INVEST. BUILD. GROW.

MANITOBA

REPORT OF ACTIVITIES 2022

Manitoba Geological Survey

Manitoba

REPORT OF ACTIVITIES
2022

Manitoba Natural Resources and Northern Development
Manitoba Geological Survey

Manitoba

Manitoba Geological Survey 2022: Report of Activities 2022; Manitoba Natural Resources and Northern Development, Manitoba Geological Survey, 127 p.

Published by:
Manitoba Natural Resources and Northern Development
Manitoba Geological Survey
360–1395 Ellice Avenue
Winnipeg, Manitoba
R3G 3P2 Canada
Telephone: 1-800-223-5215 (General Enquiry)
204-945-6569 (Publication Sales)
Fax: 204-945-8427
Email: minesinfo@gov.mb.ca
Website: manitoba.ca/minerals

ISBN: 978-0-7711-1639-1

This publication is available to download free of charge at manitoba.ca/minerals

Front cover photo:
Manitoba Geological Survey geologist Marc Rinne mapping bedrock exposures at Keeyask hydroelectric dam, northeastern Manitoba (GS2022-2, this volume).

REPORT OF ACTIVITIES 2022

Minister's Message

As Minister of Natural Resources and Northern Development, it is my pleasure to introduce the *Report of Activities 2022*, a comprehensive update on geoscience projects and activities conducted by the Manitoba Geological Survey (MGS) over the past year.

I applaud the commitment and hard work of the MGS. In the short time that I have been in my role, I had the opportunity to meet this talented team who have continued to deliver world-class geoscience publications and research. The MGS has a long-standing history of collaborating with universities, industry, Indigenous groups and government partners in Manitoba and beyond. Exemplary geoscience is foundational to exploration and mineral resource development, and drives sector investment in the province.

This year we present 12 reports, two preliminary maps and three data repository items. Manitoba's wealth of mineral resources with high potential for new discoveries include rare-earth elements, platinum-group elements, uranium, titanium, vanadium, chromite, silica, tungsten, graphite, diamonds and potash.

The MGS geoscience contributes to unlocking Manitoba's potential and advancing sustainable and responsible development of Canada's mineral resources. Continued collaboration with the Targeted Geoscience Initiative and Geo-mapping for Energy and Minerals programs, as well as the development of the 2027 Geological Atlas of the Western Canada Sedimentary Basin, highlights the wealth of public geoscience knowledge gained throughout Manitoba.

The MGS continuously updates Manitoba's geoscience knowledge base, including an innovative Mineral Deposits Database. Our leading-edge, science-based research greatly contributes to the effectiveness of mineral exploration activities in established mining camps and frontier areas.

In an effort to move forward in making the most of our shared potential and opportunities, I invite you to reach out to our MGS team to discuss their findings and talk about your needs.

When I look at Manitoba's minerals sector and the growing international demand for critical metals and key mineral resources, it is easy to see we have everything it takes to succeed in Manitoba. Let's move forward with confidence.

Original signed by

Honourable Greg Nesbitt

Manitoba Natural Resources and Northern Development

Rapport d'activités 2022

Message du ministre

À titre de ministre des Ressources naturelles et du Développement du Nord, j'ai l'honneur de présenter le *Rapport d'activités de 2022*, qui fait le point de façon exhaustive sur les projets et les activités en géoscience menés par la Direction des services géologiques (DSG) au cours de la dernière année.

J'applaudis la détermination et le travail acharné de la DSG. Dans le peu de temps qui s'est écoulé depuis mon entrée en fonctions, j'ai eu l'occasion de rencontrer cette équipe talentueuse qui continue de produire des publications et des travaux de recherche géoscientifiques de classe mondiale. La DSG collabore depuis longtemps avec le milieu universitaire, l'industrie, les groupes autochtones et ses partenaires gouvernementaux au Manitoba et ailleurs. La géoscience exemplaire est le fondement des activités d'exploration et d'exploitation des ressources minérales, qui favorise les investissements du secteur dans la province.

Cette année, nous présentons 12 rapports, deux cartes préliminaires et trois éléments du répertoire de données. Les richesses minérales du Manitoba ayant un fort potentiel de découverte comprennent les éléments des terres rares, les éléments du groupe platine, l'uranium, le titane, le vanadium, la chromite, la silice, le tungstène, le graphite, les diamants et la potasse.

Les études de géoscience de la DSG contribuent à libérer le potentiel du Manitoba et à favoriser le développement durable et responsable des ressources minérales du Canada. La collaboration soutenue à l'Initiative géoscientifique ciblée et au Programme de géocartographie de l'énergie et des minéraux, ainsi qu'à la préparation de l'Atlas géologique du bassin sédimentaire de l'Ouest canadien 2027, mettent en valeur tout le bagage de connaissances de la géoscience accumulées publiquement dans l'ensemble du Manitoba.

La DSG met à jour constamment la base de connaissances en géoscience du Manitoba, y compris une base de données sur les minéraux innovante. Nos travaux de recherche de pointe, fondés sur des données scientifiques, contribuent largement à l'efficacité des activités d'exploration minière dans les camps miniers établis et les zones inexploitées.

Afin d'aller de l'avant dans l'exploitation optimale de nos possibilités et de notre potentiel communs, je vous invite à communiquer avec les membres de l'équipe de la DSG pour discuter de leurs conclusions et de vos besoins.

Compte tenu de notre secteur des minéraux et de la demande croissante en minéraux critiques et en ressources minérales clés dans le monde, il est clair que nous avons tout ce qu'il faut pour réussir au Manitoba. Allons de l'avant avec confiance.

Origional signé par

Greg Nesbitt

Ressources naturelles et du Développement du Nord

Foreword

On behalf of the Manitoba Geological Survey (MGS), it is my privilege to present the *Report of Activities 2022*—the annual peer-reviewed volume of geoscience project results by the MGS and its partners.

With the creation of the Department of Natural Resources and Northern Development in February of 2022, the Stewardship and Resource Development (SRD) Division comprises the Manitoba Geological Survey; Forestry and Peatlands Branch; Lands and Planning Branch; Mining, Oil and Gas Branch; Consultation and Reconciliation Unit; and Business Development Services. The Manitoba Geological Survey regained its status as a branch that represents a consolidation of all geoscience-related services that SRD provides. The MGS consists of five sections: (1) Precambrian Geoscience (Christian Böhm, Chief Geologist); (2) Sedimentary Geoscience (Michelle Nicolas, Chief Geologist); (3) Geoscience Data Management (Greg Keller, Manager); (4) Rock Libraries and Laboratory (Colin Epp, Manager); and (5) the Resource Centre (Peggy Syljuberget, Manager).

The MGS conducts a wide range of investigations, which include the examination of exposed bedrock, subsurface and surficial sediments including sand, gravel and organic deposits throughout Manitoba. It also provides geoscience support for the regulatory framework and tenure systems managed by SRD, which includes oil field-pool code designations, geoscientific review of oil and gas licences and applications, borehole licence reviews, aggregate inquiries and land-use designations. By incrementally developing and advancing a detailed understanding of Manitoba's geology and geological processes, the MGS provides foundational data and unbiased technical support to inform government policy and decision-making, mineral exploration, and land-use management.

This year's 12 articles cover a diverse thematic and geographic range from greenstone belts with Ni-Cu-PGE potential, collaborative geoscience projects focusing on critical minerals, re-interpretation of old data using today's knowledge and technologies, geoscience database innovation, to state-of-the-art surficial geoscience. Some examples include renewed research and mapping of the potash layers across the basin, where better geoscientific understanding has increased the potential distribution of the potash members in Manitoba. A new bedrock-mapping project initiated at Halfway Lake in the Thompson nickel belt focuses on potentially new Ni-Cu sulphide deposits. Furthermore, the MGS is studying pegmatitic intrusions in the Kisseynew domain and the Bird River greenstone belt for their potential to host economic levels of critical minerals, including lithium.

Continued improvements to Manitoba's Mineral Deposits Database (MDD) resulted in the identification of thousands of new mineral occurrences located throughout the province. Because the new MDD captures a wide range of commodities, including several newly added critical minerals, the MGS anticipates that future updates will allow for comprehensive assessments of Manitoba's critical-mineral potential. By extracting key information from historical documents and adding newly available exploration data, the ongoing MDD update project is filling important gaps in Manitoba's mineral occurrence data and mineral potential assessments. A more comprehensive mineral occurrence dataset directly supports land-use and related economic development planning (e.g., parks and infrastructure planning within government, MGS project planning, community economic development strategies), and may trigger renewed or new exploration interest in certain areas.

Over the last year, the MGS saw several staff changes. We continue to build capacity with the hiring of Peggy Syljuberget as Manager of the Resource Centre. After more than 35 years with the MGS, Len Chackowsky set off for retirement. Len's contribution to the Geoscience Data Management section (GDMS) of the MGS will be missed, along with his fabulous sense of humour. The GDMS also lost a talented GIS specialist when Ashley Santucci left the MGS for warmer climes earlier this year. Thank you to Christine Custodio and Elena Kozak, both of whom moved to other departments, for their work as the Mining, Oil and Gas System Administrator, supporting the Manitoba Oil and Gas Well Information System (iMaQs), Petrinex and other MGS/MOG legacy systems. Finally, after six years of providing support to both staff and clients in the Resource Centre, we bid farewell to our Resource Centre specialist, Tomaz Booth.

The production of the Report of Activities, together with a wealth of other MGS publications, is not possible without the dedicated efforts of all geologists, GIS specialists, lab technicians, summer students and administrative and Corporate Services staff. Bob Davie and his team from RnD Technical provided outstanding professional technical editing services, and Craig Steffano managed report production and publication layout. I sincerely thank everyone from the MGS team for their valuable contributions.

Tafa Kennedy, Ph.D., P.Geo.

Director, Manitoba Geological Survey

Avant-propos

J'ai l'honneur de présenter, au nom de la Direction des services géologiques du Manitoba (la Direction), le *Rapport d'activités 2022*, un recueil annuel examiné par les pairs compilant les résultats de projets géoscientifiques exécutés par la Direction et ses partenaires.

Avec la création du ministère des Ressources naturelles et du Développement du Nord en février 2022, la Division de la gérance et du développement des ressources (la Division) comprend la Direction des services géologiques du Manitoba, la Direction des forêts et de la gestion des tourbières, la Direction des terres et de la planification, la Direction des mines, du pétrole et du gaz, l'Unité de consultation et de réconciliation et les Services de développement des entreprises. Les services géologiques du Manitoba ont retrouvé leur statut de direction qui représente un regroupement de tous les services liés aux géosciences que fournit la Division de la gérance et du développement des ressources. La Direction est composée de cinq sections : (1) la Section du précambrien (Christian Böhm, géologue en chef); (2) la Section de la géologie sédimentaire (Michelle Nicolas, géologue en chef); (3) la Section de la gestion des données géoscientifiques (Greg Keller, gestionnaire); (4) la Section des bibliothèques et du laboratoire des minéraux (Colin Epp, gestionnaire); et (5) le Centre de ressources (Peggy Syljuberget, gestionnaire).

La Direction mène un vaste éventail d'études, qui comprennent l'examen du substrat rocheux exposé, des matériaux en subsurface et des sédiments superficiels, comme le sable, le gravier et les dépôts organiques, à l'échelle du Manitoba. Elle fournit également un soutien géoscientifique en ce qui concerne le cadre de réglementation et les régimes fonciers gérés par la Division, ce qui inclut l'attribution de codes aux champs et gisements de pétrole, l'examen géoscientifique des permis et des demandes d'exploitation de pétrole et de gaz, l'examen des permis de forage, les enquêtes sur les agrégats et les désignations relatives à l'usage des terres. En développant progressivement une compréhension détaillée de la géologie et des processus géologiques du Manitoba, la Direction fournit des données fondamentales et un soutien technique impartial à l'appui des politiques et de la prise de décisions gouvernementales, de l'exploration minière et d'un aménagement judicieux du territoire.

Les 12 articles de cette année couvrent un large éventail thématique et géographique, allant des ceintures de roches vertes présentant un potentiel en Ni-Cu-ÉGP aux projets géoscientifiques collaboratifs axés sur les minéraux essentiels, en passant par la réinterprétation d'anciennes données à l'aide des connaissances et des technologies actuelles, l'innovation en matière de bases de données géoscientifiques et les géosciences de surface de pointe. La modernisation des recherches et de la cartographie des couches de potasse dans le bassin, où une meilleure compréhension géoscientifique a permis d'accroître la distribution potentielle des gisements de potasse au Manitoba, en est un exemple. Un nouveau projet de cartographie du substrat rocheux amorcé au lac Halfway, dans la ceinture de nickel de Thompson, vise les nouveaux gisements potentiels de sulfures de Ni-Cu. De plus, la Direction étudie les intrusions pegmatitiques du domaine de Kisseynew et de la ceinture de roches vertes de Bird River pour leur potentiel à abriter des gisements rentables de minéraux essentiels, dont le lithium.

Les améliorations continues apportées à la base de données sur les gisements minéraux du Manitoba ont permis de cerner des milliers de nouvelles occurrences minérales situées dans toute la province. La nouvelle base de données contenant un large éventail de produits, dont plusieurs minéraux essentiels récemment ajoutés, la Direction prévoit que les mises à jour futures permettront de réaliser des évaluations exhaustives du potentiel des gisements minéraux critiques du Manitoba. En extrayant des renseignements clés de documents historiques et en ajoutant des données d'exploration nouvellement disponibles, le projet en cours de mise à jour de la base de données sur les gisements minéraux comble d'importantes lacunes en ce qui concerne les données sur les occurrences minérales et les évaluations du potentiel minéral du Manitoba. Un ensemble plus complet de données sur les occurrences minérales appuie directement la planification de l'usage des terres et du développement économique connexe (p. ex., la planification des parcs et des infrastructures au sein du gouvernement, la planification des projets de la Direction, les stratégies de développement économique des communautés) et peut susciter un intérêt renouvelé ou nouveau pour l'exploration dans certaines régions.

Au cours de l'année écoulée, la Direction a connu plusieurs changements de personnel. Nous continuons à renforcer la capacité grâce à l'embauche de Peggy Syljuberget en tant que gestionnaire du Centre de ressources. Après plus de 35 années au sein de la Direction, Len Chackowsky a pris sa retraite. La contribution de Len à la Section de la gestion des données géoscientifiques de la Direction nous manquera, tout comme son merveilleux sens de l'humour. La Section a également perdu un spécialiste SIG talentueux lorsqu'Ashley Santucci a quitté la Direction pour un climat plus chaud au début de l'année. Merci à Christine Custodio et à Elena Kozak, qui ont toutes deux obtenu un poste dans d'autres ministères, pour leur travail en tant qu'administratrices du système de la section des mines, du pétrole et du gaz, leur soutien au système d'information sur les puits de pétrole et de gaz du Manitoba (iMaQs), de Petrinex ainsi que d'autres anciens systèmes des services géologiques et des mines, du pétrole et du gaz du Manitoba. Enfin, après avoir fourni un soutien au personnel et aux clients du Centre de ressources pendant six ans, nous disons au revoir à Tomaz Booth, notre spécialiste du Centre de ressources.

La production du rapport d'activités, ainsi que d'une multitude d'autres publications de la Direction, ne serait pas possible sans les efforts dévoués de tous les géologues, spécialistes SIG, techniciens de laboratoire, stagiaires et de tout le personnel des services administratifs et ministériels. Bob Davie et son équipe à RnD Technical ont fourni d'excellents services professionnels de révision technique et Craig Steffano a géré la production du rapport et la mise en pages de la publication.

Je remercie sincèrement tous les membres de l'équipe de la Direction de leurs précieuses contributions.

La directrice des services géologiques du Manitoba,
Tafa Kennedy, Ph.D., P.Geo.

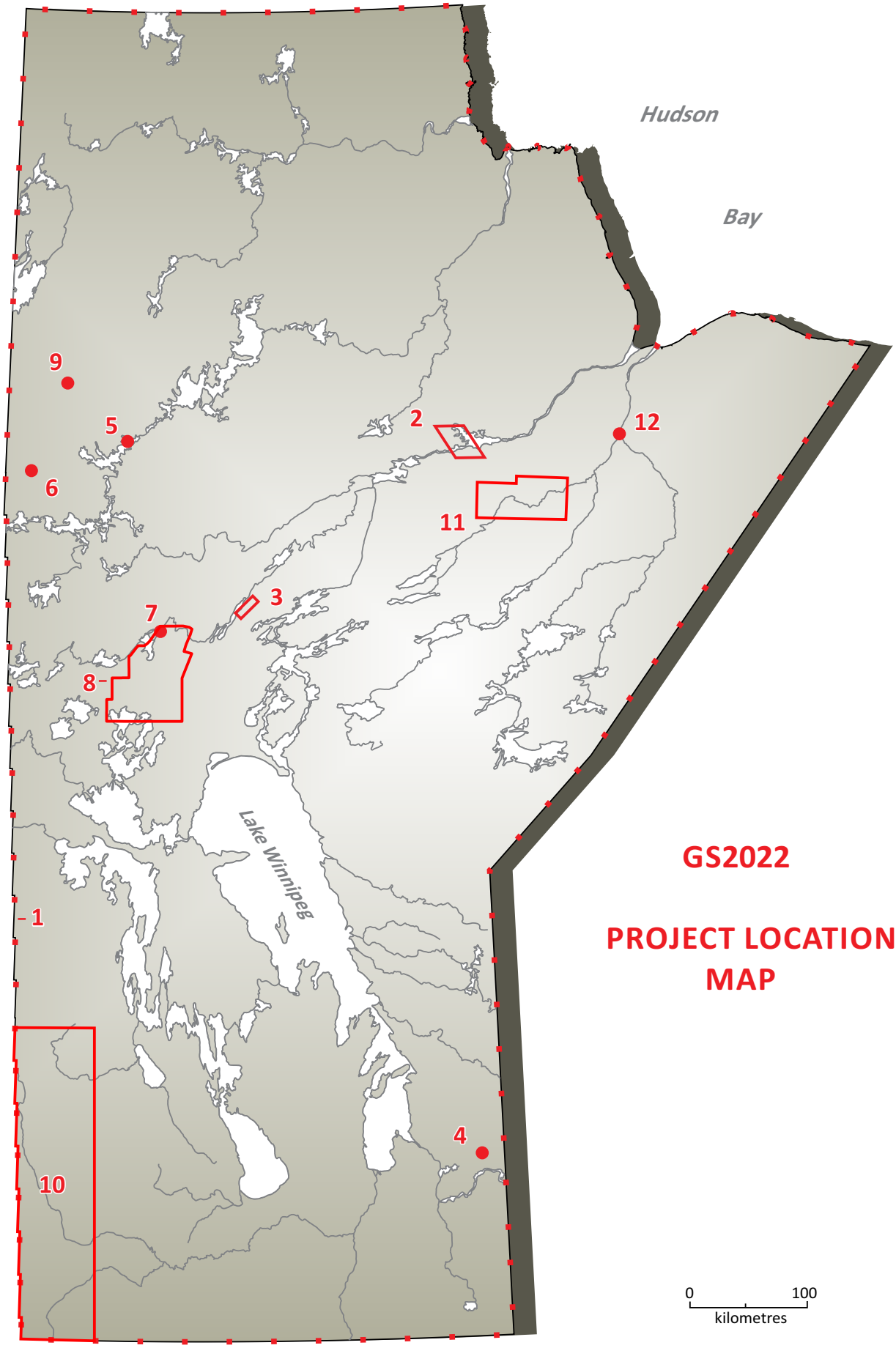
Hudson
Bay
Lake Winnipeg
1
2
3
4
5
6
7
8
9
10
11
12
GS2022
PROJECT LOCATION MAP
0
100
kilometres

Table of Contents

Minister's Message iii

Message du ministre iv

Foreword
by T. Kennedy v

Avant-propos
par T. Kennedy vi

GS2022 Project Location Map viii

PRECAMBRIAN

GS2022-1
Progress report on the Manitoba Mineral Deposits Database
by M.L. Rinne 1

GS2022-2
Updates to bedrock geology mapping in the Gull Rapids area following construction of the Keeyask hydroelectric dam, northeastern Manitoba (parts of NTS 54D5, 6)
by C.O. Böhm and M.L. Rinne 5

GS2022-3
Bedrock mapping in the Halfway Lake area, Thompson nickel belt, central Manitoba (parts of NTS 63O1, 2)
by C.G. Couëslan 12

GS2022-4
Investigating textural and geochemical relations of lithium mineralization in the Tanco pegmatite, southeastern Manitoba (part of NTS 52L6)
by C.M. Breasley, T. Martins, R.L. Linnen and L.A. Groat 25

GS2022-5
Critical minerals scoping study of the Suwannee River syenite intrusion, west-central Manitoba (part of NTS 64B4)
by T. Martins and C.G. Couëslan 36

GS2022-6
Preliminary results from targeted sampling of the Brezden Lake intrusive complex, west-central Manitoba (parts of NTS 64C4)
by T. Hnatiuk, C.G. Couëslan, A.R. Chakhmouradian and T. Martins 42

GS2022-7
Preliminary observations on emplacement controls of pegmatite dikes from the Wekusko Lake pegmatite field, north-central Manitoba (parts of 63J13, 14, 63O4)
by D. Silva, T. Martins, L. Groat and R. Linnen 49

GS2022-8
Preliminary interpretation of aeromagnetic data from poorly exposed and sub-Phanerozoic basement rocks east and southeast of Snow Lake, north-central Manitoba (parts of NTS 63F15, 16, 63G13, 14, 63J3–6, 11–14, 63K1, 2, 8, 9, 16, 63O3, 4)
by K.D. Reid 61

GS2022-9
Preliminary results of bedrock geological mapping in the Fox mine–Snake Lake area, Lynn Lake greenstone belt, northwestern Manitoba (part of NTS 64C12)
by X.M. Yang 71

PHANEROZOIC

GS2022-10
Stratigraphy and distribution of the potash-bearing members of the Devonian Prairie Evaporite, southwestern Manitoba (parts of NTS 62F, K)
by M.P.B. Nicolas and C. Yang 87

QUATERNARY

GS2022-11
Surficial geology mapping and till composition of the western Fox River greenstone belt area, northeastern Manitoba (NTS 53M15, 16, parts of 53N13, 54C4, 54D1): year two
by M.S. Gauthier and T.J. Hodder 96

GS2022-12
Quaternary stratigraphic investigations near the confluence of the Hayes and Gods rivers, northeastern Manitoba (part of NTS 54C7)
by T.J. Hodder and M.S. Gauthier 110

PUBLICATIONS

Manitoba Geological Survey Publications Released December 2021 to November 2022 122

External Publications 126

GS2022-1

Progress report on the Manitoba Mineral Deposits Database

by M.L. Rinne

Summary

Continued improvements to Manitoba's Mineral Deposits Database have resulted in the identification of thousands of new mineral occurrences located throughout the province. In this report, an overview of updates to the Mineral Deposits Database is provided, followed by a preliminary look at occurrences of Ni, Co, Cr, Pt and Pd for which location data has been compiled so far. Because the new Mineral Deposits Database is designed to capture a wide range of commodities including critical minerals, the Manitoba Geological Survey anticipates that further updates will allow for more comprehensive assessments of Manitoba's critical-mineral potential.

In Brief:

- The MGS has uncovered approximately 26 200 new or previously unrecognized mineral occurrences in Manitoba
- Preliminary compilation of Ni, Co, Cr, Pt and Pd occurrence data shows spatial association with greenstone belts
- Further updates will allow for more advanced assessments of critical mineral potential

Citation:
Rinne, M.L. 2022: Progress report on the Manitoba Mineral Deposits Database; *in* Report of Activities 2022, Manitoba Natural Resources and Northern Development, Manitoba Geological Survey, p. 1–4.

Introduction

Mineral occurrence data are an essential component of well-informed land-use plans, mineral development strategies and related mineral potential assessments. These data are also frequently used by the private sector to inform their mineral exploration decisions. Since the beginning of the Mineral Deposits Database (MDD) update in 2020, the Manitoba Geological Survey (MGS) has uncovered approximately 26 200 new or previously unrecognized mineral occurrences in Manitoba. Sample co-ordinates and other necessary information have been captured for approximately one third of the new occurrences so far, and more results are anticipated as assessment reports and sample-location maps continue to be processed.

Although much work remains to make all the mineral occurrence data publicly accessible, the MDD results collected to date provide some preliminary indication of regional mineral potential. For example, in this report, the spatial distribution of Ni, Co, Cr, Pt and Pd occurrences in Manitoba show clear relationships with the underlying geology and, in some areas, the (mostly new) occurrences could be sufficient to lead to new exploration targets. Generally speaking, these preliminary examples serve to demonstrate how the MDD and similar compilations can be used to evaluate critical-mineral potential.

Results to date

The MDD update project is effectively an exercise in software-assisted data mining from scanned industry assessment reports, supplemented with other sources. Details concerning the methods and software used to identify new mineral occurrences, along with explanations of the criteria and terminology used in the MDD, are provided in Rinne (2021a).

Approximately 26 200 occurrences have been thus far tentatively identified in Manitoba based on geochemical results or phrase-matching results (Figure GS2022-1-1). Among these new occurrences, however, only about 8000 currently have been compiled with adequate location information (i.e., sample co-ordinates). The process of georeferencing the location of each sample, which commonly requires retrieving original sample maps, is the main reason why progress has been slow in adding location information to the MDD; the MGS is looking into options to expedite this task.

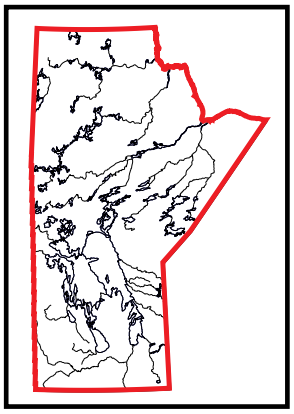

The MDD updates are shared publicly through GeoFile 5-2022 (Rinne, 2022), which supersedes a previous Data Repository Item (Rinne, 2021b). The most recent public version of GeoFile 5-2022 contains MDD updates within NTS 53E, F and all parts of Manitoba north of latitude 57°N. Occurrences will continue to be added to this GeoFile as updates progress by region.

Because new MDD entries include relevant assay data, spatial variations in elements such as Co or Ni can be explored by filtering occurrence data by grade or commodity type (e.g., Figure GS2022-1-2). Although the occurrences shown in Figure GS2022-1-2 again represent but a small portion of the total to be included in future MDD updates, there is sufficient spatial coverage to reveal regional trends. For example, elevated Co and Cr contents have been reported throughout both the Superior and Churchill provinces and trace a linear trend through both the Thompson nickel belt (TNB) and the western part of the Fox River belt (Figure GS2022-1-2a). Several volcanogenic massive sulphide

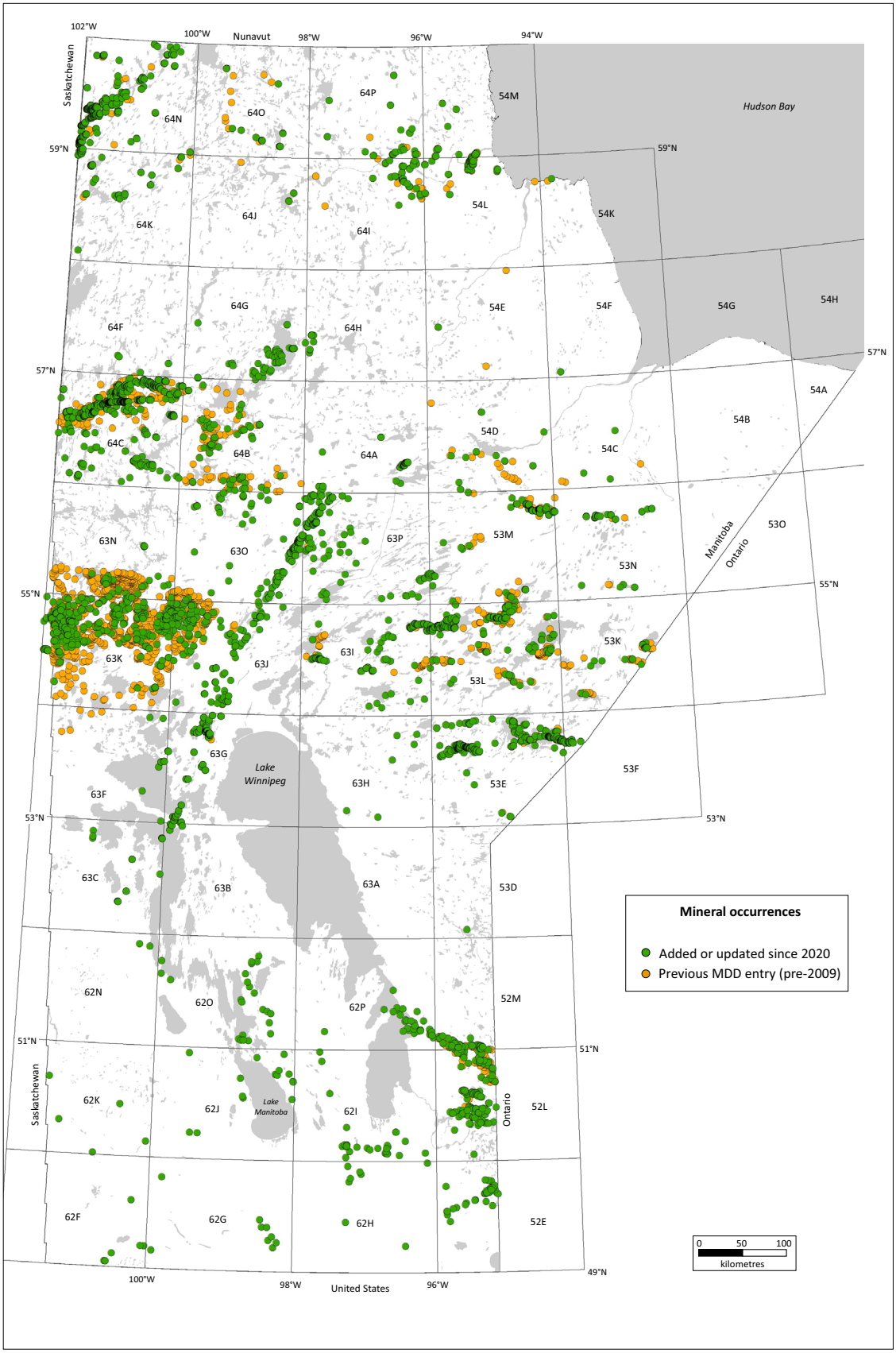

Figure GS2022-1-1: *Preliminary map of mineral occurrences added to the Manitoba Mineral Deposits Database (MDD) since 2020. Occurrences shown here represent approximately one third of total occurrences found to date; the remainder, although identified from assessment reports, have yet to be located spatially. Users should therefore note that future versions of this map will differ significantly once MDD updates have been completed. As of September 2022, occurrences in NTS 53E, F and all parts of Manitoba north of latitude 57°N have been released in Rinne (2022).*

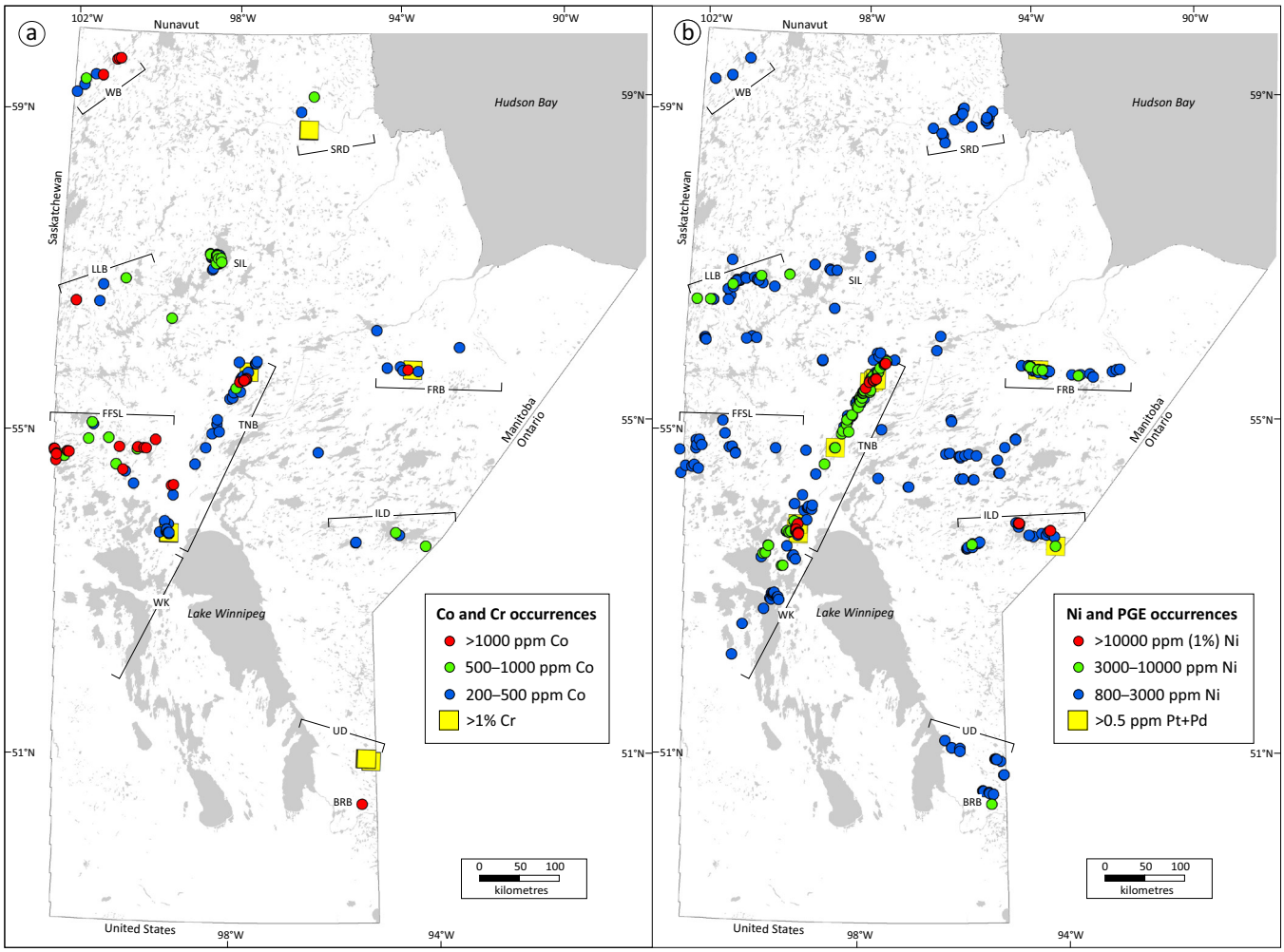

Figure GS2022-1-2: *Preliminary maps of mineral occurrences in Manitoba, limited to* ***a)*** *samples with elevated Co and Cr contents; and* ***b)*** *Ni and Pt+Pd occurrences. This figure is based on a preliminary collection of data from the new Mineral Deposits Database entries shown in Figure GS2022-1-1; as in the previous figure, only data for which location data has been collected are shown. Mine site locations and geology are omitted for clarity. Abbreviations: BRB, Bird River belt; FFSL, Flin Flon–Snow Lake belt; FRB, Fox River belt; ILD, Island Lake domain; LLB, Lynn Lake belt; SIL, Southern Indian Lake; SRD, Seal River domain; TNB, Thompson nickel belt; UD, Uchi domain; WB, Wollaston basin; WK, Winnipegosis komatiites.*

(VMS) ore samples across the Flin Flon–Snow Lake area also contain high Co contents comparable to some deposits from which Co is extracted (e.g., Slack et al., 2017), perhaps implying potential for local Co byproduction from these ore deposits. Anomalous Co contents are also scattered across parts of the Seal River domain, the Wollaston basin and an as yet unexplained cluster of Co-bearing basalt outcrops across part of the Southern Indian Lake area (Figure GS2022-1-2a).

Nickel, which is commonly included in assay results listed in most assessment reports, reveals similar regional trends (Figure GS2022-1-2b). Even though most of the new Ni occurrences in MDD updates are presently lacking location data (and are therefore omitted from the map), the number of occurrences shown in Figure GS2022-1-2b is in many locations sufficient to reveal linear belts, corresponding mostly to greenstone belts such as the Lynn Lake, Island Lake or Bird River belts. Elevated Ni results also clearly trace the Fox River belt and TNB extending into the buried segments of the Winnipegosis komatiite belt.

Platinum-group elements (PGE) such as Pt and Pd are not as commonly reported in assessment files. Occurrences of Pt and Pd for which locations have currently been compiled relate to TNB deposit ores, part of the western Fox River sill, and an occurrence in the Island Lake region at Rose Lake (Figure GS2022-1-2b). There is limited information concerning the Rose Lake occurrence (Rose Lake is too small to display at the map scale); drilling in the area reportedly intersected sulphide-mineralized pyroxenite and gabbro and later surface assays near Rose Lake returned 0.5 ppm Au, 0.06% Co, 1.94% Cu, 0.75% Ni, 0.48 ppm Pd and 0.41 ppm Pt (Assessment File 92726, Manitoba Natural Resources and Northern Development, Winnipeg).

Economic considerations

By extracting key information from historical documents, the ongoing MDD update project is filling important gaps in Manitoba's mineral occurrence data and mineral potential assessments. A more comprehensive mineral occurrence dataset directly sup-

ports land-use and related economic development planning (e.g., parks and infrastructure planning within government, geological survey project planning or community economic development strategies) and may trigger renewed or new exploration interest in certain areas.

Mineral occurrence criteria were selected to ensure that critical minerals—resources deemed essential to Canada's economic security and for the transition to a low-carbon economy (Natural Resources Canada, 2021)—are fully captured in MDD updates. In addition to improving data coverage around known deposits, further compilation of critical-minerals data from established mining areas may also reveal overlooked potential for byproduct extraction from some ores. Results of the MDD update have demonstrated that not only are there many potentially significant critical-mineral occurrences hidden among historical assay results and rock descriptions, but also that these are not limited to established mining districts.

Acknowledgments

The author thanks C. Böhm and M. Nicolas (Manitoba Geological Survey) for their reviews, and J. Janssens (University of Manitoba) for her tireless assistance with the Mineral Deposits Database, especially in dealing with poor-quality scans and georeferencing sample locations.

References

Natural Resources Canada 2021: Critical minerals; Natural Resources Canada, URL <https://www.nrcan.gc.ca/our-natural-resources/minerals-mining/critical-minerals/23414> [September 2022].

Rinne, M.L. 2021a: Updates to the Manitoba Mineral Deposits Database, east-central and northwestern Manitoba (NTS 53E, F, 64J, K, N, O); in Report of Activities 2021, Manitoba Agriculture and Resource Development, Manitoba Geological Survey, p. 1–7, URL <https://manitoba.ca/iem/geo/field/roa21pdfs/GS2021-1.pdf> [October 2022].

Rinne, M.L. 2021b: Updates to the Manitoba Mineral Deposits Database, east-central Manitoba (NTS 53E, F); Manitoba Agriculture and Resource Development, Manitoba Geological Survey, Data Repository Item DRI2021019, Microsoft® Excel® file, URL <https://manitoba.ca/iem/info/libmin/DRI2021019.xlsx> [November 2021].

Rinne, M.L. 2022: Updates to the Manitoba Mineral Deposits Database, east-central and northern Manitoba (parts of NTS 53; 54; 64); Manitoba Natural Resources and Northern Development, Manitoba Geological Survey, GeoFile 5-2022, Microsoft® Excel® file, URL <https://manitoba.ca/iem/info/libmin/geofile5.zip> [October 2022].

Slack, J.F., Kimball, B.E. and Shedd, K.B. 2017: Cobalt; Chapter F *in* Critical mineral resources of the United States–Economic and environmental geology and prospects for future supply, K.J. Schulz, J.H. DeYoung, R.R. Seal and D.C. Bradley (ed.), U.S. Geological Survey, Professional Paper 1802, p. F1–F40.

GS2022-2

Updates to bedrock geology mapping in the Gull Rapids area following construction of the Keeyask hydroelectric dam, northeastern Manitoba (parts of NTS 54D5, 6)

by C.O. Böhm and M.L. Rinne

In Brief:

- Bedrock mapping of outcrops made accessible or created by Keeyask hydroelectric dam construction at Gull Rapids allow for minor changes of the regional geology
- Regionally thick glacial overburden limit bedrock exposures but warrant a future surficial mapping and sampling study

Citation:
Böhm, C.O. and Rinne, M.L. 2022: Updates to bedrock geology mapping in the Gull Rapids area following construction of the Keeyask hydroelectric dam, northeastern Manitoba (parts of NTS 54D5, 6); *in* Report of Activities 2022, Manitoba Natural Resources and Northern Development, Manitoba Geological Survey, p. 5–11.

Summary

Bedrock geological studies in the Gull Rapids area were previously conducted in 2003–2004, to document the geological record prior to construction of the Keeyask hydroelectric dam. The addition of bedrock geological data collected in summer 2022 from previously nonexistent or inaccessible exposures allows for some updates of the regional geology mapping done in the Keeyask dam region of the Gull Rapids area, specifically the geology as portrayed at a scale of 1:250 000. The new bedrock data, in combination with high-resolution aeromagnetic data to probe beneath regionally thick overburden cover, refine the geology shown on the existing 1:250 000 scale bedrock compilation. The ubiquitous glacial overburden in the region evidently resulted in misinterpretation of contact positions and distribution of geological units, and may warrant the undertaking of surficial geological studies in the Keeyask hydroelectric dam area.

Introduction

In 2003 and 2004, the Manitoba Geological Survey (MGS), in collaboration with the universities of Alberta and Waterloo and supported by Manitoba Hydro, undertook detailed bedrock mapping at 1:1000 to 1:200 scales in the Gull Rapids area (Böhm et al., 2003a, b, 2006; Bowerman et al., 2004; Downey et al., 2004), west of Gillam, where the lower Nelson River spills into Stephens Lake (present site of the Keeyask hydroelectric dam; Figure GS2022-2-1). The 2003 and 2004 bedrock mapping and follow-up analytical studies provided a detailed record of the geology at Gull Rapids. In conjunction with the Gull Rapids studies, mapping of areas upstream the lower Nelson River to Split Lake were conducted in 2003–2005 (Hartlaub et al., 2003, 2004; Kuiper et al., 2003, 2004; Hartlaub and Kuiper, 2004; Kuiper and Lin, 2004a, b). Together, these studies provided a record of the geology east of Stephens Lake along the lower Nelson River prior to the Keeyask hydroelectric dam construction, which resulted in water level alterations and changes in bedrock exposures and access.

Since the completion of the aforementioned geological studies, an approximately 25 km long all-weather access road was built by Manitoba Hydro between Provincial Road 280 northeast of Split Lake and the Keeyask hydroelectric dam site (Figure GS2022-2-1). This new road, together with aggregate quarry sites along the way, provides access to potential bedrock exposures for a previously largely inaccessible and geologically poorly documented transect along this portion of the Superior boundary zone (Figure GS2022-2-1).

The northern access road to the Keeyask dam and changes in exposure at Gull Rapids due to hydroelectric dam construction warranted collection of new geological information both along the road corridor and at the dam site. Permission granted by Manitoba Hydro to use the access road and work onsite at the Keeyask dam area allowed the MGS to proceed with geological mapping and sampling work in August 2022, when the authors conducted two weeks of geological fieldwork in the Keeyask dam area (Figure GS2022-2-1). This geological fieldwork included

- one week of geological mapping and sampling along and off the Keeyask dam northern access road, focused on possible bedrock exposures accessible by truck and foot traverses; and
- one week of detailed geological follow-up mapping in the Keeyask dam area, focused on new or changed bedrock exposures accessible by truck and on foot, providing an update to the previous bedrock mapping at Gull Rapids.

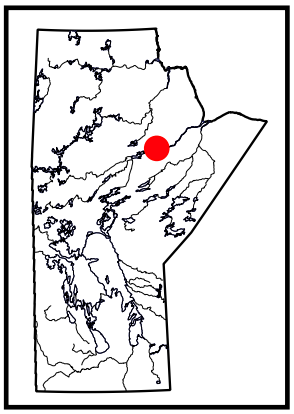

Bedrock geology of the Keeyask dam region

Gull Rapids (location of the Keeyask hydroelectric dam) is located at the northwestern margin of the Superior craton in northeastern Manitoba. It is situated between variably retrogressed Archean granulites of the Split Lake block (northwestern Superior province) to the southwest and Paleopro-

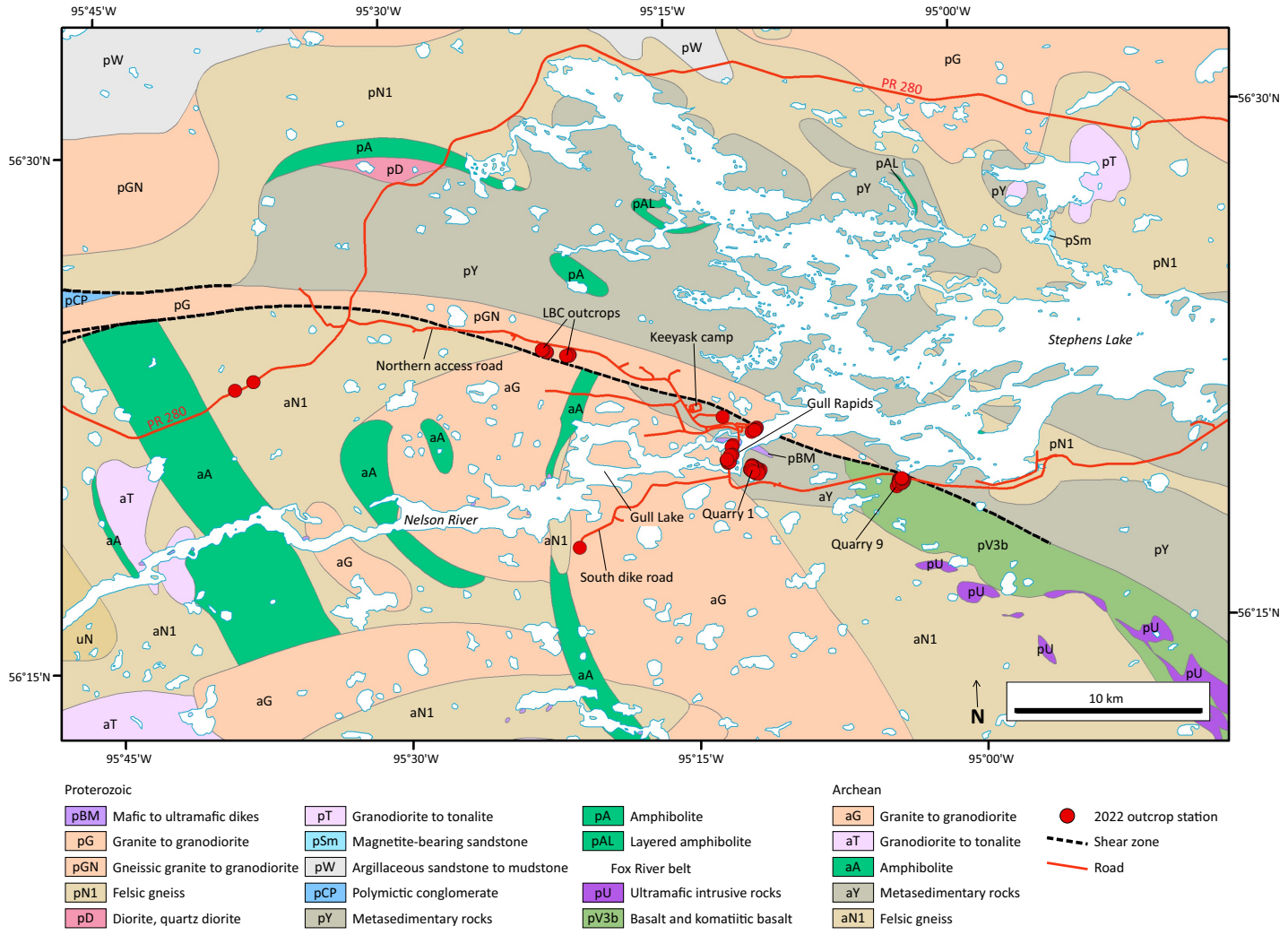

Figure GS2022-2-1: *Regional bedrock geology of the Keeyask hydroelectric dam area, modified after the 1:250 000 scale Precambrian bedrock geology map issued by the Manitoba Geological Survey (2022). The 2022 station locations (red circles) were accessed primarily by road and on foot, with access to the Keeyask dam site via a side road off Provincial Road 280 (PR 280, labeled). Locations referenced in the text (Keeyask main camp, quarry 1, quarry 9, south dike road) are labeled near map centre. Abbreviation: LBC, Looking Back creek.*

terozoic amphibolite-facies sedimentary and igneous rocks of the eastern Kisseynew domain (southeast Trans-Hudson orogen) to the north and east (Figure GS2022-2-1). The Gull Rapids area, located along the lower Nelson River, includes a spectacularly exposed sequence of late Archean, multiply deformed and upper-amphibolite– to granulite–facies supracrustal rocks that are juxtaposed against, and derived from, middle Archean, granulite-facies orthogneiss of the Split Lake block (Böhm et al., 1999). Extensive, late Archean felsic injection sheets and anatectic melts crosscut the supracrustal rocks and orthogneiss, and are further truncated by large numbers of Paleoproterozoic mafic dikes. The Gull Rapids area records a complex tectonic history, the bulk of which occurred during late Archean (Kenoran) rather than Paleoproterozoic (Hudsonian) orogenesis (Downey et al., 2009).

Early investigations of the Gull Rapids area delineated supracrustal rocks, which are abundant just east of Gull Rapids at Stephens Lake, as being part of the Paleoproterozoic Burntwood group (Haugh and Elphick, 1968; Haugh, 1969; Corkery, 1975, 1985). Detailed mapping in the Gull Rapids region in 2003 and 2004, combined with lithogeochemical, isotopic and geochronological analyses, identified more lithological and structural complexity than was previously known. From west to east, the following are the principal, dominantly south-trending lithological building blocks at Gull Rapids (e.g., Böhm et al., 2006): Mesoarchean granodiorite and derived gneissic rocks (3.18–3.14 Ga and 2.86–2.85 Ga; Bowerman et al., 2004), Archean amphibolite interpreted as metabasalt and metagabbro, Archean metasedimentary rocks including dominantly iron-rich metagreywacke gneiss (ca. 2.70 Ga youngest detrital zircons; Bowerman et al., 2004) with banded iron formation and rare lenses of ultramafic to mafic metaconglomerate, voluminous Neoarchean granitoid injection sheets and pegmatite dikes (ca. 2.69–2.61 Ga; Downey et al., 2009), and west- to northwest-trending Paleoproterozoic mafic dikes (2.07 Ga; Bowerman et al., 2004). For detailed descriptions of the lithologies and structures at Gull Rapids con-

sult Böhm et al. (2003a, b), Bowerman et al. (2004) and Downey et al. (2004).

Field observations at Gull Rapids further indicated that the supracrustal units are multiply deformed, based on the development of multiple foliations and refolded folds (Böhm et al., 2003a, b; Downey et al., 2004). Detailed structural examinations by Downey (2005) delineated five generations of deformation at Gull Rapids, some of which were subsequently dated by Downey et al. (2009) between ca. 2.69 Ga (D_1) and 2.61 Ga (D_4).

Due to the earthworks and construction of the Keeyask hydroelectric generation site at Gull Rapids and resulting upstream flooding, the western two-thirds of the documented bedrock geological record, summarized at 1:5000 scale in Böhm et al. (2006), has become inaccessible.

Newly mapped bedrock exposures

Quarry 1

Detailed mapping was carried out at a bedrock quarry approximately 500 by 250 m located immediately southeast of the Keeyask dam (Figure GS2022-2-2). The dominant lithology along the southern and western sides of the quarry is massive to foliated, layered grey granodiorite, locally showing a character-

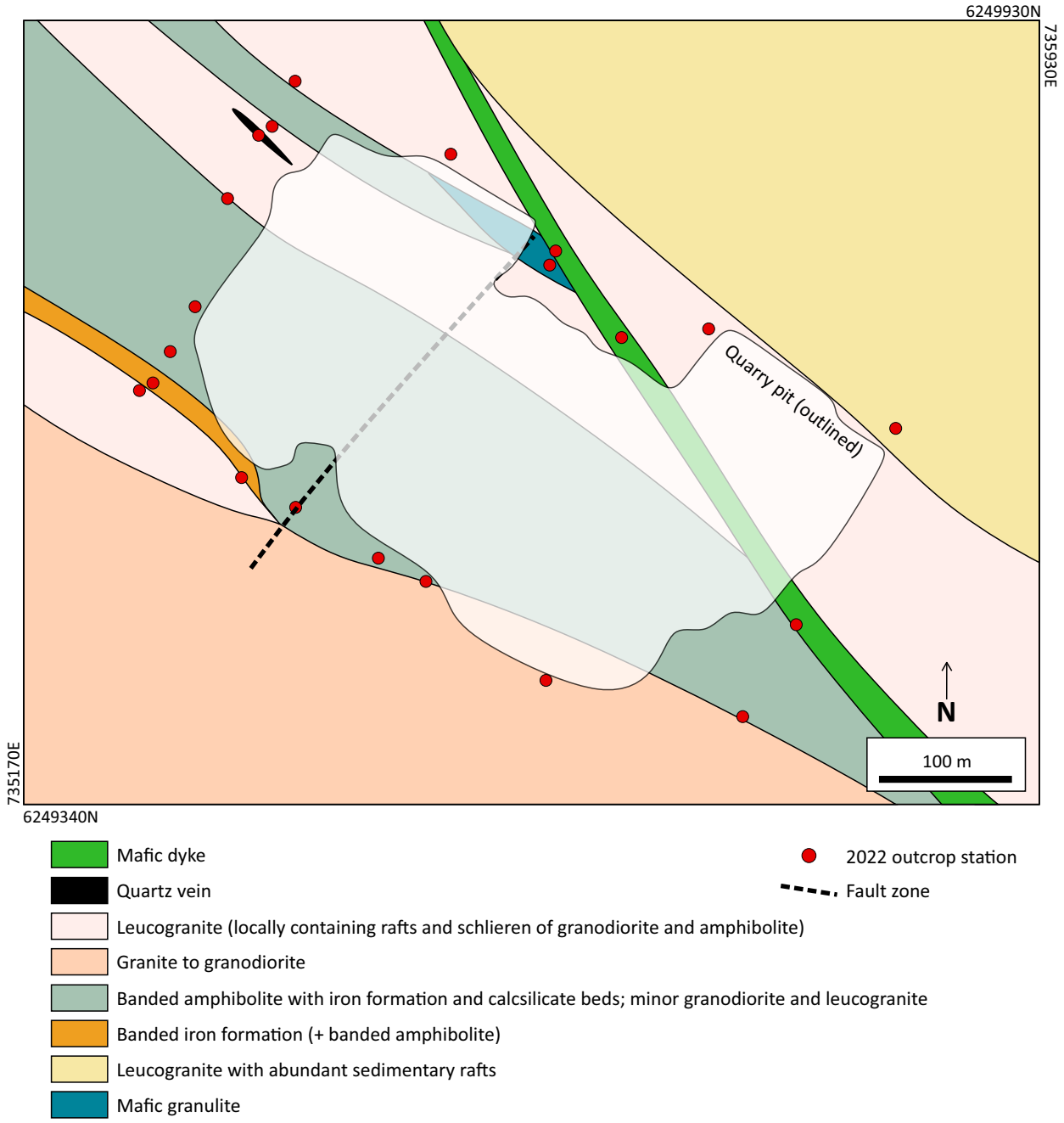

Figure GS2022-2-2: *Bedrock geological sketch map of quarry 1, located southeast of the Keeyask dam (all co-ordinates are in UTM Zone 14, NAD83).*

istic texture of black retrogressed garnet-amphibole clots. Along the western side of the quarry, the granodiorite is injected by leucogranite and the granitic units include abundant amphibolite interpreted as xenoliths or rafts (Figure GS2022-2-3a). The amphibolite is fine grained and dark grey green on fresh and weathered surfaces, and is commonly layered. Several 1–2 m wide, strongly deformed layers and lenses of mainly oxide-facies banded iron formation are hosted within the amphibolite (Figure GS2022-2-3b) and are prominently exposed at the northwestern corner of the quarry. Calcsilicate layers up to 2 m wide have also been observed in the layered amphibolite (Figure GS2022-2-3c), largely exposed near the granodiorite contact along the southwestern side of the quarry.

The northern and eastern parts of the quarry are dominated by leucogranite that is coarse grained to pegmatitic and contains up to 10% biotite in aggregates and clots. Along the southeastern side of the quarry, leucogranite includes xenoliths of biotite gneiss interpreted as paragneiss. A southeast-trending (~140°) mafic dike at least 10 m thick transects the eastern part of the quarry (Figure GS2022-2-2).

The northeastern side of the quarry exposes medium- to coarse-grained, layered to banded and commonly folded amphibolite interpreted as retrogressed mafic granulite. This interpretation is based on abundant feldspathic mobilizate and melt pods (Figure GS2022-2-3d). As elsewhere, the amphibolite is injected by leucogranite. A prominent zone of chloritic phyllite a few metres wide marks a brittle-ductile shear zone with locally abundant quartz veining that trends approximately 225° across the quarry. In summary, the rock types exposed at quarry 1 represent a remarkable variety and are similar to the main lithological units along the eastern part of Gull Rapids along strike to the north-northwest (Böhm et al., 2006).

Quarry 9

Quarry 9 is located east-southeast of the Keeyask dam, in an area outlined as basalt on the 1:250 000 scale Precambrian bedrock geology map issued by the Manitoba Geological Survey in 2022 (Figure GS2022-2-1). Detailed mapping of this quarry revealed bedrock consisting almost entirely of foliated, grey, medium- to coarse-grained gneissic granodiorite with schlieren structures (Figure GS2022-2-3e). The gneissic granodiorite locally hosts quartz veins and leucogranitic pegmatite dikes up to 1 m in width. A single 1–2 m wide zone of biotite phyllite trends northwest across the quarry and is interpreted as a minor shear zone. The northeastern corner of the quarry exposes a contact, trending approximately 120°, between a massive diabase dike and gneissic granodiorite. Small diabase offshoots into the gneissic granodiorite suggest the latter to be Archean.

Western end of the south dike road

One exposure of layered felsic gneiss was found about 100 m north of the western termination of the south dike road (Figure GS2022-2-1). The light grey-beige weathered gneiss contains 10–15% fine-grained biotite, mostly along thin seams, and sparse feldspar porphyroclasts up to 4 cm in diameter. The gneiss is interpreted as a granodiorite intrusion and contains up to 20% medium- to coarse-grained quartzofeldspathic mobilizate layers and pods. Gneissosity is steeply dipping and strikes approximately 350°, mimicking the regional fabric of similar felsic intrusive gneisses in the Keeyask dam area.

Looking Back creek

A series of outcrops occur along a ridge dropping off to Looking Back creek, south of the Keeyask dam northern access road (labeled LBC outcrops in Figure GS2022-2-1; the creek is too small to display at the map scale). All exposures along the ridge display highly strained and altered gneiss (Figure GS2022-2-3f), with a main quartzofeldspathic component and up to 30% interlayered mafic bands and lenses. The felsic gneiss layers are greyish green on fresh surfaces, and characteristically tend to weather pale pink to orange. Mafic bands are commonly strongly sheared and resorbed with abundant pale green epidote alteration. Gneissosity and main foliation strike west to northwest. Locally abundant deformed quartz veining follows gneissosity and weaves into east- to southeast-trending shear bands. Gneissic layering commonly varies from a few millimetres to a few centimetres in size. The highly strained gneiss shows abundant intrafolial folding and dextral shearing, representing a major brittle–ductile deformation zone likely subparallel or related to the regional Assean Lake deformation zone.

Future studies

Thick drift cover, from Gull Rapids and extending beyond Provincial Road 280 to the north, blankets bedrock except for a few exposures along Looking Back creek and warrants surficial geological investigations along the northern access road (vast sand deposits) and the lower Nelson River in the Keeyask dam area (high till banks). Surficial mapping and sampling of glacial deposits and erosional features would provide valuable information on the nature, composition and derivation of glacial sediments, including aggregate materials in the region.

Economic considerations

The northwestern Superior craton margin is the site of many exploration targets, most prominently economic nickel in the prolific Thompson nickel belt and shear-hosted gold associated with ancient crust and regional deformation zones at Assean Lake. The extent of the Thompson nickel belt and Assean Lake ancient crust, forming part of the Superior boundary zone, is only partially delineated; the extensions of these zones remain important economic targets. Further mapping along the Superior craton margin contributes to an understanding of the tectonic configuration of this complex zone; it will provide a valuable tool for outlining possible new targets for nickel and gold exploration.

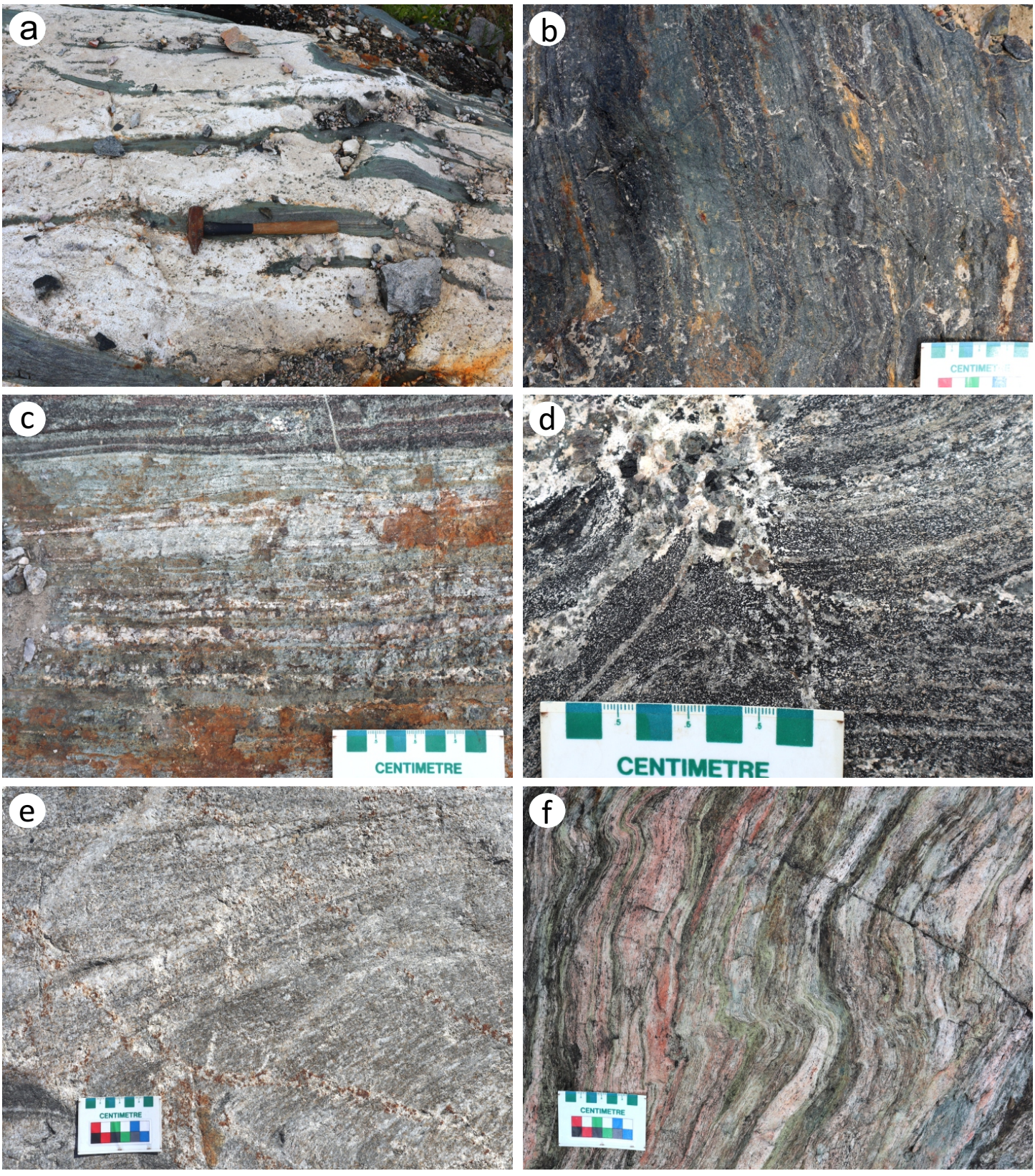

Figure GS2022-2-3: *Outcrop photographs from the Keeyask dam area showing:* ***a)*** *leucogranite with abundant amphibolite rafts (quarry 1);* ***b)*** *layered amphibolite and oxide-facies iron formation (quarry 1);* ***c)*** *pale calcsilicate beds within layered amphibolite (darker amphibolite visible at the top of image; quarry 1);* ***d)*** *amphibolite interpreted as retrogressed mafic granulite (quarry 1);* ***e)*** *gneissic granodiorite (quarry 9); and* ***f)*** *intensely strained gneiss with minor kink bands (near the LBC outcrops shown on Figure GS2022-2-1).*

The formation, emplacement and preservation of diamondiferous kimberlites is broadly controlled by the presence of thick Archean cratonic lithosphere combined with crustal-scale sutures and lineaments (e.g., faults, dike swarms). Geophysical and isotopic investigations (e.g., Böhm et al., 2000; Coyle et al., 2004a, b; Thomas, 2007; Böhm et al., 2008) have proven the existence of ancient crust, regional sutures and dike swarms extending along the Superior boundary zone into the Keeyask dam area. The presence of promising kimberlite-indicator-mineral trends and a greater understanding of ice-flow directions during glaciation has led to northeastern Manitoba being targeted as a likely source for these indicators (e.g., Keller, 2019; Gauthier et al., 2021).

Acknowledgments

The authors thank T. Middleton (Manitoba Hydro) for discussions and generous support of this project.

References

Böhm, C.O., Heaman, L.M., Creaser, R.A. and Corkery, M.T. 1999: Archean tectonic evolution of the northwestern Superior craton margin: U-Pb zircon results from the Split Lake Block; Canadian Journal of Earth Sciences, v. 37, no. 12, p. 1973–1987.

Böhm, C.O., Heaman, L.M., Creaser, R.A. and Corkery, M.T. 2000: Discovery of pre-3.5 Ga exotic crust at the northwestern Superior Province margin, Manitoba; Geological Society of America, Geology, v. 28, no. 1, p. 75–78.

Böhm, C.O., Bowerman, M.S. and Downey, M.W. 2003a: Geology of the Gull Rapids area, Manitoba (part of NTS 54D6); Manitoba Industry, Economic Development and Mines, Manitoba Geological Survey, Preliminary Map PMAP2003-3, scale 1:5000, URL <https://manitoba.ca/iem/info/libmin/PMAP2003-3.zip> [October 2022].

Böhm, C.O., Bowerman, M.S. and Downey, M.W. 2003b: Bedrock mapping in the Gull Rapids area, northern Manitoba (NTS 54D6); *in* Report of Activities 2003, Manitoba Industry, Economic Development and Mines, Manitoba Geological Survey, p. 92–104, URL <https://manitoba.ca/iem/geo/field/roa03pdfs/GS-13.pdf> [October 2022].

Böhm, C.O., Bowerman, M.S. and Downey, M.W. 2006: Bedrock geology of the Gull Rapids area, Manitoba (part of NTS 54D6); Manitoba Science, Technology, Energy and Mines, Manitoba Geological Survey, Open File Report OF2006-32, DVD-ROM, URL <https://manitoba.ca/iem/info/libmin/OF2006-32.zip> [October 2022].

Böhm, C.O., Zwanzig, H.V. and Creaser, R.A. 2008: Sm-Nd isotope technique as an exploration tool: delineating the northern extension of the Thompson nickel belt, Manitoba, Canada; Economic Geology, v. 102, p. 1217–1231.

Bowerman, M.S., Böhm, C.O., Hartlaub, R.P., Heaman, L.M. and Creaser, R.A. 2004: Preliminary geochemical and isotopic results from the Gull Rapids area of the eastern Split Lake Block, northwestern Superior Province, Manitoba (parts of NTS 54D5 and 6); *in* Report of Activities 2004, Manitoba Industry, Economic Development and Mines, Manitoba Geological Survey, p. 156–170, URL <https://manitoba.ca/iem/geo/field/roa04pdfs/GS-14.pdf> [October 2022].

Corkery, M.T. 1975: Gull Rapids; Manitoba Mines, Resources and Environmental Management, Mineral Resources Division, Exploration and Geological Survey Branch, Preliminary Map 1975N-4, scale 1:50 000.

Corkery, M.T. 1985: Geology of the lower Nelson River project area; Manitoba Energy and Mines, Geological Services, Geological Report GR82-1, 66 p., URL <https://manitoba.ca/iem/info/libmin/GR82-1.zip> [October 2022].

Coyle, M., Kiss, F. and Oneschuk, D. 2004a: First vertical derivative of the magnetic field, Gull Rapids, Manitoba (NTS 54D6); Manitoba Industry, Economic Development and Mines, Manitoba Geological Survey, Open File Report OF2004-13, scale 1:50 000, URL <https://manitoba.ca/iem/info/libmin/OF2004-13.pdf> [October 2022].

Coyle, M., Kiss, F. and Oneschuk, D. 2004b: Residual total magnetic field, Gull Rapids, Manitoba (NTS 54D6); Manitoba Industry, Economic Development and Mines, Manitoba Geological Survey, Open File Report OF2004-14, scale 1:50 000, URL <https://manitoba.ca/iem/info/libmin/OF2004-14.pdf> [October 2022].

Downey, M.W., 2005. The structural geology, kinematics and timing of deformation at the Superior craton margin, Gull Rapids, Manitoba; M.Sc. thesis. University of Waterloo, Waterloo, Ontario, 131 p.

Downey, M.W., Lin, S. and Böhm, C.O. 2004: New insights into the structural geology and timing of deformation at the Superior craton margin, Gull Rapids, Manitoba (NTS 54D6); *in* Report of Activities 2004, Manitoba Industry, Economic Development and Mines, Manitoba Geological Survey, p. 171–186, URL <https://manitoba.ca/iem/geo/field/roa04pdfs/GS-15.pdf> [October 2022].

Downey, M.W., Lin, S., Böhm, C.O. and Rayner, N.M. 2009: Timing and kinematics of crustal movement in the Northern Superior superterrane: insights from the Gull Rapids area of the Split Lake Block, Manitoba; Precambrian Research, v. 168, p. 134–148.

Gauthier, M.S., Breckenridge, A. and Hodder, T.J. 2021: Patterns of ice recession and ice stream activity for the MIS 2 Laurentide Ice Sheet in Manitoba, Canada; Boreas, v. 51, no. 2, p. 274–298.

Hartlaub, R.P. and Kuiper, Y.D. 2004: Geology of central and north Split Lake, Manitoba (parts of NTS 54D4, 5, 6 and 64A1, 8); Manitoba Industry, Economic Development and Mines, Manitoba Geological Survey, Preliminary Map PMAP2004-1, scale 1:25 000, URL <https://manitoba.ca/iem/info/libmin/PMAP2004-1.pdf> [October 2022].

Hartlaub, R.P., Heaman, L.M., Böhm, C.O. and Corkery, M.T. 2003: Split Lake Block revisited: new geological constraints from the Birthday to Gull rapids corridor of the lower Nelson River (NTS 54D5 and 6); *in* Report of Activities 2003, Manitoba Industry, Economic Development and Mines, Manitoba Geological Survey, p. 114–117, URL <https://manitoba.ca/iem/geo/field/roa03pdfs/GS-15.pdf> [October 2022].

Hartlaub, R.P., Böhm, C.O., Kuiper, Y.D., Bowerman, M.S. and Heaman, L.M. 2004: Archean and Paleoproterozoic geology of the northwestern Split Lake Block, Superior Province, Manitoba (parts of NTS 54D4, 5, 6 and 64A1); *in* Report of Activities 2004, Manitoba Industry, Economic Development and Mines, Manitoba Geological Survey, p. 187–194, URL <https://manitoba.ca/iem/geo/field/roa04pdfs/GS-16.pdf> [October 2022].

Haugh, I. 1969: Gull Rapids–Moose Lake, Manitoba Mines and Natural Resources, Mines Branch, Preliminary Map 1969C-1, scale 1:31 680.

Haugh, I. and Elphick, S.C. 1968: Kettle Rapids–Moose Lake area; *in* Summary of Geological Fieldwork 1968, Manitoba Mines and Natural Resources, Mines Branch, Geological Paper GP 3/68, p. 29–37, URL <https://manitoba.ca/iem/info/libmin/GP3-68.pdf> [October 2022].

Keller, G.R. 2019: Manitoba Kimberlite Indicator Mineral Database (version 3.2); Manitoba Growth, Enterprise and Trade, Manitoba Geological Survey, zipped Microsoft® Access® 2016 database, URL <https://manitoba.ca/iem/geo/diamonds/MBKIMDB_32.zip> [September 2022].

Kuiper, Y.D. and Lin, S. 2004a: Structural geology of the Aiken River deformation zone, Manitoba (parts of NTS 64A1 and 2); Manitoba Industry, Economic Development and Mines, Manitoba Geological Survey, Preliminary Map PMAP2004-3, scale 1:50 000, URL <https://manitoba.ca/iem/info/libmin/PMAP2004-3.pdf> [October 2022].

Kuiper, Y.D. and Lin, S. 2004b: Structural geology of the Aiken River deformation zone, York Landing area, Manitoba (part of NTS 64A1); Manitoba Industry, Economic Development and Mines, Manitoba Geological Survey, Preliminary Map PMAP2004-4, scale 1:20 000, URL <https://manitoba.ca/iem/info/libmin/PMAP2004-4.pdf> [October 2022].

Kuiper, Y.D., Lin, S., Böhm, C.O. and Corkery, M.T. 2003: Structural geology of the Assean Lake and Aiken River deformation zones, northern Manitoba (NTS 64A1, 2 and 8); *in* Report of Activities 2003, Manitoba Industry, Economic Development and Mines, Manitoba Geological Survey, p. 105–113, URL <https://manitoba.ca/iem/geo/field/roa03pdfs/GS-14.pdf> [October 2022].

Kuiper, Y.D., Lin, S., Böhm, C.O. and Corkery, M.T. 2004: Structural geology of the Aiken River deformation zone, Manitoba (NTS 64A1 and 2); *in* Report of Activities 2004, Manitoba Industry, Economic Development and Mines, Manitoba Geological Survey, p. 201–208, URL <https://manitoba.ca/iem/geo/field/roa04pdfs/GS-18.pdf> [October 2022].

Manitoba Geological Survey 2022: New edition of the 1:250 000 scale Precambrian bedrock geology compilation map of Manitoba; Manitoba Natural Resources and Northern Development, Manitoba Geological Survey, GeoFile 3-2022, scale 1:250 000, URL <https://manitoba.ca/iem/info/libmin/geofile3-2022.zip> [October 2022].

Thomas, M.D. 2007: Magnetic domains in the area of the Assean Lake high resolution aeromagnetic survey: a new perspective on regional geology; Geological Survey of Canada, Open File 5507, 29 p.

GS2022-3

Bedrock mapping in the Halfway Lake area, Thompson nickel belt, central Manitoba (parts of NTS 63O1, 2)

by C.G. Couëslan

In Brief:

- A new bedrock mapping project was initiated at Halfway Lake, in the southern Thompson nickel belt
- Two sedimentary associations were identified: a calcsilicate-semipelite assemblage, and a quartzite-pelite assemblage
- A mineralized ultramafic body is known to be associated with the calcsilicate-semipelite assemblage, and sulphidic pelite layers in the quartzite-pelite assemblage could be viable sources of sulphur for intruding ultramafic magmas and the generation of Ni-Cu sulphide deposits

Citation:
Couëslan, C.G. 2022: Bedrock mapping in the Halfway Lake area, Thompson nickel belt, central Manitoba (parts of NTS 63O1, 2); *in* Report of Activities 2022, Manitoba Natural Resources and Northern Development, Manitoba Geological Survey, p.12–24.

Summary

A new bedrock mapping project was initiated by the Manitoba Geological Survey at Halfway Lake, 80 km south-southwest of Thompson, in the Thompson nickel belt (TNB). Several mineralized ultramafic bodies are known to underlie the lake. The aim of the project is to update mapping with respect to Ospwagan group stratigraphy and to search for possible Paint sequence rocks. Much of the lake is underlain by Archean orthogneiss with rare metre-scale screens of Archean metasedimentary rocks. A large granite–tonalite intrusion of uncertain age occurs along roughly 12 km of the western shoreline. The intrusion is characterized by the presence of disseminated, pinhead-sized garnet. A calcsilicate-semipelite assemblage occurs at the north end of a bay in east-central Halfway Lake. This assemblage is tentatively correlated with the Thompson formation of the Ospwagan group. Outcrops of quartzite-pelite assemblage rocks occur throughout the Halfway Lake area and could be correlative with the upper stratigraphy of the Ospwagan group, or possibly the Garand quartzite of the Paint sequence. Mafic volcanic rocks occur along a 12 km strike length in south-central Halfway Lake and are tentatively correlated with the Bah Lake assemblage of the Ospwagan group. The volcanic rocks are intruded by an irregular body, or several bodies, of foliated granite. A quartz monzonite intrusion with a strike length of approximately 14 km occurs along the southeastern shoreline of the lake.

The majority of rocks in the Halfway Lake area are characterized by a northeast-trending, subvertical S_2 gneissosity, with the exception of later granitoid intrusions. The gneissosity is folded by upright, northeast- and southwest-plunging isoclinal F_3 folds. The isoclinal folds are accompanied by an axial-planar S_3 foliation. Sinistral, mylonitic shear zones commonly occur along the limbs of major fold structures and are subparallel to S_3. Upper-amphibolite–facies mineral assemblages in pelitic rocks suggest that peak metamorphism outlasted D_2 and continued until at least early D_3.

Current models for the generation of Ni-Cu deposits in the TNB call for the intrusion of ultramafic magmas into sulphidic Ospwagan group rocks, leading to sulphur saturation of the magma and the precipitation and concentration of Ni-Cu sulphides. Ultramafic bodies at Halfway Lake are associated with both the calcsilicate-semipelite and quartzite-pelite assemblages. The presence of sedimentary sulphide within the quartzite-pelite assemblage, including metre-scale beds of sulphidic pelite, indicate that it could be a viable source of sulphur for an intruding ultramafic magma and the generation of Ni-Cu sulphides. A mineralized ultramafic body associated with the calcsilicate-semipelite assemblage was the focus of exploration between 1992 and 2008. Similar metamorphic grade, and structural and mineralization styles as found at the Thompson mine, suggest that exploration targeting F_3 fold structures for thickened zones of sulphide in hinge zones, and mineralization hosted by metasedimentary rocks rather than by intrusions, could be viable strategies in the Halfway Lake area.

Introduction

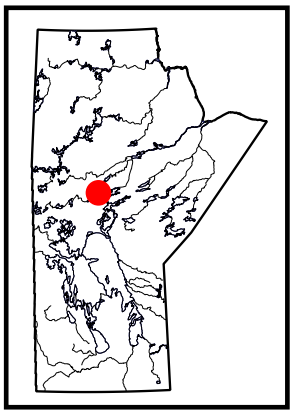

Halfway Lake is located 80 km south-southwest of Thompson in the southern Thompson nickel belt (TNB; Figure GS2022-3-1). It is situated between Provincial Highway 6 and the Hudson Bay Railway line. The Halfway Lake area has been the focus of airborne and ground geophysical surveys, diamond drilling and outcrop mapping by various companies from 1958 to present, and several ultramafic bodies have been delineated underlying the lake (Macek et al., 2006; Griffin et al., 2012). Current mineral dispositions in the Halfway Lake area are held by Anglo American plc, CanAlaska Uranium Ltd., CaNickel Mining Ltd. and Vale Canada Ltd. (Manitoba Mineral Resources, 2013). Shoreline mapping by the MGS was last conducted on Halfway Lake in 1980 (Macek, 1980; Macek and Scoates, 1980), prior to the formal definition of the Ospwagan group stratigraphy and Paint sequence rocks (Bleeker and Macek, 1988; Bleeker, 1990; Zwanzig et al., 2007; Couëslan, 2016, 2022b). The geology of the area was updated in 2006 by correlating the shoreline mapping with the Ospwagan group stratigraphy and incorporating drillcore and geophysical data (Macek et al., 2006).

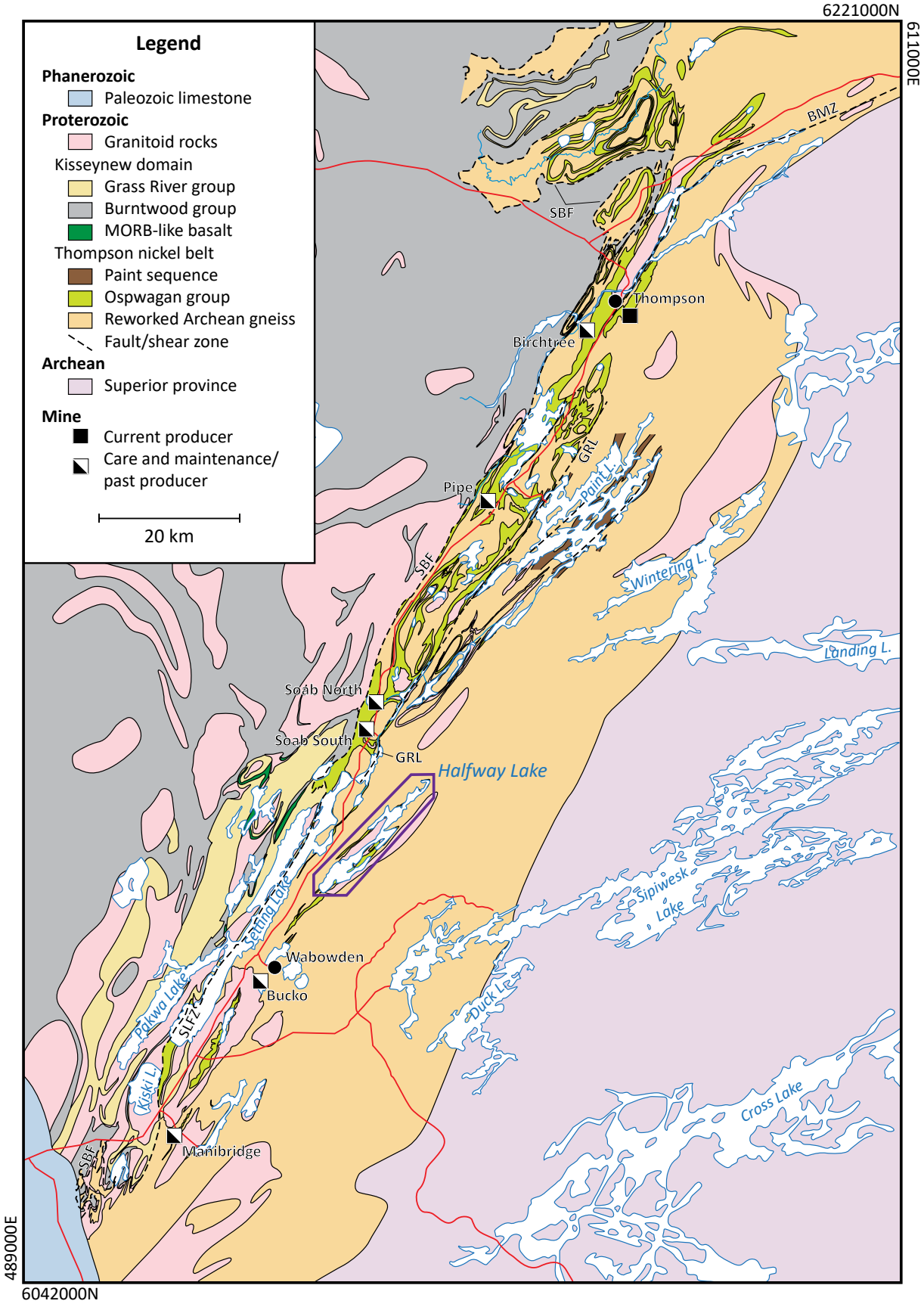

Figure GS2022-3-1: *Simplified geological map of the Thompson nickel belt, central Manitoba (modified from Macek et al., 2006; Couëslan, 2016). Purple outline indicates the location of the study area. Abbreviations: BMZ, Burntwood mylonite zone; GRL, Grass River lineament; SBF, Superior boundary fault; SLFZ, Setting Lake fault zone.*

A new bedrock-mapping project was initiated at Halfway Lake in July of 2022. Mapping was conducted at a scale of 1:20 000 utilizing the stratigraphic framework for the Thompson nickel belt. The goal of the project is to update mapping with respect to the Ospwagan group stratigraphy, and to characterize the mafic rocks of southeastern Halfway Lake, which are believed to be correlative with the Bah Lake assemblage. In addition, a search was made for possible Paint sequence rocks misidentified as Archean basement gneiss or as 'ghost successions' of the Ospwagan group (Zwanzig et al., 2007).

Regional geology

The TNB forms a segment of the Superior boundary zone, flanked to the northwest by the Kisseynew domain of the Trans-Hudson orogen and to the southeast by the Pikwitonei granulite domain (PGD) of the Superior craton. The TNB is underlain largely by reworked Archean gneiss of the Superior craton, which is typically quartzofeldspathic with enclaves of mafic to ultramafic rock; clearly recognizable paragneiss is rare. It is commonly migmatitic and characterized by complex internal structures that are the result of multiple generations of Archean and Paleoproterozoic deformation and metamorphism. The gneiss is interpreted to be derived from the adjacent PGD, which was subjected to amphibolite- to granulite-facies metamorphic conditions from ca. 2720 to 2640 Ma (Hubregtse, 1980; Mezger et al., 1990; Heaman et al., 2011; Guevara et al., 2020; Couëslan, 2021). The granulites of the PGD were exhumed and unconformably overlain by the Paleoproterozoic supracrustal rocks of the Ospwagan group and Paint sequence prior to intrusion of the Molson dike swarm and associated ultramafic intrusions at ca. 1880 Ma (Bleeker, 1990; Zwanzig et al., 2007; Heaman et al., 2009; Scoates et al., 2017). The Archean basement gneiss and Proterozoic supracrustal rocks were subjected to multiple generations of deformation, and metamorphic conditions ranging from middle-amphibolite facies to lower-granulite facies, during the Trans-Hudson orogeny (Bleeker, 1990; Burnham et al., 2009; Couëslan and Pattison, 2012).

The dominant phase of penetrative deformation is D_2, which affected the Ospwagan group, Paint sequence and ca. 1880 Ma magmatic rocks. This deformation phase resulted in the formation of F_2 nappe structures, which incorporated the underlying Archean gneiss. The nappe structures have been interpreted as either east verging (Bleeker, 1990; White et al., 2002) or southwest verging (Zwanzig et al., 2007; Burnham et al., 2009). The recumbent folds are associated with regionally penetrative S_2 fabrics. The D_2 phase of deformation is interpreted to be the result of convergence between the Superior craton margin and the Reindeer zone of the Trans-Hudson orogen from ca. 1830 to 1800 Ma. The D_3 phase of deformation resulted in isoclinal folds with vertical to steeply southeast-dipping axial planes (Bleeker, 1990; Burnham et al., 2009). Mylonite zones with subvertical stretching lineations parallel many of the regional F_3 folds. Tightening of D_3 structures continued during D_4, marked by localized retrograde greenschist-facies metamorphism along northeast-striking, mylonitic and cataclastic shear zones that commonly record southeast-side-up sinistral movement (Bleeker, 1990; Burnham et al., 2009). The geometry of metamorphic-field gradients in the belt are primarily controlled by regional D_3–D_4 structures (Couëslan and Pattison, 2012).

Ospwagan group stratigraphy

The following summary of the Ospwagan group is sourced largely from Bleeker (1990) and Zwanzig et al. (2007). The Paleoproterozoic Ospwagan group unconformably overlies Archean basement gneiss in the TNB (Figure GS2022-3-2). The lowermost unit of the Ospwagan group is the Manasan formation, which is made up of two members: the lower M1 member, consisting of layered to laminated sandstone with local conglomerate layers near the base; and the overlying M2 member, consisting of semipelitic rock. The Manasan formation is interpreted as a transgressive, fining-upward sequence deposited along a passive margin. This siliciclastic system grades into the overlying calcareous sedimentary rocks of the Thompson formation.

The Thompson formation consists of three members: the T1 member comprises a variety of calcareous–siliceous rocks, including chert, calcsilicate and impure marble; the T2 member is a semipelitic calcareous gneiss that is rarely present; and the T3 member consists of impure dolomitic marble with local horizons of calcsilicate. The Thompson formation represents a transition from a siliciclastic-dominated to a carbonate-dominated system.

The Pipe formation is subdivided into three members. The P1 member consists of a graphite-rich, sulphide-facies iron formation at the base (the locus of the Pipe II and Birchtree orebodies), overlain by a silicate-facies iron formation. The top of the P1 member consists of a reddish, laminated, siliceous rock. The P1 member grades into the overlying pelitic rocks of the P2 member, the top of which is marked by a sulphide-facies iron formation (the locus of the Thompson orebody). The overlying P3 member consists of a wide variety of rock types, including laminated, siliceous sedimentary rocks; silicate-, carbonate- and local oxide-facies iron formations; and semipelitic rocks, calcsilicate and a local horizon of relatively pure dolomitic marble. The Pipe formation represents a mix of chemical sediments and fine to very fine siliciclastics that were deposited in either an open-marine environment (Zwanzig et al., 2007) or during the development of a foredeep basin (Bleeker, 1990).

The Setting formation is divided into two members and is defined to include all siliciclastic rocks above the uppermost iron formation of the P3 member. The S1 member consists of rhythmically interbedded quartzite and pelitic schist with local garnet-rich pods, which are interpreted as calcareous concretions and are characteristic of the S1 member. The S2 member consists of thickly layered greywacke, with local horizons grading from conglomeratic at the base to pelitic at the top. No contact has been observed between the S1 and S2 members. It is

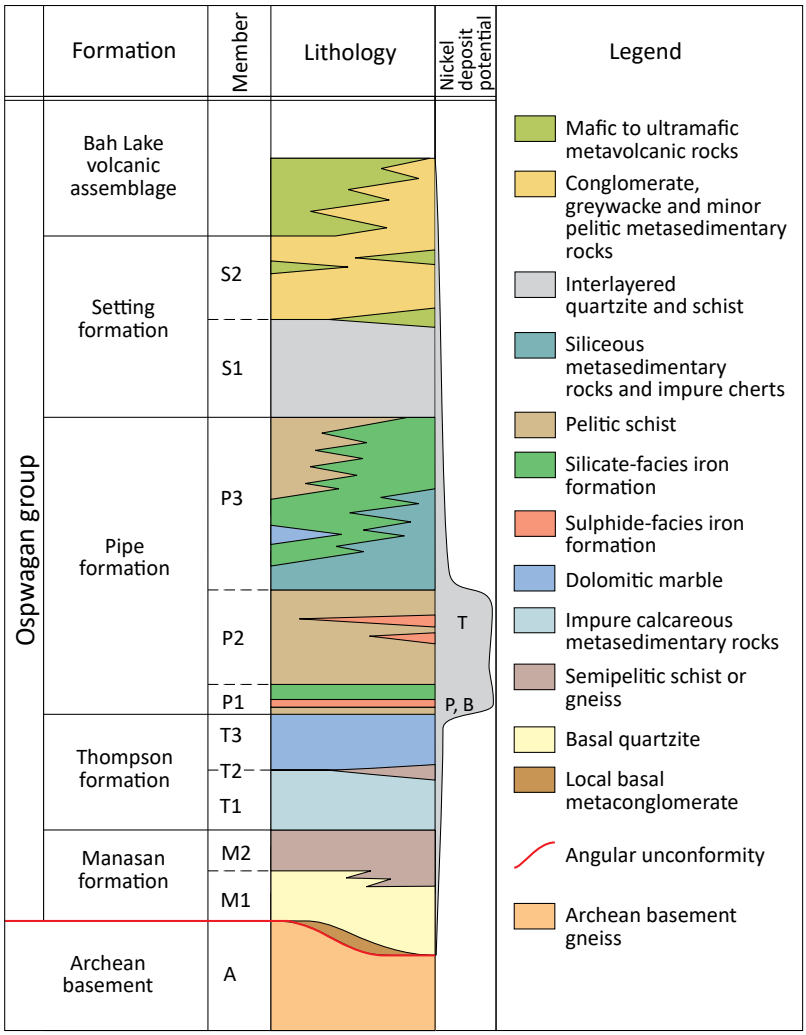

Figure GS2022-3-2: *Schematic lithostratigraphic section of the Ospwagan group (modified from Bleeker, 1990). Abbreviations: B, stratigraphic location of the Birchtree orebody; P, stratigraphic location of the Pipe II orebody; T, stratigraphic location of the Thompson orebody.*

possible that they represent a lateral facies change as opposed to a vertical succession. The Setting formation is interpreted as turbidite deposits in a relatively deep-marine environment, possibly a foredeep basin (Bleeker, 1990). The coarse clastic material and thick turbidite bedding of the S2 member may record the shallowing of the basin, the onset of active tectonism or a lateral sedimentary facies change to a submarine-channel or upper-fan environment (Zwanzig et al., 2007).

At the top of the Ospwagan group is the Bah Lake assemblage, which consists of mafic to ultramafic volcanic rocks dominated by massive to pillowed basalt flows with local picrite and minor synvolcanic intrusions. The Bah Lake assemblage is dominated by a high-Mg suite, similar to normal mid-ocean–ridge basalt (N-MORB), which occurs throughout much of the main TNB; and an incompatible-element–enriched suite, similar to enriched mid-ocean–ridge basalt (E-MORB), that occurs in the northwestern Setting Lake area and along the margin of the Kisseynew domain (Zwanzig, 2005). The enriched suite is interpreted to overlie the high-Mg suite; however, it is uncertain if this represents a stratigraphic or tectonic relationship. The Bah Lake assemblage may suggest the onset of active rifting in the TNB (Zwanzig, 2005; Zwanzig et al., 2007), or that the foredeep was magmatically active (Bleeker, 1990).

A maximum age for the Ospwagan group is provided by a ca. 1974 Ma zircon recovered from Setting formation greywacke (Bleeker and Hamilton, 2001); however, inherited zircons younger than ca. 2600 Ma are rare. A minimum age is provided by crosscutting amphibolitized dikes interpreted to be part of the Molson dike swarm, and the possibly comagmatic Ni-ore–bearing ultramafic sills, that intruded the Ospwagan group at all stratigraphic levels at ca. 1880 Ma (Bleeker, 1990; Heaman et al., 2009; Scoates et al., 2017). Ospwagan group rocks yield crustal-residence Nd-model ages of ca. 3.22–2.82 Ga, which is typically younger than model ages obtained from the Archean basement (ca. 3.70–3.14 Ga; Böhm et al., 2007).

Granulite-facies assemblages in semipelitic and pelitic rocks of the Ospwagan group can become almost indistinguishable from the Archean basement gneiss; however, petrological end members such as marble, quartzite and iron formation remain recognizable at the highest metamorphic grades and can be used

as marker horizons. Basement-like gneiss or migmatite successions between isolated but still recognizable marker horizons may represent 'ghost successions' of the Ospwagan group (Zwanzig et al., 2007). Distinguishing Archean from Ospwagan group rocks at high metamorphic grade may require the use of lithogeochemistry or Sm-Nd isotope geochemistry (Böhm et al., 2007; Zwanzig et al., 2007).

Paint sequence rocks

The Paint sequence occurs as three northeast-striking belts of metasedimentary rocks in the Paint Lake area (Figure GS-2022-3-1) and continues southwest along strike to the Phillips Lake area (Couëslan, 2016, 2022b). To date, the sequence has only been recognized east of the Grass River lineament in areas of granulite-facies metamorphism where primary textures and structures are all but obliterated save for centimetre-scale compositional layering. The Paint sequence is subdivided into two lithological packages. The Klippen wacke is the most widespread member of the sequence and is characterized by centimetre- to metre-thick layering of more mud-rich and more sand-rich beds. Pods of in-situ and in-source leucosome are abundant. Outcrops of wacke are characterized by rusty weathered surfaces because of the presence of minor but ubiquitous pyrrhotite. Rare flakes of molybdenite can be present. The wacke contains subordinate interbeds of iron formation as discontinuous layers and lenses <3 m thick. Iron formations are typically of the silicate facies; however, significant pyrrhotite and magnetite can be present. The Garand quartzite is not as widely distributed and is only exposed at Paint Lake. It consists of interbedded quartzite and pelite with rare garnet-rich pods, which are interpreted as concretions. The pelite contains abundant graphite and pyrrhotite, and is characterized by rusty weathered surfaces. The stratigraphic relationships between the Klippen wacke and Garand quartzite, and the Paint sequence and Ospwagan group, are unknown.

A maximum age for the Klippen wacke is provided by five ca. 1970 Ma detrital zircon grains (Couëslan, 2022b) present in samples from both Paint and Phillips lakes. The Paint sequence rocks are intruded by relatively straight-walled mafic dikes, which are tentatively interpreted to be part of the Molson dike swarm, suggesting a minimum age of ca. 1880 Ma for the sequence. The Paint sequence rocks differ from the Ospwagan group rocks in having a significant detrital zircon component younger than ca. 2600 Ma, a wider range of crustal-residence Nd-model ages (ca. 3.57–2.92 Ga), and unique trace-element compositions (Couëslan, 2016, 2022b). Paint sequence rocks have been misidentified as part of the Archean basement and as ghost successions of Ospwagan group rocks.

Geology of the Halfway Lake area

Bedrock exposures in the Halfway Lake area are limited by extensive Quaternary deposits. The majority of outcrop occurs along the lakeshore and varies from poor to excellent in quality (Macek and Scoates, 1980). The Halfway Lake area is interpreted to be underlain by several highly attenuated dome-and-basin–like structures of Ospwagan group rocks (Macek et al., 2006; Burnham et al., 2009). The structures are enclosed by Archean basement gneiss and interpreted to have Manasan formation at the margins and Pipe formation or Bah Lake assemblage in the cores. Ultramafic rocks are present within all of these structures and are hosted predominantly at the top of the Manasan formation, or within the Pipe formation (Macek et al., 2006). A mineralized ultramafic body in the east-central part of the lake has been the focus of the majority of exploration in the Halfway Lake area (cf. 'Economic considerations'; Griffin et al., 2012; Assessment Files 72495 and 74607, Manitoba Natural Resources and Northern Development, Winnipeg).

Most of the Ospwagan group rocks underlie the lakebed, but the compilation mapping of Macek et al. (2006) indicates shoreline exposures throughout the area, including a 7 km long zone of Bah Lake assemblage rocks in the south-central part of the lake. A large garnet-bearing granite intrusion outcrops along the west shore of the lake (Assessment File 99528; Macek et al., 2006), and hornblende monzonite outcrops along much of the southeast shore in the Clarence Evans Bay area (Macek et al., 2006). The majority of shoreline outcrops consist of Archean basement gneiss. The Archean basement gneiss consist of grey hornblende-biotite gneiss, and migmatitic multicomponent gneiss (Macek and Scoates, 1980). The Halfway Lake area is believed to have attained upper-amphibolite–facies conditions during the Trans-Hudson orogeny (Couëslan and Pattison, 2012). The compilation work of Macek et al. (2006) suggests the presence of ghost succession Ospwagan Group rocks in the southern Halfway Lake area.

Results of 2022 mapping

Mapping during the 2022 field season was restricted to the lakeshore. Inland and underwater geology in Figure GS2022-3-3 is largely interpreted and modified from Macek et al. (2006). In several parts of the lake, shoreline observations were difficult to reconcile with previous mapping. In general, the extent of Ospwagan group exposures on Halfway Lake appears to be less than that indicated by previous compilation work. It is hoped that future study of archived drillcore will help to resolve some of these issues. All rock units described below, with the possible exception of the latest intrusive rocks, were metamorphosed to at least amphibolite-facies conditions. To improve the readability of the text, the 'meta-' prefix has been omitted from rock names.

Archean rocks

Archean orthogneiss, undivided

Much of the Halfway Lake area is underlain by tonalitic to granodioritic rocks with a well-developed gneissosity (Figure GS2022-3-4a). The gneissic rocks are typically grey to pinkish grey, medium to coarse grained, foliated to strongly foliated,

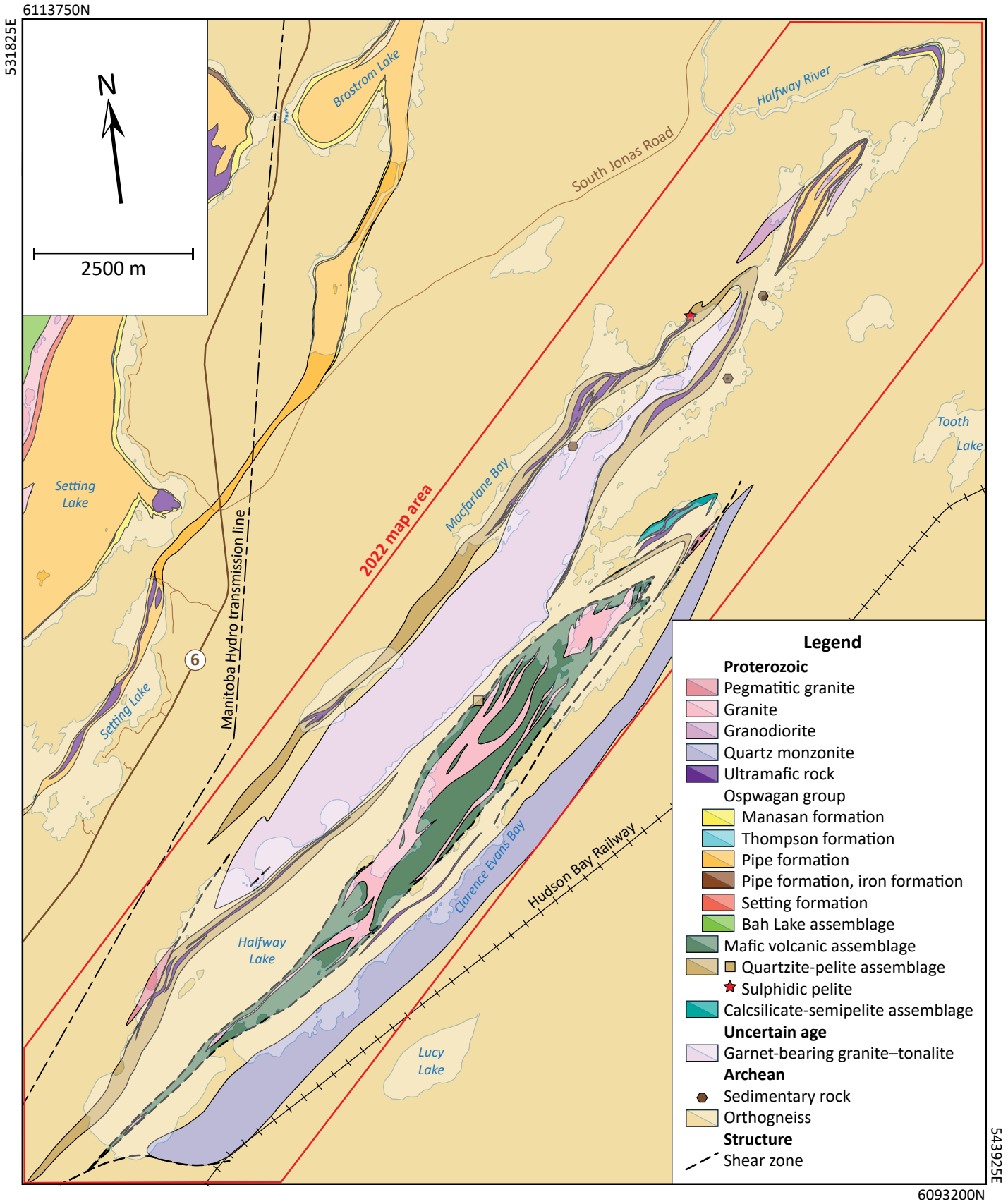

Figure GS2022-3-3: *Bedrock geology map of the Halfway Lake area, central Manitoba (simplified from Couëslan, 2022a). Lighter shade of a colour indicates a body of water. Geology outside of the 2022 map area is from Macek et al. (2006).*

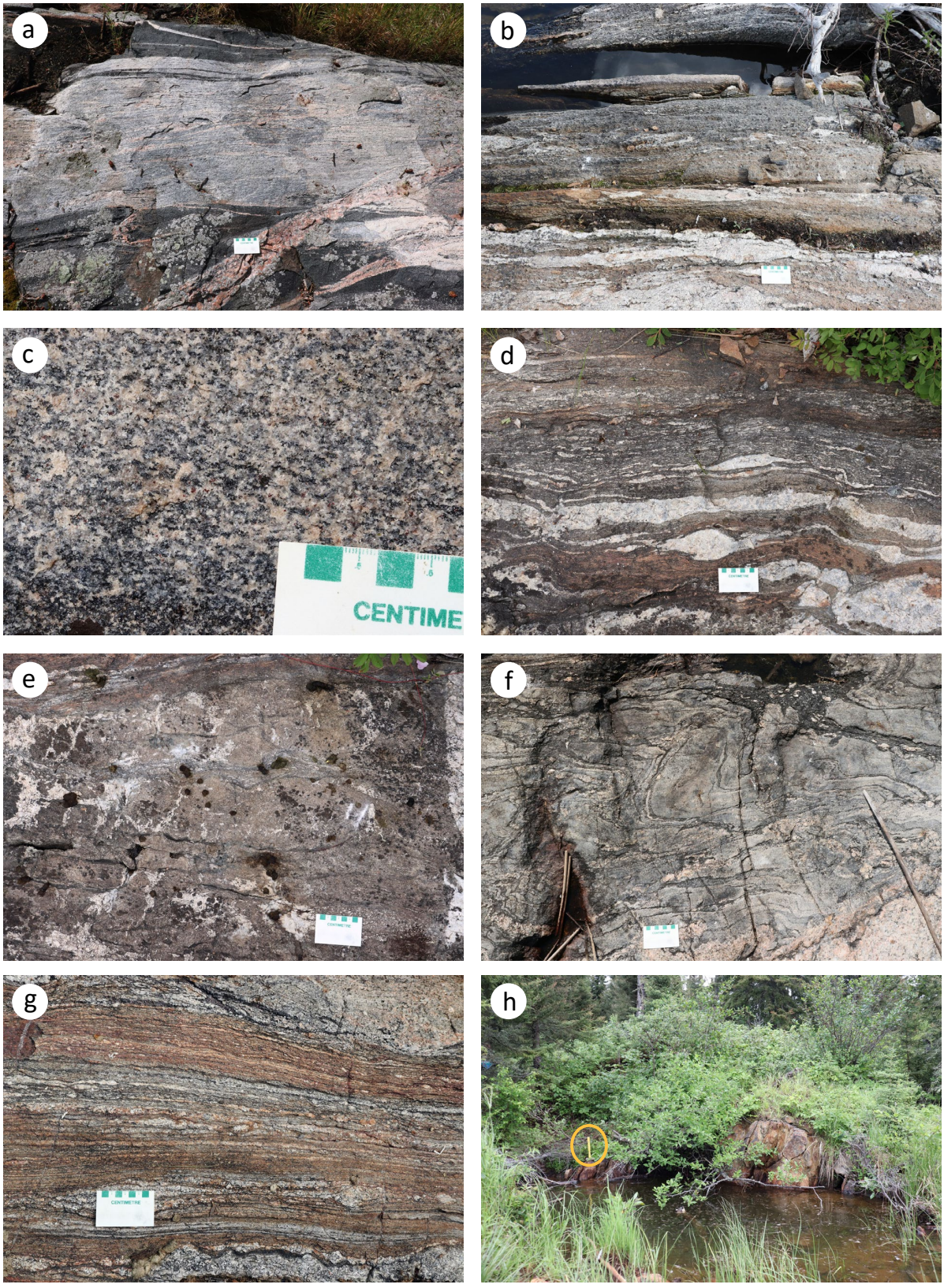

Figure GS2022-3-4: *Outcrop images from Halfway Lake:* ***a)*** *Archean biotite orthogneiss with discontinuous layers of plagioclase amphibolite (interpreted as diabase dikes) and crosscut by pegmatitic granite dikes;* ***b)*** *Archean sedimentary rock, likely derived from wacke;* ***c)*** *garnet-hornblende granodiorite–tonalite of uncertain age with garnet occurring as pinhead-sized grains in the groundmass;* ***d)*** *tremolite-bearing semipelite and* ***e)*** *calc-silicate from the calcsilicate-semipelite assemblage;* ***f)*** *quartzite with pelite laminations from the quartzite-pelite assemblage, the rocks are folded by F_3 minor folds and an intrusion of pegmatitic granite is present in the lower right corner;* ***g)*** *high-strain wacke interlayered with quartzite from the quartzite-pelite assemblage;* ***h)*** *graphitic and sulphidic pelite from the quartzite-pelite assemblage in an outcrop that is approximately 5 m wide (circled hammer for scale).*

and locally magnetic. They are most commonly biotite bearing, but can contain hornblende in place of, or in addition to, biotite. Biotite and hornblende typically form discontinuous, mafic-rich laminations separated by quartzofeldspathic layers; however, alternating mafic and felsic layers <4 cm thick can also occur. Garnet is relatively common, but generally makes up <3% of the rock and occurs as dark red grains randomly distributed throughout the groundmass. Magnetite locally occurs in trace amounts. Local, diffuse, hornblende-rich bands <20 cm thick could represent Archean mafic dikes. Local granitic to granodioritic pods and discontinuous layers <20 cm thick could represent attenuated leucosome.

Archean sedimentary rocks

Several outcrops in northern Halfway Lake consist of discrete, metre-scale screens of sedimentary rock surrounded by Archean orthogneiss (Figures GS2022-3-3 and GS2022-3-4b). The screens are quartzofeldspathic, with 10–30% biotite and either minor garnet or cummingtonite with trace amounts of garnet, and were likely derived from wacke. They are characterized by compositional layering on a scale of <20 cm. Local rusty layers <10 cm thick contain up to 5% pyrrhotite. These sedimentary rocks are interpreted as Archean because they are of limited extent and enclosed by Archean orthogneiss.

Rocks of uncertain age

Garnet-bearing intrusion

A garnet-bearing intrusion approximately 12 km long occurs along much of the western shoreline of Halfway Lake (Figure GS2022-3-3). The intrusion consists largely of garnet-biotite granite–granodiorite but grades into garnet-hornblende granodiorite–tonalite toward the northeast. The granite–granodiorite is pink to pinkish grey, whereas the granodiorite–tonalite is pinkish grey to grey weathering and beige on fresh surfaces (Figure GS2022-3-4c). Both phases are coarse grained, foliated, locally magnetic and locally gneissic, with either diffuse biotite laminations or flattened clots of hornblende that give the rock a spotted appearance. Red garnet typically occurs in trace amounts as fine, pinhead-sized grains. Trace amounts of magnetite occur in the groundmass; however, local pods of leucosome <15 cm thick can contain 3–5% magnetite. The leucosome is commonly attenuated and forms discontinuous bands in the rock. The granodiorite–tonalite is locally intruded by pegmatite dikes that contain prismatic hornblende up to 3 cm long. The garnet-bearing intrusion is tentatively interpreted as Archean because of the weakly developed gneissosity and presence of leucosome; however, it could be a pre-D_2 intrusion similar to the ca. 1885 Ma Clarke Lake pluton east of the former Manibridge mine (Percival et al., 2005).

Paleoproterozoic rocks

Calcsilicate-semipelite assemblage

The calcsilicate-semipelite assemblage outcrops at the northern end of a bay in east-central Halfway Lake (Figure GS2022-3-3). This sedimentary rock assemblage consists of semipelite and calcsilicate intercalated on a metre to sub-metre scale. The semipelite forms a coarse-grained, foliated to strongly foliated diatexite that is grey to rusty brown weathering and purplish brown to brown-grey on fresh surfaces (Figure GS2022-3-4d). It is relatively calcareous, with 10–20% diopside or tremolite and 10–20% biotite in a quartzofeldspathic groundmass. Minor pyrrhotite is locally present. The calcsilicate is brown weathering and grey-green on fresh surfaces. It varies from medium to coarse grained and from massive to foliated, and is locally magnetic. It is diopside and quartz rich, with minor biotite and carbonate and trace to minor amounts of pyrrhotite. The calcsilicate is internally layered with alternating biotite-rich and diopside-rich strata <15 cm thick (Figure GS2022-3-4e), and it can contain discontinuous layers of marble <5 cm thick. The marble is white, medium to coarse grained and foliated. It is diopside rich with minor serpentinized olivine and phlogopite, and trace amounts of pyrrhotite and a mineral tentatively identified as titanite or possibly a member of the humite group. The semipelite-calcsilicate assemblage is tentatively correlated with the Thompson formation of the Ospwagan group.

Quartzite-pelite assemblage

Outcrops of the quartzite-pelite assemblage occur scattered throughout the Halfway Lake area (Figure GS2022-3-3). The assemblage consists of quartzite with subordinate wacke and sulphidic pelite. The majority of outcrops are dominated by quartzite; however, the wacke and sulphidic pelite can be dominant. The quartzite is light grey weathering and beige on fresh surfaces. It is medium to coarse grained and foliated, and contains 10–20% plagioclase with minor biotite and pink–violet garnet, and trace amounts of pyrrhotite. The quartzite occurs as layers <1 m thick separated by pelitic laminations <1 cm thick (Figure GS2022-3-4f), which contain garnet, sillimanite, biotite, graphite and sulphide. The pelitic laminations are commonly associated with a rusty orange staining of the outcrop. The quartzite contains local layers of wacke <1 m thick and rare, fine-grained, garnet-rich pods or 'concretions' <3 cm thick.

The wacke, or quartz-rich pelite, is grey-brown to rusty orange, medium to coarse grained and foliated to protomylonitic. It typically consists of interlayered quartz-rich and biotite-rich laminations and contains minor pink–violet garnet and local sillimanite and graphite. The prevalence of orange weathering suggests the ubiquitous presence of disseminated pyrrhotite (Figure GS2022-3-4g). In the rare instances where the wacke is the dominant rock in outcrop, it contains beds of internally layered to laminated quartzite <30 cm thick. The wacke commonly contains discontinuous layers of leucosome <10 cm thick and boudinaged

layers of plagioclase amphibolite <50 cm thick, which are locally garnet bearing.

The sulphidic and graphitic pelite is rusty weathering and brown-grey on fresh surfaces. It is coarse grained, strongly foliated and magnetic. The rock forms a quartzofeldspathic diatexite with 10–20% biotite, 10–12% sillimanite, 3–5% pyrrhotite, 3–5% graphite and trace amounts of pink–violet garnet. In northern Halfway Lake, the pelite forms a gossanous outcrop approximately 5 m wide that disappears beneath overburden in both directions across strike (Figure GS2022-3-4h).

The affinity of the quartzite-pelite assemblage is uncertain. The presence of minor iron formation in the assemblage was interpreted from geophysics and drillcore by Macek et al. (2006), which led them to correlate these rocks with the Pipe formation of the Ospwagan group. However, no chemical sedimentary rocks were observed during the course of mapping, which would argue against correlation with the Pipe formation. The quartzite-pelite assemblage is lithologically most similar to the Setting formation rocks of the Ospwagan group, with the sulphidic pelite possibly representing a sliver of the P2 member pelite of the Pipe formation. Alternatively, it could be correlative with the Garand quartzite of the Paint sequence. It is hoped that lithogeochemical and isotopic analyses will provide additional insight.

Mafic volcanic assemblage

Outcrops of plagioclase amphibolite, which are interpreted to be of mafic volcanic origin, occur along a strike length of approximately 12 km and underlie much of a long peninsula in south-central Halfway Lake (Figure GS2022-3-3). The mafic volcanic rocks are dark grey-green, medium to coarse grained and foliated. The rocks are hornblende and plagioclase rich, with <20% clinopyroxene, local biotite and trace amounts of titanite. The unit varies from relatively homogeneous to diffusely and discontinuously layered on a scale <40 cm (Figure GS2022-3-5a). Local layers have a spotted appearance caused by plagioclase clots <1 cm across. Garnet was observed in one of these layers with plagioclase coronas of varying thickness (Figure GS2022-3-5b). This suggests that the plagioclase clots are pseudomorphous after garnet; however, it is possible that, in other instances, they represent recrystallized phenocrysts or amygdules. Local layers <3 m thick contain small (<2 cm) nebulitic pods of equal proportions of quartz, plagioclase and green amphibole ± garnet. These layers could represent basaltic breccia. Other outcrops are characterized by irregular, plagioclase-rich, vein-like networks, which could represent deformed pillow selvages (Figure GS2022-3-5c). Possible interpillow material in these outcrops forms plagioclase-rich lenses with hornblende, quartz and minor garnet. Rare pods of quartz-carbonate contain minor clinopyroxene, suggesting that they predate or are synchronous with relatively high-grade metamorphism.

A relatively small band of quartzite-pelite assemblage was found along the narrow channel in central Halfway Lake, in close spatial association with the mafic volcanic rocks; however, no direct contact relationship could be determined. The mafic volcanic rocks are interpreted to be Paleoproterozoic in age because there is no evidence for partial melting, which would be expected if these rocks were derived from Archean mafic rocks of the adjacent PGD. These rocks are tentatively correlated with the Bah Lake assemblage of the Ospwagan group.

Diabase

Relatively homogeneous layers of plagioclase amphibolite occur in all of the previously described units throughout the Halfway Lake area. These layers are sharp sided and vary from discontinuous and boudinaged (Figure GS2022-3-4a) to relatively continuous at the outcrop scale. They are typically <1.5 m wide and conformable with the gneissosity, but rarely form layers or zones close to 20 m. The amphibolite is dark grey, medium to coarse grained and foliated, and consists of hornblende with 30–50% plagioclase. The amphibolite is locally garnet bearing, and this variety may be more commonly associated with rocks of the quartzite-pelite assemblage. The relatively homogeneous plagioclase amphibolite is interpreted as metamorphosed and attenuated gabbro and diabase dikes, likely correlative with the Molson dikes; however, homogeneous amphibolite associated with the mafic volcanic rocks could represent massive flows or related subvolcanic intrusions.

Quartz monzonite

The quartz monzonite forms much of the southeastern shoreline of the lake and is believed to extend over approximately 14 km (Figure GS2022-3-3). It is dark green-pink to green-grey weathering and dark pink on fresh surfaces, coarse grained and foliated. It is relatively homogeneous, with attenuated dikes of granite and pegmatite that locally contain hornblende <2 cm across. The monzonite contains 20–30% mafic minerals, usually dominated by hornblende with subordinate biotite; however, local zones contain approximately equal proportions of hornblende and biotite. These zones are reddish in colour, suggesting a higher potassium feldspar content, and could be the result of localized metasomatism. Local amphibole-rich lenses and pods <15 cm across could represent cognate xenoliths (Figure GS2022-3-5d). The amphibole-rich pods also contain abundant clinopyroxene and biotite, and minor feldspar.

The compilation map of Macek et al. (2006) indicates that rare map-scale lenses of ultramafic rock occur within the monzonite. Assuming the ultramafic rock is intrusive into the monzonite, it would imply the monzonite is older than ca. 1880 Ma and could suggest an affinity with the 1883 Ma Paint Lake syenite (Couëslan, 2016). Alternatively, if the ultramafic rock represents a large-scale xenolith, the monzonite could be related to the ca. 1835 Ma Bucko quartz monzonite intrusion south of Wabowden (Bleeker et al., 1995).

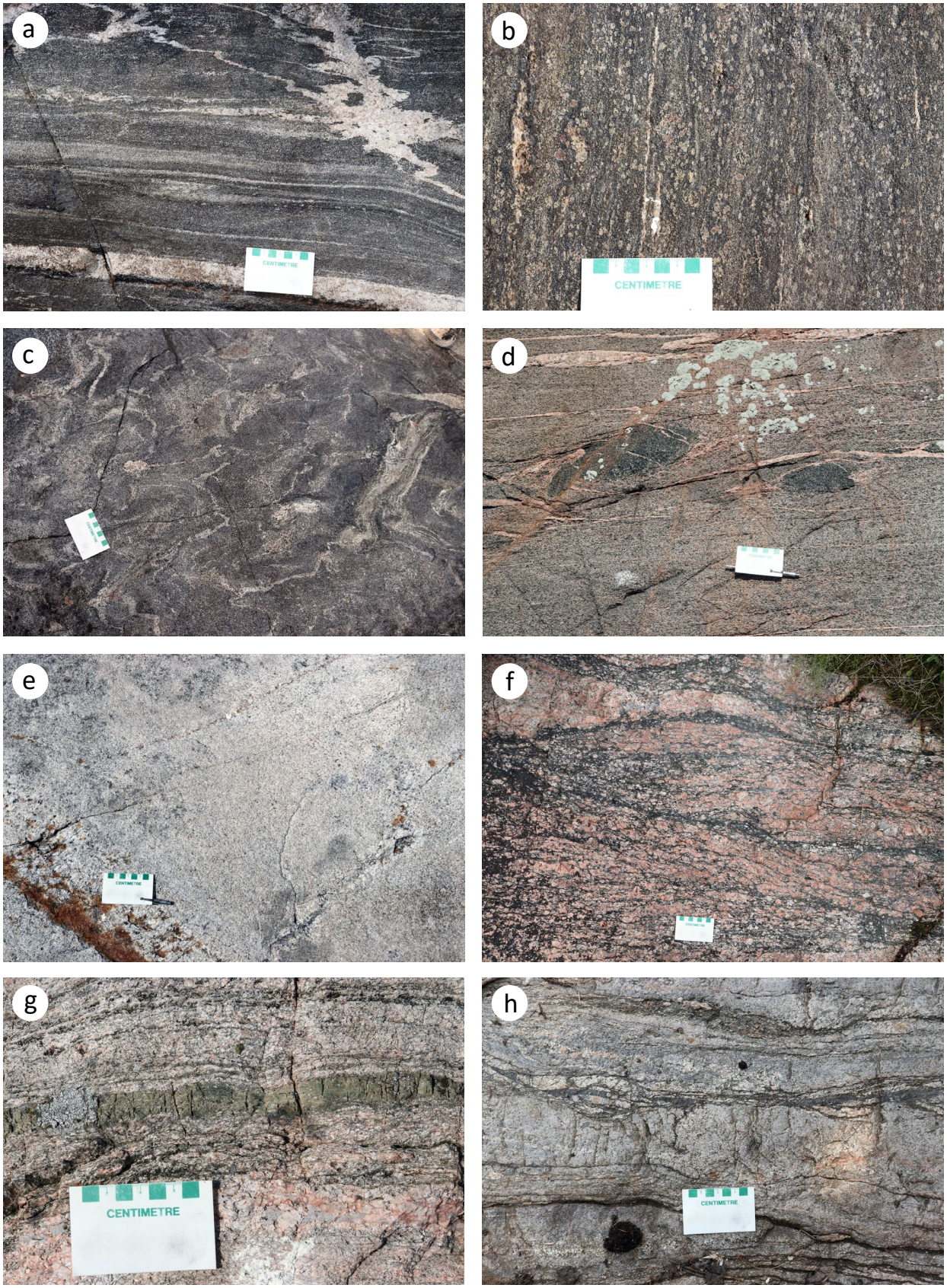

Figure GS2022-3-5: *Outcrop images from the Halfway Lake area:* ***a)*** *diffusely and discontinuously layered plagioclase amphibolite interpreted as mafic volcanic rocks;* ***b)*** *plagioclase clots and garnet with plagioclase corona in mafic volcanic rocks;* ***c)*** *irregular, plagioclase-rich veins in the mafic volcanic rocks likely represent deformed pillow selvages;* ***d)*** *mafic pods within quartz monzonite could represent cognate xenoliths;* ***e)*** *granodiorite from the north basin of Halfway Lake;* ***f)*** *shear zone of mylonitized pegmatite;* ***g)*** *ultramylonite seam in high-strain outcrop of garnet-hornblende granodiorite–tonalite;* ***h)*** *pseudotachylite vein in quartzite.*

Other granitoid rocks

Several isolated reefs and rocky points of granodiorite occur in the northern basin of the lake (Figure GS2022-3-3). The granodiorite is light grey to pinkish white, coarse grained, foliated and homogeneous (Figure GS2022-3-5e). Mafic minerals typically consist of minor biotite; however, trace amounts of sulphide and hornblende can be present. Outcrops locally contain schlieren of biotite gneiss.

An irregular body, or several bodies, of pink granite intrude the mafic volcanic rocks in southern Halfway Lake (Figure GS2022-3-3). The granite is coarse grained and foliated, and contains minor biotite. Hornblende was noted in place of biotite at one location. It is relatively homogeneous, with diffuse patches of leucosome or pegmatite and sparse schlieren.

Dikes of pegmatitic granite occur in all outcrops of the Halfway Lake area and are generally <5 m wide (Figure GS2022-3-4a, f); however, local map-scale (>20 m wide) intrusions of pegmatite are present. They are typically pink and granitic with minor biotite, and can locally contain trace amounts of garnet. There is evidence for multiple generations of pegmatite. The dikes can be strongly foliated and conformable, or attenuated parallel to the regional gneissosity; or foliated and crosscutting the gneissosity; or massive and crosscutting all fabrics. In addition, foliated pegmatite dikes are observed crosscutting other foliated pegmatite dikes. The massive dikes locally display comb-textured biotite or quartz. Rare white pegmatite is typically associated with the mafic volcanic rocks (Figure GS2022-3-5a).

Structural and metamorphic geology

All rocks in the Halfway Lake area, with the exception of Paleoproterozoic intrusive rocks, display a northeast-trending, subvertical S_2 gneissosity. The gneissosity in supracrustal rocks is defined by the attenuation of primary compositional layering (S_0). The gneissosity is folded by upright, northeast- and southwest-plunging, isoclinal F_3 folds. The isoclinal folds are accompanied by an axial-planar S_3 foliation that affected all rocks except the massive pegmatite dikes. The foliation is commonly defined by a quartz fabric in outcrops. The S_2 gneissosity is commonly attenuated parallel to the S_3 foliation, but local outcrops display a divergence of up to 45°. Protomylonitic to mylonitic shear zones are relatively common and subparallel to S_3 (Figure GS2022-3-5f). The shear zones are dominantly sinistral and are locally accompanied by discrete seams of ultramylonite <3 cm thick (Figure GS2022-3-5g). The shear zones typically occur along the limbs of major fold structures and, most notably, appear to enclose the mafic volcanic assemblage. Rare pseudotachylite veins (D_4?) are typically found overprinting ductile shear zones (Figure GS2022-3-5h).

Pelitic rocks from the Halfway Lake area are migmatitic and appear from hand sample to contain a peak metamorphic assemblage of quartz–plagioclase–K-feldspar–biotite–sillimanite–garnet. This mineral assemblage is typical for upper-amphibolite–facies pelitic rocks. Although this mineral assemblage is typically found within the S_2 gneissosity, it was locally observed within S_3 mylonitic shear zones. This suggests that peak metamorphic conditions outlasted D_2 and continued until at least early D_3. Clinopyroxene is relatively common in the rocks of the mafic volcanic assemblage; however, no orthopyroxene was observed. This suggests that granulite-facies metamorphic conditions were not attained during the Paleoproterozoic.

Economic considerations

The most widely accepted model for generating Ni-Cu deposits in the TNB invokes the intrusion of ultramafic magmas into sulphide-rich horizons of the Pipe formation of the Ospwagan group (Figure GS2022-3-2). There the magmas scavenged sulphide from the host sedimentary rocks, leading to sulphur saturation of the melt and the precipitation and concentration of sulphides enriched in Ni and Cu. As a result, ultramafic bodies hosted by Pipe formation rocks are considered the most likely to host mineralization and are prime exploration targets in the TNB (Bleeker, 1990; Layton-Matthews et al., 2007; Zwanzig et al., 2007).

The recently recognized Paint sequence consists of sulphide-bearing wacke with minor iron formation and quartz arenite interbedded with sulphidic and graphitic pelite (Couëslan, 2016). These sedimentary rocks were deposited sometime after ca. 1970 Ma but likely prior to the intrusion of the Molson swarm and Thompson-type ultramafic bodies at ca. 1880 Ma (Couëslan, 2022b). Therefore, there is also potential for the sulphide-bearing Paint sequence rocks to host mineralized ultramafic intrusions.

Although the affinity of the quartzite-pelite assemblage is not constrained, the presence of ubiquitous rusty orange weathering suggests the existence of disseminated sulphide, and local metre-scale layers of sulphidic pelite indicate greater concentrations of sulphide. A number of ultramafic bodies were interpreted by Macek et al. (2006) to be present within this sedimentary assemblage, which would have been a potential source of sulphide for intruding magmas.

The calcsilicate-semipelite assemblage of east-central Halfway Lake is tentatively correlated with the Thompson formation of the Ospwagan group. The presence of pyrrhotite (locally up to 5%) within this assemblage could indicate proximity to the overlying sulphide-facies iron formation of the P1 member (Pipe formation). The contact between the Thompson and Pipe formations correlates with the same stratigraphic level as the ore horizons at the Pipe II and Birchtree mines of Vale Ltd. (Bleeker, 1990). A mineralized ultramafic body in this vicinity was the focus of exploration for Falconbridge Ltd. (now Glencore plc) and Crowflight Minerals Inc. (now Canickel Mining Ltd.) between 1992 and 2008. The best mineralized intersections to date include 1.38% Ni over 17.55 m (drillcore HW95-05; Assessment File 72905) and 1.58% Ni over 13.03 m (drillcore HW08-02; Assessment File 74607).

Intersections of Ni mineralization at Halfway Lake include ultramafic-hosted disseminated and net-textured sulphide, similar to mineralization in much of the Thompson belt, as well as metasedimentary-hosted semisolid to solid sulphide, similar to mineralization at the Thompson mine (Assessment Files 74504, 74607). The metamorphic grade at Halfway Lake is comparable to that of the Thompson mine area, which implies a similar ductile structural regime, with sulphides deforming in a plastic or viscous manner. A considerable portion of the Thompson orebody is contained within an F_3 hinge zone, with mineralization also associated with parasitic F_3 fold structures along one of the limbs (Lightfoot et al., 2017). Although it occurs at the same stratigraphic level as a train of ultramafic bodies, most of the Ni ore at the Thompson mine is hosted by Pipe formation rocks (Bleeker, 1990; Lightfoot et al., 2017).

Future exploration at Halfway Lake might consider targeting F_3 fold structures to look for thickened zones of sulphide plunging along fold hinges. The mineralized ultramafic body mentioned in the previous paragraph occurs along the west limb of an F_3 fold, not far from the hinge zone. Additional fold hinges and zones of thickening occur in the northern part of Halfway Lake, in the vicinity of the sulphidic pelite exposure. It should also be remembered that sulphide could have remobilized under high-grade metamorphic conditions and need not be directly associated with ultramafic bodies. Exploration at the same stratigraphic level as ultramafic bodies could reveal the presence of mineralization that is hosted by sedimentary rocks rather than by the intrusion.

The relatively common occurrence of garnet in Archean orthogneiss and garnet-bearing intrusions at Halfway Lake, combined with sparse screens of Archean sedimentary rocks, could be potential sources of confusion while logging drillcore in the Halfway Lake area. The presence of garnet alone cannot be used as an indicator for sedimentary protolith, and small isolated intersections of metasedimentary rock may not be good indicators for the existence of Ospwagan group or other assemblages with the potential to host Ni-mineralized ultramafic bodies. An observation that may be useful in separating low-potential Archean rocks from higher potential Paleoproterozoic sedimentary rocks is the colour and distribution of garnet. It was observed that garnet within the Archean orthogneiss (and garnet-bearing intrusion) is generally dark red and randomly disseminated throughout the rock. Garnet within the quartzite-pelite assemblage rocks is typically pink to violet and is more abundant along pelitic (aluminous/mafic-rich) layers.

Acknowledgments

Thanks to T. Hnatiuk (University of Manitoba) for providing excellent field assistance; C. Epp and P. Belanger for logistical support; L. Chackowsky and H. Adediran for GIS expertise; and M. Rinne and C. Böhm for their reviews of this report. Thanks also to C. Beaumont-Smith for discussions on access and geology of the Halfway Lake area. Special thanks to T. McCracken, J. Gogal, and B. Gogal from Gogal Air Services in Snow Lake for providing invaluable air support, which made this project possible.

References

Bleeker, W. 1990: Evolution of the Thompson Nickel Belt and its nickel deposits, Manitoba, Canada; Ph.D. thesis, University of New Brunswick, Fredericton, New Brunswick, 400 p.

Bleeker, W. and Hamilton, M.A. 2001: New SHRIMP U-Pb ages for the Ospwagan group: implications for the SE margin of the Trans-Hudson orogen; Geological Association of Canada–Mineralogical Association of Canada, Joint Annual Meeting, St. John's, Newfoundland, May 27–30, 2001, Abstracts, v. 26, p. 15.

Bleeker, W. and Macek, J.J. 1988: Thompson Nickel Belt project – Pipe Pit mine (part of 63O/8NE); *in* Report of Field Activities 1988, Manitoba Energy and Mines, Minerals Division, p. 111–115, URL <https://manitoba.ca/iem/geo/field/rfa88.zip> [August 2022].

Bleeker, W., Nägerl, P. and Machado, N. 1995: The Thompson Nickel Belt, Manitoba: some new U-Pb ages; Geological Association of Canada–Mineralogical Association of Canada Joint Annual Meeting, Victoria, British Columbia, May 17–19, 1995, Program with Abstracts, v. 20, p. A-8.

Böhm, C.O., Zwanzig, H.V. and Creaser, R.A. 2007: Sm-Nd isotope technique as an exploration tool: delineating the northern extension of the Thompson Nickel Belt, Manitoba, Canada; Economic Geology, v. 102, p. 1217–1231.

Burnham, O.M., Halden, N., Layton-Matthews, D., Lesher, C.M., Liwanag, J., Heaman, L., Hulbert, L., Machado, N., Michalak, D., Pacey, M., Peck, D.C., Potrel, A., Theyer, P., Toope, K. and Zwanzig, H. 2009: CAMIRO project 97E-02, Thompson Nickel Belt: final report, March 2002, revised and updated 2003; Manitoba Science, Technology, Energy and Mines, Manitoba Geological Survey, Open File OF2008-11, 434 p. plus appendices and GIS shape files for use with ArcInfo®, URL <https://manitoba.ca/iem/info/libmin/OF2008-11.zip> [August 2022].

Couëslan, C.G. 2016: Geology of the Paint and Phillips lakes area, Thompson nickel belt, central Manitoba (parts of NTS 63O1, 8, 9, 63P5, 12); Manitoba Growth, Enterprise and Trade, Manitoba Geological Survey, Geoscientific Report GR2016-1, 44 p. and 1 map at 1:50 000 scale, URL <https://manitoba.ca/iem/info/libmin/GR2016-1.zip> [August 2022].

Couëslan, C.G. 2021: Bedrock geology of the central Sipiwesk Lake area, Pikwitonei granulite domain, central Manitoba (part of NTS 63P4); Manitoba Agriculture and Resource Development, Manitoba Geological Survey, Geoscientific Report GR2021-1, 47 p. plus 1 appendix and 1 map at 1:20 000 scale, URL <https://manitoba.ca/iem/info/libmin/GR2021-1.zip> [August 2022].

Couëslan, C.G. 2022a: Bedrock geology of the Halfway Lake area, central Manitoba (parts of NTS63O1, 2); Manitoba Natural Resources and Northern Development, Manitoba Geological Survey, Preliminary Map PMAP2022-1, scale 1:25 000, URL <https://manitoba.ca/iem/info/libmin/PMAP2022-1.pdf> [November 2022].

Couëslan, C.G. 2022b: Characterization of ultramafic-hosting metasedimentary rocks and implications for nickel exploration at Phillips Lake, Thompson nickel belt, central Manitoba (part of NTS 63O1); Manitoba Natural Resources and Northern Development, Manitoba Geological Survey, Geoscientific Paper GP2022-1, 33 p. and 4 appendices, URL <https://manitoba.ca/iem/info/libmin/GP2022-1.zip> [August 2022].

Couëslan, C.G. and Pattison, D.R.M. 2012: Low-pressure regional amphibolite-facies to granulite-facies metamorphism of the Paleoproterozoic Thompson Nickel Belt, Manitoba; Canadian Journal of Earth Sciences, v. 49, p. 1117–1153.

Griffin, L.A., Martin, P.L. and Broili, C.C. 2012: CaNickel Mining Limited NI 43-101 technical report regarding update to reserves and resources for the Bucko Lake nickel project Wabowden, Manitoba; NI 43-101 report prepared for CaNickel Mining Ltd., 133 p., URL <https://canickel.com/static/20121019_Technical_Report.pdf> [March 2022].

Guevara, V.E., MacLennan, S.A., Dragovic, B., Caddick, M.J., Schoene, B., Kylander-Clark, A.K.C. and Couëslan, C.G. 2020: Polyphase zircon growth during slow cooling from ultrahigh temperature: an example from the Archean Pikwitonei granulite domain; Journal of Petrology, v. 61, art. egaa021, URL <https://doi.org/10.1093/petrology/egaa021> [October 2022].

Heaman, L.M., Böhm, C.O., Machado, N., Krogh, T.E., Weber, W. and Corkery, M.T. 2011: The Pikwitonei Granulite Domain, Manitoba: a giant Neoarchean high-grade terrane in the northwest Superior Province; Canadian Journal of Earth Sciences, v. 48, p. 205–245.

Heaman, L.M., Peck, D. and Toope, K. 2009: Timing and geochemistry of 1.88 Ga Molson Igneous Events, Manitoba: insights into the formation of a craton-scale magmatic and metallogenic province; Precambrian Research, v. 172, p. 143–162, URL <https://doi.org/10.1016/j.precamres.2009.03.015> [October 2022].

Hubregtse, J.J.M.W. 1980: The Archean Pikwitonei granulite domain and its position at the margin of the northwestern Superior Province (central Manitoba); Manitoba Energy and Mines, Manitoba Geological Survey, Geological Paper GP80-3, 16 p., URL <https://manitoba.ca/iem/info/libmin/GP80-3.pdf> [August 2022].

Layton-Matthews, D., Lesher, C.M., Burnham, O.M., Liwanag, J., Halden, N.M., Hulbert, L. and Peck, D.C. 2007: Magmatic Ni-Cu-platinum-group element deposits of the Thompson Nickel Belt; *in* Mineral Deposits of Canada: A Synthesis of Major Deposit-Types, District Metallogeny, the Evolution of Geological Provinces, and Exploration Methods, W.D. Goodfellow (ed.), Geological Association of Canada, Mineral Deposits Division, Special Publication No. 5, p. 409–432.

Lightfoot, P.C., Stewart, R., Gribbin, G. and Mooney, S.J. 2017: Relative contribution of magmatic and post-magmatic processes in the genesis of the Thompson Mine Ni-Co sulfide ores, Manitoba, Canada; Ore Geology Reviews, v. 83, p. 258–286.

Macek, J.J. 1980: Halfway Lake; Manitoba Department of Energy and Mines, Mineral Resources Division, Preliminary Map 1980T-1, 1:25 000 scale.

Macek, J.J. and Scoates, R.F.J. 1980: Thompson Nickel Belt project (parts of 63O/1, 2); *in* Report of Field Activities 1980, Manitoba Department of Energy and Mines, Mineral Resources Division, p. 23–29, URL <https://manitoba.ca/iem/geo/field/roa80.pdf> [August 2022].

Macek, J.J., Zwanzig, H.V. and Pacey, J.M. 2006: Thompson Nickel Belt geological compilation map, Manitoba (parts of NTS 63G, J, O, P and 64A and B); Manitoba Science, Technology, Energy, and Mines, Manitoba Geological Survey, Open File Report OF2006-33, digital map on CD, URL <https://manitoba.ca/iem/info/libmin/OF2006-33.zip> [August 2022].

Manitoba Mineral Resources 2013: Mineral Dispositions, Manitoba; *in* Map Gallery – Mining and Quarrying, Manitoba Mineral Resources, Manitoba Geological Survey, URL <https://rdmaps.gov.mb.ca/Html5Viewer/index.html?viewer=MapGallery_Mining.MapGallery> [March 2022].

Mezger, K., Bohlen, S.R. and Hanson, G.N. 1990: Metamorphic history of the Archean Pikwitonei granulite domain and the Cross Lake subprovince, Superior Province, Manitoba, Canada; Journal of Petrology, v. 31, p. 483–517.

Percival, J.A., Whalen, J.B. and Rayner, N. 2005: Pikwitonei–Snow Lake Manitoba transect (parts of NTS 63J, O and P), Trans-Hudson Orogen–Superior Margin Metallotect Project: new results and tectonic interpretation; *in* Report of Activities 2005, Manitoba Industry, Economic Development and Mines, Manitoba Geological Survey, p. 69–91, URL <https://manitoba.ca/iem/geo/field/roa05pdfs/GS-09.pdf> [August 2022].

Scoates, J.S., Scoates, J.R.F., Wall, C.J., Friedman, R.M. and Couëslan, C.G. 2017: Direct dating of ultramafic sills and mafic intrusions associated with Ni-sulfide mineralization in the Thompson nickel belt, Manitoba, Canada; Economic Geology, v. 112, p. 675–692.

White, D.J., Lucas, S.B., Bleeker, W., Hajnal, Z., Lewry, J.F. and Zwanzig, H.V. 2002: Suture-zone geometry along an irregular Paleoproterozoic margin: the Superior boundary zone, Manitoba, Canada; Geology, v. 30, p. 735–738.

Zwanzig, H.V. 2005: Geochemistry, Sm-Nd isotope data and age constraints of the Bah Lake assemblage, Thompson Nickel Belt and Kisseynew Domain margin: relation to Thompson-type ultramafic bodies and a tectonic model (NTS 63J, O and P); *in* Report of Activities 2005, Manitoba Industry, Economic Development and Mines, Manitoba Geological Survey, p. 40–53, URL <https://manitoba.ca/iem/geo/field/roa05pdfs/GS-06.pdf> [August 2022].

Zwanzig, H.V., Macek, J.J. and McGregor, C.R. 2007: Lithostratigraphy and geochemistry of the high-grade metasedimentary rocks in the Thompson Nickel Belt and adjacent Kisseynew Domain, Manitoba: implications for nickel exploration; Economic Geology, v. 102, p. 1197–1216.

GS2022-4

Investigating textural and geochemical relations of lithium mineralization in the Tanco pegmatite, southeastern Manitoba (part of NTS 52L6)

by C.M. Breasley[1], T. Martins, R.L. Linnen[2] and L.A. Groat[1]

In Brief:

- Samples of the Tanco pegmatite were taken from underground mining faces showing different spodumene textures
- Spodumene at the Tanco pegmatite can be classified into four textural groups which show complex internal geochemical zonation highlighted by cathodoluminescence imaging and LA-ICP-MS
- Future analysis will include using micro-CT to quantify the variable proportions of spodumene and quartz ratios within intergrowths

Citation:
Breasley, C.M., Martins, T., Linnen, R.L. and Groat, L.A. 2022: Investigating textural and geochemical relations of lithium mineralization in the Tanco pegmatite, southeastern Manitoba (part of NTS 52L6); *in* Report of Activities 2022, Manitoba Natural Resources and Northern Development, Manitoba Geological Survey, p. 25–35.

Summary

Underground samples were collected from the Tanco pegmatite in southeastern Manitoba in early May 2022 to investigate the textural varieties of spodumene and Li mineralization trends. Thin-section petrography, cathodoluminescence imaging, electron probe microanalysis, and laser-ablation inductively coupled plasma–mass spectrometry (LA-ICP-MS) were done at the University of Manitoba in late May 2022. Preliminary observations show four distinct groups of spodumene textures at Tanco: 1) classic spodumene and quartz intergrowths (SQUI) as shown by elongated unidirectional texture; 2) micro-SQUI with symplectic radial texture, replacing the classic SQUI; 3) equant SQUI, which forms larger, stubby, equant interlocking crystals; and 4) primary platy spodumene that is not necessarily associated with quartz. Cathodoluminescence imaging revealed a complex internal zonation sequence within the SQUI. Preliminary LA-ICP-MS results showed that the classic and micro-SQUI are geochemically similar, whereas equant SQUI has a highly variable trace-element composition. Future work will include subsequent LA-ICP-MS studies to determine the geochemical variability, which defines the zonation within the spodumene.

Introduction

The genesis and significant economic potential of pegmatites make them a fascinating field of study in economic geology. The Li-Cs-Ta (LCT) Tanco pegmatite in southeastern Manitoba represents one of the most economically important and fractionated pegmatitic bodies in the world. It has been the subject of numerous studies that have contributed significantly to understanding of pegmatite petrogenesis (Černý, 2005).

This project was initiated in August 2021 when two weeks of fieldwork were completed at the Tanco mine in order to collect a variety of drillcore and subsurface samples (Breasley et al., 2021). Preliminary visualization of spodumene and quartz intergrowths (SQUI) using X-ray computed tomography (micro-CT) was presented at AME Roundup 2022 (Breasley et al., 2022a). The bulk of Li mineralization at Tanco occurs as SQUI, which may have formed by the breakdown of petalite (Černý and Ferguson, 1972). Rietveld analysis of SQUI indicates that they can consist of up to 80% spodumene and 19.1% quartz (Breasley et al., 2022a). This contradicts the hypothesis of an idealized breakdown of petalite, which should result in a SQUI vol. % ratio of ~60% spodumene and ~40% quartz.

This project aims to better constrain the different types of SQUI, analyze proportional variability of spodumene and quartz within these types, and characterize compositions and timing of formation of additional Li-bearing minerals. Analysis of the compositional variability of SQUI (using X-ray computed tomography, electron backscatter diffraction, and powder X-ray diffraction Rietveld methods) will reveal information on their crystallization history. The results from this study are expected to help explain the notable lack of abundant petalite within the Li-rich zones of the pegmatite examined here. Furthermore, studying variability of the SQUI groups at Tanco is of economic importance to the mineral processing protocols for different styles of mineralization.

Due to unprecedented high-water levels in the region, access to the Tanco mine as initially planned did not take place. Fieldwork conducted at the Tanco mine in early May 2022 consisted of subsurface sampling instead. A range of subsurface samples were collected to investigate the textural variability of Li mineralization, enrichment in different zones, and spatial trends within the pegmatite. The work carried out at the University of Manitoba involved analysis of the samples collected in 2021, including thin-section petrography, cathodoluminescence (CL) imaging, electron probe microanalysis (EPMA),

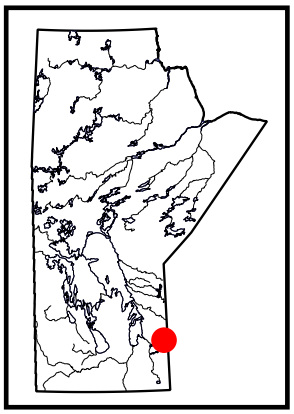

[1] Department of Earth, Ocean and Atmospheric Science, University of British Columbia, 2207 Main Mall #2020, Vancouver, British Columbia V6T 1Z4
[2] Department of Earth Sciences, Western University, 1151 Richmond St. N., London, Ontario N6A 5B7

and laser-ablation inductively coupled plasma–mass spectrometry (LA-ICP-MS). These analytical results were presented at the Goldschmidt 2022 meeting (Breasley et al., 2022b), and are summarized in this report.

Geological setting

The Tanco pegmatite is part of the Bernic Lake group of pegmatites of the Cat Lake–Winnipeg River pegmatite district in southeastern Manitoba (Figure GS2022-4-1). This district is situated in the southern limb of the Bird River greenstone belt (2.75–2.72 Ga; Gilbert, 2006). Rock assemblages within the belt are separated into northern and southern assemblages constituting part of the Archean Superior province.

The Bernic Lake formation (2724.6 ±1 Ma; Gilbert, 2008) is a 2 by 45 km, dominantly mafic, volcanic-rich unit. It is located in the southern assemblage of the Bird River greenstone belt and hosts the Tanco gabbro, into which the Tanco pegmatite was emplaced. The Tanco gabbro crystallized at 2723.1 ±0.8 Ma and was subsequently metamorphosed along with surrounding lithologies of the region in an amphibolite-grade Abukuma-style system (Černý, 2005; Gilbert, 2008; Kremer, 2010). The Tanco gabbro and Bernic Lake formation are hypothesized to have formed during a single episode of magmatism because of their similar ages and spatial relationships (Kremer, 2010). Gilbert (2006, 2007, 2008) provided detailed descriptions of the various lithologies of the Bird River greenstone belt.

The extensive Cat Lake–Winnipeg River pegmatite district is divided into two subdistricts: the Winnipeg River and the Cat Lake–Maskwa Lake subdistricts (Černý et al., 1981). The Bernic Lake pegmatite group that hosts the Tanco pegmatite forms part of the Winnipeg River subdistrict. The multiple pegmatites of the Bernic Lake group are notably enriched in Li, however Li enrichment in the Tanco pegmatite far exceeds the volume and grade of mineralization of the other Li-rich pegmatites of the group.

Tanco pegmatite

The morphology of the Tanco pegmatite intrusion is bilobate, with maximum dimensions of 1520 m in length, 1060 m in width and 100 m in thickness (Černý, 2005). Uranium-lead tantalite dating (Camacho et al., 2012) showed an intrusive age of 2641 ±3 Ma, similar to a U-Pb zircon age of 2647.4 ±1 Ma reported by Kremer (2010). These data are concurrent with the hypothesized reactivation of the Bernic Lake shear zone during the period of ca. 2650–2640 Ma, which facilitated emplacement

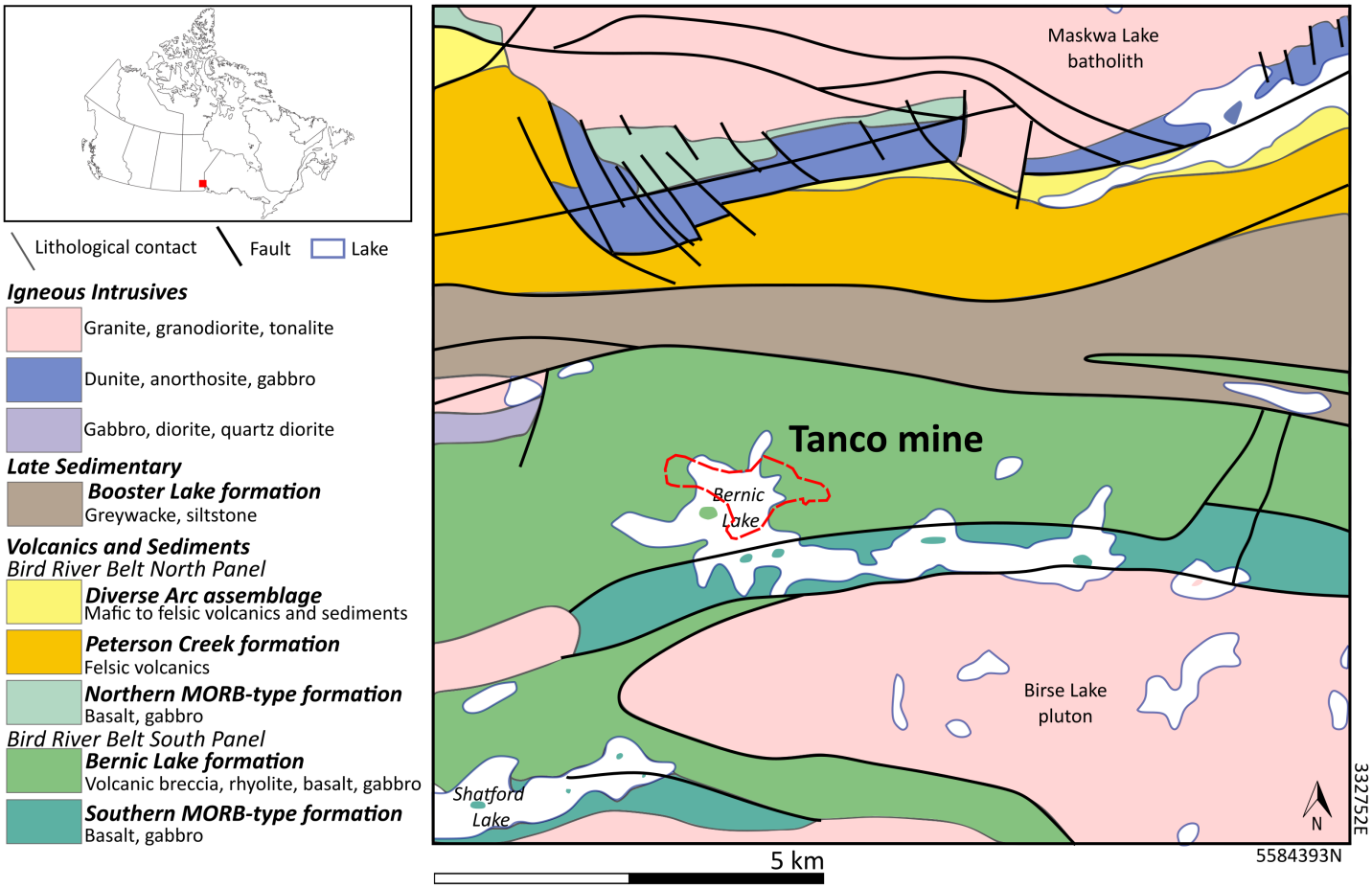

Figure GS2022-4-1: *Location and local geology surrounding the Tanco pegmatite (dashed red outline; Stilling et al., 2006) in southeastern Manitoba. Adapted from Breasley et al. (2021) and Gilbert (2008). Abbreviation: MORB, mid-ocean–ridge basalt.*

of the igneous body along the west-trending fault system in the surrounding area (Kremer, 2010; Martins et al., 2013).

The Tanco pegmatite is classified as a petalite subtype, attributed to complex LCT pegmatites (Černý and Ercit, 2005). The mineralogy of the Tanco pegmatite lacks considerable petalite; spodumene is the dominant Li aluminosilicate phase. Spodumene and quartz intergrowths that form the bulk of Li mineralization are hypothesized to have formed via the breakdown of petalite as a re-equilibration reaction. The pegmatite has a peraluminous composition that is generally depleted in Fe, Mg and Ca (Stilling et al., 2006). Other Li minerals used to classify pegmatites, such as lepidolite, amblygonite-montebrasite and primary spodumene, are also present (Černý, 2005).

Mineralized zones

Tanco has been divided into nine major mineralized zones (zones 10 to 90), which contain several subzones differentiated on the basis of their differences in mineralogy, geochemistry and textures (Figure GS2022-4-2). The nature of zonation and geo-

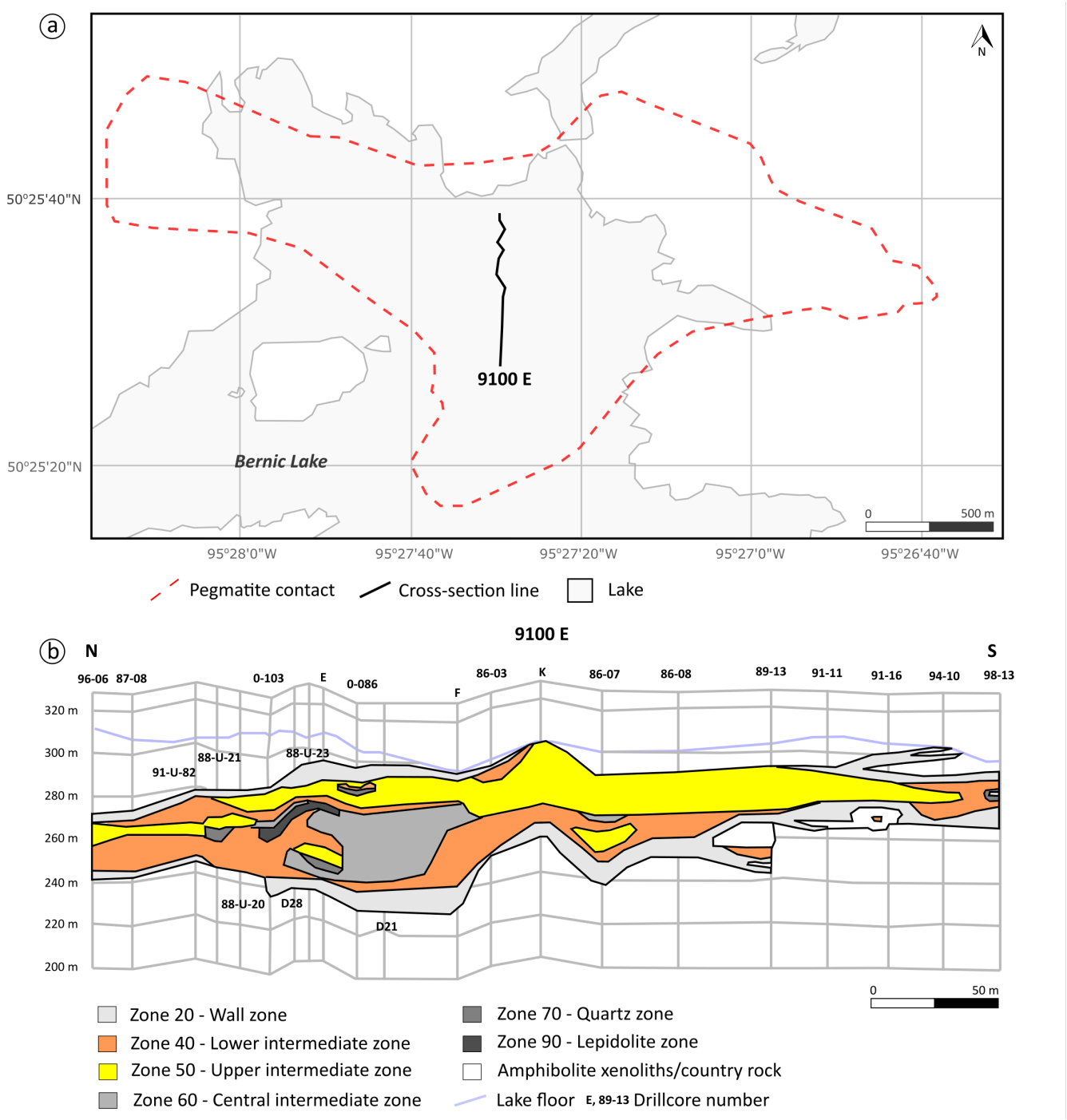

Figure GS2022-4-2: a) *Location of Tanco pegmatite and line of cross-section shown in (b);* ***b)*** *Cross-section of zones based on drillcore data (adapted from Stilling et al., 2006, Figure 6).*

graphical location of the zones at Tanco reveals information on the evolution of the pegmatite melts and Li mineralization over time. Previous works (Černý et al., 1998; Černý, 2005; Stilling et al., 2006) presented detailed descriptions of these zones. In this report we present an overview of the Tanco zones detailed in the literature and in historical core logs written by Tanco mine geologists, and include descriptions of several subzones.

Zone 01 (overburden): Lake and till sediments.

Zone 05 (host rock): The host rock is generally called amphibolite, but it is much more diverse and gabbroic in composition in some areas. The amphibolite host rock surrounding Tanco comprises 54% Fe-hornblende, 37% plagioclase (An_{38}), 4% ilmenite, 1% apatite and 4% quartz, with minor epidote, biotite, chlorite and almandine (Morgan and London, 1987). It was subjected to multiple metasomatic events during crystallization of the Tanco pegmatite (Morgan and London, 1987).

Zone 10 (border zone): The border zone is a fine-grained contact zone with amphibolite, representing portions of the Tanco pegmatite that crystallized first. It is composed of a very thin band of quartz and albite, which locally penetrates the host rock. This zone, less than 30 cm thick, is the least geochemically evolved section of the pegmatite (Stilling et al., 2006).

Zone 20 (wall zone): The wall zone consists of simple pegmatite that is roughly representative of the bulk composition of the Tanco pegmatite. The mineralogy of this zone is composed predominantly of megacrystic microcline-perthite, quartz, albite and curvilamellar lithian muscovite. Minor components include beryl, tourmaline, muscovite, lithian muscovite and perthite. Some notable features of this zone include red perthite, exocontact tourmaline growths perpendicular to the contact with country rock, and white beryl. This zone hosts giant potassium feldspar phenocrysts in a medium-grained groundmass. Aplitic bands are commonly found in the footwall of the wall zone. This zone is up to 35 m thick in the footwall (Černý, 2005).

Zone 22 (simple pegmatites): Isolated blebs of pegmatites are simple in mineralogy, and not enriched in metals. They are commonly found above and below the main mineralized Tanco body, within the country rock.

Zone 30 (aplitic albite zone): This zone consists of albite, quartz and muscovite, with minor tantalum oxides, beryl, apatite, tourmaline, cassiterite, ilmenite, zircon and sulphides. This zone is generally pale blue-white and contains dark brown and black clots of remobilized Ta/Nb–bearing minerals. The blue colour is attributed to micro-scale blades of massive albite. This zone is of particular interest due to its distinctive textures that include multiple undulatory layered growths and fracture infill structures. The banded nature represents progressive crystallization fronts. Zone 30 is >16 m thick in some areas. Another interesting feature of this zone includes the presence of a 'beryl fringe' at contact zones with other units (Stilling et al., 2006) and the typical association with Ta and Nb mineralization. Some spatial trends of this zone include ragged lenses of mineralization in the eastern area of the pegmatite, where they are found beside the wall zone, grading locally into zone 60 (Černý et al., 1998). In the western side of the Tanco deposit, zone 30 is found throughout zone 60 and in contact with zones 40 and 20 (Černý et al., 1996).

Zone 36 (aplitic albite – muscovite and quartz after microcline (MQM) zone): In this zone, the abundance of zone 30 aplite is greater than zone 60 MQM secondary alteration. The rock in this zone is typically green or white, with coarser crystalline growth than the massive blue albite. This zone often contains beryl and is associated commonly with Ta mineralization.

Zone 39 (aplitic albite – lepidolite zone): Zone 30 albite is more abundant in this zone than zone 90 lepidolite.

Zone 40 (lower intermediate (mixed) zone): This zone is highly internally variable and is often used to describe chaotic zones in historical drillcore. Common components include microcline-perthite, albite, quartz, spodumene (with SQUI crystals up to 2 m in length) and amblygonite. Minor components include lithian muscovite, lithiophilite, lepidolite, petalite, and tantalum oxides. This zone can be distinguished from zone 50 (see below) by the notable abundance of feldspars. Zone 40 is medium- to coarse-grained, remarkably heterogeneous, and can be up to 25 m in thickness. Radial fans of albite and mica commonly surround the feldspar-dominant minerals (Černý et al., 1996).

Zone 45 (low-grade spodumene zone): This zone represents the mixed zone but is more enriched in SQUI. It has a higher sodium content than zone 50, with common blue-white aplite bands and patches. Thin-section analysis revealed a highly complex internal mineralogy, indicative of high-temperature remobilization processes, including relatively high-temperature/pressure spodumene phases. However, multiple generations of aplite are found at Tanco, therefore it is unknown whether the aplites in zone 45 are genetically linked to those in zone 30.

Zone 50 (upper intermediate (spodumene) zone): Major components in this zone include giant crystals of spodumene and quartz (in multiple co-existent textural forms) and amblygonite. Minor components include microcline-perthite, pollucite, lithiophilite, petalite, eucryptite, tantalum oxides, albite and lithian muscovite. Historical drill logs suggest the presence of minor quartz pods, triphylite and apatite. This zone is up to 24 m thick, and generally has a gradational contact with zone 40. The lack of albite and mica differentiates this zone from zone 40. Vugs are commonly found in this zone (Černý et al., 1996), which is the most enriched in Li and is known for containing the largest spodumene crystals within the Tanco deposit.

Zone 60 (central intermediate (MQM) zone): This zone is hypothesized to be entirely metasomatic in origin and displays a variety of colours, including green, yellow and brown. It is the main zone of Ta mineralization, and commonly contains mixtures of zones 30 and 90. Major components include microcline-perthite, quartz, albite and muscovite. Minor components include beryl, tantalum oxides, zircon, ilmenite, spodumene, sulphides, lithiophilite, apatite and cassiterite. This zone is medium- to

coarse-grained. It is up to 45 m thick with notably sharp contacts that locally are seen to grade into zones 30 and 90 (Černý et al., 1996).

Zone 63 (MQM (aplitic albite) zone): This zone is a mixture between zones 60 and 30. MQM is found as green, coarser micaceous domains with blue aplitic albite and common white beryl. MQM is found in greater abundance in this zone than in the aplitic albite zone.

Zone 69 (MQM (lepidolite) zone): This is a mix of zones 60 and 90, with MQM in greater quantities than lepidolite. Lepidolite can range from fine micro-crystals to fine interlocked equant growths.

Zone 67 (quartz-rich MQM zone): This is a mixture of zones 60 and 70 (the quartz zone), with quartz being the dominant mineral.

Zone 70 (quartz zone): Zone 70 comprises massive monomineralic quartz lenses. It is difficult to distinguish in drillcore from quartz pods present in other zones and can contain minor amblygonite and spodumene. A distinctive feature of this zone is that it is often surrounded by a potassium feldspar cap that contains crystals of SQUI oriented normal to the contact. Zone 70 represents a truly highly evolved pegmatitic 'core' and is found in the eastern side of the Tanco deposit. Pink quartz of this zone is noted to contain minor petalite (Stilling et al., 2006).

Zone 80 (pollucite zone): This zone is almost entirely composed of monomineralic pollucite. Minor components include quartz, spodumene, petalite, muscovite, lepidolite, albite, microcline and apatite. This zone is geochemically part of zone 50 and is gradational between them, although it is large enough in scale to be defined as a new unit. It hosts a remarkably pure (75%) pollucite unit and is commonly crosscut by late veins of lepidolite, quartz and feldspar. This zone comprises several lens-like bodies found above zone 50. The largest segment of this zone is found in the eastern portion of the Tanco pegmatite (Černý et al., 1996).

Zone 58 (low-grade pollucite zone): This zone is found surrounding zone 80. Common components include pollucite mixed with SQUI, potassium feldspar, quartz, amblygonite and petalite.

Zone 90 (lepidolite zone): This zone is hypothesized to have formed from metasomatism, with purple lithian muscovite having replaced primary feldspar. Microlite is the dominant tantalum mineral found intermixed with MQM alteration in this zone. Thin-section microscopy and scanning electron microscopy (SEM) imaging revealed microlite crystals to be highly internally zoned. Dominant minerals include lithian muscovite, lepidolite and microcline-perthite. Minor components include albite, quartz, beryl, tantalum oxides, cassiterite and zircon. This zone is <18 m thick and is composed predominantly of fine-grained micas. It is economically important because of high concentrations of rubidium and cesium micas, and tantalum and niobium oxides. This zone forms two major bodies that trend east-west, along with multiple smaller bodies found within zone 60 (Černý et al., 1996).

Zone 93 (lepidolite–aplitic albite zone): This is a mixture of zones 90 and 30. Lepidolite is found in greater abundance here than in the aplitic albite zone.

Zone 96 (lepidolite-MQM zone): This zone contains a mix of zones 90 and 60, with the lepidolite being the main mineralization.

Zone 99 (potassium feldspar zone): This zone is typically composed of massive potassium feldspar crystals, and contains minor amblygonite-montebrasite.

Lithium at Tanco

Lithium is a critical element because it plays a major role in the global transition to green energy sources as a vital component in rechargeable batteries. Studying the nature of mineralization and Li distribution is therefore key to understanding the behaviour and mechanism of concentration of this important element.

The Li aluminosilicate relationships at Tanco can be explained by a reaction path that shows the nature of primary Li mineral crystallization (London, 1986, 1990, 2008; Černý et al., 1998). The crystallization path shows an initial primary petalite phase that crystallized from a hydrous granitic melt. As the melt cooled, it crossed the petalite-spodumene reaction boundary, where the bulk of petalite is hypothesized to have broken down into SQUI. The crystallization path then shows a period of primary spodumene growth, followed by a transition to primary eucryptite growth as the spodumene-eucryptite reaction boundary is crossed at 270°C and 1.8 kbar (180 megapascals (MPa); Figure GS2022-4-3).

Extensive re-equilibration of spodumene to eucryptite did not occur, due to the presence of exsolved CO_2 liquid and lack of hydrated fluids, which inhibit breakdown of spodumene (Černý and London, 1983). Černý and Ferguson (1972) found that the SQUI at Tanco had similar bulk composition to petalite, and therefore concluded that all spodumene and quartz intergrowths at Tanco were a result of the breakdown from petalite. The variable coarseness of SQUI, reduction in volume during recrystallization (18.6%), and subsequent silica migration are hypothesized to explain the deviations from the petalite composition (Černý and Ferguson, 1972).

There are multiple Li-bearing minerals at Tanco, such as lithian mica, which are abundant in the lepidolite zone (zone 90). Little research has taken place to assess the Li distribution between these mineral phases, which could have economic value.

Lithium-bearing minerals

The Tanco pegmatite is well known for its extensive mineralogy, with in excess of 100 minerals having been identified (Černý, 2005; Martins et al., 2013). This report addresses and describes the Li-bearing mineral phases. A full description of the other

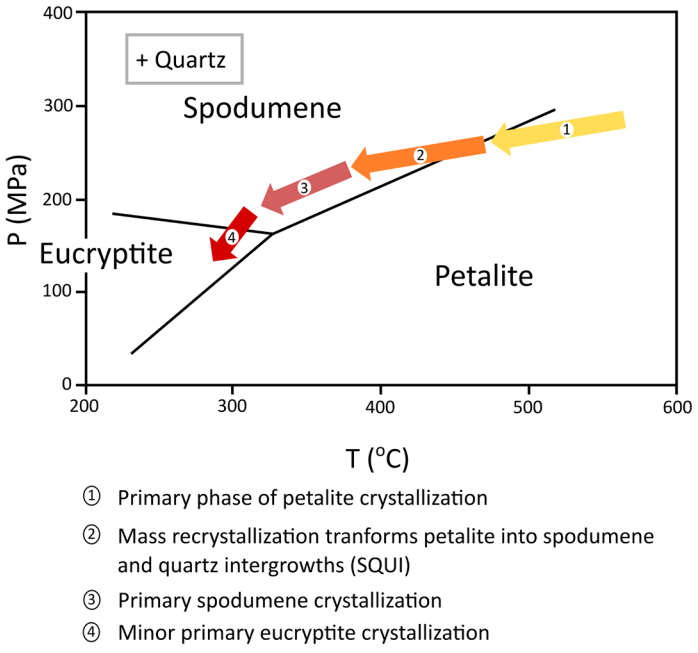

Figure GS2022-4-3: *Li silicate phase diagram showing the proposed crystallization path of the Tanco pegmatite (adapted from London, 2008, Figure 7-7). Abbreviations: MPa, megapascals; P, pressure; T, temperature.*

minerals at Tanco may be found in Černý et al. (1996) and Černý (2005). A summary of these mineral descriptions can be found in Breasley et al. (2021).

Silicates

Li aluminosilicates

Petalite occurs in zones 50 and 80 (Černý and Ferguson, 1972). Petalite is uncommon in the Tanco pegmatite and is thought to have been mostly replaced by SQUI (London, 1986, 1990; Černý et al., 1998).

Spodumene is typically milky white in colour, except near the contacts with gabbroic rafts where it can be pale green. It ranges in size from micro-SQUI texture to megacrysts up to 2 m long (Černý and Ferguson, 1972). Černý and Ferguson (1972) described three different types of spodumene at the Tanco pegmatite: 1) secondary breakdown product of petalite into SQUI; 2) primary spodumene; and 3) spodumene that has broken down and recrystallized into spodumene and quartz. The recrystallized type of spodumene is distinct from SQUI and occurs as coarser crystals that lack the intimate intergrowth textures shown by SQUI. Lithium is currently being mined at Tanco from zones 40 and 50, where 90% of the spodumene is SQUI.

Eucryptite at Tanco is grey to pink, with a distinct red-orange fluorescence in ultraviolet light (Černý, 1972). Crystals are up to 4 cm long and are intergrown with SQUI or in crosscutting vein structures.

Tourmaline

Tourmaline is easily distinguishable and abundant in many zones. In zones 10, 20, 30 and 60, the tourmaline crystals tend to be brown or black, and locally are green in colour. Pink and green tourmalines are found in zones 40 and 50 (Selway et al., 2000b). Tourmalines present a detailed geochemical evolution series and are also found in contact zones with the country rock (Selway et al., 2000a).

Elbaite is a common Na-Li–bearing tourmaline at Tanco. It can be found in a variety of colours, including pink (locally rubellite), green and blue (due to iron content; Selway et al., 2000b).

Rossmanite (the X-site-vacant variety of tourmaline) is present at Tanco, often found as either core or rim of evolved zoned elbaite in zone 40 or 50 (Selway et al., 2000b).

Micas

A wide variety of micas are present in nearly all zones of the Tanco pegmatite. There are noticeable changes in the growth habits of micas, from curvilinear 'ballpeen' crystals to normal micaceous books (Figure GS2022-4-4). The mica crystallography and chemistry at Tanco were described by Rinaldi et al. (1972) and were investigated in relation to Ta mineralization by Van Lichtervelde et al. (2008). Micas at Tanco exist as a substitution series of dioctahedral muscovite (which contains Al>Li) to trioctahedral lepidolite (which contains Li>Al; Van Lichtervelde et al., 2007).

Although zone 90 is termed the lepidolite zone, the dominant mineral in this zone is fine equant growths of lithian muscovite. These purple equant intergrowths show the highest Li contents on average out of all the micas at Tanco (7% Li_2O; Van Lichtervelde et al., 2008). True lepidolite (trilithionite-polylithionite) is found in association with lithian muscovite in zone 90.

Other silicates

Holmquistite occurs in association with epidote, chlorite, albite, calcite, titanite, iron/titanium oxides and quartz in country rock close to contacts with the pegmatite.

Holmquistite is interpreted to have been formed in a late-stage crystallization event, as veins crosscut the previously metasomatically altered country rock. Holmquistite in the Tanco country rock is interpreted to have replaced actinolite (London, 1986).

Phosphates

Amblygonite-montebrasite

Mineral phases from the amblygonite-montebrasite series occur as large primary crystals up to 1.5 m in size but can also be present as smaller tabular aggregates (1–3 cm in size). Montebrasite can be present as a secondary phase along grain boundaries and fractures (Černá et al., 1972). Amblygonite occurs in three main zones of Tanco as white, pink and yellow crystals with vari-

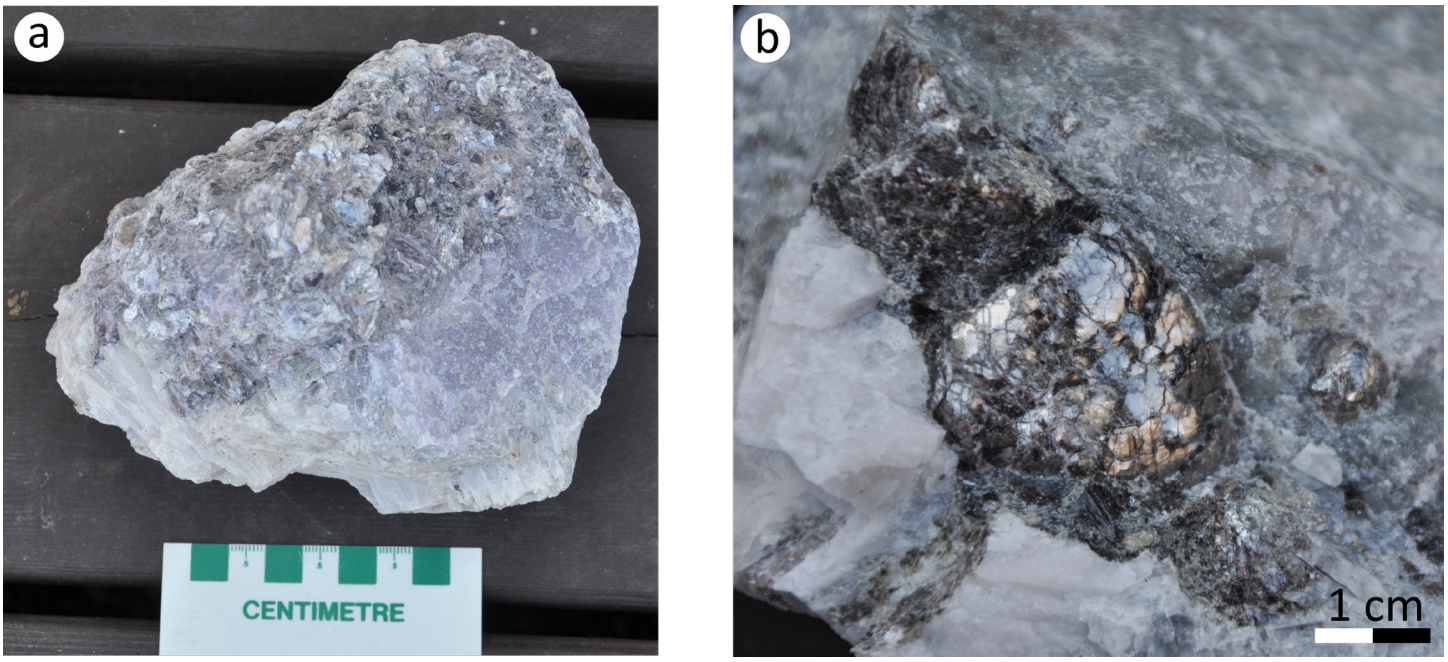

Figure GS2022-4-4: *Images of micas from Tanco showing different growth habits:* ***a)*** *pale purple lithian muscovite crystallized in mesh of mica books (1–3 cm);* ***b)*** *ballpeen mica growth habit of muscovite.*

able fluorine content (4–6.8%; Černá, 1970). Fluorine content is associated with the colour sequence of amblygonite at Tanco, with decreasing fluorine content leading to a transition from pink to white to yellow in the amblygonite (Černá, 1970). Where in its primary form, amblygonite is commonly replaced by fluorine-poor montebrasite via late-stage hydrothermal alteration (Černá, 1970; Černá et al., 1972).

Lithiophosphate and lithiophilite

Lithiophosphate is found as a secondary assemblage from hydrothermal alteration of zone 50 (Simpson, 1974). Lithiophosphate can be found in crystals up to 5 cm in size and is often found in association with quartz, cesian analcime and cookeite as cavity infills (Černý, 1972). Lithiophilite is found in a series with triphylite in zones 10 through to 60 (Černý et al., 1996). It occurs as coarse brown-orange crystals up to 40 cm in size.

Tancoite

Tancoite is an orthorhombic-dipyramidal anhydrous phosphate discovered at Tanco (Ramik et al., 1980). It is typically found in association with lithiophosphate and apatite in zone 50, within secondary hydrothermal vugs.

Clay minerals

Generally, clays at Tanco formed only as a result of secondary breakdown reactions and hydrothermal alteration.

Cookeite is often found as a breakdown product of spodumene and is associated with muscovite. Cavities in zones 40 and 50 host cookeite and it is also found as an epitaxial growth on earlier phases in zones 50 and 60 (Černý, 1972).

Preliminary results

Petrography

Thin-section petrography was used to devise a textural grouping scheme for the spodumene at the Tanco mine from zone 50 (Breasley et al., 2022b).

1) Classic SQUI (Figure GS2022-4-5a, b) shows elongated spodumene and quartz laths, which are intimately intergrown and have a dominant singular orientation. The modal composition is highly variable, with a range of spodumene to quartz ratios visible in thin section. The crystals show prominent cleavage and lack internal mottling. Classic SQUI contains a varied suite of crystal sizes, grouped here into fine (<0.5 cm), medium (0.5–1 cm), and coarse (>1 cm). Classic green SQUI occurs proximal to gabbroic rafts and wallrock, which formed green crystals from Fe contamination. Petalite parental skeletal crystals, which are hypothesized to have broken down into classic SQUI, locally create bounding structures for oriented growth observed in hand sample, and were previously noted in the literature (Černý and Ferguson, 1972).
2) Micro-SQUI crystals (Figure GS2022-4-5c, d) are milky white, massive, and microcrystalline in hand sample. This SQUI variety represents symplectic intergrowth of internally mottled spodumene (with abundant inclusions of quartz, zircon and mica) and quartz. The characteristic habit forms localized radial, elongated fans of symplectite (100–600 µm in length) and commonly textures of very fine intergrowths with no

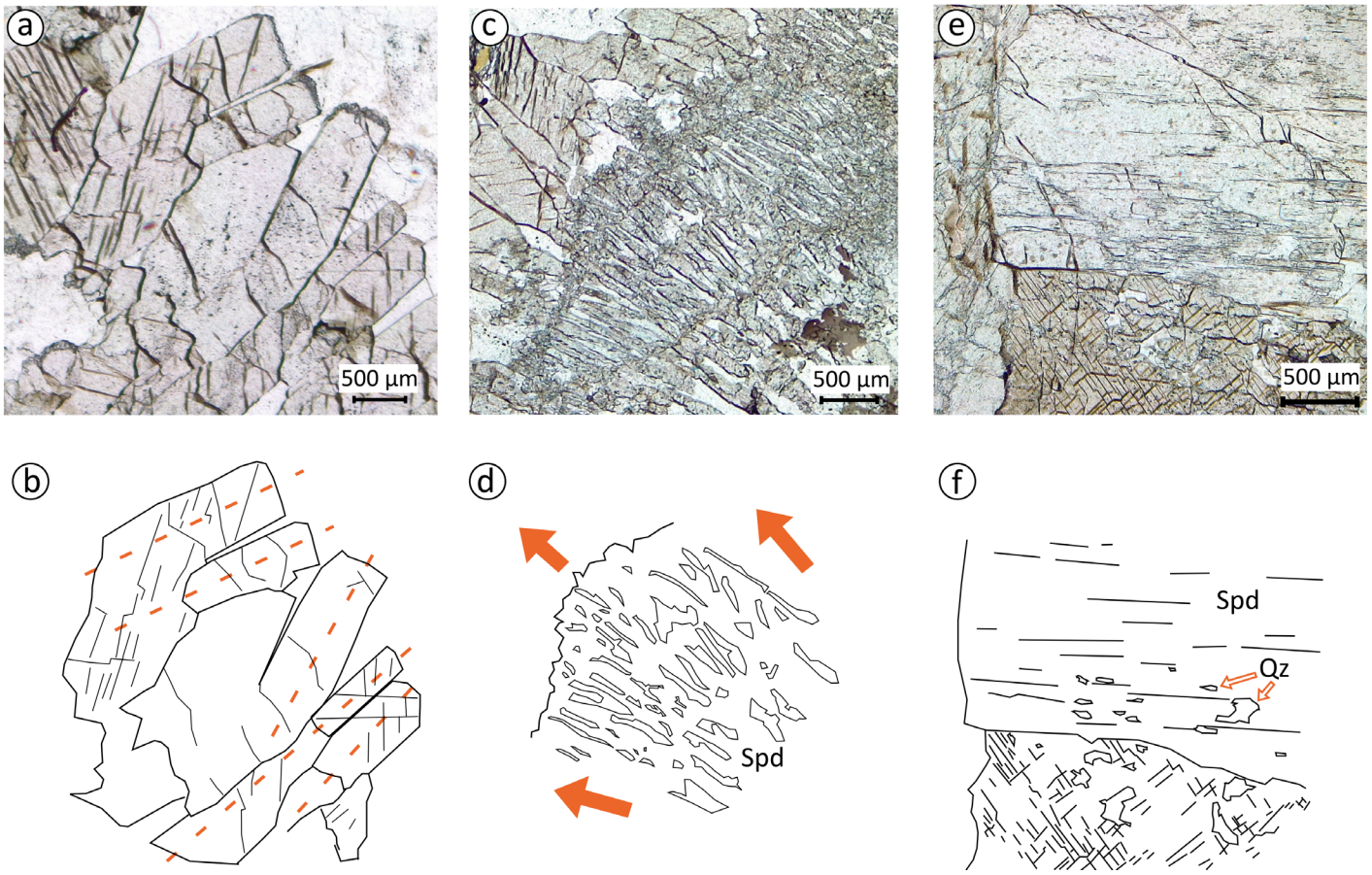

Figure GS2022-4-5: *Photomicrographs and schematic representations of different varieties of spodumene-quartz intergrowth (SQUI; adapted from Breasley et al., 2022b):* ***a)*** *PPL image of classic SQUI;* ***b)*** *digitization of representative classic SQUI showing strong crystallographic orientation of growth (orange dashed line);* ***c)*** *PPL image of micro-SQUI;* ***d)*** *digitization of representative micro-SQUI showing radial symplectic growth (highlighted by orange arrows);* ***e)*** *PPL image of equant SQUI;* ***f)*** *digitization of representative equant SQUI showing interlocking boundaries with surrounding crystals. Abbreviations: PPL, plane polarized light; Qz, quartz; Spd, spodumene.*

obviously elongated crystals of spodumene (<20–50 µm in length). Samples have a high internal textural variability and are in both sharp and gradational breakdown contacts with classic SQUI. In thin section, the micro-SQUI texture is interpreted to represent fluid-flow pathways, with microcrystalline reprecipitation of minerals (Figure GS2022-4-5c).

3) Equant SQUI (Figure GS2022-4-5e, f) shows angular crystal boundaries, and spodumene and quartz are not intimately intergrown. Spodumene crystals grew contemporaneously with quartz, and crystals are in planar contact. Spodumene contains micro inclusions of quartz, eucryptite and mica that lack preferred orientation.

4) Primary spodumene forms larger platy crystals of monomineralic spodumene. It is locally found in association with quartz, but commonly occurs as large monomineralic masses.

Cathodoluminescence imaging and electron probe microanalysis

The use of cathodoluminescence (CL) imaging revealed highly complex internal zoning within spodumene grains (Figure GS2022-4-6). The internal zoning can be caused by trace-element variations within the spodumene, as well as structural variations (Wise and Brown, 2019). Electron probe microanalysis (EPMA) of the spodumene showed minimal variation of bulk elements between spodumene from all sample groups. The silicate values of all EPMA points were averaged for internal LA-ICP-MS calibration.

Laser-ablation inductively coupled plasma–mass spectrometry

Trace-element compositions of spodumene were determined using a combination of LA-ICP-MS points and linear ablations. Due to mass interferences, two ablations were used per point and line to minimize data error (low resolution: 55 µm, and medium resolution: 80 µm). Similar CL-zoned regions were selected for each resolution, to maximize comparability of points between low and medium resolutions. The external standard used was NIST 610 synthetic glass; the internal standard used was silicate values from EPMA. A known 'unknown' of BCR basalt (400 ppm Li) was also used as an internal standard. The low-resolution data acquisition included analyses for Li, Be, Mg, Al, Mn,

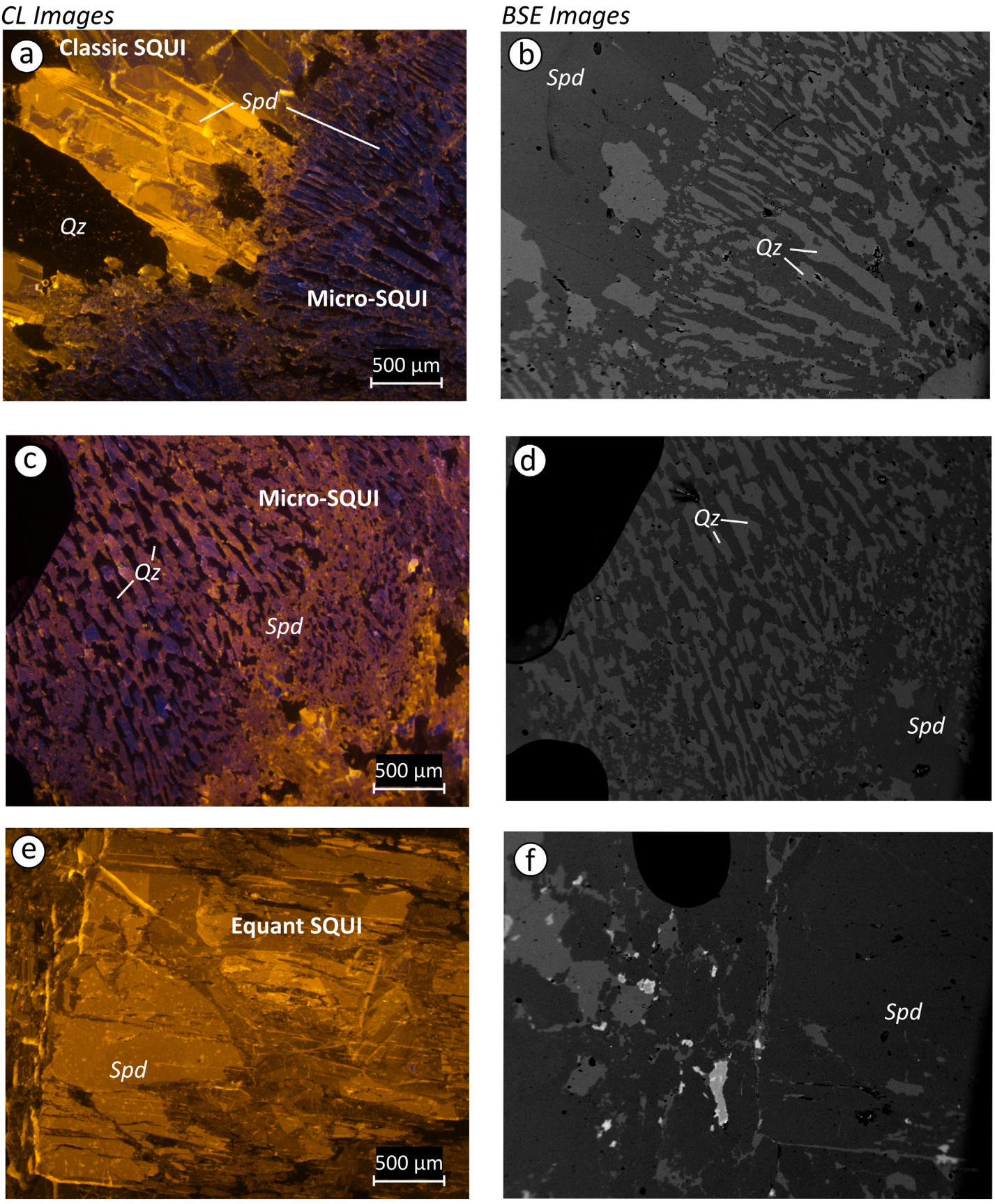

Figure GS2022-4-6: *Cathodoluminescence (CL) and backscattered electron (BSE) imagery of different spodumene samples (all photos are at the same scale):* ***a)*** *sample 22 SII SQUI A showing classic SQUI and second generation of micro-SQUI growth (blue symplectite fan);* ***b)*** *BSE image of classic and micro-SQUI showing notable lack of zonation;* ***c)*** *sample 91-14 B4C1 C showing micro-SQUI texture;* ***d)*** *BSE image of micro-SQUI;* ***e)*** *sample 91-9 B4C1 K showing equant SQUI with chaotic zonation;* ***f)*** *BSE image of equant SQUI. Abbreviations: Qz, quartz; Spd, spodumene.*

Co, Ni, Zn, Rb, Zr, Sn, Cs, Ba, Hf, Ta and Tl. Medium-resolution measurements included Na, K, V, Cr, Fe, Ge and Nb.

Preliminary results

Classic and micro-SQUI are generally geochemically similar when found adjacent to one another in thin section but show different concentrations of Mn, Sn and Ge. Green classic SQUI show highest Fe contents in all of the classic SQUI category. Equant SQUI show little geochemical trace-element similarities to classic and micro-SQUI.

Future work

Subsequent studies will further utilize micro-CT to visualize and quantify the variable proportions of spodumene to quartz in SQUI. Breasley et al. (2021, 2022a) showed that the density differences between spodumene and quartz crystals are sufficient to provide contrast on micro-CT scans in 2-D and 3-D to an impressive level of detail. This method will be developed and used to create 3-D renderings of the different groups of SQUI presented in this report. Origins and formation conditions of the spodumene, and textural and geochemical variability of the different groups will be examined and delineated. The abundance of SQUI at Tanco provides a unique opportunity to constrain this information.

Studying the variety of Li-bearing minerals will give insight into the Li partitioning between crystalline phases during melt crystallization and subsequent metasomatism. Microprobe analysis, LA-ICP-MS, and powder X-ray diffraction will aid in this part of the study, as well as the attempt to identify petalite.

Economic considerations

Pegmatites are lucrative exploration targets because of their potential to host significant enrichments of critical elements (Linnen et al., 2012). Lithium, cesium and tantalum are all recognized as critical minerals by the Government of Canada (2021). This project focuses on lithium, which is currently used mainly in rechargeable batteries (U.S. Geological Survey, 2022). This battery technology will undoubtedly play a significant role as the world transitions to a decarbonized economy (Zubi et al., 2018). Therefore, studying pegmatites that contain economic quantities of these elements will be key to maintaining the economic competitiveness and resource security of Canada into the future. Minor associations of other economically important elements at Tanco are notable, such as Be and Rb.

The province of Manitoba has multiple sources of Li associated with Li-bearing pegmatites and brines (Manitoba Geological Survey, 2022). The Tanco pegmatite, which is the focus of this study, is the most economically viable. The research avenues detailed in this report explore the nature of Li mineralization and distribution trends within Tanco, which will have implications for targeting and understanding Li sources elsewhere. Future work will help confirm the trends seen in the mine and allow the quantification of Li in different minerals to show the behaviour of the highly volatile nature of this element during primary crystallization and post-crystallization remobilization.

Acknowledgments

The authors sincerely thank the Tanco Sinomine team for their enthusiasm and support in this project, notably S. Rankmore and J. Champagne. Special gratitude is extended to C. Deveau (Sinomine Resource Group Co. Ltd.) for continued support in this project. The geology team at Tanco, including A. Hutchins and I. Zhou, were invaluable in assisting at the mine and discussing ideas. A debt of gratitude is extended to all employees at the Tanco mine, without whom this project could have never taken place. Thanks are extended to the Manitoba Geological Survey for their continuing logistical and field support. The authors also extend their thanks towards T. Hnatiuk for valuable field assistance and to P. Yang for aid with analyses from the University of Manitoba. Edits provided by E. Yang and C. Böhm assisted in improving drafts of this manuscript. RnD Technical editing services are acknowledged for assistance in editorial work, and C. Steffano is thanked for layout and final edits.

References

Breasley, C.M., Martins, T., Groat, L.A. and Linnen, R.L. 2021: Results of a preliminary investigation into the lithium mineralization, distribution trends and remobilization in the Tanco pegmatite, southeastern Manitoba (part of NTS 52L6); *in* Report of Activities 2021, Manitoba Agriculture and Resource Development, Manitoba Geological Survey, p. 8–17, URL <https://manitoba.ca/iem/geo/field/roa21pdfs/GS2021-2.pdf> [May 2022].

Breasley, C.M., Linnen, R.L., Barker, I.R., Groat, L.A. and Martins, T. 2022a: Utilizing X-ray computed tomography to visualise lithium silicate minerals: insights into mineralization at the Tanco pegmatite, Manitoba; AME Roundup 2022, January 31–February 3, 2022, Vancouver, British Columbia, poster presentation.

Breasley, C.M., Martins, T., Linnen, R.L. and Groat, L.A. 2022b: Textures and trace element geochemistry of spodumene at the Tanco pegmatite, Manitoba, Canada; Goldschmidt 2022, July 10–15, 2022, Honolulu, Hawaii, poster presentation.

Camacho, A., Baadsgaard, H., Davis, D.W. and Černý, P. 2012: Radiogenic isotope systematics of the Tanco and Silverleaf granitic pegmatites, Winnipeg River pegmatite district, Manitoba; The Canadian Mineralogist, v. 50, no. 6, p. 1775–1792.

Černá, I. 1970: Mineralogy and paragenesis of amblygonite-montebrasite with special reference to the Tanco (chemalloy) pegmatite, Bernic Lake, Manitoba; M.Sc. thesis, University of Manitoba, Winnipeg, Manitoba, 90 p.

Černá, I., Černý, P. and Ferguson, R.B. 1972: The Tanco pegmatite at Bernic Lake, Manitoba, III – Amblygonite-montebrasite; The Canadian Mineralogist, v. 11, no. 3, p. 643–659.

Černý, P. 1972: The Tanco pegmatite at Bernic Lake, Manitoba, VII – Eucryptite; The Canadian Mineralogist, v. 11, no. 3, p. 708–713.

Černý, P. 2005: The Tanco rare-element pegmatite deposit, Manitoba: regional context, internal anatomy, and global comparisons; *in* Rare-Element Geochemistry and Mineral Deposits, R.L. Linnen and I.M. Samson (ed.), Geological Association of Canada, Short Course Notes, v. 17, p. 127–158.

Černý, P. and Ercit, T.S. 2005: The classification of granitic pegmatites revisited; The Canadian Mineralogist, v. 43, no. 6, p. 2005–2026.

Černý, P. and Ferguson, R.B. 1972: The Tanco pegmatite at Bernic Lake, Manitoba, IV – Petalite and spodumene relations; The Canadian Mineralogist, v. 11, no. 3, p. 660–678.

Černý, P. and London, D. 1983: Crystal chemistry and stability of petalite; Tschermaks mineralogische und petrographische Mitteilungen, v. 31, no. 1, p. 81–96.

Černý, P., Ercit, T.S. and Vanstone, P.T. 1996: Petrology and mineralization of the Tanco rare element pegmatite, southeastern Manitoba; Geological Association of Canada–Mineralogical Association of Canada, Joint Annual Meeting, May 27–29, 1996, Winnipeg, Manitoba, Field Trip Guidebook A4.

Černý, P., Ercit, T. and Vanstone, P. 1998: Mineralogy and petrology of the Tanco rare-element pegmatite deposit, southeastern Manitoba; International Mineralogical Association, 17th General Meeting, August 10, 1998, Toronto, Ontario, Field Trip Guidebook B6, 74 p.

Černý, P., Trueman, D.L., Ziehlke, D.V., Goad, B.E. and Paul, B.J. 1981: The Cat Lake–Winnipeg River and the Wekusko Lake pegmatite fields, Manitoba; Manitoba Energy and Mines, Manitoba Resources Division, Economic Geology Report ER80-1, 215 p., URL <https://manitoba.ca/iem/info/libmin/ER80-1.zip> [May 2022].

Gilbert, H.P. 2006: Geological investigations in the Bird River area, southeastern Manitoba (parts of NTS 52L5N and 6); *in* Report of Activities 2006, Manitoba Science, Technology, Energy and Mines, Manitoba Geological Survey, p. 184–205, URL <https://manitoba.ca/iem/geo/field/roa06pdfs/GS-17.pdf> [May 2022].

Gilbert, H.P. 2007: Stratigraphic investigations in the Bird River greenstone belt, Manitoba (part of NTS 52L5, 6); *in* Report of Activities 2007, Manitoba Science, Technology, Energy and Mines, Manitoba Geological Survey, p. 129–143, URL <https://manitoba.ca/iem/geo/field/roa07pdfs/GS-12.pdf> [May 2022].

Gilbert, H.P. 2008: Stratigraphic investigations in the Bird River greenstone belt, Manitoba (part of NTS 52L5, 6); *in* Report of Activities 2008, Manitoba Science, Technology, Energy and Mines, Manitoba Geological Survey, p. 121–138, URL <https://manitoba.ca/iem/geo/field/roa08pdfs/GS-11.pdf> [May 2022].

Government of Canada 2021: Critical minerals, URL <https://www.nrcan.gc.ca/criticalminerals> [March 2021].

Kremer, P.D. 2010: Structural geology and geochronology of the Bernic Lake area in the Bird River greenstone belt, Manitoba: evidence for syn-deformational emplacement of the Bernic Lake pegmatite group; M.Sc. thesis, University of Waterloo, Waterloo, Ontario, 91 p.

Linnen, R.L., Van Lichtervelde, M. and Černý, P. 2012: Granitic pegmatites as sources of strategic metals; Elements, v. 8, no. 4, p. 275–280.

London, D. 1986: Magmatic-hydrothermal transition in the Tanco rare-element pegmatite: evidence from fluid inclusions and phase-equilibrium experiments; American Mineralogist, v. 71, no. 3–4, p. 376–395.

London, D. 1990: Internal differentiation of rare-element pegmatites: a synthesis of recent research; *in* Ore-bearing Granite Systems: Petrogenesis and Mineralizing Processes, H.J. Stein and J.L. Hannah (ed.), Geological Society of America, Special Paper, v. 246, p. 35–50.

London, D. 2008: Rare-element pegmatites; Chapter 7 *in* Pegmatites, The Canadian Mineralogist, Special Publication 10, p. 108–114.

Manitoba Geological Survey 2022: Lithium in Manitoba; Manitoba Natural Resources and Northern Development, Manitoba Geological Survey, URL <https://manitoba.ca/iem/geo/lithium/index.html> [June 2022].

Martins, T., Kremer, P. and Vanstone, P. 2013: The Tanco mine: geological setting, internal zonation and mineralogy of a world-class rare element pegmatite deposit; Geological Association of Canada–Mineralogical Association of Canada, Joint Annual Meeting, May 22–24, 2013, Field Trip Guidebook FT-C1; Manitoba Innovation, Energy and Mines, Manitoba Geological Survey, Open File OF2013-8, 17 p., URL <https://manitoba.ca/iem/info/libmin/gacmac/OF2013-8_FT-C1.pdf> [May 2022].

Morgan, G.B. and London, D. 1987: Alteration of amphibolitic wallrocks around the Tanco rare-element pegmatite, Bernic Lake, Manitoba; American Mineralogist, v. 72, no. 11–12, p. 1097–1121.

Ramik, R.A., Sturman, B.D., Dunn, P.J. and Povarennykh, A.S. 1980: Tancoite, a new lithium sodium aluminum phosphate from the Tanco pegmatite, Bernic Lake, Manitoba; The Canadian Mineralogist, v. 18, no. 2, p. 185–190.

Rinaldi, R., Černý, P. and Ferguson, R.B. 1972: The Tanco pegmatite at Bernic Lake, Manitoba, VI – Lithium-rubidium-cesium micas; The Canadian Mineralogist, v. 11, no. 3, p. 690–707.

Selway, J.B., Novák, M., Černý, P. and Hawthorne, F.C. 2000a: The Tanco pegmatite at Bernic Lake, Manitoba, XIII – Exocontact tourmaline; The Canadian Mineralogist, v. 38, no. 4, p. 869–876.

Selway, J.B., Černý, P., Hawthorne, F.C. and Novák, M. 2000b: The Tanco pegmatite at Bernic Lake, Manitoba, XIV – Internal tourmaline; The Canadian Mineralogist, v. 38, no. 4, p. 877–891.

Simpson, F.M. 1974: The mineralogy of pollucite and beryl from the Tanco pegmatite at Bernic Lake, Manitoba; M.Sc. thesis, University of Manitoba, Winnipeg, Manitoba, 71 p.

Stilling, A., Ćerný, P. and Vanstone, P.J. 2006: The Tanco pegmatite at Bernic Lake, Manitoba, XVI – Zonal and bulk compositions and their petrogenetic significance; The Canadian Mineralogist, v. 44, no. 3, p. 599–623, URL <https://doi.org/10.2113/gscanmin.44.3.599>.

U.S. Geological Survey 2022: Final list of critical minerals 2022; International Energy Agency, URL <https://www.iea.org/policies/15271-final-list-of-critical-minerals-2022> [June 2022].

Van Lichtervelde, M., Salvi, S., Beziat, D. and Linnen, R.L. 2007: Textural features and chemical evolution in tantalum oxides: magmatic versus hydrothermal origins for Ta mineralization in the Tanco Lower Pegmatite, Manitoba, Canada; Economic Geology, v. 102, no. 2, p. 257–276.

Van Lichtervelde, M., Grégoire, M., Linnen, R.L., Béziat, D. and Salvi, S. 2008: Trace element geochemistry by laser ablation ICP-MS of micas associated with Ta mineralization in the Tanco pegmatite, Manitoba, Canada; Contributions to Mineralogy and Petrology, v. 155, no. 6, p. 791–806.

Wise, M.A. and Brown, C.D. 2019: Cathodoluminescence (CL) microscopy–a technique for understanding the dynamics of pegmatite crystallization; The Canadian Mineralogist, v. 57, no. 5, p. 821–823.

Zubi, G., Dufo-López, R., Carvalho, M. and Pasaoglu, G. 2018: The lithium-ion battery: state of the art and future perspectives; Renewable and Sustainable Energy Reviews, v. 89, p. 292–308.

GS2022-5

Critical minerals scoping study of the Suwannee River syenite intrusion, west-central Manitoba (part of NTS 64B4)

by T. Martins and C.G. Couëslan

Summary

In the summer of 2022, a reconnaissance study was carried out focusing on the Suwannee River syenite intrusion, one of several syenite bodies in the Kisseynew domain of Manitoba. These types of intrusions can be associated with rare-earth–element mineralization. Rare-earth elements are considered critical by the governments of Manitoba and Canada. Field observations of the Suwannee River syenite were hindered by extensive lichen and moss coverage. The Suwannee River syenite is composed of a main hornblende-bearing phase that seems to be dominant in the majority of outcrops. Two additional phases of the syenite include a more leucocratic phase and a phase characterized by equant mafic clots. A similar syenite with mafic clots is also observed at other syenite complexes in the Kisseynew domain. The Suwannee River syenite is crosscut by leucogranite and pegmatite at various scales. Future work will include whole-rock geochemistry, petrography and isotope-geochronology studies.

In Brief:

- Detailed field description of Suwannee River syenite is presented; the syenite has not been studied since 1972
- The MGS continuously studies syenitic intrusions from the Kisseynew domain with potential to host critical mineral mineralization
- Goals of this study are understanding economic importance of syenite intrusions and its tectonic significance in the Trans-Hudson orogen

Citation:
Martins, T. and Couëslan, C.G. 2022: Critical minerals scoping study of the Suwannee River syenite intrusion, west-central Manitoba (part of NTS 64B4); *in* Report of Activities 2022, Manitoba Natural Resources and Northern Development, Manitoba Geological Survey, p. 36–41.

Introduction

This report summarizes the preliminary findings of a critical minerals scoping study of the Suwannee River syenite in west-central Manitoba during July of 2022. The Suwannee River syenite is located roughly 38 km south of Leaf Rapids. The syenite outcrops are exposed over an area approximately 1.56 km in length and 1.27 km in width, and are only accessible by air. The area was mapped by Schledewitz (1972) and has not been studied in detail since then. The primary objective of this project is to examine the intrusive body along the Suwannee River for its potential to host critical element mineralization.

The rare-earth elements (REEs) are a group of elements considered critical for Manitoba (Manitoba Geological Survey, 2022b) and for Canada (Government of Canada, 2021). The current findings are part of a larger study initiated by the Manitoba Geological Survey (MGS) in 2011 that focuses on rare metals and the economic potential of different rocks that host critical elements in various parts of the province (Manitoba Geological Survey, 2022c). The Kisseynew domain (KD) in Manitoba hosts several syenite occurrences with potential for REE mineralization (e.g., Martins et al., 2011).

Geological setting

The Suwannee River syenite (Figure GS2022-5-1), mapped by Schledewitz (1972), is located in the north flank of the KD, a division proposed by Zwanzig (2008). The KD is a metasedimentary basin in the internal zone of the Trans-Hudson orogen dominated by metamorphosed greywacke and mudstone of the Burntwood group, which is interpreted to have been deposited in coalescing turbidite fans (Bailes, 1980; Zwanzig, 1999). The Burntwood group was deposited between ca. 1860 and 1840 Ma (Machado et al., 1999). Early folding and thrusting (D_1) occurred during 1842–1835 Ma and predated peak metamorphism in the KD. The D_1 deformation phase was accompanied by the intrusion of calcalkaline plutons from ca. 1840 to 1820 Ma. The youngest calcalkaline intrusions in the KD are represented by the enderbitic Touchbourne suite, which was intruded prior to the main tectonometamorphic event between ca. 1830 and 1820 Ma (Gordon et al., 1990; Machado et al., 1999). Two generations of nappe-like folding (F_2–F_3, 1820–1800 Ma) were accompanied by the intrusion of peraluminous granitoids (1820–1810 Ma; Kraus and Menard, 1997; White, 2005). The majority of the KD experienced low-pressure granulite-facies metamorphic conditions of 750 ±50°C and 5.5 ±1.0 kbar (Gordon, 1989) following D_2 (White, 2005). Peak metamorphic conditions continued through D_3. Folding and faulting continued during D_4 and D_5 until after ca. 1790 Ma (Zwanzig, 1999).

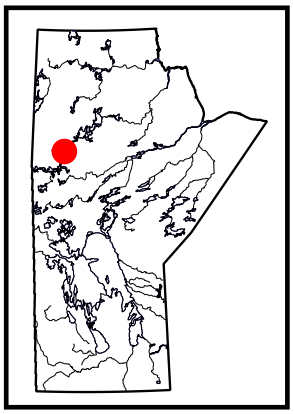

The tectonic setting of the Kisseynew basin continues to be a matter of debate. It has been interpreted as a back-arc basin to the Flin Flon volcanic-arc domain (e.g., Ansdell et al., 1995; Ansdell, 2005; Corrigan et al., 2009). However, intra-arc– and forearc-basin–environments were also proposed

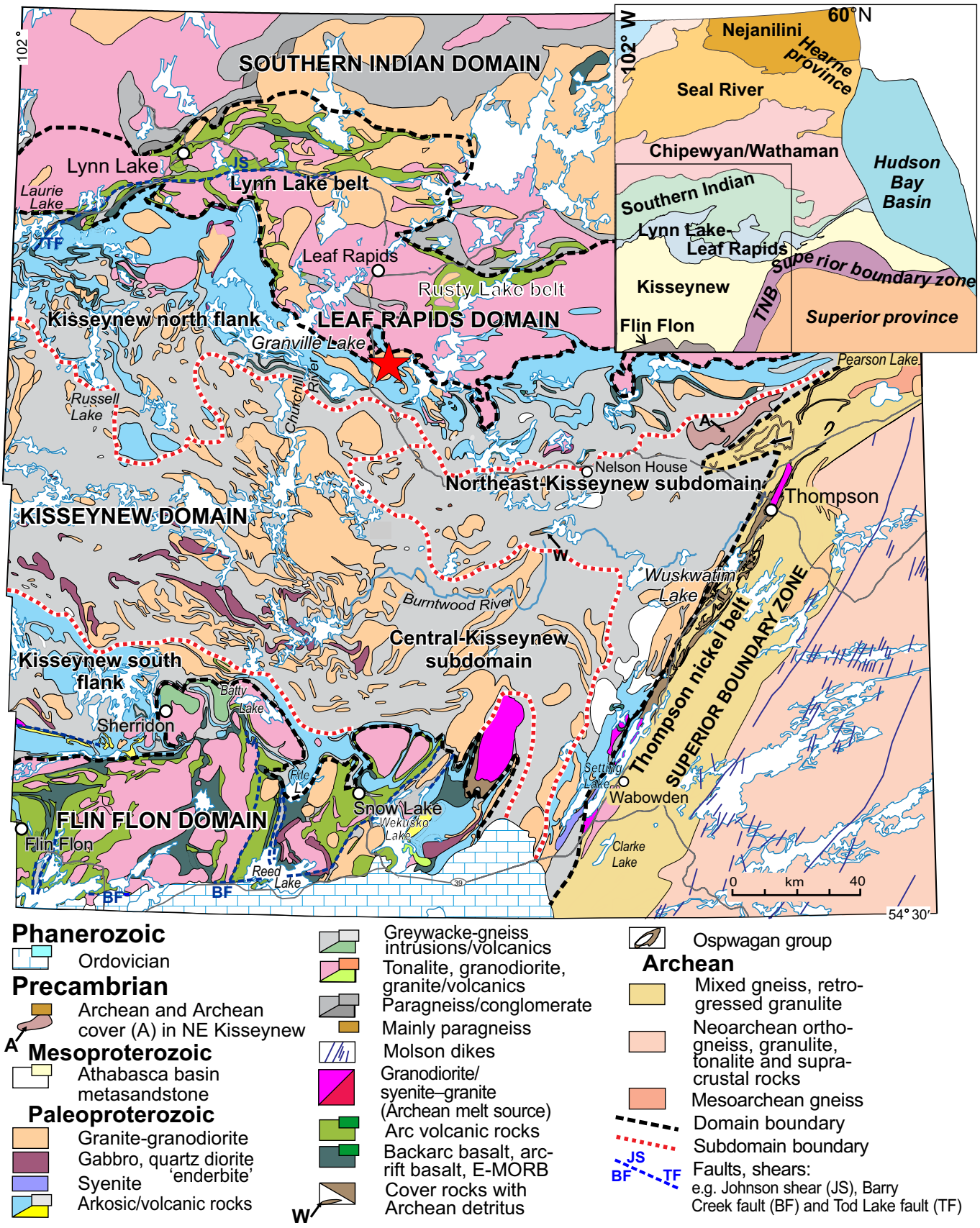

Figure GS2022-5-1: *Geology of the Kisseynew and surrounding domains, simplified and modified after Murphy and Zwanzig (2021). The location of the Suwannee River syenite is indicated with a star. The inset shows the domains of the Trans-Hudson orogen in Manitoba (after Manitoba Geological Survey, 2022a), with the location of the figure outlined. Abbreviations: E-MORB, enriched mid-ocean–ridge basalt; NE, northeastern; TNB, Thompson nickel belt; W, Wuskwatim Lake sequence.*

for the development of the KD, with a complex evolution during continental convergence and collision (Zwanzig, 1999; Zwanzig and Bailes, 2010; Murphy and Zwanzig, 2021).

Geology of the Suwannee River syenite

Schledewitz (1972) described the Suwannee River intrusion as a pear-shaped body of hornblende syenite occurring north of the Suwannee River. It is clearly defined in regional geophysical surveys by its intermediate magnetic intensity (Geological Survey of Canada, 1963) compared to the surrounding granitoid rocks. The body appears to be bound along its western margin by a fault, as indicated by a strong north-trending topographic lineament (Figure GS2022-5-2) and an abrupt aeromagnetic gradient (Schledewitz, 1972). Geological mapping by Schledewitz (1972) suggests that the syenite is surrounded by foliated quartz monzonite and granite. The foliation in the country rocks is interpreted as conformable with the margin of the syenite body; however, the contacts are not exposed.

The outcrops in the study area are extensively covered in lichen and moss, and surrounded by mature forest. These conditions make full and detailed observations of the outcrops difficult. The rock surrounding the syenite intrusion appears to consist of homogeneous pink granite that is coarse grained to pegmatitic, weakly foliated and magnetic. In an outcrop along the west side of the syenite intrusion (station 113-22-001; Figure GS2022-5-2), the granite is characterized by a weak, steeply dipping and northeast-trending fabric. The granite is composed of quartz (20–35%), biotite (3–5%), similar amounts of K-feldspar and plagioclase, and trace amounts of magnetite.

From the limited outcrop observations, the main phase of the syenite is relatively homogeneous, dark pink when fresh (locally reddish pink), buff-pink weathered, medium grained, foliated and locally magnetic (Figure GS2022-5-3a). It is composed of K-feldspar and plagioclase (40–50%), hornblende (10–20%), quartz (10–15%), clinopyroxene (7–15%), biotite (2–5%), titanite (1%), allanite (trace–1%) and trace amounts of magnetite. The mafic phases (i.e., hornblende, clinopyroxene, titanite and alla-

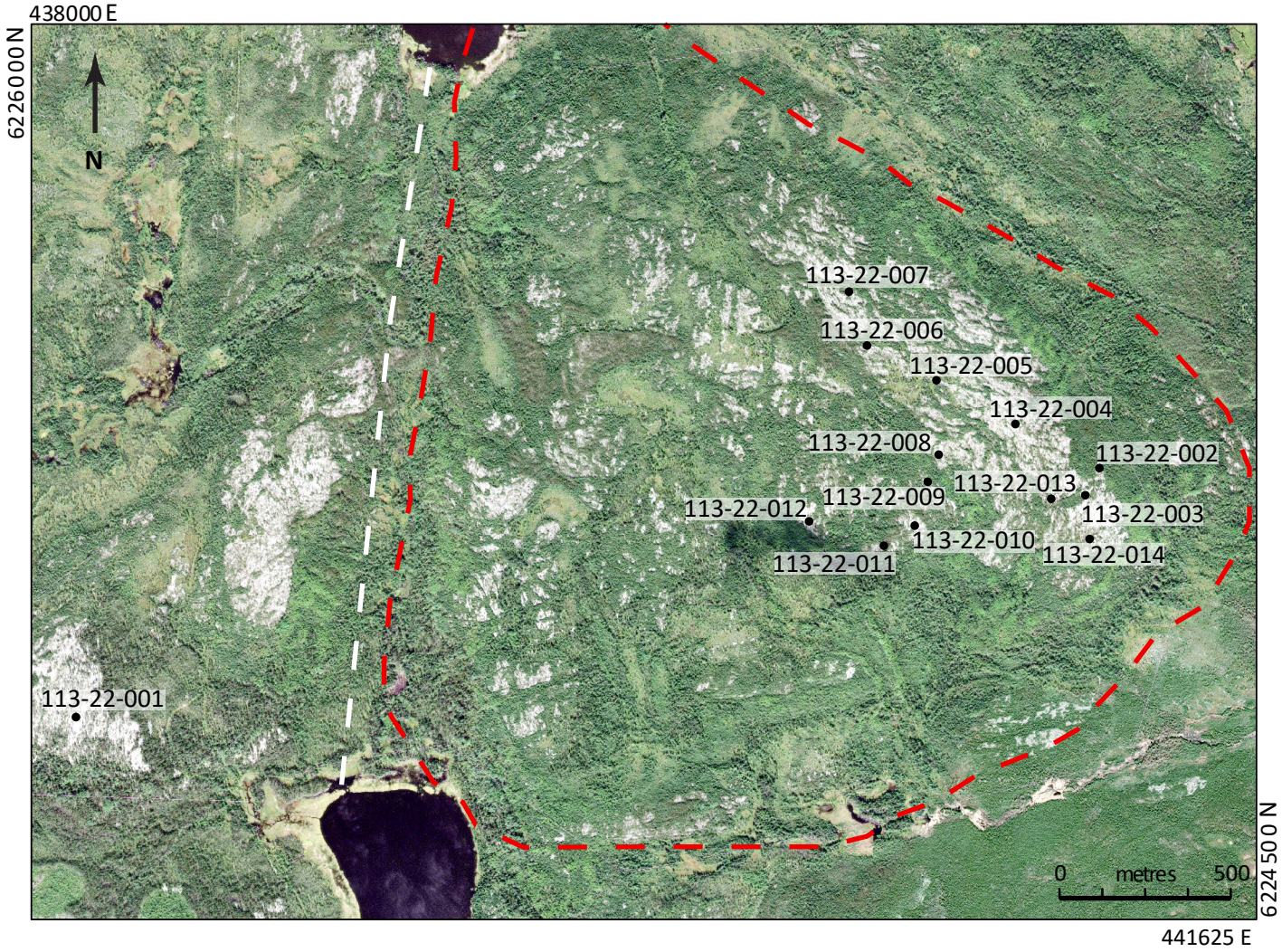

Figure GS2022-5-2: *Satellite image of the Suwannee River syenite. The white dashed line marks a strong topographic lineament and the red dashed line delineates the syenite body (after Schledewitz, 1972). Sources: Esri, Maxar, GeoEye, Earthstar Geographics, CNES/Airbus DS, USDA, USGS, AeroGRID, IGN, and the GIS User Community.*

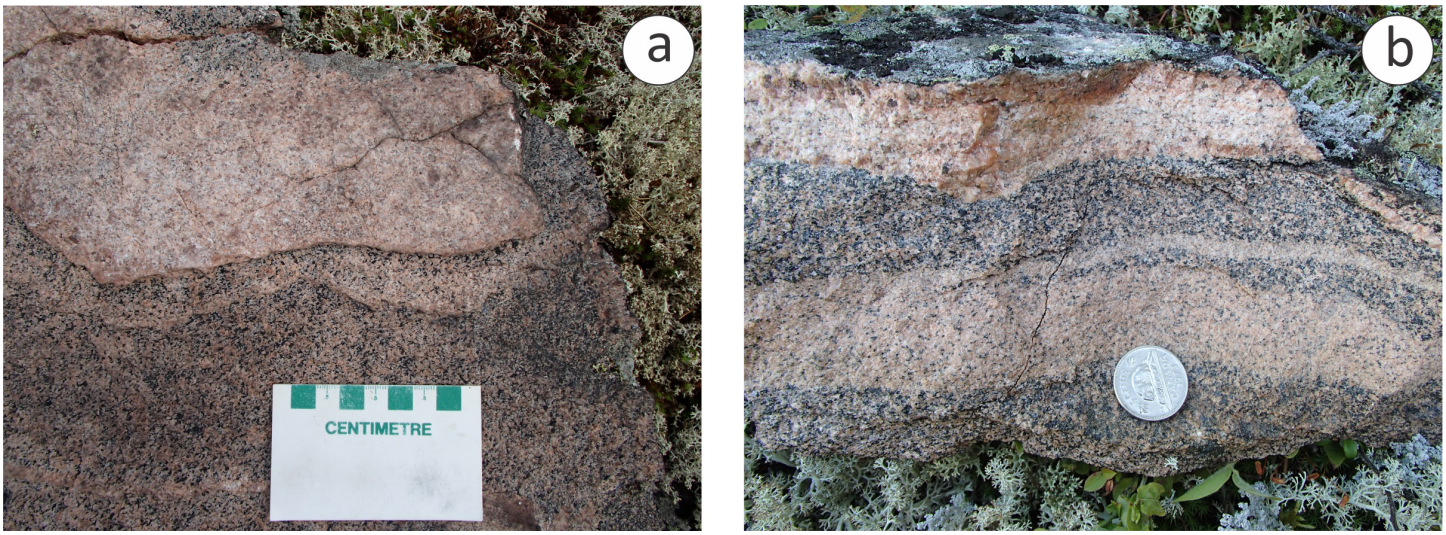

Figure GS2022-5-3: *Outcrop photographs of the main phase of the Suwannee River syenite and its textural variation:* ***a)*** *main phase of foliated hornblende syenite (under scale card), with a more leucocratic phase of the syenite at the top of the image;* ***b)*** *banded aspect of the syenite, showing alternating mafic compositions.*

nite) commonly occur as aggregates that are locally flattened and occasionally weathered to a combination of clay minerals and oxides. Local recessive weathering of the mafic minerals gives the rock a mottled appearance. In a few outcrops, the syenite shows vuggy weathering over areas ranging from 7 to 20 cm across. The main phase of the syenite locally alternates with bands of more leucocratic syenite (Figure GS2022-5-3b). The more leucocratic phase is pink, medium grained and foliated. Composition is similar to the main phase of syenite: K-feldspar and plagioclase (50–60%), hornblende (5–10%), quartz (10–15%), clinopyroxene (7–10%), biotite (2–5%), titanite (1%) and trace amounts of allanite and magnetite.

Another syenite phase, characterized by equant mafic clots composed of mostly hornblende, was observed at a few stations (Figure GS2022-5-4a). It contains K-feldspar (50–60%), quartz (20–30%), hornblende (7–10%) and trace amounts of titanite. A syenite phase with a similar texture was previously described at Eden Lake (colloquially called 'chicken pox' syenite; Couëslan, 2005; Mumin, 2010) and was also recently discovered at Brezden Lake (Hnatiuk et al., 2022). This syenitic phase is either cut by the main phase of the syenite body or contains xenoliths of the main phase. Limited outcrop exposures do not allow for definitive interpretation. Schledewitz (1972) described a similar phase of the syenite with a pink feldspathic groundmass distinctively spotted with equant greenish black hornblende.

A clinopyroxene-rich rock was identified in one outcrop at the contact with a pegmatite dike and a xenolith of quartz-rich biotite gneiss (Figure GS2022-5-4b). The clinopyroxene-rich rock is dark green, coarse to very coarse grained, massive and nonmagnetic. Clinopyroxene forms discrete euhedral prisms varying in size from 1 to 3 cm. This coarse-grained rock contains clinopyroxene (30–60%), quartz (10–20%), K-feldspar (10–20%), titanite (2–3%) and allanite (trace–1%). It is possible that this rock is the product of alkali metasomatism.

Leucogranite (Figure GS2022-5-4c) crosscuts the main phase of the syenite. This was also observed by Schledewitz (1972), who described the syenite as cut by fine-grained microcline-quartz veins and dikes. The leucogranite is pink, coarse grained, nonmagnetic and massive. It contains K-feldspar (40–60%), quartz (30–40%), plagioclase (10–15%), hornblende (2–5%), clinopyroxene (1–2%), allanite (trace–2%) and titanite (trace amounts). Quartz often occurs as discrete equant crystals. Allanite occurs as glassy to resinous black grains up to 2 mm in size. The leucogranite locally forms the dominant phase of outcrops and contains rafts of the main-phase syenite <1 m across. Pegmatite dikes (up to 1.5 m in width) also crosscut the main phase of the syenite. The granitic pegmatite contains quartz, feldspars and muscovite, and has pods of massive quartz <30 cm thick that locally form the cores of dikes. Other pegmatite dikes contain a core area enriched in K-feldspar (or possibly plagioclase stained by Fe oxides) with albitic rims, and were observed with comb-textured feldspar at the contacts with the syenite (Figure GS2022-5-4d).

Economic considerations

In 2021, the Government of Canada released a list of 31 elements considered critical for the sustainable economic success of the country and its allies, and to position Canada as a leading mining nation (Government of Canada, 2021). Rare-earth elements are part of this list and are used for a number of applications, most notably permanent magnets and batteries (Alonso et al., 2012), which are essential for the transition to clean energies and decarbonization of Canada's economy. Canada continues to renew its intention to grow domestic and global supply chains for the green and digital economy, as highlighted in the govern-

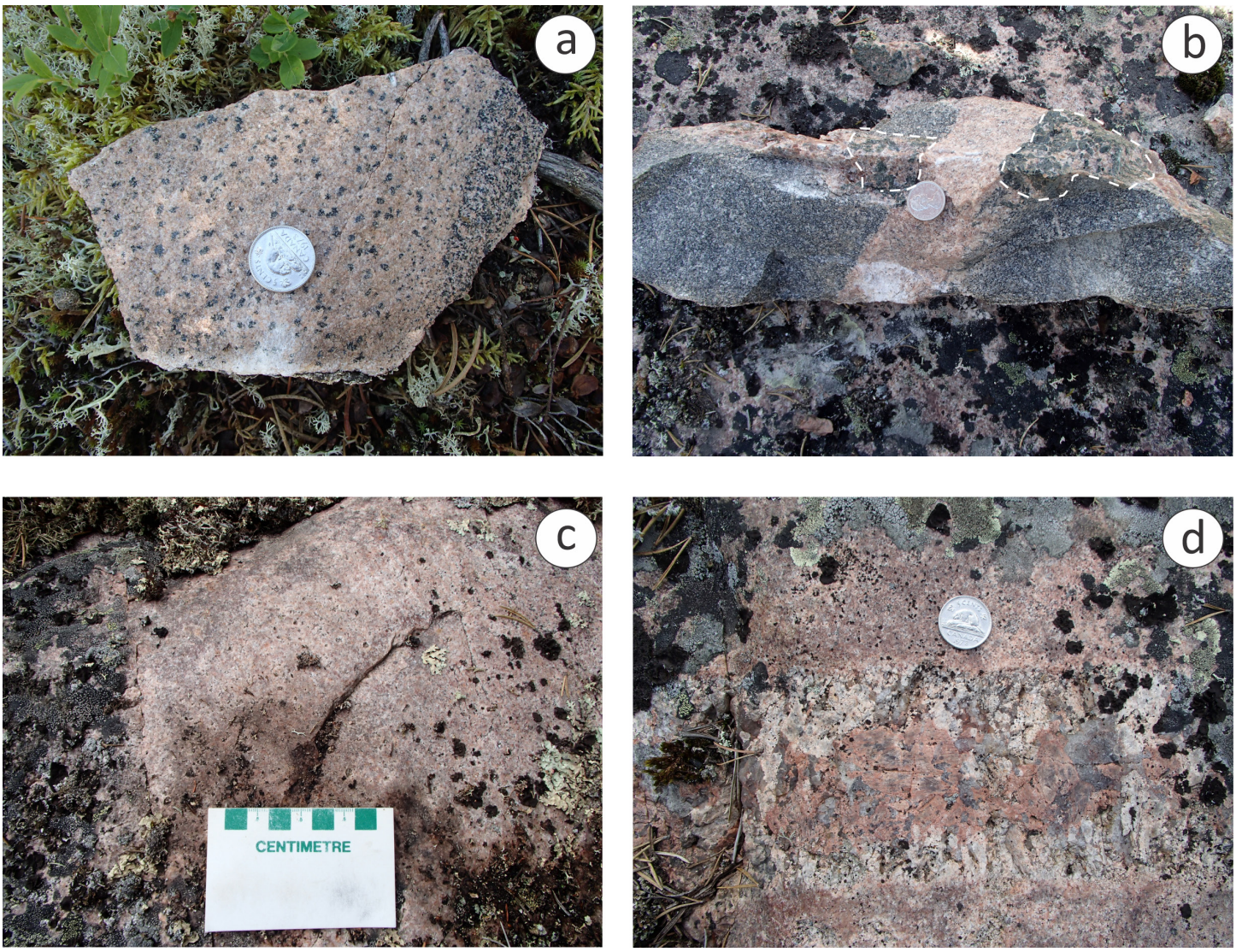

Figure GS2022-5-4: *Outcrop photographs of the Suwannee River syenite with textural variations and later intrusive phases:* ***a)*** *syenite phase with equant mafic clots;* ***b)*** *very coarse grained clinopyroxene rock (outlined in white) at the contact with pegmatite and a raft of quartz-rich biotite gneiss;* ***c)*** *detail of the leucogranite;* ***d)*** *crosscutting granitic pegmatite with pink feldspar core.*

ment's most recent discussion paper (Government of Canada, 2022).

Preliminary results from fieldwork suggest that the mineralogy (e.g., clinopyroxene, titanite, allanite) and some textures (e.g., mafic clots) of the Suwannee River syenite are similar to those of the syenite bodies observed at Brezden Lake (Martins et al., 2012; Hnatiuk et al., 2022), Burntwood Lake (Martins et al., 2011) and Eden Lake (Chakhmouradian et al., 2008), which are known for their potential to host REE mineralization. Future work planned for the Suwannee River syenite includes whole-rock geochemical analyses from representative samples, along with detailed petrographic work from thin sections. Additional analyses could include Sm-Nd isotopes and in-situ laser-ablation geochronology studies. Results from these studies will help in understanding the full economic potential of the Suwannee River syenite and its tectonic implications.

Acknowledgments

Field logistical support and services provided at the Manitoba Geological Survey's Midland Sample and Core Library (Winnipeg, Manitoba) by C. Epp and P. Belanger were essential for the success of this project. The GIS support provided by L. Chackowsky and H. Adediran is truly appreciated. Edits by T. Kennedy and C. Böhm helped improve earlier drafts of the manuscript. RnD Technical provided technical editing services. C. Steffano took great care of the layout and final editing. Many thanks to T. Hnatiuk from the University of Manitoba for his competent and always enthusiastic field assistance.

References

Alonso, E., Sherman, A.M., Wallington, T.J., Everson, M.P., Field, F.R., Roth R. and Kirchain, R.E. 2012: Evaluating rare earth element availability: a case with revolutionary demand from clean technologies; Environmental Science & Technology, v. 46, no. 6, p. 3406–3414.

Ansdell, K.M. 2005: Tectonic evolution of the Manitoba-Saskatchewan segment of the Paleoproterozoic Trans-Hudson Orogen, Canada; Canadian Journal of Earth Sciences, v. 42, no. 4, p. 741–759.

Ansdell, K.M., Lucas, S.B., Connors, K. and Stern, R.A. 1995: Kisseynew metasedimentary gneiss belt, Trans-Hudson orogen (Canada): back-arc origin and collisional inversion; Geology, v. 23, no. 11, p. 1039–1043.

Bailes, A.H. 1980: Origin of early Proterozoic volcaniclastic turbidites, south margin of the Kisseynew sedimentary gneiss belt, File Lake, Manitoba; *in* Early Precambrian Volcanology and Sedimentology in the Light of the Recent, E. Dimroth, J.A. Donaldson and J. Veizer (ed.), Precambrian Research, v. 12, no. 1–4, p. 197–225.

Chakhmouradian, A.R., Mumin, A.H., Demény, A. and Elliott, B. 2008: Postorogenic carbonatites at Eden Lake, Trans-Hudson Orogen (northern Manitoba, Canada): geological setting, mineralogy and geochemistry; Lithos, v. 103, p. 503–526.

Corrigan, D., Pehrsson, S., Wodicka, N. and de Kemp, E. 2009: The Palaeoproterozoic Trans-Hudson Orogen: a prototype of modern accretionary processes; *in* Ancient Orogens and Modern Analogues, J.B. Murphy, J.D. Keppie and A.J. Hynes (ed.), Geological Society of London, Special Publications, v. 327, p. 457–479.

Couëslan, C.G. 2005: Geochemistry and petrology of the Eden Lake carbonatite and associated silicate rocks; M.Sc. thesis, University of Western Ontario, London, Ontario, 201 p.

Geological Survey of Canada 1963: Rat Lake, Manitoba; Geological Survey of Canada, Aeromagnetic Series Map, Map 2387G, scale 1:63 360.

Gordon, T.M. 1989: Thermal evolution of the Kisseynew sedimentary gneiss belt, Manitoba: metamorphism at an early Proterozoic accretionary margin; *in* Evolution of Metamorphic Belts, J.S. Daly, R.A. Cliff and B.W.D. Yardley (ed.), Geological Society of London, Special Publications, v. 43, p. 233–243.

Gordon, T.M., Hunt, P.A., Bailes, A.H. and Syme, E.C. 1990: U-Pb ages from the Flin Flon and Kisseynew belts, Manitoba: chronology of crust formation at an Early Proterozoic accretionary margin; *in* The Early Proterozoic Trans-Hudson Orogen of North America; J.F. Lewry and M.R. Stauffer (ed.), Geological Association of Canada, Special Paper 37, p. 177–199.

Government of Canada 2021: Critical minerals, URL <https://www.nrcan.gc.ca/our-natural-resources/minerals-mining/critical-minerals/23414> [July 2022].

Government of Canada 2022: Canada's critical minerals strategy: discussion paper; opportunities from exploration to recycling: powering the green and digital economy for Canada and the world, URL <https://www.canada.ca/content/dam/nrcan-rncan/documents/critical-minerals-discussion-paper-eng-2.pdf>[August 2022].

Hnatiuk, T., Couëslan, C.G., Chakhmouradian, A.R. and Martins, T. 2022: Preliminary results from targeted sampling of the Brezden Lake intrusive complex, west-central Manitoba (parts of NTS 64C4); *in* Report of Activities 2022, Manitoba Natural Resources and Northern Development, Manitoba Geological Survey, p. 42–48, URL <https://manitoba.ca/iem/geo/field/roa22pdfs/GS2022-6.pdf> [November 2022].

Kraus, J. and Menard, T. 1997: A thermal gradient at constant pressure: implications for low- to medium-pressure metamorphism in a compressional tectonic setting, Flin Flon and Kisseynew domains, Trans-Hudson Orogen, central Canada; Canadian Mineralogist, v. 5, no. 5, p. 1117–1136.

Machado, N., Zwanzig, H. and Parent, M. 1999: U-Pb ages of plutons, sedimentation, and metamorphism of the Paleoproterozoic Kisseynew metasedimentary belt, Trans-Hudson Orogen (Manitoba, Canada); Canadian Journal of Earth Sciences, v. 36, no. 11, p. 1829–1842.

Manitoba Geological Survey 2022a: Bedrock geology of Manitoba; Manitoba Natural Resources and Northern Development, Manitoba Geological Survey, Open File OF2022-2, scale 1:1 000 000, URL <https://manitoba.ca/iem/info/libmin/OF2022-2.pdf> [November 2022].

Manitoba Geological Survey 2022b: Critical minerals in Manitoba; Manitoba Agriculture and Resource Development, Manitoba Geological Survey, URL <https://manitoba.ca/iem/geo/commodity/files/comm_criticalminerals.pdf> [August 2022].

Manitoba Geological Survey 2022c: Rare metals in Manitoba; Manitoba Agriculture and Resource Development, Manitoba Geological Survey, URL <https://manitoba.ca/iem/geo/raremetals/index.html> [August 2022].

Martins, T., Couëslan, C.G. and Böhm, C.O. 2011: The Burntwood Lake alkali-feldspar syenite revisited, west-central Manitoba (part of NTS 63N8); *in* Report of Activities 2011, Manitoba Innovation, Energy and Mines, Manitoba Geological Survey, p. 79–85, URL <https://manitoba.ca/iem/geo/field/roa11pdfs/GS-8.pdf> [August 2022].

Martins, T., Couëslan, C.G. and Böhm, C.O. 2012: Rare metals scoping study of the Brezden Lake intrusive complex, western Manitoba (part of NTS 64C4); *in* Report of Activities 2012, Manitoba Innovation, Energy and Mines, Manitoba Geological Survey, p. 115–123, URL <https://manitoba.ca/iem/geo/field/roa12pdfs/GS-10.pdf> [August 2022].

Mumin, H. 2010: The Eden Lake rare metal (REE, Y, U, Th, Phosphate) carbonatite complex, Manitoba: updated report; Medallion Resources Ltd., NI 43-101 report, 110 p. plus six appendices.

Murphy, L.A. and Zwanzig, H.V. 2021: Geology of the Wuskwatim–Granville lakes corridor, Kisseynew domain, Manitoba (parts of NTS 63O, P, 64A–C); Manitoba Agriculture and Resource Development, Manitoba Geological Survey, Geoscientific Report GR2021-2, 94 p., URL <https://manitoba.ca/iem/info/libmin/GR2021-2.zip> [August 2022].

Schledewitz, D.C.P. 1972: Geology of the Rat Lake area; Manitoba Mines, Resources and Environmental Management, Mines Branch, Publication 71-2B, 57 p., URL <https://manitoba.ca/iem/info/libmin/PUB71-2B.zip> [July 2022].

White, D.J. 2005: High-temperature, low-pressure metamorphism in the Kisseynew domain, Trans-Hudson orogen: crustal anatexis due to tectonic thickening?; Canadian Journal of Earth Sciences, v. 42, no. 4, p. 707–721.

Zwanzig, H.V. 1999: Structure and stratigraphy of the south flank of the Kisseynew Domain in the Trans-Hudson Orogen, Manitoba: implications for 1.845–1.77 Ga collision tectonics; Canadian Journal of Earth Sciences, v. 36, no. 11, p. 1859–1880.

Zwanzig, H.V. 2008: Correlation of lithological assemblages flanking the Kisseynew Domain, Manitoba (parts of NTS 63N, 63O, 64B, 64C): proposal for tectonic/metallogenic subdomains; *in* Report of Activities 2008, Manitoba Science, Technology, Energy and Mines, Manitoba Geological Survey, p. 38–52, URL <https://manitoba.ca/iem/geo/field/roa08pdfs/GS-4.pdf> [July 2022].

Zwanzig, H.V. and Bailes, A.H. 2010: Geology and geochemical evolution of the northern Flin Flon and southern Kisseynew domains, Kississing–File lakes area, Manitoba (parts of NTS 63K, N); Manitoba Innovation, Energy and Mines, Manitoba Geological Survey, Geoscientific Report GR2010-1, 135 p., URL <https://manitoba.ca/iem/info/libmin/GR2010-1.zip> [July 2022].

GS2022-6

Preliminary results from targeted sampling of the Brezden Lake intrusive complex, west-central Manitoba (parts of NTS 64C4)

by T. Hnatiuk[1], C.G. Couëslan, A.R. Chakhmouradian[1] and T. Martins

Summary

The Brezden Lake intrusive complex is an alkali-rich pluton of largely syenitic composition. The complex is hosted in a granodiorite intrusion within the Burntwood group metasedimentary rocks of the Kisseynew domain. The Brezden Lake intrusive complex consists predominantly of silica-saturated syenites, which are classified into several subunits based on field, macroscopic and petrographic observations. Foliated and massive syenite, quartz syenite, calcite-bearing melasyenite and pegmatoid syenite are interpreted to represent multiple intrusive phases and products of their evolution. The syenites were intruded by dikes of lamprophyre-like rocks, akin to vogesite, and calcite-carbonatite. The discovery of carbonatite and associated fenitic alteration expands exploration potential for rare-earth elements in this part of Manitoba significantly further west of the Eden Lake carbonatitic-alkaline complex and beyond the Lynn Lake belt.

In Brief:

- The Brezden Lake intrusive complex consists predominantly of silica saturated syenites
- The syenites were intruded by dikes of lamprophyre-like rock, as well as calcite carbonatite
- The discovery of carbonatite and associated fenitic alteration indicates potential for rare-earth element mineralization

Citation:
Hnatiuk, T., Couëslan, C.G., Chakhmouradian, A.R. and Martins, T. 2022: Preliminary results from targeted sampling of the Brezden Lake intrusive complex, west-central Manitoba (parts of NTS 64C4); *in* Report of Activities 2022, Manitoba Natural Resources and Northern Development, Manitoba Geological Survey, p. 42–48.

Introduction

Field observations and preliminary petrographic results from five days of reconnaissance sampling of the Brezden Lake intrusive complex (BLIC) in west-central Manitoba during June 2022 are summarized in this report. Previous studies of the BLIC by the Manitoba Geological Survey are described in Lenton (1981), McRitchie (1988) and Martins et al. (2012). The 2012 project resulted in the discovery of metasomatized syenites that locally contain interstitial calcite. This finding was significant in that it demonstrated the potential for carbonatite magmatism in the area.

Historically, the BLIC has been considered similar to the Eden Lake complex (ELC), which is located approximately 110 km northeast of the study area and known to host calcite-carbonatite (Chakhmouradian et al., 2008) and associated rare-earth element (REE) mineralization (Mumin, 2010; Medallion Resources, 2011). The primary objective of the 2022 sampling program was to follow up on the work completed in 2012 by Martins et al. (2012) and to investigate the BLIC for large-scale lithological or structural variations, as well as the possible presence of carbonatites and REE mineralization.

Regional geology

The westernmost edge of the BLIC is located approximately 600 m east of Brezden Lake, which can be reached by floatplane from Lynn Lake situated some 95 km to the south-southwest. The BLIC is exposed over a length of approximately 4 km with a maximum width of 800 m (Figure GS2022-6-1). The BLIC is hosted in a granodiorite intrusion within the metasedimentary Burntwood group, which itself lies within the northern flank of the Kisseynew domain (KD). The KD is part of the internal zone of the Trans-Hudson orogen and is bound to the north by the Leaf Rapids domain, to the east and southeast by the Superior boundary zone, and to the south by the Flin Flon domain (Lenton, 1981; Ansdell et al., 1995; Corrigan et al., 2007).

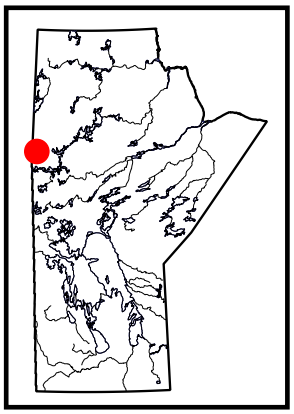

The KD tectonic environment has been interpreted as either a back-arc (Ansdell et al., 1995) or fore-arc basin (Zwanzig, 1999). In recent years, the back-arc regime has become accepted as the most likely tectonic model for the KD (Ansdell, 2005; Corrigan et al., 2009). The KD is a belt of upper-amphibolite– to lower-granulite–facies metasedimentary gneisses, which consist predominantly of the Burntwood group metaturbidite (Corrigan et al., 2007). However, arkose-derived gneisses of the Sickle group (terrestrial equivalent to the Burntwood group) are exposed on the northern flank of the KD. The Sickle group was deposited unconformably on the Granville complex, which is interpreted as back-arc metabasalts with slightly altered mid-ocean–ridge basalt (MORB) affinity (Murphy and Zwanzig, 2021).

[1] Department of Earth Sciences, University of Manitoba, Winnipeg, Manitoba

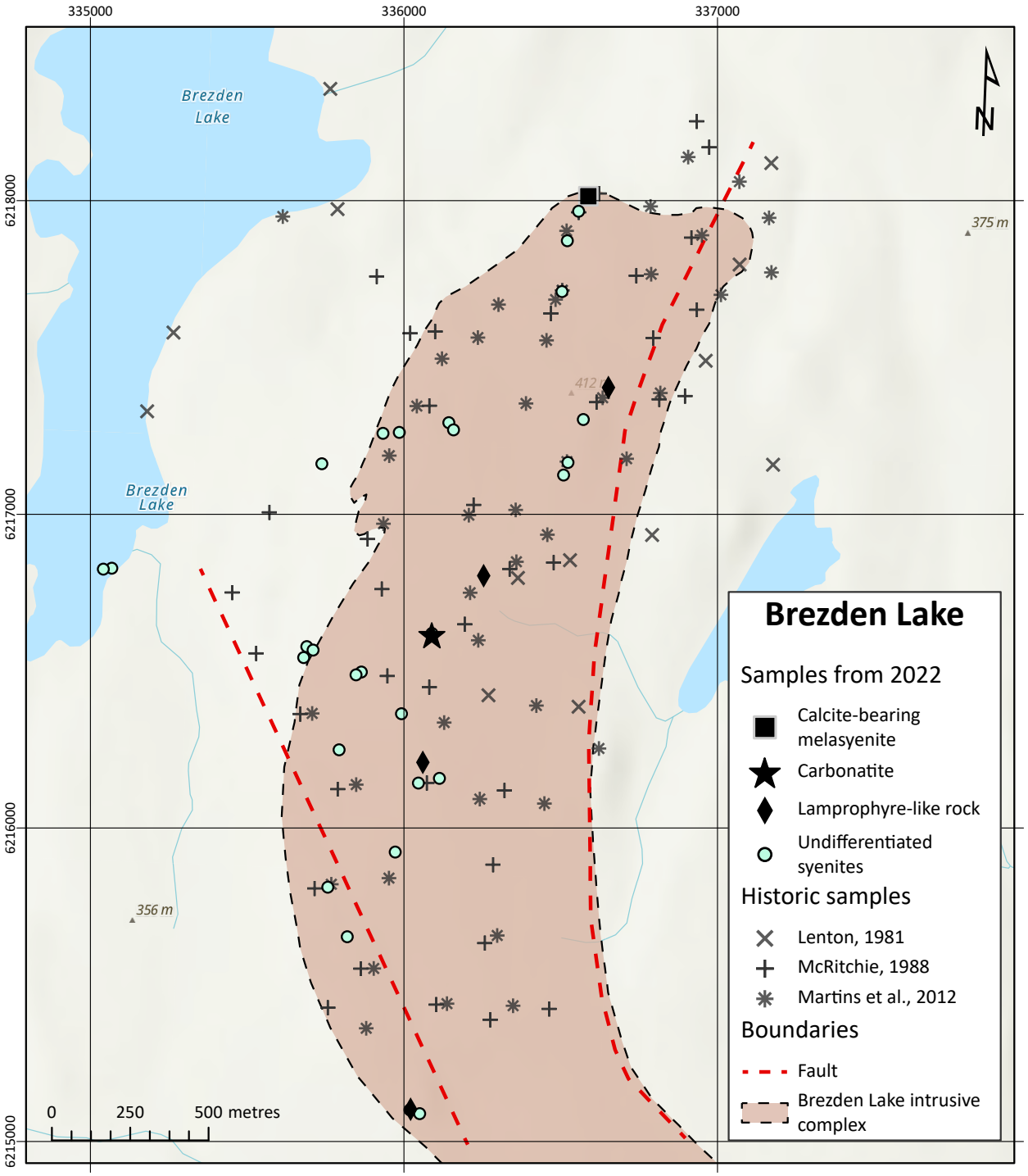

Figure GS2022-6-1: *Simplified geological map showing the extent of the Brezden Lake intrusive complex, west-central Manitoba (after Martins et al., 2012; all co-ordinates are projected in UTM Zone 14N, NAD 83).*

The BLIC is emplaced in a granodiorite intrusion hosted exclusively in the Burntwood group but lies approximately 6 km south of the Sickle group rocks at Russell Lake (Martins and Couëslan, 2019). The Burntwood group, which was deposited between ca. 1.86 and 1.84 Ga, grades laterally and vertically into the fluvial to alluvial deposits along the flanks of the KD (1.85–1.84 Ga; Machado et al., 1999; Zwanzig, 2008 Corrigan et al., 2009). Sedimentation was followed by a period of calcalkaline arc magmatism and D_1 deformation dated at 1.84–1.83 Ga (Machado et al., 1999; Zwanzig, 1999; Hollings and Ansdell, 2002). The KD collided with the Superior boundary zone between 1.84 and 1.82 Ga, which resulted in two deformation phases (D_2–D_3) at 1.82–1.81 Ga (White, 2005). The D_2–D_3 phases produced nappe-like folds accompanied by peak metamorphic conditions in the central KD (750 ±50°C, 5.5 ±1 kbar; Gordon, 1989). Peak metamorphic conditions were not homogeneous across the KD, whose peripheral areas are characterized by lower grades of metamorphism. Lenton (1981) reported peak conditions for the

Brezden Lake area to be 600–630°C and 2.5 kbar. This period of deformation and metamorphism was coeval with the emplacement of a voluminous granitoid suite. Advection from the granitic intrusions is thought to be the cause of high-temperature conditions after the cessation of D_3 (Kraus and Menard, 1997). The F_4 folds and D_5 faults are the last major deformation phases and occurred after 1.79 Ga. This period was accompanied by retrograde metamorphism and dike emplacement until 1.78 Ga. (Machado et al., 1999).

Description of the Brezden Lake intrusive complex units

The following rock-unit descriptions are based on multiple outcrop, hand-specimen and petrographic observations, and build upon the previous work and interpretations presented in Martins et al. (2012). The carbonatite, fenite, and lamprophyre-like rocks were identified in the course of this current study and, therefore, more detailed descriptions of these units are provided in this report.

Syenites

The bulk of the BLIC is composed of modally and texturally diverse syenites (syenite, quartz syenite, melasyenite, calcite-bearing melasyenite), whose mineralogy is dominated by K-feldspar and plagioclase. Plagioclase is predominantly sodic in composition (<15 mol. % anorthite), as indicated by its optical characteristics. Quartz and a variety of ferromagnesian silicates are common minor constituents in these rocks but locally gain the status of major rock-forming minerals (in quartz syenite and melasyenite, respectively). Wide variations in the morphology and distribution of these minerals are responsible for textural variants such as spotted, pegmatoid, foliated, massive and inequigranular syenites. Volumetrically, the most common rock type by far is pink, massive, fine- to medium-grained syenite. In addition to feldspars, this rock contains on average 6 vol.% quartz (locally up to 20%, grading into quartz syenite) and up to 15 vol. % greenish-black clinopyroxene and/or calcium amphibole. Wedge-shaped, brown titanite crystals and black platy biotite are the only accessory minerals identifiable in hand specimens.

Significant grain-size variations are common at the outcrop scale, leading to tabular and lenticular bodies of pegmatoid syenite showing complex crosscutting relationships (Figure GS2022-6-2a). Near the BLIC margins, clinopyroxene, amphibole and feldspar crystals (or their aggregates) exhibit preferred orientations subparallel to the contact and the proportion of dark-coloured minerals generally decreases toward the interior of the complex. Away from the marginal zone, clinopyroxene and amphibole crystals are randomly oriented, subhedral in morphology and generally do not exceed several millimetres in size. However, in pegmatoid varieties, ferromagnesian silicates are euhedral and reach several centimetres in diameter.

Based on limited outcrop observations, early massive to foliated syenite is crosscut by pegmatite dikes and lenses, which in turn are crosscut by younger, fine-grained melasyenite (Figure GS2022-6-2a).

Quartz syenite

This rock type contains the same minerals as the syenite units described above. However, quartz syenite is commonly much coarser-grained and differs by its higher modal content of quartz (up to 20 vol. %) and plagioclase (25 vol. %) relative to the predominant syenite varieties. Quartz syenite is more abundant close to the contacts of the BLIC, particularly in the midsection. One notable exception is a spotted variety, which contains ovoid aggregates of ferromagnesian silicates in a leucocratic fine-grained mesostasis. The majority of foliated syenites observed are quartz syenite.

Melasyenite

Melasyenite is the least abundant variety of syenite exposed at the BLIC and typically shows extensive iron staining on weathered surfaces due to decomposition of ferromagnesian silicates. All observed melasyenite is foliated, regardless of its location in the BLIC. The melasyenite differs from the predominant syenite units by its higher modal proportion of clinopyroxene and calcium amphibole (35 vol. %). Other dark-coloured constituents (biotite and titanite) do not exceed a few per cent in abundance. Melasyenite is typically medium grained; however, a single dike of fine-grained melasyenite was observed crosscutting a pegmatite dike but could not be sampled (Figure GS2022-6-2a). The medium-grained syenite variety is crosscut by pegmatite dikes (Figure GS2022-6-2a), lamprophyre-like rocks and calcite-carbonatite.

Calcite-bearing melasyenite

This unit was observed along the northwestern edge of a ridge forming the northernmost exposure of the BLIC (Figure GS2022-6-1). In outcrop, the melasyenite is structurally uniform, but crosscut by multiple pegmatite dikes (Figure GS2022-6-2b). The rock is patchy green, fine grained and appears pitted on weathered surfaces. The green colour of the rock is due to the high modal percentage of clinopyroxene (50–55 vol. %). Albite and orthoclase (identified by their optical properties) each constitute approximately 20 vol. % of the rock, whereas quartz does not exceed 5 vol. % in abundance. The presence of interstitial calcite grains, which are present throughout the rock and explain the surface pitting, should be noted.

Pegmatoid syenite

Pegmatite was observed throughout the BLIC and crosscuts most other units, except for late fine-grained melasyenite dikes (Figure GS2022-6-2a–c). In addition to well-defined tabular intrusions with sharp contacts (dikes), a smaller number of pegmatoid

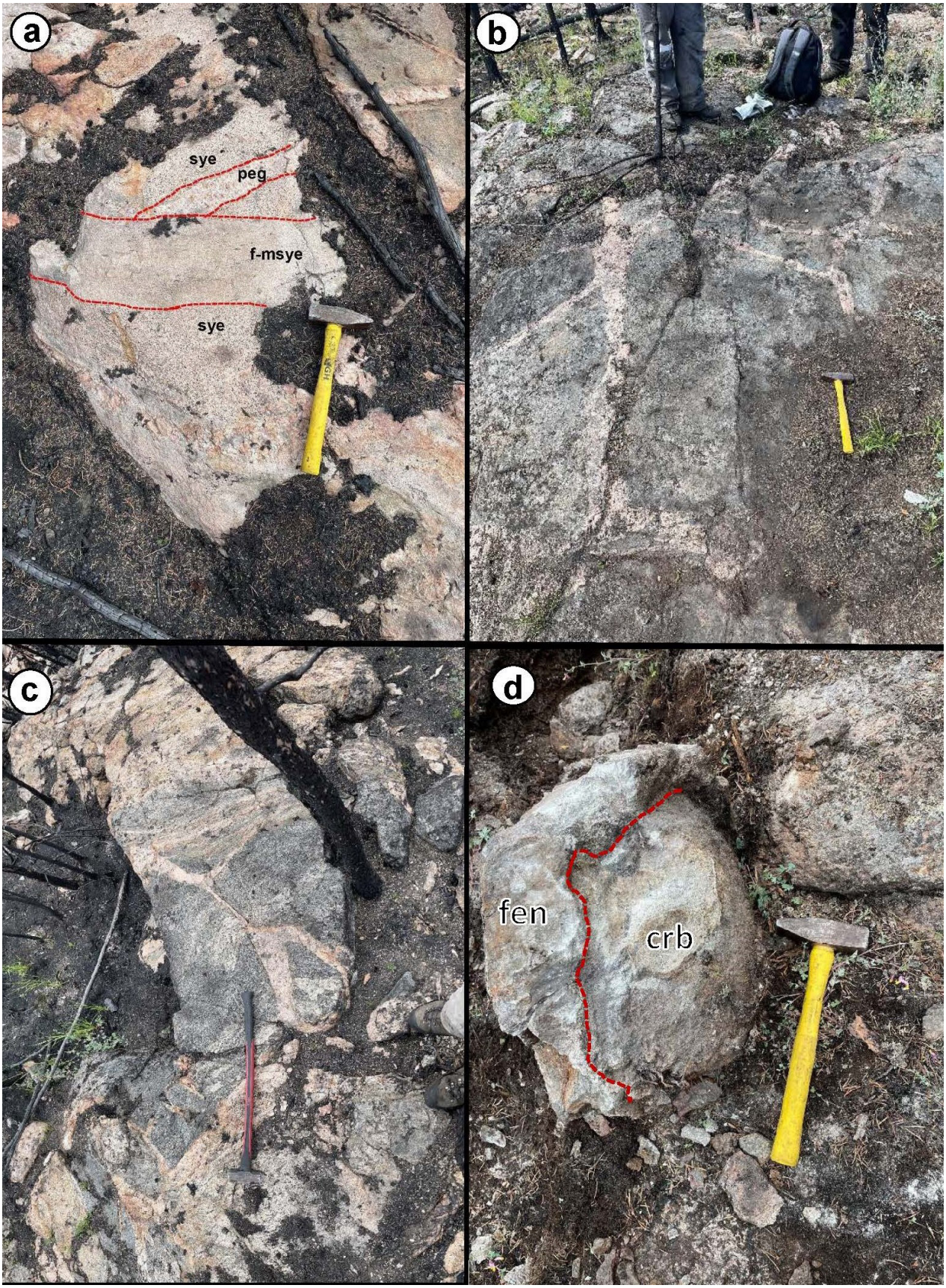

Figure GS2022-6-2: *Outcrop photographs from the Brezden Lake intrusive complex, with examples of contacts and crosscutting relationships:* ***a)*** *fine-grained melasyenite (f-msye) crosscutting pegmatite dike (peg), both emplaced in syenite (sye);* ***b)*** *multiple pegmatite veins crosscutting melasyenite host;* ***c)*** *pegmatite veins (pink) crosscut lamprophyre-like rock;* ***d)*** *recessively weathered carbonatite (crb) and adjacent fenite (fen).*

syenite pods were observed; their contacts with the host syenites are diffuse, resulting from gradual grain coarsening. This textural change is accompanied by a decrease in the modal content of plagioclase in the pegmatoid variety and its enrichment in quartz and black calcium amphibole. No preferential orientation was evident in the distribution of pegmatite bodies, but some areas within the BLIC show a greater density of dikes (Figure GS2022-6-2b). Locally, areas of concentrated crosscutting pegmatite represent megabreccias comprising rafts of metasomatized country rocks cemented by medium-grained and pegmatoid syenites. Mineralogically, the pegmatoid rocks are similar to one another, with the predominance of sub- to anhedral microcline-perthite and quartz (~1–5 cm across), and euhedral clinopyroxene, amphibole and titanite crystals (each up to 3 cm in length).

Lamprophyre-like rocks

In comparison with the calcite-bearing melasyenite (see above), dark-coloured inequigranular rocks containing large (up to 2 cm across) euhedral phenocrysts of calcium amphibole set in a fine-grained clinopyroxene-feldspar mesostasis are much more common. Visually, these rocks resemble amphibole-phyric feldspathic lamprophyres (vogesite and spessartites) and, hence, are referred to as lamprophyre-like rocks in the present report. The exposures of these rocks are restricted to recessed areas within syenites more resistant to weathering, which precluded accurate determination of their structural and dimensional characteristics. A series of isolated outcrops of this unit, each measuring up to several tens of square metres, were observed in the central and west-central parts of the BLIC. Based on limited field evidence, the lamprophyre-like rocks occur as thick dikes, which are possibly arranged in clusters. The lamprophyre-like rocks appear to crosscut the massive syenite and, in turn, are intruded by pegmatite dikes (Figure GS2022-6-2c).

Mineralogically, the lamprophyre-like rocks comprise amphibole rhombs (20–25 vol. %) immersed in a fine-grained mesostasis of sub- to euhedral clinopyroxene and anhedral microcline-perthite (30–35 vol. % each). Minor to accessory constituents include sodic plagioclase, apatite, titanite and allanite. The amphibole crystals are poikilitic with numerous small (<1 mm) inclusions of apatite, allanite, titanite and clinopyroxene. Locally, the density of inclusions is such that their host amphibole should be more appropriately termed 'oikocryst' rather than 'phenocryst'. In addition to discrete inclusions, oikocrysts in some lamprophyre-like rocks enclose lithic clusters of clinopyroxene and apatite (~75 and 15 vol. %, respectively), associated with accessory plagioclase, titanite and allanite.

Carbonatite and associated fenite

A calcite-carbonatite dike crosscutting foliated melasyenite was identified at a single outcrop in the central part of the BLIC (Figures GS2022-6-1, 2d). The carbonatite exposure is recessed and appears tan on the weathered surface. Locally, the exocontact zone is darker coloured, owing to its enrichment in clinopyroxene, and coarser grained relative to wallrock further away from the carbonatite. The exocontact rock comprises anhedral microcline-perthite, quartz and plagioclase (~40–45, 20–25 and 10–15 vol. %, respectively) associated with prismatic clinopyroxene (10–15 vol. %), which is variably replaced by calcium amphibole. Euhedral crystals of titanite and apatite (<1 mm in length) are accessory constituents (Figure GS2022-6-3a). The observed textural and mineralogical variations are interpreted as the product of alkali metasomatism (fenitization) of the wallrock syenite at its contact with the carbonatite (Le Bas, 2008; Elliott et al., 2018). Consequently, the exocontact parageneses are interpreted as fenite rather than quartz syenite.

The calcite-carbonatite is distinctly banded parallel to the dike margins. The banding is expressed on a millimetre to centimetre scale and involves both textural and modal variations. Macroscopically, the rock comprises inequigranular, mosaic-textured calcite, euhedral black clinopyroxene, yellowish-green apatite prisms, brownish-black titanite, andradite and allanite grains. The latter three minerals are visible in hand specimen but are reliably distinguished from one another only in thin section.

Calcite makes up approximately 70 vol. % of the rock. Calcite grains are anhedral and range from 0.2 to 7 mm in size. In predominantly carbonate areas, calcite grains form a recognizable mosaic pattern with triple junctions. Most of the grains exhibit polysynthetic twinning and, in some cases, bent or tapering-out twin lamellae (Figure GS2022-6-3b). Also ubiquitous are undulatory extinction, grain-boundary bulging, lineage and core-mantle structures (Figure GS2022-6-3b, c). All these microtextural characteristics are indicative of low-strain deformation and syndeformational recrystallization (Chakhmouradian et al., 2015). The carbonatite contains elongate syenite xenoliths, as well as isolated xenocrysts of microcline, plagioclase and quartz locally mantled by calcsilicate phases.

Clinopyroxene and apatite are ubiquitous minor constituents (~10 vol. % each) and occur as prismatic crystals ranging from 0.3 to 2.0 and from 0.2 to 1.5 mm in length, respectively. The clinopyroxene is pleochroic, varying from pale yellow to pale green in plane-polarized light. A large proportion of the grains are fractured and replaced by minute elongate crystals of bluish-green amphibole and pale-brown biotite along the fractures. Apatite crystals of crudely prismatic habit show concentric zonation in cross-polarized light (Figure GS2022-6-3b) and cathodoluminescence images. Their blue luminescence is indicative of elevated REE contents (Barbarand and Pagel, 2001; Chakhmouradian et al., 2017).

Economic considerations

Carbonatites are economically important sources for REE and host the largest REE deposits known (i.e., the Bayan Obo and Mianning–Dechang deposits in China and the Mountain Pass deposit in the United States). China is currently the largest producer of REE ore concentrate worldwide (168 000 t in 2021; Cor-

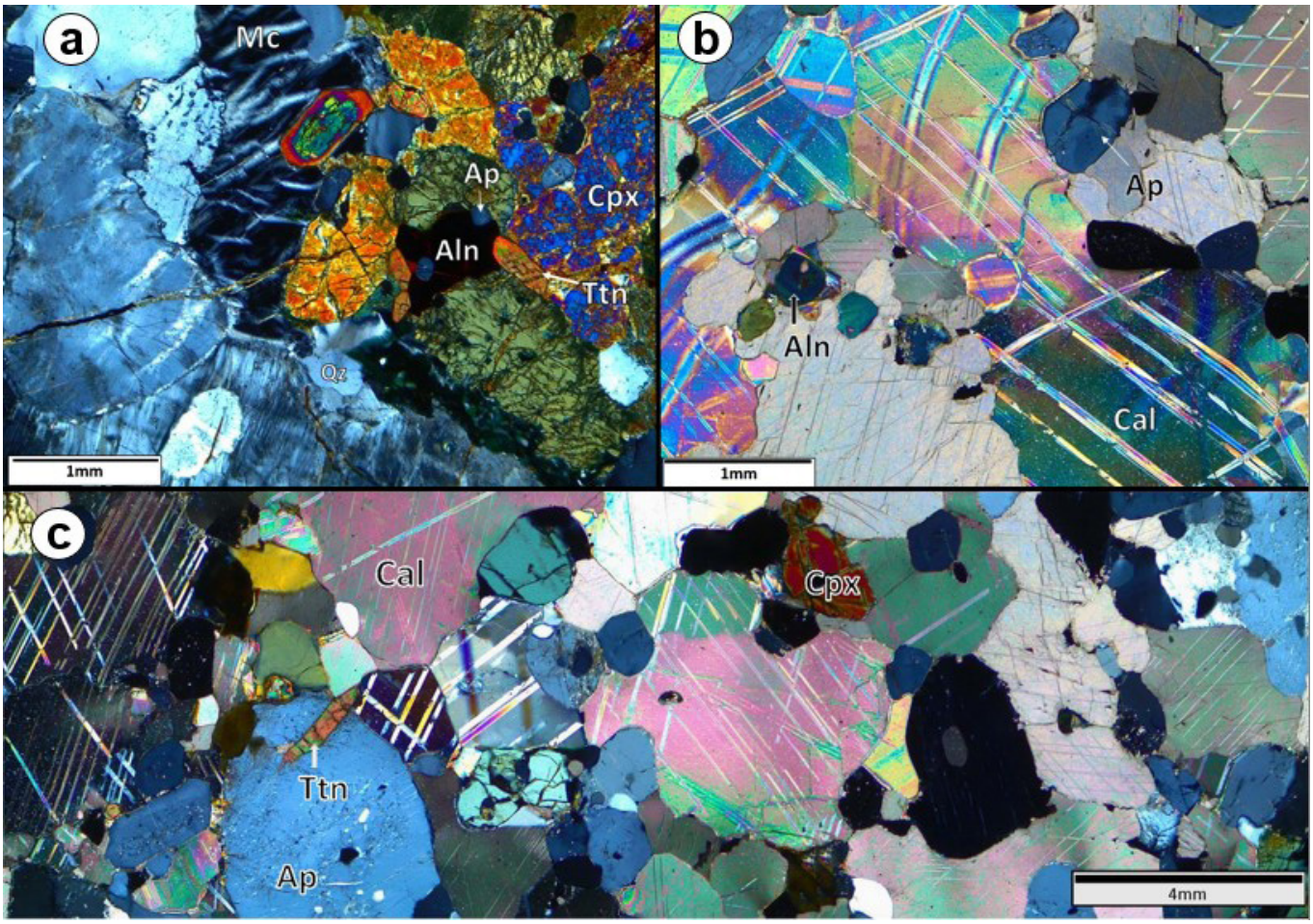

Figure GS2022-6-3: *Photomicrographs, taken in cross-polarized light, of representative textures and mineral associations in fenite and calcite-carbonatite from the study area:* ***a)*** *fenite composed of microcline (Mc), apatite (Ap), allanite (Aln), clinopyroxene (Cpx), quartz (Qz) and zoned titanite (Ttn);* ***b)*** *deformation textures in carbonatite, mechanical twinning in calcite (Cal), and grain-size variations due to dynamic recrystallization;* ***c)*** *further example of the microtextural characteristics shown in photo b.*

dier, 2022). The Mountain Pass mine in California is the second largest producer, with an annual output of 43 000 t; however, all its production is currently exported (Cordier, 2022). Increased demand for REE, spurred on by the electronics and green-technology industries, has created a need for economically viable REE deposits, as well as stable and reliable sources of REE, outside of the current producers. This has prompted the Government of Canada to include REE to the list of critical minerals (Natural Resources Canada, 2021) and support mineral exploration and research efforts focused on REE under the Targeted Geoscience Initiative (TGI) and other programs.

The BLIC is geologically similar to the ELC, situated some 110 km north-northwest in the Lynn Lake Paleoproterozoic greenstone belt. The ELC, predominantly composed of syenites, hosts calcite-carbonatite and associated REE mineralization and has been the subject of REE exploration in recent years (Medallion Resources, 2011). The newly discovered carbonatite occurrence at the BLIC further underscores this similarity, particularly given the nearly identical textural characteristics and mineralogy of this rock at both localities (Chakhmouradian et al., 2008). At the same time, there are significant petrographic differences between the syenites at Brezden and Eden lakes. Firstly, the BLIC appears to lack cumulate rocks akin to foliated coarse-grained melasyenites in the western part of the ELC. Secondly, amphibole and biotite are far more common in the Brezden Lake suite, attesting to a much higher level of activity of water and alkalis in its parental magma(s). Thirdly, lamprophyres are a prominent lithology in the BLIC, but were not observed at Eden Lake. These petrographic differences suggest not only that the BLIC magmas are of a more evolved nature but also that the prevailing geotectonic regime prevented volatile loss during their emplacement. Overall, the preliminary results of the current work indicate significant REE exploration potential outside the Lynn Lake belt, including the BLIC, but probably tied to similar processes in the lithospheric mantle.

Acknowledgments

The present project is supported by Natural Resources Canada under the Targeted Geoscience Initiative program. Many thanks are due to P. Belanger, C. Cameron and C. Epp at the Midland Sample and Core Library of the Manitoba Geological Survey for their help with fieldwork logistics, expediting and sample

preparation. In addition, L. Chackowsky and H. Adediran are acknowledged for GIS support; C. Böhm, for reviewing a draft of this report; and C. Steffano, for report layout.

References

Ansdell, K.M. 2005: Tectonic evolution of the Manitoba-Saskatchewan segment of the Paleoproterozoic Trans-Hudson Orogen, Canada; Canadian Journal of Earth Sciences, v. 42, no. 4, p. 741–759.

Ansdell, K.M., Lucas, S.B., Connors, K. and Stern, R.A. 1995: Kisseynew metasedimentary gneiss belt, Trans-Hudson orogen (Canada): back-arc origin and collisional inversion; Geology, v. 23, no. 11, p. 1039–1043.

Barbarand, J. and Pagel, M. 2001: Cathodoluminescence study of apatite crystals; American Mineralogist, v. 86, p. 473–484.

Chakhmouradian, A.R., Mumin, A.H., Demény, A. and Elliott, B. 2008: Postorogenic carbonatites at Eden Lake, TransHudson Orogen (northern Manitoba, Canada): geological setting, mineralogy and geochemistry; Lithos, v. 103, p. 503–526.

Chakhmouradian, A.R., Reguir, E.P. and Zaitsev, A.N. 2015: Calcite and dolomite in intrusive carbonatites. I. Textural variations; Mineralogy and Petrology, v. 110, p. 333–360.

Chakhmouradian, A.R., Reguir, E.P., Zaitsev, A.N., Couëslan, C., Xu, C., Kynický, J., Mumin, A.H. and Yang, P. 2017: Apatite in carbonatitic rocks: compositional variation, zoning, element partitioning and petrogenetic significance; Lithos, v. 275, p. 188–213.

Cordier, D.J. 2022: Mineral commodity summaries 2022–rare-earths; Mineral Commodities Summaries, January 2022, U.S. Geological Survey, URL <https://pubs.usgs.gov/periodicals/mcs2022/mcs2022-rare-earths.pdf> [October 2022].

Corrigan, D., Galley, A. and Pehrsson, S. 2007: Tectonic evolution and metallogeny of the southwestern Trans-Hudson Orogen; Mineral deposits of Canada: a synthesis of major deposit types, district metallogeny, the evolution of geological provinces, and exploration methods, W.D. Goodfellow (ed.); Geological Association of Canada, Mineral Deposits Division, Special Publication, no. 5, p. 881–902.

Corrigan, D., Pehrsson, S., Wodicka, N. and de Kemp, E. 2009: The Palaeoproterozoic Trans-Hudson Orogen: a prototype of modern accretionary processes; Geological Society of London, Special Publications, v. 327, p. 457–479.

Elliott, H.A.L., Wall, F., Chakhmouradian, A.R., Siegfried, P.R., Dahlgren, S., Weatherley, S., Finch, A.A., Marks, M.A.W., Dowman, E. and Deady, E. 2018: Fenites associated with carbonatite complexes: a review; Ore Geology Reviews, v. 93, p. 38–59, URL <https://doi.org/10.1016/j.oregeorev.2017.12.003>.

Gordon, T.M. 1989: Thermal evolution of the Kisseynew sedimentary gneiss belt, Manitoba: metamorphism at an early Proterozoic accretionary margin; *in* Evolution of metamorphic belts, J.S. Daly, R.A. Cliff and B.W.D. Yardley (ed.), Geological Society of London, Special Publication, no. 43, p. 233–243.

Hollings, P. and Ansdell, K. 2002: Paleoproterozoic arc magmatism imposed on an older backarc basin: implications for the tectonic evolution of the Trans-Hudson orogen, Canada; GSA Bulletin, v. 114, p. 153–168.

Kraus, J. and Menard, T. 1997: A thermal gradient at constant pressure: implications for low- to medium-pressure metamorphism in a compressional tectonic setting, Flin Flon and Kisseynew domains, Trans-Hudson Orogen, central Canada; Canadian Mineralogist, v. 5, no. 5, p. 1117–1136.

Le Bas, M.J. (2008): Fenites associated with carbonatites; The Canadian Mineralogist, v. 46, p. 915–932.

Lenton, P.G. 1981: Geology of the MacKnight–McCallum lakes area; Manitoba Department of Energy and Mines, Mineral Resources Division, Manitoba Geological Survey, Geological Report GR79-1, 39 p., URL <https://manitoba.ca/iem/info/libmin/GR79-1.zip> [April 2022].

Machado, N., Zwanzig, H. and Parent, M. 1999: U-Pb ages of plutons, sedimentation, and metamorphism of the Paleoproterozoic Kisseynew metasedimentary belt, Trans-Hudson Orogen (Manitoba, Canada); Canadian Journal of Earth Sciences, v. 36 no. 11, p. 1829–1842.

Martins, T. and Couëslan, C.G. 2019: Geological investigations in the Russell–McCallum lakes area, northwestern Manitoba (parts of NTS 64C3–6); *in* Report of Activities 2019, Manitoba Agriculture and Resource Development, Manitoba Geological Survey, p. 30–41, URL <https://manitoba.ca/iem/geo/field/roa19pdfs/GS2019-3.pdf> [October 2022].

Martins, T., Couëslan, C.G. and Böhm, C.O. 2012: Rare metals scoping study of the Brezden Lake intrusive complex, western Manitoba (part of NTS 64C4); *in* Report of Activities 2012, Manitoba Innovation, Energy and Mines, Manitoba Geological Survey, p. 115–123, URL <https://manitoba.ca/iem/geo/field/roa12pdfs/GS-10.pdf> [October 2022].

McRitchie, W.D. 1988: Alkaline intrusions of the Churchill Province, Eden Lake (64C/9) and Brezden Lake (64C/4); *in* Report of Activities 1988, Manitoba Energy and Mines, Minerals Division, p. 5–11, URL <https://manitoba.ca/iem/geo/field/rfa88.zip> [October 2022].

Medallion Resources 2011: Medallion to shift Eden Lake exploration focus to rare-earth bearing carbonatite; Medallion Resources, press release, February 3, 2011, URL <https://medallionresources.com/2011/02/medallion-to-shift-eden-lake-exploration-focus-to-rare-earth-bearing-carbonatite/> [October 2022].

Mumin, H. 2010: The Eden Lake rare metal (REE, Y, U, Th, phosphate) carbonatite complex Manitoba "Updated Report"; Medallion Resources Ltd, NI43-101, p. 87–94.

Murphy, L.A. and Zwanzig, H.V. 2021: Geology of the Wuskwatim–Granville lakes corridor, Kisseynew domain, Manitoba (parts of NTS 63O, P, 64A–C); Manitoba Agriculture and Resource Development, Manitoba Geological Survey, Geoscientific Report GR2021-2, p. 94, URL <https://manitoba.ca/iem/info/libmin/GR2021-2.zip> [October 2022].

Natural Resources Canada 2021: Government of Canada, Natural Resources Canada, URL <https://www.nrcan.gc.ca/our-natural-resources/minerals-mining/critical-minerals/23414> [October 2022].

White, D.J. 2005: High-temperature, low-pressure metamorphism in the Kisseynew domain, Trans-Hudson orogen: crustal anatexis due to tectonic thickening?; Canadian Journal of Earth Sciences, v. 42, no. 4, p. 707–721.

Zwanzig, H.V. 1999: Structure and stratigraphy of the south flank of the Kisseynew domain in the Trans-Hudson Orogen, Manitoba: implications for 1.845–1.77 Ga collision tectonics; Canadian Journal of Earth Sciences, v. 36, no. 11, p. 1859–1880.

Zwanzig, H.V. 2008: Correlation of lithological assemblages flanking the Kisseynew Domain, Manitoba (parts of NTS 63N, 63O, 64B, 64C): proposal for tectonic/metallogenic subdomains; *in* Report of Activities 2008, Manitoba Science, Technology, Energy and Mines, Manitoba Geological Survey, p. 38–52, URL <https://manitoba.ca/iem/geo/field/roa08pdfs/GS-4.pdf> [October 2022].

GS2022-7

Preliminary observations on emplacement controls of pegmatite dikes from the Wekusko Lake pegmatite field, north-central Manitoba (parts of 63J13, 14, 63O4)

by D. Silva[1], T. Martins, L. Groat[2] and R. Linnen[3]

In Brief:

- Wekusko pegmatite field is comprised of multiple types of pegmatites including spodumene-bearing pegmatite dikes
- Pegmatite dikes are temporally related to brittle-ductile deformation events, and structurally related to major shear zones and faults
- Pegmatite dikes emplacement is associated with three hostrock dilation modes: (1) tension gashes; (2) tension gashes en échelon; and (3) pull-apart shearing

Citation:
Silva, D., Martins, T., Groat, L. and Linnen, R. 2022: Preliminary observations on emplacement controls of pegmatite dikes from the Wekusko Lake pegmatite field, north-central Manitoba (parts of NTS 63J13, 14, 63O4); *in* Report of Activities 2022, Manitoba Natural Resources and Northern Development, Manitoba Geological Survey, p. 49–60.

Summary

This report outlines recent field observations of lithium-bearing pegmatite dikes in the Wekusko pegmatite field in north-central Manitoba, along with possible mechanisms of pegmatite emplacement. Two main categories of pegmatite dikes are defined in the Wekusko pegmatite field: 1) barren pegmatite dikes, and 2) spodumene-bearing pegmatite dikes. Most of the spodumene-bearing pegmatite dikes have a coarse-grained mineral assemblage of albite, quartz, K-feldspar, muscovite, spodumene and tourmaline, and are located close to regional-scale fault zones (Crowduck Bay shear zone, Herb Lake and Roberts Lake faults). These regional discontinuities facilitated melt transport, and emplacement at mid-crust level. Three mechanisms of emplacement of the spodumene-bearing pegmatites are proposed: 1) oriented subparallel to the strike of shear zones in pull-apart openings (Violet-Thompson group of pegmatite dikes); 2) oriented subparallel to the main tectonic stress direction in tension-gash openings (Sherritt-Gordon group of pegmatite dikes); and 3) oriented subparallel to the main tectonic stress direction, at a high angle to probable second-degree shear faults and aligned in en échelon formation (Green Bay group of pegmatite dikes).

Introduction

Electric-powered transportation and the transition towards more sustainable electrical storage and energy production has increased the demand for lithium, nickel, cobalt, tantalum and rare-earth elements. Canada identifies these elements as 'critical minerals', in part because of the risk of supply to the manufacturing industry, or their economic and/or military importance (Natural Resources Canada, 2021). Rare-element pegmatites play a strategic role in the green revolution because they contain high concentrations of critical minerals, particularly lithium, making them targets for mineral exploration.

Manitoba is a well-established jurisdiction for lithium-bearing pegmatite exploration and mining due to the large number of known occurrences and large size of some deposits (e.g., Tanco deposit in southeast Manitoba; Černý et al., 2005). This report focuses on the Wekusko Lake pegmatite field located in north-central Manitoba, which is known to be enriched in lithium. The Wekusko Lake pegmatite field is located approximately 25 km east of the town of Snow Lake. Because of the high lithium potential, there are currently several exploration campaigns targeting spodumene pegmatites in the region (Foremost Lithium Resource & Technology Ltd., 2022; Snow Lake Lithium, 2022). This report is a summary of mineralogical and structural observations of dikes from the Wekusko Lake pegmatite field during the summer of 2022, and includes a preliminary interpretation of the mode and structural controls on emplacement of the lithium-mineralized pegmatite dikes in the region.

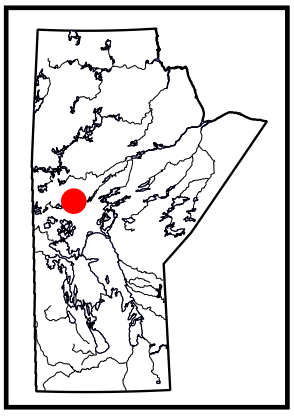

Regional geology

The Wekusko Lake pegmatite field is located within the Snow Lake subdomain of the Flin Flon domain (Černý et al., 1981; Gordon et al., 1990; Lucas et al., 1996; Ansdell, 2005; Zwanzig and Bailes, 2010). The Snow Lake subdomain lies within the southeastern exposed Reindeer zone of the Trans-Hudson orogen (David et al., 1996; Connors et al., 1999). It is bounded to the north and east by the Kisseynew domain (Figure GS2022-7-1; David et al., 1996; Connors et al., 1999). The Snow Lake subdomain is underlain by three major Paleoproterozoic tectonostratigraphic packages dated 1.88–1.83 Ga: 1) accreted Flin Flon arc and ocean-floor assemblages forming the Flin Flon–Glennie complex

[1] Department of Earth, Ocean and Atmospheric Sciences, The University of British Columbia, Vancouver, British Columbia, davidbsilva237@gmail.com
[2] Department of Earth, Ocean and Atmospheric Sciences, The University of British Columbia, Vancouver, British Columbia
[3] Department of Earth Sciences, Western University, London, Ontario

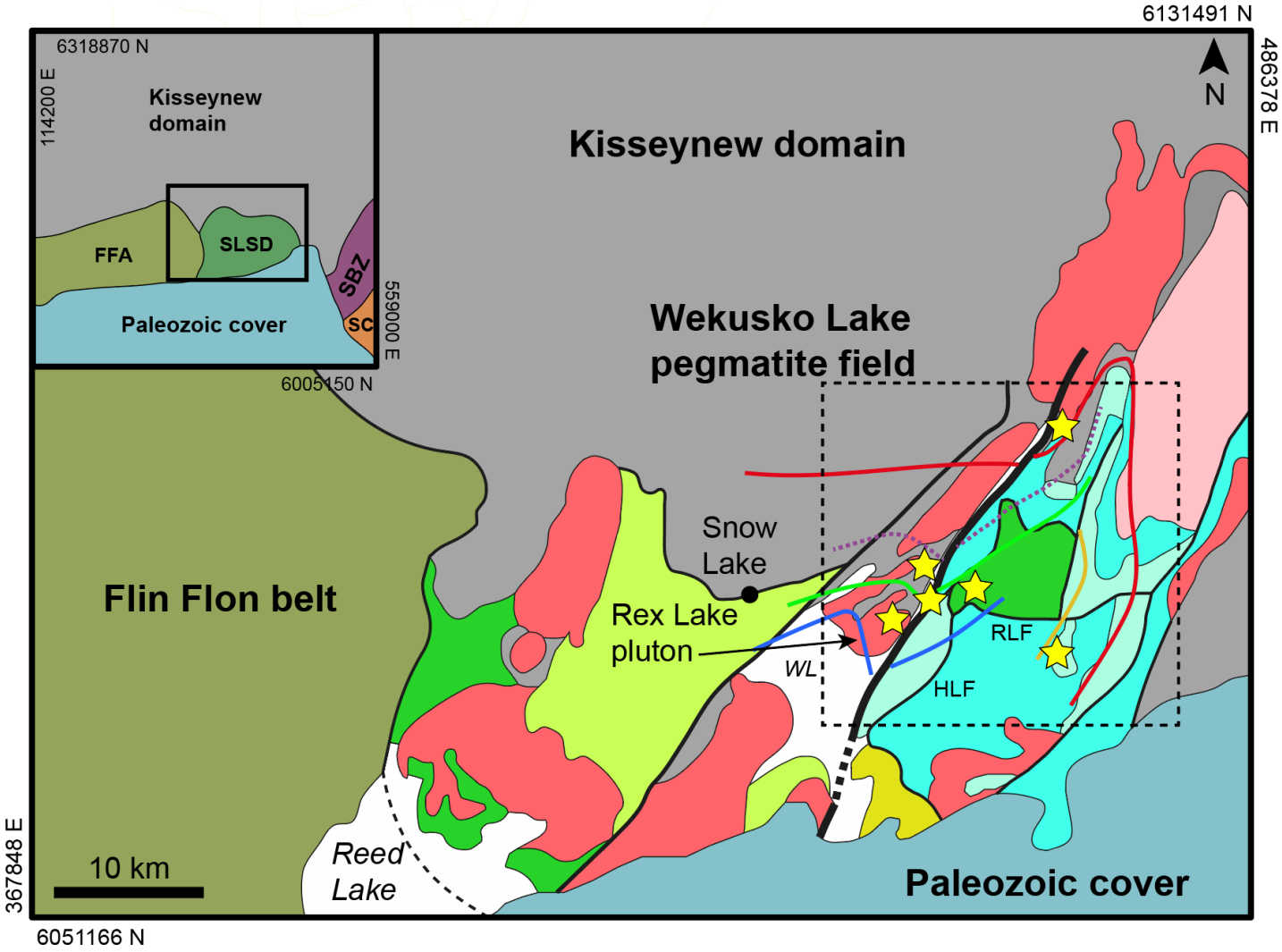

Pre-accretion assemblages (1.87–1.92 Ga)

- Juvenile arc metavolcanic rocks
- Ocean floor metabasalt

Successor arc and basin deposits (1.83–1.87 Ga)

- Missi Group: undivided; continental sandstone/volcanics
- Schist-Wekusko assemblage
- Late successor-arc plutons
- Early to middle successor-arc pluton

Metamorphic isograds

- Staurolite-in
- Andalusite-in
- Sillimanite-in
- Staurolite-out
- Melting-in

- Pegmatite dikes
- Crowduck Bay shear zone
- Faults
- Inferred faults

Figure GS2022-7-1: *Simplified geology of the Snow Lake subdomain (modified after Galley et al., 2007), with the Wekusko Lake pegmatite field outlined by dashed black box. Inset tectonic elements map of the Trans-Hudson orogen of central Saskatchewan and Manitoba is modified after Hoffman (1988). Metamorphic isograds after Lazzarotto (2020). Abbreviations: FFA, Flin Flon arc assemblage; HLF, Herb Lake fault; RLF, Roberts Lake fault; SBZ, Superior boundary zone; SC, Superior craton; SLSD, Snow Lake subdomain; WL, Wekusko Lake. All co-ordinates are in UTM Zone 14, NAD83.*

(Gordon et al., 1990; Stern et al., 1993; Stern and Lucas, 1994; David et al., 1996; Ansdell et al., 1999; Machado et al., 2000; Reid, 2021a, b); 2) Burntwood group turbidite deposits (Bailes, 1980; Zwanzig, 1990); and 3) Missi group alluvial-fluvial sandstones (Figure GS2022-7-1; Ansdell, 1993; Ansdell and Connors, 1995; Ansdell and Norman, 1995; Reid, 2021a, b). All these units are intruded by 1.84–1.83 Ga late successor-arc plutons in the Snow Lake region (Gordon et al., 1990; David et al., 1996; Whalen et al., 1999). In the south, the Reindeer zone is unconformably overlain by a Paleozoic dolomitic limestone cover (Connors et al., 1999). The Flin Flon domain has a metamorphic field gradient that ranges from lower greenschist facies in the south to upper amphibolite facies in the north, at the boundary with the Kisseynew domain (Černý et al., 1981; Lewry et al., 1994; Kraus and Menard, 1997). In the Snow Lake area, the metamorphic field gradient ranges from upper greenschist–lower amphibolite facies to upper amphibolite facies, with migmatitic zones towards the north, northeast and east from Wekusko Lake (Bailes, 1985; Lazzarotto, 2020).

The Snow Lake region has undergone four deformational events (D_1–D_4) before craton stabilization at 1.70–1.65 Ga (Schneider et al., 2007). Deformation event D_1 is associated with accretion of the Flin Flon–Glennie arc at 1.88–1.87 Ga (Lucas et al., 1996; Connors et al., 1999; Schneider et al., 2007; Stewart et al., 2018). This was followed by D_2, which recorded south to southwest compression at 1.84–1.81 Ga and involved the collision of the Kisseynew domain and Flin Flon–Glennie arc with the Sask craton (Zwanzig, 1990; Connors, 1996; Connors et al., 1999). Peak metamorphism was attained at ca. 1.81 Ga and coincided with the transition between D_2 and D_3 in the east Snow Lake area (Connors et al., 2002). The main tectonic stress direction changed from northeast-southwest to northwest-southeast compression during the D_3 event and is linked to the formation of the Crowduck Bay shear zone, Herb Lake and Roberts Lake regional transpressional faults (Connors and Ansdell, 1994; Kraus and Williams, 1994; Connors et al., 2002). The D_4 phase could be a continuation of D_3 and recorded mostly brittle deformation (Lucas et al., 1994; Fedorowich et al., 1995).

Pegmatite dikes of the Wekusko Lake field intruded several lithologies, including conglomerate to quartzofeldspathic gneiss from the Missi group, and metabasalt to basaltic andesite of N-MORB (normal mid-ocean–ridge basalt) affinity from the Snow Lake arc assemblage (Syme et al., 2000; Benn et al., 2018). The pegmatite dikes range from barren to lithium-bearing, with spodumene as the dominant lithium ore mineral (Černý et al., 1981; Martins et al., 2017). Černý et al. (1981) subdivided the Wekusko Lake pegmatite field into three mineralized groups: Sherritt-Gordon, Green Bay, and Violet-Thompson. One pegmatite from the Green Bay group yielded a U-Pb columbite age of 1780 ±8.1 Ma (Martins et al., 2019), while the other two groups remain undated. Benn et al. (2019) interpreted this pegmatite emplacement to be late D_3 to D_4, which postdates the ca. 1.81 Ga peak metamorphism. Černý et al. (1981) interpreted the evolved pegmatite dikes to be the product of fractional crystallization of surrounding successor-arc granite suites; however, this leaves a roughly 50 m.y. time gap between the crystallization of the granite suites and the emplacement of the pegmatite dikes. Alternatively, Benn et al. (2019) relate the petrogenesis of the pegmatite dikes to the partial melting of metasedimentary rocks.

Field description of pegmatite dikes

Numerous occurrences of pegmatite dikes were visited for this study, mainly in the areas of 1) north to northeast Wekusko Lake (Wekusko Lake/Crowduck Bay, Sherritt-Gordon, Green Bay and Violet-Thompson pegmatite groups), 2) Dion Lake, and 3) North Grass River. The subdivisions of Černý et al. (1981) are used to simplify the general description of the pegmatite occurrences. In addition, descriptions of the Rex Lake pluton outcrops and drillcore from 1911 Gold Corporation's exploration campaign are briefly discussed. All localities presented in Figure GS2022-7-2 were sampled for future geochemical and microstructural work.

Wekusko Lake/Crowduck Bay pegmatite dikes

The Wekusko Lake/Crowduck Bay pegmatite dikes occur as multiple, 1 to 2 m thick intrusions along the northeast arm of Wekusko Lake and on islands located in Crowduck Bay (Figure GS2022-7-3a). These pegmatite dikes are medium grained to very coarse grained, and have a simple mineralogy of albite, quartz, K-feldspar and muscovite, with trace tourmaline and garnet (Figure GS2022-7-3b–d). The muscovite content of the dikes varies, with greater abundances typically close to the country rock contact. Tourmaline is rarely present, and garnet is commonly observed adjacent to mafic xenoliths or hostrock contacts. No lithium mineralization was observed in this group of pegmatites. Based on mineralogy, these pegmatite dikes can be categorized as part of the muscovite class of Černý and Ercit (2005).

Books of muscovite are subparallel to the 038° strike of the pegmatite dikes observed on some of the islands in Crowduck Bay (Figure GS2022-7-3c). The muscovite books are also oriented subparallel to the Crowduck Bay shear zone (Figure GS2022-7-3c). The dikes intrude metasedimentary rocks of the Missi group. The pegmatite dikes commonly feature postemplacement hematization along crosscutting fractures. Postemplacement hematization is common in pegmatite dikes of the Wekusko Lake pegmatite field (Benn et al., 2018) and can make the identification of feldspars difficult due to the pink colouring associated with the metasomatic process (e.g., Gysi et al., 2016; Benn et al., 2018). Tourmalinization of the hostrock is commonly observed adjacent to pegmatite contacts.

Sherritt-Gordon group (B1, B2 and Grass River dikes)

Pegmatite dikes from the Sherritt-Gordon group contain lithium mineralization, which places them in the category of lithium-cesium-tantalum (LCT) rare-element pegmatites, based on

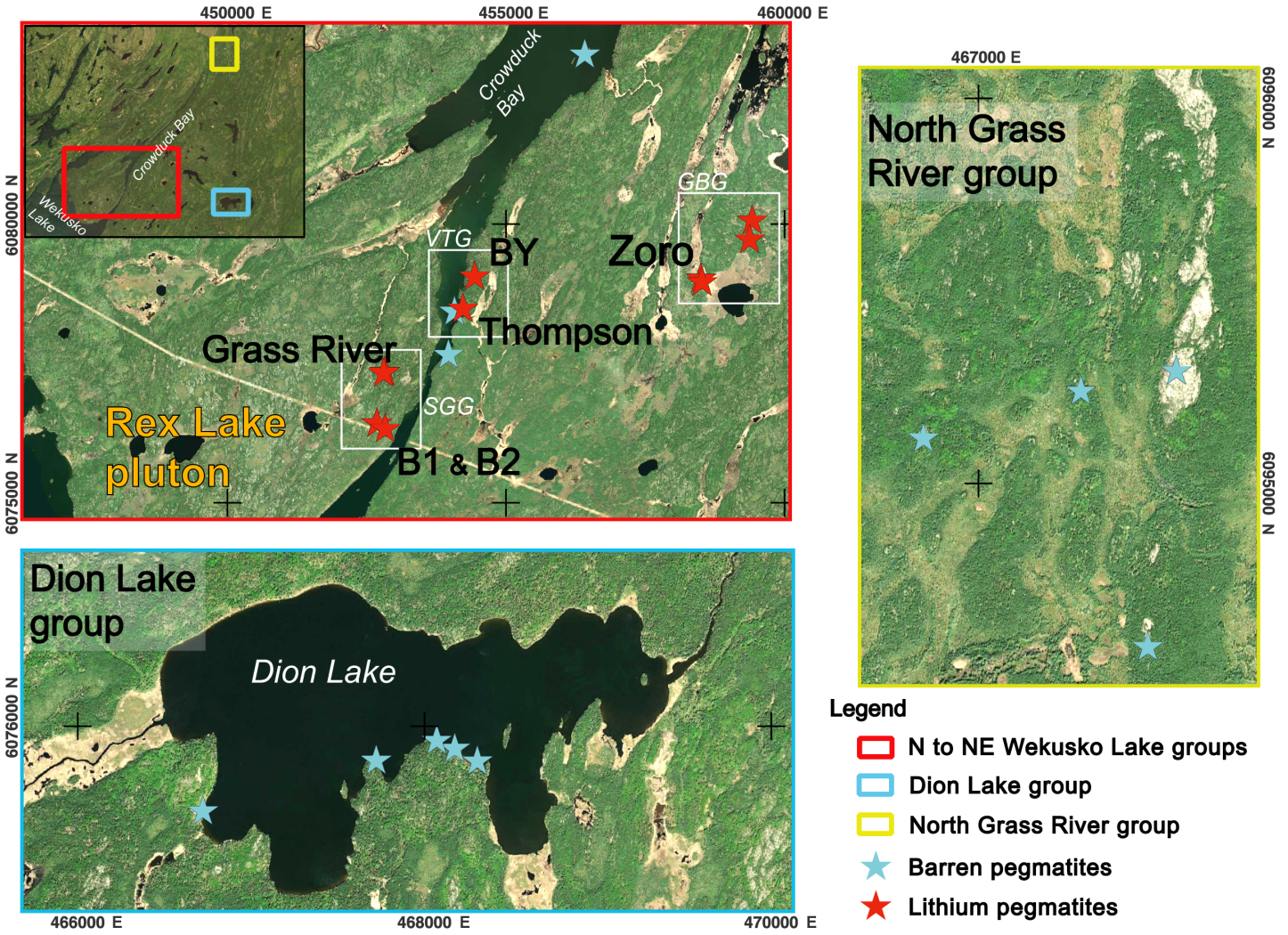

Figure GS2022-7-2: *Satellite imagery showing the locations of the pegmatite dikes visited and sampled during the summer 2022 fieldwork. Abbreviations: GBG, Green Bay pegmatite group; N, north; NE, northeast; SGG, Sherritt-Gordon pegmatite group; VTG, Violet-Thompson pegmatite group. Satellite images are copyright 2022 Maxar. All co-ordinates are in UTM Zone 14, NAD83.*

the classification of Černý and Ercit (2005). The lithium mineralization occurs as green spodumene (Figure GS2022-7-4a–c). This group of metre-scale pegmatite dikes is located east-northeast of the Rex Lake pluton (Figure GS2022-7-2) and intrudes bodies of leucocratic gabbro west of the Crowduck Bay shear zone. The main orientation of these pegmatite dikes ranges between 110 and 140°, with steep east dips of 60–70°. The pegmatite dikes are the focus of exploration by Foremost Lithium Resource & Technology Ltd. (Foremost Lithium; pegmatite occurrences B1, B2 and barren B3 pegmatite dike) and Snow Lake Lithium Ltd. (Snow Lake Lithium; Grass River pegmatite occurrences) in this region. All the dikes in this group are extremely coarse grained (i.e., main crystal size is >10 cm), with varying amounts of albite, K-feldspar, quartz, muscovite and spodumene within a single pegmatite body. There is no clear mineral zonation within the dikes apart from a more fine-grained, centimetre-scale border zone (Figure GS2022-7-4a). Accessory phases include tourmaline, apatite, garnet, and less commonly albite with a cleavelandite habit. Increased concentration of tourmaline is observed close to dike margins, locally as parallel bands or tourmaline that is perpendicular to the contact.

Spodumene occurs as elongate prisms up to 50 cm in length and 8 cm in width, or as equant basal sections 0.5–2.0 cm across (Figure GS2022-7-4a–c). The spodumene prisms in the Grass River dikes are oriented 045° and suborthogonal to the pegmatite orientation. Spodumene grains in the B1 and B2 occurrences have two main orientations, at 160° and 230° (Figure GS2022-7-4c).

Green Bay group

This group consists of at least 13 previously defined LCT-type pegmatite dikes that intruded mostly metabasalt to basaltic andesite of the Snow Lake arc-assemblage, and less commonly quartzofeldspathic gneiss of the Missi group (Figure GS2022-7-1; Benn et al., 2018). This group is located ~4 km east of the Crow-

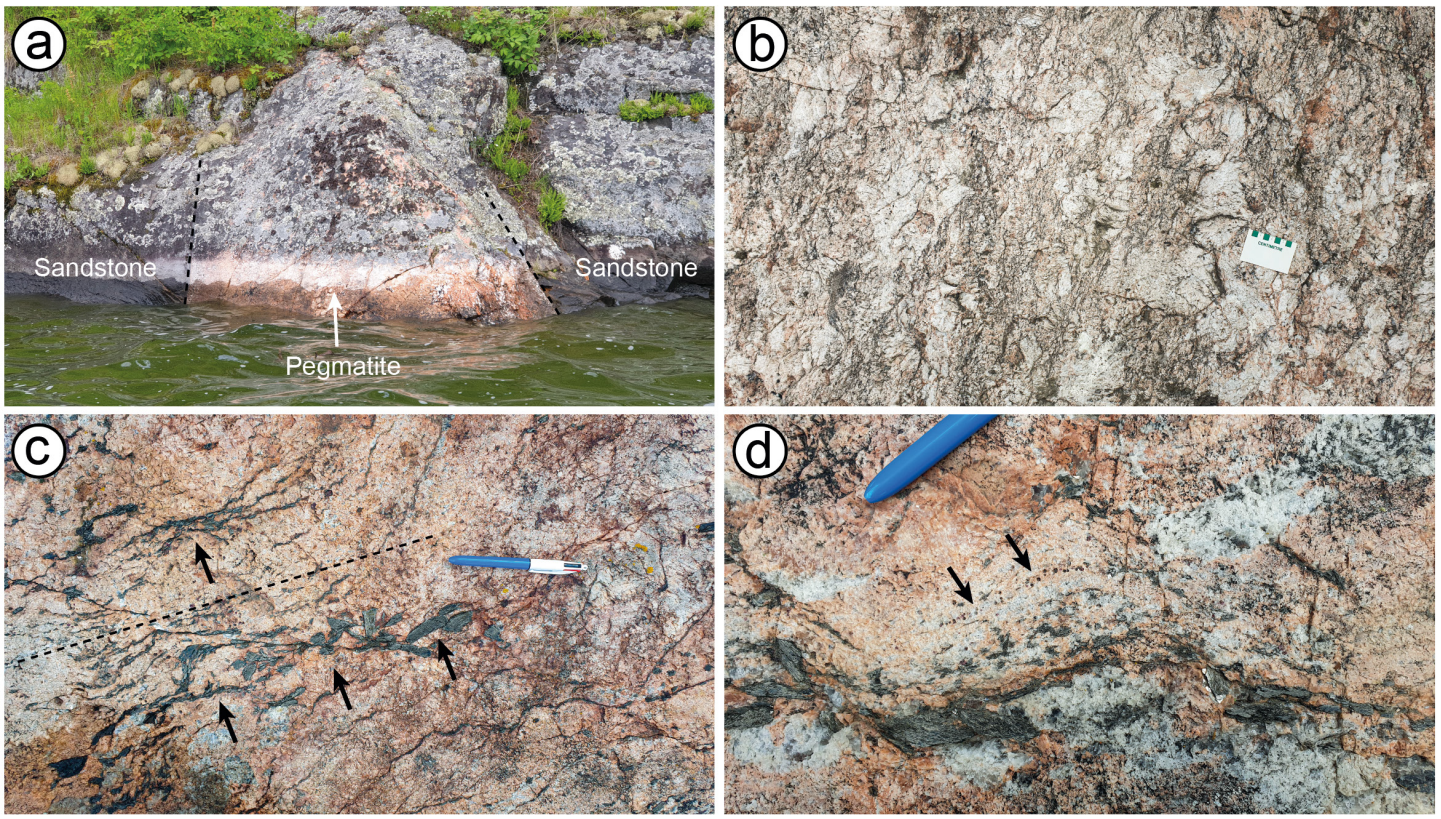

Figure GS2022-7-3: *Outcrop photographs showing pegmatite dikes from Wekusko Lake and Crowduck Bay:* ***a)*** *subvertical, hematized pegmatite dike (within black dashed lines) intruding Missi group sandstone;* ***b)*** *example of simple mineralogical composition (albite-quartz-muscovite) of this group of pegmatite dikes;* ***c)*** *preferred orientation of muscovite books (orientation is subparallel to dashed line; black arrows point to muscovite books);* ***d)*** *garnet trails (arrows) in pegmatite located in Crowduck Bay. Scale bar in (b) is in centimetres, pen for scale in panels (c) and (d) is 15 cm long.*

duck Bay shear zone, proximal to the Roberts Lake thrust fault (Figure GS2022-7-2). The Green Bay group is composed of multiple lithium-mineralized pegmatite dikes, in which the Zoro dike 1 is the largest of the group, with a similar style of mineralization as the Sherritt-Gordon group. The Zoro dike 1 is well characterized by 23 drillholes completed by Foremost Lithium (Fedikow and Zelligan, 2018). The pegmatite is zoned and trends roughly north-south for over 300 m (Benn et al., 2018). The dike contains a coarse-grained mineral assemblage of albite, quartz, K-feldspar, muscovite and spodumene (Figure GS2022-7-5a; Černý et al., 1981). The spodumene is green and up to 10 cm in length in the intermediate and core zones of the pegmatite dike (Figure GS2022-7-5a and -b). Benn et al. (2018) observed additional mineral phases such as beryl, apatite, iron and manganese phosphate minerals, garnet, zircon and columbite-group minerals. In outcrops visited during this study, spodumene appeared to be evenly distributed in the intermediate and central zones of the pegmatite. As previously reported by Benn et al. (2018), the dike has a discrete border zone characterized by smaller grain-size, sequential millimetre-size tourmaline bands close to the contact, and the presence of spodumene close to the boundary between the intermediate and border zones (Figure GS2022-7-5a). Columbite-group mineral U-Pb ages yielded a crystallization age of 1780 ±8.1 Ma (Martins et al., 2019). Deformation of feldspar and muscovite in the Zoro pegmatite dike 1 was previously reported by Martins et al. (2017), and field observations by Benn et al. (2018) suggest pegmatite emplacement and crystallization prior to the latest stages of regional deformation.

Violet-Thompson group (Thompson Brothers and BY dikes)

The Thompson Brothers and BY pegmatite occurrences are located adjacent to the Crowduck Bay shear zone, northeast of the Rex Lake pluton (Figure GS2022-7-2). The Violet-Thompson pegmatite group intruded a sequence of Missi group pebble to cobble conglomerate. Both occurrences are classified as LCT rare-element pegmatites and contain spodumene, albite, quartz, K-feldspar, muscovite and black tourmaline (Figure GS2022-7-6a–d). The outcrop of the Thompson Brothers dike is up to 10 m wide. The pegmatite is steeply dipping and is exposed for about 130 m along a strike of 035°. Drilling has traced the continuation of the dike for an additional 900 m (Snow Lake Lithium, 2022). The Thompson Brothers pegmatite shows a preferred alignment of spodumene crystals (overall trend is 160°) oblique to the dike orientation. The spodumene fabric is subperpendicular to the orientation of the Crowduck Bay shear zone (Figure GS2022-7-6a–c), which is consistent with the observations of Černý et al. (1981). This mineral fabric is possibly magmatic, and is dis-

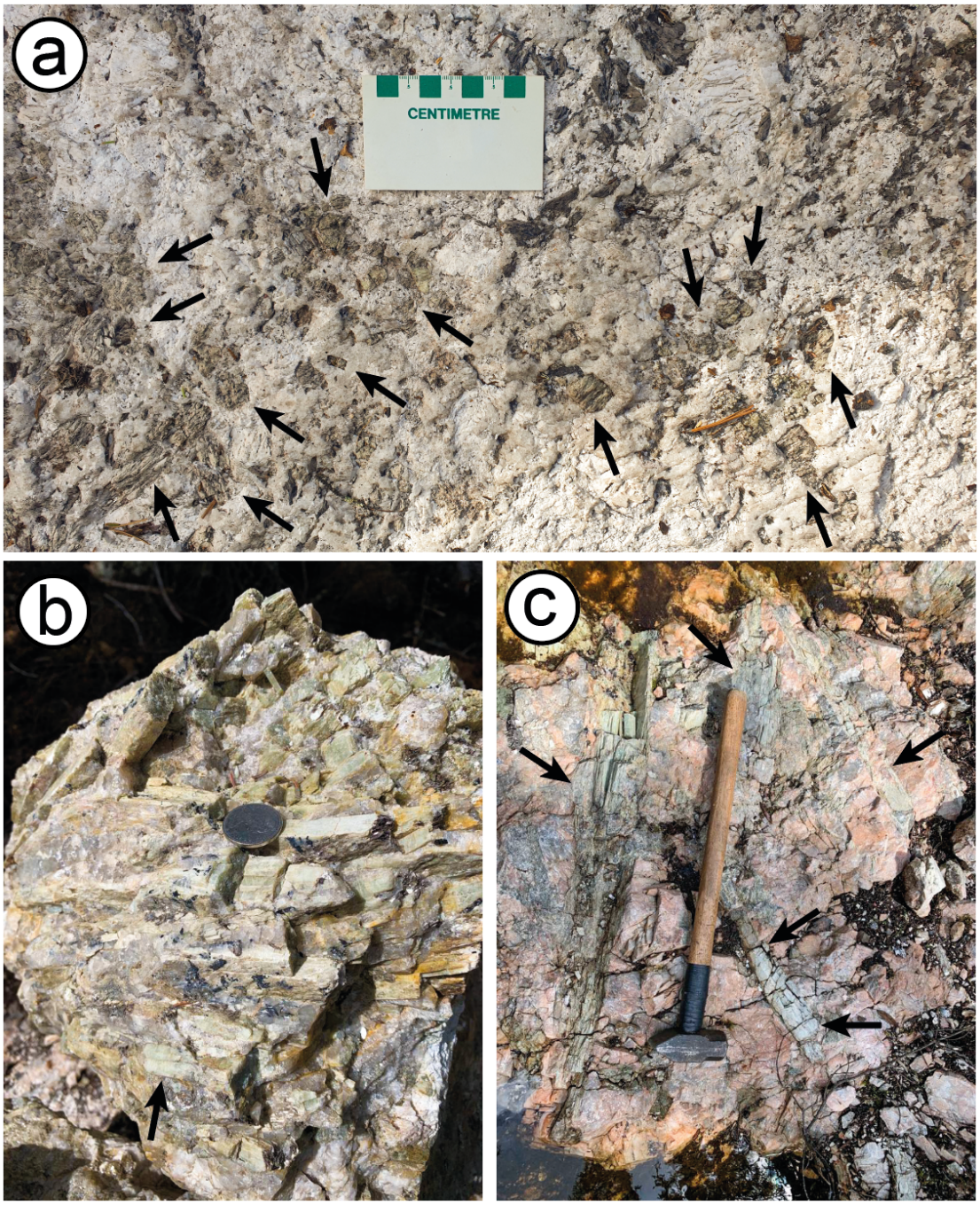

Figure GS2022-7-4: *Outcrop photographs of spodumene mineralization in the Sherritt-Gordon group of pegmatite dikes:* ***a)*** *spodumene (black arrows) in albite-quartz matrix, B2 pegmatite;* ***b)*** *very coarse-grained, elongate green spodumene crystals (black arrow) in B2 pegmatite (coin for scale is 2.4 cm in diameter);* ***c)*** *large spodumene crystals (black arrows) in B1 pegmatite (hammer for scale is 50 cm long).*

rupted by shear zones oriented subparallel to the pegmatite contact. The spodumene is reoriented closer to the trend of the dike by the shear zones (Figure GS2022-7-6a, -c). The BY pegmatite occurrence is mineralogically similar to the Thompson Brothers dike; however, a spodumene fabric is only developed as a comb structure close to the dike margin.

Dion Lake and North Grass River pegmatite dikes

These pegmatite occurrences are described separately from the previous groups because they are peripheral to the Wekusko Lake area. The North Grass River pegmatite dikes are located farther north, and the Dion Lake pegmatite dikes are located farther east (Figure GS2022-7-2). These spatially distinct occurrences are described together because they are both characterized by 1) a lack of observed lithium or other rare-element mineralization; 2) simple, medium- to coarse-grained mineralogy of albite, quartz and muscovite, with only apatite, garnet and possibly tourmaline as accessory mineral phases (Figure GS2022-7-7a); and 3) large size (one pegmatite body in the main north-south-oriented North Grass River pegmatite group is up to 1 km

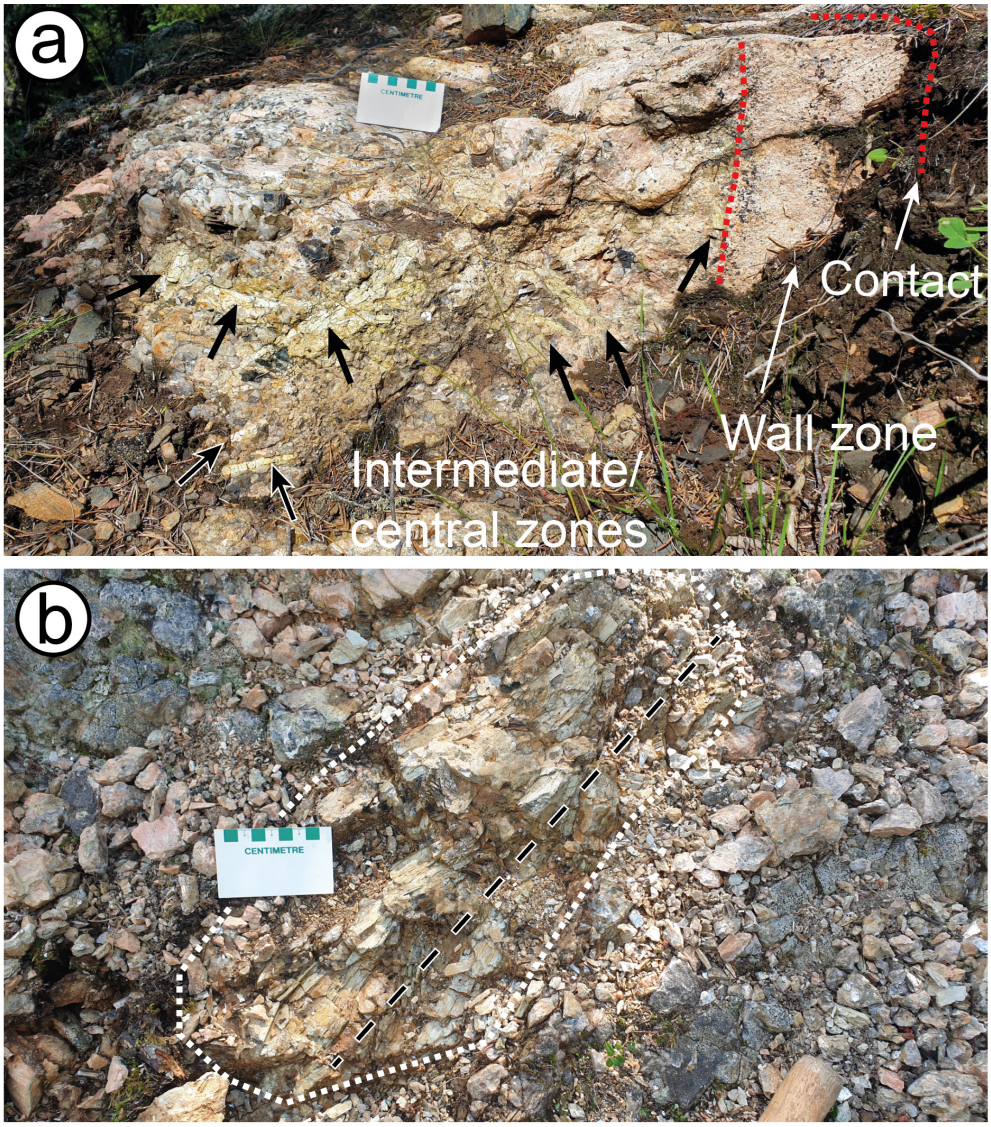

Figure GS2022-7-5: *Outcrop photographs of the Zoro pegmatite dike 1 (Green Bay group):* ***a)*** *spodumene crystals (black arrows) within the intermediate/central zones and the contact with the wall zone (within red dashed lines) of the dike;* ***b)*** *example of spodumene crystals' main orientation in the Zoro pegmatite dike (black and white dashed lines).*

in length and 80 m in thickness; Figure GS2022-7-2). Based on their mineralogy, these pegmatite occurrences are classified as muscovite-type (Černý and Ercit, 2005).

The Dion Lake dikes are locally hematized and locally contain oxide and sulphide minerals close to fractures oriented approximately 040°. These pegmatite dikes intruded rocks of high metamorphic grade of the Missi group east of the Wekusko Lake area.

Rex Lake pluton

The Rex Lake pluton (1832 ±4 Ma; Gordon et al., 1990) was documented and sampled in both outcrop and drillcore to assess if it could be parental to part of the Wekusko Lake pegmatite field via crystal fractionation, and to determine the structural mechanisms of pegmatite dike emplacement within and around the pluton. The Rex Lake pluton consists dominantly of medium-grained granodiorite, with local, weak to strong hematization near fractures. Small, subvertical felsic dikes with varying orientations (i.e., 160°, 235°, 300°) crosscut the main granodiorite (Figure GS2022-7-7b). Local tourmaline occurs as grains up to 1–2 cm long in the cores of the felsic dikes. Mafic xenoliths up to 20–30 cm wide are prevalent throughout the pluton (Figure GS2022-7-7b). Drillcore from 1911 Gold Corporation shows weak chlorite alteration, with local sulphides in fractures. Local pegmatitic dikes up to 1 m wide are mineralogically simple, as described in 1911 Gold Corporation's diamond-drill core confidential logs. More mafic subdomains of the pluton consist of porphyritic leucocratic gabbro with plagioclase phenocrysts up to 4 cm.

Preliminary two-dimensional emplacement model of lithium-mineralized pegmatite dikes

The location, strike, and in some cases spodumene fabrics, of lithium-mineralized dikes in the Wekusko Lake pegmatite field

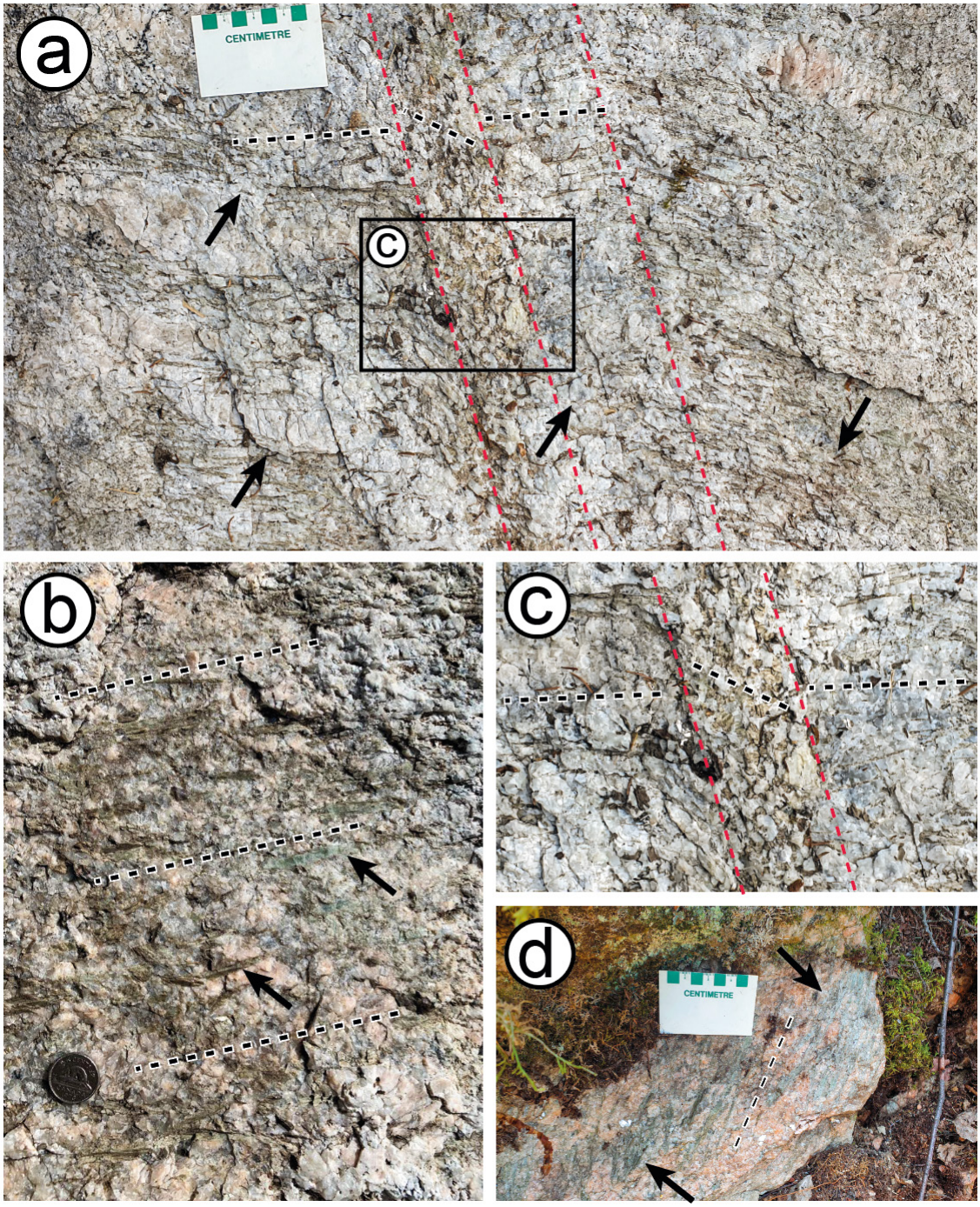

Figure GS2022-7-6: *Outcrop photographs showing pegmatite dikes from the Violet-Thompson group:* ***a)*** *and* ***b)*** *pervasive mineral fabric (black dashed lines) in the Thompson Brothers pegmatite dike and post- to late-crystallization shear planes (red dashed lines) slightly rotating the mineral fabric (black arrows pointing at aligned spodumene crystals; coin for scale in b) is 2.1 cm in diameter);* ***c)*** *close-up of shear planes (red dashed lines) at high angle to mineral fabric (black dashed lines) observed in the Thompson Brothers pegmatite dike;* ***d)*** *aligned spodumene crystals (comb structure; black arrows) close to pegmatite contact (contact outside of photograph) in BY pegmatite dike. Fabric orientation is represented by black dashed line with white outline.*

suggest that emplacement was structurally controlled. The strike of the Sherritt-Gordon group of dikes, located west of the Crowduck Bay shear zone, is oriented subparallel to the D_3 maximum compressional stress (northwest-southeast). This orientation suggests emplacement in Mode-I (extensional; Irwin, 1957) tension-gash openings, with spodumene crystals oriented perpendicular to the contact of the pegmatites (Figure GS2022-7-8).

The Violet-Thompson pegmatite group is located east of, and proximal to, the Crowduck Bay shear zone. The dikes are oriented subparallel to the adjacent structure, and are probably related to shear corridors formed subparallel to the Crowduck Bay shear zone (Figure GS2022-7-8; Černý et al., 1981). Syndeformational, dilational crystallization of the Thompson Brothers pegmatite is inferred from the dominant mineral fabric, which is oblique to

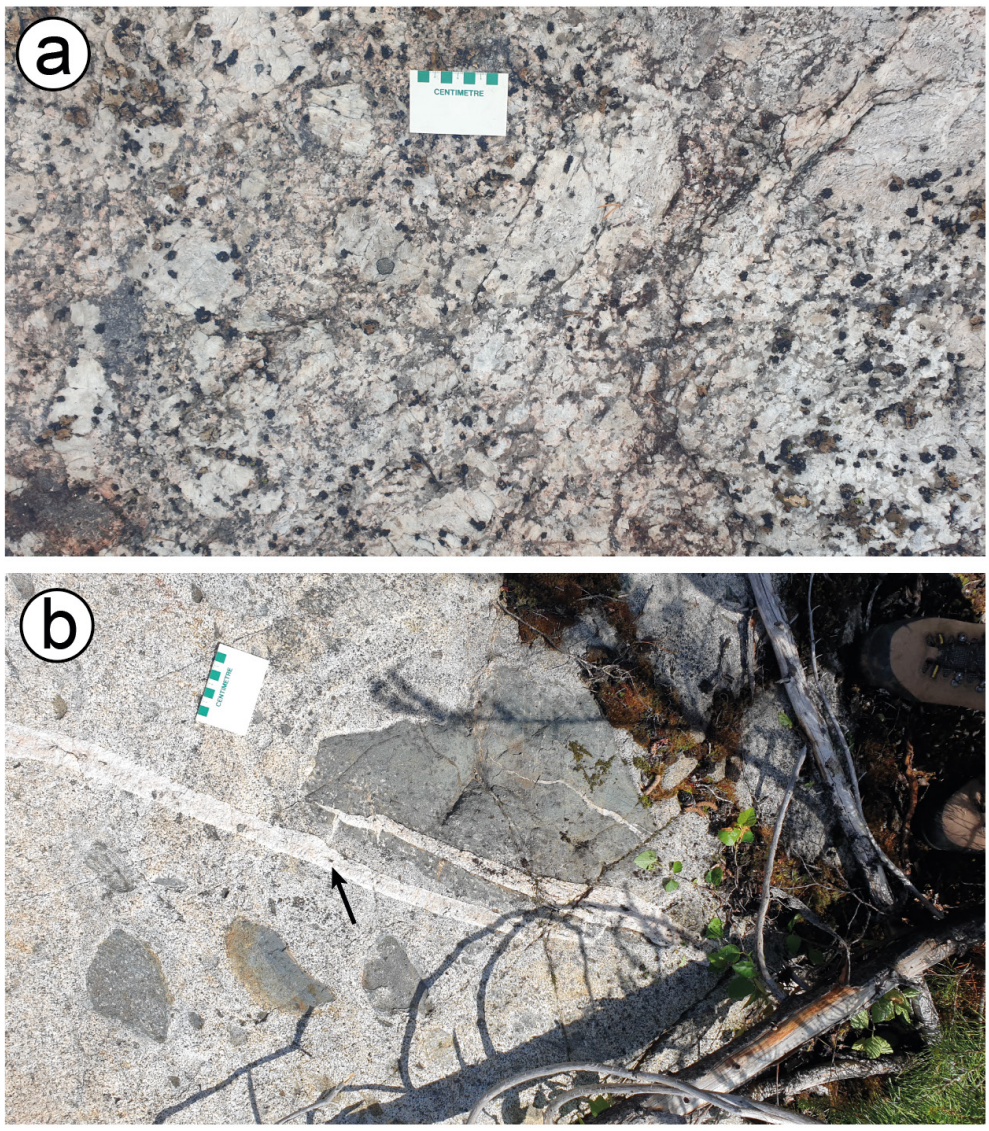

Figure GS2022-7-7: *Outcrop photographs of nonmineralized rocks:* ***a)*** *North Grass River pegmatite dike with simple mineralogical composition (albite-quartz-muscovite);* ***b)*** *Rex Lake pluton granodiorite with mafic xenoliths and crosscut by felsic dikes (black arrow indicates tourmaline in felsic dike). Scale card in both photos is in centimetres.*

the dike margins (Figure GS2022-7-6a, -d; Černý et al., 1981). Pegmatite-hosted shear planes are oriented subparallel to the dike margins, and mineral fabrics proximal to these shear planes are rotated in the direction of shearing (Figure GS2022-7-6a, -c).

Pegmatite dikes of the Green Bay group are emplaced as a series of northwest-trending en échelon–like dikes. Regional-scale, east-northeast-trending lineaments present in the area could represent shear structures. The pegmatite dikes appear to be emplaced between these lineaments as a succession of en échelon tension gashes (Figure GS2022-7-8; Černý et al., 1981). This area is also proximal to the intersection of two main thrust faults (Roberts Lake and Herb Lake faults). Similar regional-scale structures have been proposed as conduits for the transportation of melt within the crust (Deveaud et al., 2013; Piazolo et al., 2020; Silva et al., 2018, 2022). The strike of the Zoro dike 1 appears to be rotated towards a north-trending orientation by the proximity of the north-northeast-trending Herb Lake fault (Figure GS2022-7-8).

Economic considerations

Canada, and particularly Manitoba, are major players in the green revolution because of an abundance of lithium-bearing pegmatite occurrences such as the Tanco pegmatite and pegmatites in the Wekusko Lake field. The Wekusko Lake pegmatite field has considerable economic potential because of a high concentration of lithium-mineralized dikes, favourable mineralogy for lithium extraction, and central location for the Canadian lithium market.

The increasing need for critical minerals, and growing necessity to reduce our dependence on fossil fuels, highlights the political and economic importance of discovering new rare-element pegmatite deposits and increasing our knowledge of already

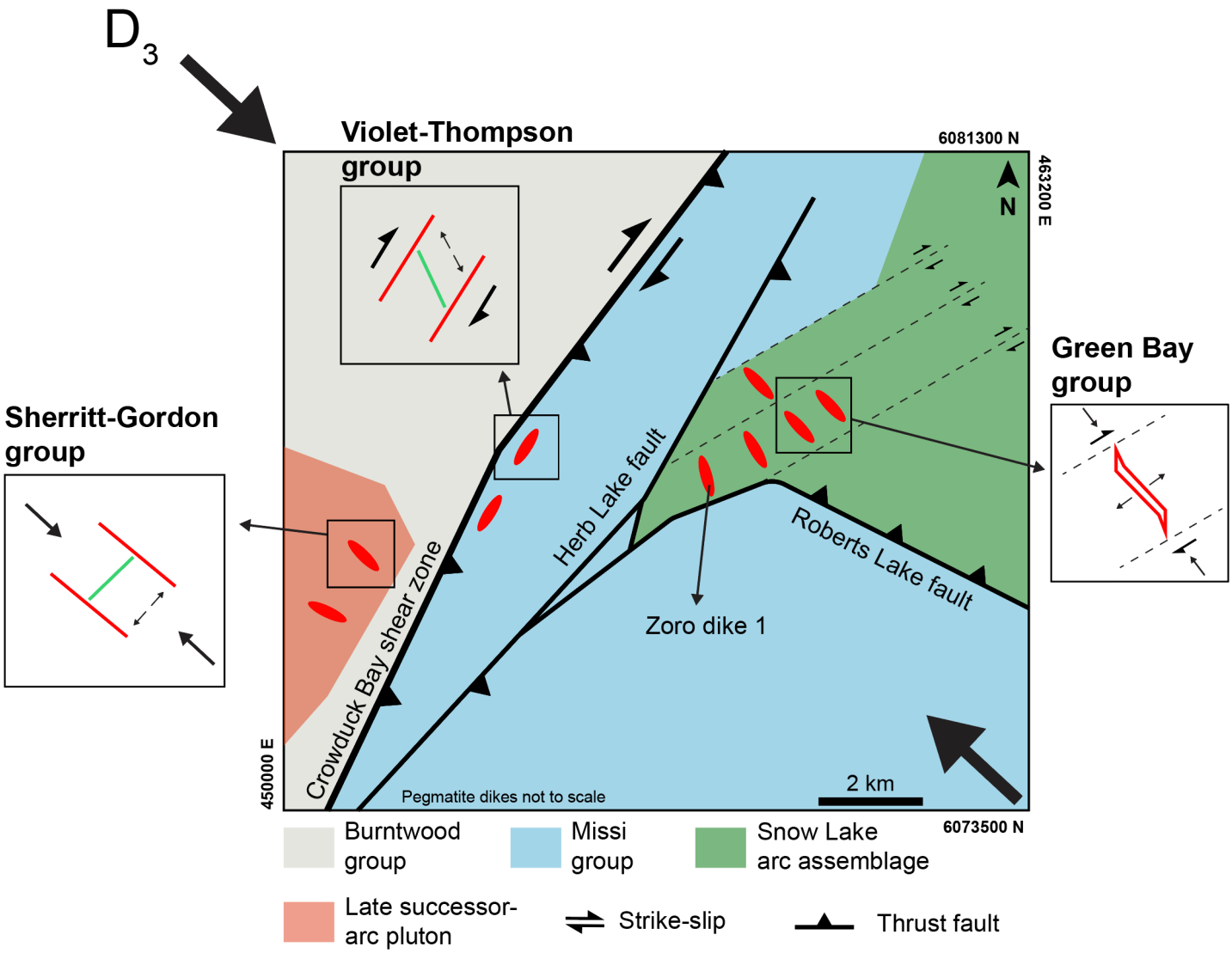

Figure GS2022-7-8: *Preliminary schematic model for the structurally controlled emplacement of lithium-mineralized dikes in the Wekusko Lake pegmatite field. In main portion of figure and in insets, thick black arrows indicate the direction of main tectonic stress during D_3. In the Sherritt-Gordon and Violet-Thompson group insets, the red lines indicate the longitudinal boundaries of the pegmatite dikes and the green lines indicate the elongation of the spodumene crystals. In the Green Bay group inset, the dashed black lines indicate probable strike-slip fault discontinuities.*

known deposits. To achieve these goals, it is necessary to assess probable emplacement mechanisms, the relationship between pegmatite bodies and tectonic structures, and the style and mode of lithium mineralization. The Wekusko Lake pegmatite field in north-central Manitoba is located within a historical and active mining district, with excellent access and developed infrastructure, and a well-studied regional geology. Its lithium resources are the focus of ongoing research as well as active exploration by two companies (Foremost Lithium and Snow Lake Lithium).

Acknowledgments

Thanks to Foremost Lithium Resource & Technology Ltd. and Snow Lake Lithium Ltd. for access to their pegmatite properties and drillcore, and for providing accommodation in Snow Lake. We also thank 1911 Gold Corporation for access to their Rex Lake core at their Bissett, Manitoba property. Field and logistical support from the Manitoba Geological Survey is also gratefully acknowledged. The project benefited from discussions with M. Fedikow and J. Ziehlke. This study is supported by a Mitacs Accelerate Industrial Postdoc grant with Foremost Lithium Resource & Technology Ltd. as financial and logistical partner. Edits from reviewers C. Couëslan and C. Böhm are truly appreciated.

References

Ansdell, K.M. 1993: U-Pb constraints on the timing and provenance of fluvial sedimentary rocks in the Flin Flon and Athapapuskow basins, Flin Flon domain, Trans-Hudson orogen, Manitoba and Saskatchewan; *in* Radiogenic Age and Isotopic Studies, Report 7, Geological Survey of Canada, no. 93-2, p. 49–57.

Ansdell, K.M. 2005: Tectonic evolution of the Manitoba-Saskatchewan segment of the Paleoproterozoic Trans-Hudson orogen, Canada; Canadian Journal of Earth Sciences, v. 42, no. 4, p. 741–759.

Ansdell, K.M. and Connors, K.A. 1995: Geochemistry of mafic volcanic rocks, east Wekusko Lake, Manitoba; Proceedings Lithoprobe Trans-Hudson Orogen Transect Meeting, Regina, no. 48, p. 198–205.

Ansdell, K.A. and Norman, A.R. 1995: U-Pb geochronology and tectonic development of the southern flank of the Kisseynew Belt, Trans-Hudson orogen, Canada; Precambrian Research, v. 72, p. 147–167.

Ansdell, K.M., Connors, K.A., Stern, R.A. and Lucas, S.B. 1999: Coeval sedimentation, magmatism, and fold-thrust belt development in the Trans-Hudson Orogen: geochronological evidence from the Wekusko Lake area, Manitoba, Canada; Canadian Journal of Earth Sciences, v. 36, no. 2, p. 293–312.

Bailes, A.H. 1980: Origin of early Proterozoic volcaniclastic turbidites, south margin of the Kisseynew sedimentary gneiss belt, File Lake, Manitoba; Precambrian Research, v. 12, no. 1–4, p. 197–225.

Bailes, A.H. 1985: Geology of the Saw Lake area; Manitoba Energy and Mines, Geological Services, Geological Report GR83-2, 47 p., URL <https://manitoba.ca/iem/info/libmin/GR83-2.zip> [September 2022].

Benn, D., Linnen, R.L. and Martins, T. 2018: Geology and bedrock mapping of the Wekusko Lake pegmatite field (northeastern block), central Manitoba (part of NTS 63J13); *in* Report of Activities 2018, Manitoba Growth, Enterprise and Trade, Manitoba Geological Survey, p. 79–88, URL <https://manitoba.ca/iem/geo/field/roa18pdfs/GS2018-7.pdf> [September 2022].

Benn, D., Martins, T. and Linnen, R.L. 2019: Interpretation of U-Pb isotopic dates of columbite-group minerals in pegmatites, Wekusko Lake pegmatite field, central Manitoba (part of NTS 63J13); *in* Report of Activities 2019, Manitoba Agriculture and Resource Development, Manitoba Geological Survey, p. 52–59, URL <https://manitoba.ca/iem/geo/field/roa19pdfs/GS2019-5.pdf> [September 2022].

Černý, P. and Ercit, T. 2005: The classification of granitic pegmatites revisited; The Canadian Mineralogist, v. 43, no. 6, p. 2005–2026.

Černý, P., Linnen, R.L. and Samson, I.M. 2005: The Tanco rare-element pegmatite deposit, Manitoba: regional context, internal anatomy, and global comparisons; Geological Association of Canada, GAC Short Course, no. 17, p. 127–158.

Černý, P., Trueman, D.L., Zeihlke, D.V., Goad, B.E. and Paul, B.J. 1981: The Cat Lake-Winnipeg River and the Wekusko Lake pegmatite fields, Manitoba; Manitoba Department of Energy and Mines, Mineral Resources Division, Economic Geology Report ER80-1, 216 p., URL <https://manitoba.ca/iem/info/libmin/ER80-1.zip> [September 2022].

Connors, K.A. 1996: Unraveling the boundary between turbidites of the Kisseynew belt and volcano-plutonic rocks of the Flin Flon belt, eastern Trans-Hudson orogen, Canada; Canadian Journal of Earth Sciences, v. 33, p. 811–829.

Connors, K.A. and Ansdell, K.M. 1994: Timing and significance of thrust faulting along the boundary between the Flin Flon-Kisseynew domains, eastern Trans-Hudson orogen; *in* Proceedings Lithoprobe Trans-Hudson Orogen Transect, Saskatoon, no. 38, p. 112–122.

Connors, K.A., Ansdell, K.M. and Lucas, S.B. 1999: Coeval sedimentation, magmatism, and fold-thrust development in the Trans-Hudson orogen: propagation of deformation into an active continental arc setting, Wekusko Lake area, Manitoba; Canadian Journal of Earth Sciences, v. 36, no. 2, p. 275–291.

Connors, K., Ansdell, K. and Lucas, S. 2002: Development of a transverse to orogen parallel extension lineation in a complex collisional setting, Trans-Hudson orogen, Manitoba, Canada; Journal of Structural Geology, v. 24, no. 1, p. 89–106.

David, J., Bailes, A.H. and Machado, N. 1996: Evolution of the Snow Lake portion of the Paleoproterozoic Flin Flon and Caisson belts, Trans-Hudson orogen, Manitoba, Canada; Precambrian Research, v. 80, p. 107–124.

Deveaud, S., Gumiaux, C., Gloaguen, E. and Branquet, Y. 2013: Spatial statistical analysis applied to rare-element LCT-type pegmatite fields: an original approach to constrain faults-pegmatites-granites relationships; Journal of Geosciences, v. 58, no. 2, p. 163–182.

Fedikow, M. and Zelligan, S. 2018: NI 43-101 Technical Report on the Zoro Lithium Project, Snow Lake, Manitoba; filed by Far Resources Inc., URL <https://webfiles.thecse.com/FAT-NR-20180905-TechReport-FINAL.pdf> [September 2022].

Fedorowich, J.S., Kerrich, R. and Stauffer, M.R. 1995: Geodynamic evolution and thermal history of the central Flin Flon belt, Trans-Hudson Orogen: constraints from structural development, $^{40}Ar/^{39}Ar$, and stable isotope geothermometry; Tectonics, v. 14, p. 472–503.

Foremost Lithium Resource & Technology Ltd. 2022: Properties; URL <https://foremostlithium.com/> [September 2021].

Galley, A.G., Syme, E.C. and Bailes, A.H. 2007: Metallogeny of the Paleoproterozoic Flin Flon belt, Manitoba and Saskatchewan; Geological Association of Canada, Mineral Deposits Division, St. John's, Newfoundland, Special Publication 5, p. 533509–552531.

Gordon, T., Hunt, P., Bailes, A. and Syme, E. 1990: U-Pb ages from the Flin Flon and Kisseynew belts, Manitoba: chronology of crust formation at an early Proterozoic accretionary margin; *in* The Early Proterozoic Trans-Hudson Orogen of North America, J.F. Lewry and M.R. Stauffer (ed.), Geological Association of Canada, Special Paper 37, p. 177–199.

Gysi, A.P., Williams-Jones, A.E. and Collins, P. 2016: Lithogeochemical vectors for hydrothermal processes in the Strange Lake peralkaline granitic REE-Zr-Nb deposit; Economic Geology, v. 111, no. 5, p. 1241–1276.

Hoffman, P. 1988: United Plates of America, the birth of a craton: Early Proterozoic assembly and growth of Laurentia; Annual Review of Earth and Planetary Sciences, v. 16, no. 1, p. 543–603.

Irwin, G. 1957: Analysis of stresses and strains near the end of a crack traversing a plate; Journal of Applied Mechanics, v. 24, p. 361–364.

Kraus, J. and Menard, T. 1997: A thermal gradient at constant P: implications for low- to medium-P metamorphism in a compressional tectonic setting, Flin Flon and Kisseynew domains, Trans-Hudson orogen, central Canada; Canadian Mineralogist, v. 35, p. 1117–1136.

Kraus, J. and Williams, P.F. 1994: Cleavage development and timing of metamorphism in the Burntwood Group across the Threehouse synform, Snow Lake, Manitoba: a new paradigm; Proceedings Lithoprobe Trans-Hudson Orogen Transect, Saskatoon, no. 38, p. 230–238.

Lazzarotto, M.C. 2020: Metamorphism of the Flin Flon greenstone belt, Manitoba; Ph.D. thesis, University of Calgary, Calgary, Alberta.

Lewry, J., Hajnal, Z., Green, A., Lucas, S.B., White, D., Stauffer, M.R., Ashton, K.E., Weber, W. and Clowes, R. 1994: Structure of Paleoproterozoic continent-continent collision zone: a LITHOPROBE seismic reflection profiles across the Trans-Hudson orogen, Canada; Tectonophysics, v. 232, no. 1–4, p. 143–160.

Lucas, S.B., Stern, R.A., Syme, E.C., Reilly, B.A. and Thomas, D.J. 1996: Intra-oceanic tectonics and the development of continental crust: 1.92–1.84 Ga evolution of the Flin Flon belt, Canada; Geological Society of America Bulletin, v. 108, p. 602–629.

Lucas, S.B., White, D., Hajnal, Z., Lewry, J., Green, A., Clowes, R., Zwanzig, H., Ashton, K., Schledewitz, D., Stauffer, M., Norman, A., Williams, P.F. and Spence, G. 1994: Three-dimensional collisional structure of the Trans-Hudson orogen, Canada; Tectonophysics, v. 232, p. 161–178.

Machado, N., Zwanzig, H. and Parent, M. 2000: U-Pb ages of plutonism, sedimentation, and metamorphism of the Paleoproterozoic Kisseynew metasedimentary belt, Trans-Hudson Orogen (Manitoba, Canada); Canadian Journal of Earth Sciences, v. 36, no. 11, p. 1829–1842.

Martins, T., Benn, D. and McFarlane, C. 2019: Laser-ablation inductively coupled plasma–mass spectrometry (LA-ICP-MS) analyses of columbite grains from Li-bearing pegmatites, Wekusko Lake pegmatite field (northeastern block), central Manitoba (part of NTS 63J13); Manitoba Agriculture and Resource Development, Manitoba Geological Survey, Data Repository Item DRI2019003, Microsoft® Excel® file, URL <https://manitoba.ca/iem/info/libmin/DRI2019003.xlsx> [September 2022].

Martins, T., Linnen, R., Fedikow, M. and Singh, J. 2017: Whole-rock and mineral geochemistry as exploration tools for rare-element pegmatite in Manitoba: examples from the Cat Lake–Winnipeg River and Wekusko Lake pegmatite fields (parts of NTS 52L6, 63J13); *in* Report of Activities 2017, Manitoba Growth, Enterprise and Trade, Manitoba Geological Survey, p. 42–51, URL <https://manitoba.ca/iem/geo/field/roa17pdfs/GS2017-5.pdf> [September 2022].

Natural Resources Canada 2021: Critical minerals; URL <https://www.nrcan.gc.ca/our-natural-resources/minerals-mining/critical-minerals/23414/> [September 2022].

Piazolo, S., Daczko, N., Silva, D. and Raimondo, T. 2020: Melt-present shear zones enable intracontinental orogenesis; Geology, v. 48, no. 7, p. 643–648.

Reid, K.D. 2021a: Bedrock geology of the Stuart Bay–Chickadee Lake area (east of Wekusko Lake), north-central Manitoba (parts of NTS 63J12, 13); Manitoba Agriculture and Resource Development, Manitoba Geological Survey, Preliminary Map PMAP2021-1, scale 1:15 000, URL <https://manitoba.ca/iem/info/libmin/PMAP2021-1.pdf> [October 2022].

Reid, K.D. 2021b: Results of bedrock geological mapping in the Stuart Bay–Chickadee Lake area (east of Wekusko Lake), north-central Manitoba (parts of NTS 63J12, 13); *in* Report of Activities 2021, Manitoba Agriculture and Resource Development, Manitoba Geological Survey, p. 29–39, URL <https://manitoba.ca/iem/geo/field/roa21pdfs/GS2021-4.pdf> [October 2022].

Schneider, D., Heizler, M., Bickford, M., Wortman, G., Condie, K. and Perilli, S. 2007: Timing constraints of orogeny to cratonization: thermochronology of the Paleoproterozoic Trans-Hudson orogen, Manitoba and Saskatchewan, Canada; Precambrian Research, v. 153, p. 65–95.

Silva, D., Daczko, N., Piazolo, S. and Raimondo, T. 2022: Glimmerite: a product of melt-rock interaction within a crustal-scale high-strain zone; Gondwana Research, v. 105, p. 160–184.

Silva, D., Lima, A., Gloaguen, E., Gumiaux, C., Noronha, F. and Deveaud, S. 2018: Spatial geostatistical analysis applied to the Barroso-Alvão rare-elements pegmatite field (northern Portugal); *in* Frontiers in Information Systems (Volume 1): GIS – An Overview of Applications, A.C. Teodoro (ed.), Bentham Science Publishers, Sharjah, United Arab Emirates, p. 67–101.

Snow Lake Lithium 2022: Presentation; URL <https://snowlakelithium.com/presentation/> [September 2021].

Stern, R.A. and Lucas, S.B. 1994: U-Pb zircon age constraints on the early tectonic history of the Flin Flon accretionary collage, Saskatchewan; *in* Current Research, Part F, Geological Survey of Canada, no. 94-F, p. 75–86.

Stern, R.A., Lucas, S.B., Syme, E.C., Bailes, A.H., Thomas, D.J., Leclair, A.D. and Hulbert, L. 1993: Geochronological studies in the Flin Flon domain, Manitoba-Saskatchewan, NATMAP Shield Margin Project area: results for 1992–1993; *in* Radiogenic Age and Isotopic Studies, Report 7, Geological Survey of Canada, no. 93-2, p. 59–70.

Stewart, M.S., Lafrance, B. and Gibson, H.L. 2018: Early thrusting and folding in the Snow Lake camp, Manitoba: tectonic implications and effects on volcanogenic massive sulfide deposits; Canadian Journal of Earth Sciences, v. 55, no. 8, p. 935–957.

Syme, E.C., Lucas, S.B., Bailes, A.H. and Stern, R.A. 2000: Contrasting arc and MORB-like assemblages in the Paleoproterozoic Flin Flon Belt, Manitoba, and the role of intra-arc extension in localizing volcanic-hosted massive sulphide deposits; Canadian Journal of Earth Sciences, v. 36, no. 11, p. 1767–1788.

Whalen, J.B., Syme, E.C. and Stern, R.A. 1999: Geochemical and Nd isotopic evolution of Paleoproterozoic arc-type granitoid magmatism in the Flin Flon Belt, Trans-Hudson orogen, Canada; Canadian Journal of Earth Sciences, v. 36, no. 2, p. 227–250.

Zwanzig, H.V. 1990: Kisseynew gneiss belt in Manitoba: stratigraphy, structure, and tectonic evolution; *in* The Early Proterozoic Trans-Hudson Orogen of North America, J.F. Lewry and M.R. Stauffer (ed.), Geological Association of Canada, Special Paper 37, p. 95–120.

Zwanzig, H.V. and Bailes, A.H. 2010: Geology and geochemical evolution of the northern Flin Flon and southern Kisseynew domains, Kississing–File lakes area, Manitoba (parts of NTS 63K, N); Manitoba Innovation, Energy and Mines, Manitoba Geological Survey, Geoscientific Report GR2010-1, 135 p., URL <https://manitoba.ca/iem/info/libmin/GR2010-1.zip> [September 2022].

GS2022-8

Preliminary interpretation of aeromagnetic data from poorly exposed and sub-Phanerozoic basement rocks east and southeast of Snow Lake, north-central Manitoba (parts of NTS 63F15, 16, 63G13, 14, 63J3–6, 11–14, 63K1, 2, 8, 9, 16, 63O3, 4)

by K.D. Reid

In Brief:

- The area east and south of Snow Lake is subdivided into 13 aeromagnetic domains based on total magnetic intensity and structural patterns
- Each aeromagnetic domain is subdivided lithologically and often contain multiple rocks types
- Sub-Phanerozoic basement rocks of the eastern Trans-Hudson orogen contain a variety of economically significant mineral deposit types

Citation:
Reid, K.D. 2022: Preliminary interpretation of aeromagnetic data from poorly exposed and sub-Phanerozoic basement rocks east and southeast of Snow Lake, north-central Manitoba (parts of NTS 63F15, 16, 63G13, 14, 63J3–6, 11–14, 63K1, 2, 8, 9, 16, 63O3, 4); *in* Report of Activities 2022, Manitoba Natural Resources and Northern Development, Manitoba Geological Survey, p. 61–70.

Summary

The Manitoba Geological Survey is conducting research on metavolcanic and metasedimentary rocks of Paleoproterozoic age that extend beneath Phanerozoic limestone and dolomite south and southeast of Snow Lake in north-central Manitoba. The goal is to produce new 1:50 000 scale geological maps using industry and government aeromagnetic, lithological, geochemical and geochronological data. Presented here are brief descriptions of 13 interpreted aeromagnetic domains in the project area and their proposed lithological subdivisions. In the northern half of the study area, some lithological subdivisions have been tested by reviewing drillcore and the associated geochemical and geochronological analytical results.

Introduction

Isotopically juvenile volcanic-arc and arc-rift sequences are economic producers of volcanogenic massive-sulphide (VMS) in the Flin Flon domain (FFD), and, as such, have long been subject to extensive exploration. Volcanogenic massive-sulphide orebodies commonly have both magnetic and conductive properties detectable by airborne magnetic and electromagnetic surveys, thus these surveys are routinely applied exploration tools. South of where the FFD is exposed, Phanerozoic limestone and dolomite cover rocks have little magnetic response and thus behave largely as 'transparent' material, allowing the more magnetic basement rocks to be observed.

The project area extends over an irregular 9350 km^2 area southeast of Snow Lake (Figure GS2022-8-1), covering both poorly exposed and sub-Phanerozoic basement rocks along the southeasterly flank of the FFD. This report provides a summary of the interpreted aeromagnetic domains and potential lithological subdivisions for the project area as determined from magnetic intensity, internal magnetic complexity and electrical conductivity. In addition, some aspects of drillcore observations are reviewed from previous work (e.g., Simard et al., 2010; Reid, 2020).

Regional setting

The FFD is one of a series of volcanic-sedimentary assemblages that make up the internal Reindeer zone of the Paleoproterozoic Trans-Hudson orogen (Lewry, 1990). In Manitoba, 1.92–1.87 Ga juvenile island-arc, juvenile ocean-floor/back-arc and ocean-island basalt (Syme et al., 1999) were tectonically accreted during 1.88–1.87 Ga closure of the Manikewan Ocean (e.g., Stauffer, 1984; Lucas et al., 1996). Successor-arc plutonism (1.87–1.84 Ga) 'stitched' this accretionary complex. Southwest-directed thrusting resulted in uplift and erosion during the waning stages of successor-arc magmatism (e.g., Ansdell et al., 1999). This led to deposition of voluminous continental alluvial-fluvial deposits (Paleoproterozoic metasediments; medium blue in Figure GS2022-8-1) and broadly coeval marine turbidites (Paleoproterozoic greywacke; light grey in Figure GS2022-8-1) into the Kisseynew paleobasin to the north (ca. 1.85–1.84 Ga; Zwanzig, 1990; Lucas et al., 1996). South-directed thrusting continued and resulted in the FFD being overthrust by nappes of marine turbidites of the Kisseynew domain (Zwanzig, 1990). Arc and successor-arc processes were followed by a protracted interval of deformation and metamorphism in the Trans-Hudson orogen (1.84–1.69 Ga) related to collision between the juvenile Paleoproterozoic Reindeer zone and Archean cratons (Gordon et al., 1990; Lewry, 1990; Ansdell et al., 1995).

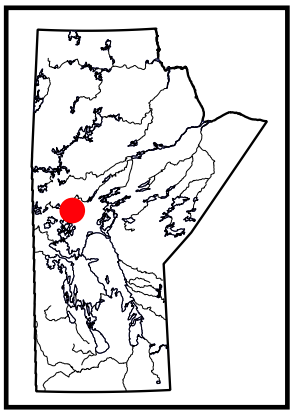

Previous work

Leclair et al. (1997) conducted regional mapping of the sub-Phanerozoic portion of the FFD in the early 1990s by integration of high-resolution aeromagnetic and gravity data. Leclair's compila-

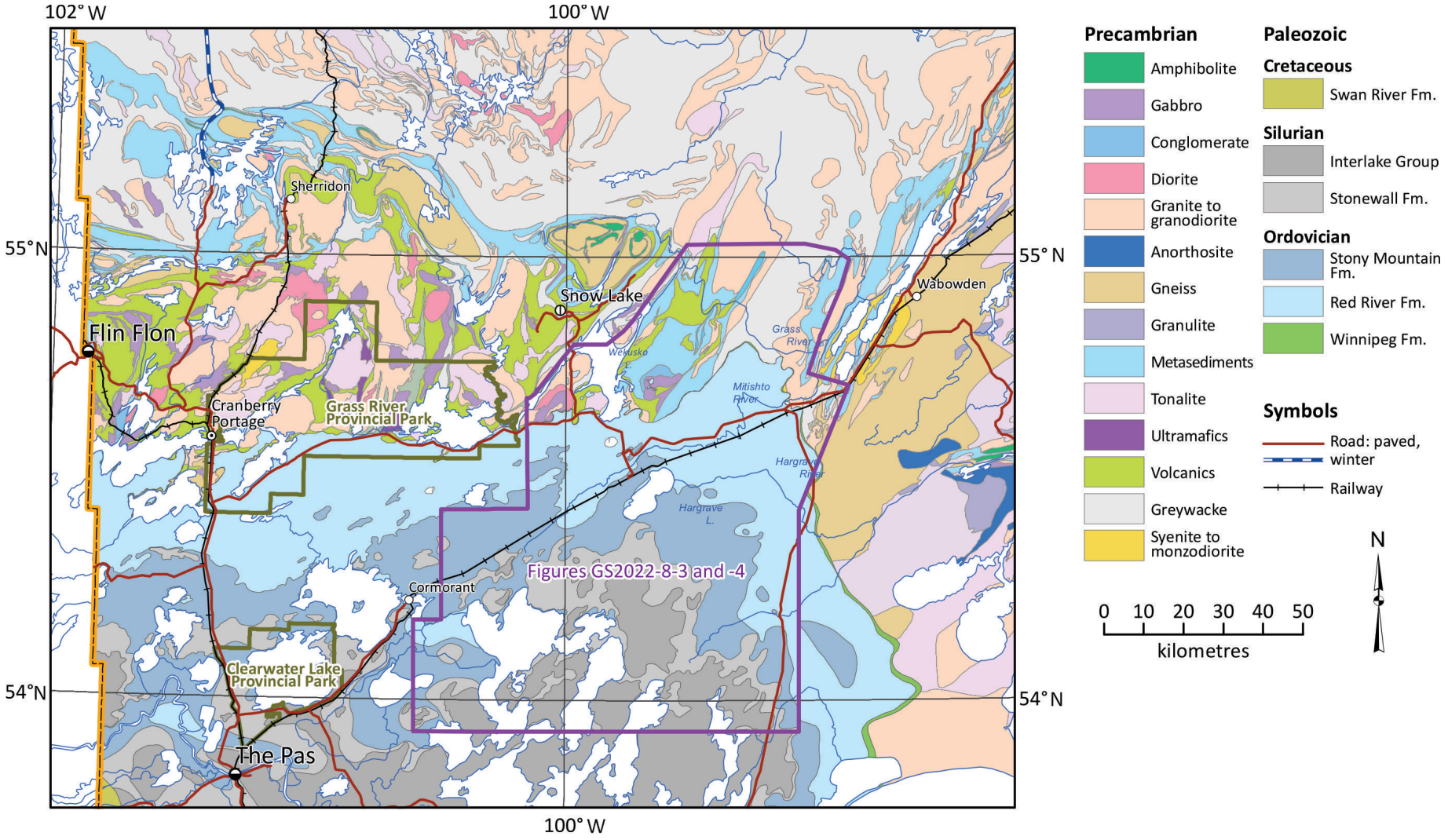

Figure GS2022-8-1: *Geology of the Flin Flon domain in west-central Manitoba (geology from Manitoba Geological Survey, 2022), with the study area outlined in purple. Rocks in the northern portion of the study area are poorly exposed. Abbreviation: Fm., Formation.*

tion resulted in the recognition of several major domains (Figure GS2022-8-2). Some rock assemblages similar to those found in the exposed portion of the FFD and Kisseynew domain were recognized in the sub-Phanerozoic, whereas others appear to be unique to the sub-Phanerozoic. In the project area, Leclair et al. (1997) recognized four lithotectonic domains in the FFD (Figure GS2022-8-2): 1) the 1.83 Ga Cormorant batholith; 2) the Clearwater domain (interpreted to be correlative to the 1.90–1.88 Ga Snow Lake assemblage); 3) the Eastern Kisseynew domain; and 4) the Superior boundary zone.

Simard and McGregor (2009) started compilation of new geochronological, isotopic and geochemical data to aid in mapping the sub-Phanerozoic portion of the Flin Flon and Kisseynew domains, with the objective of characterizing the various geophysical domains outlined by Leclair et al. (1997). Simard et al. (2010) conducted detailed work on eight poorly understood VMS deposits from the Clearwater and Eastern Kisseynew domains, showing that they formed in different lithotectonic environments. They were able to show that deposits in the Clearwater domain (Moose, Limestone, Sylvia, Kofman deposits) are hosted in bimodal tholeiitic to transitional oceanic-arc rocks at 'lower metamorphic grade', whereas those of the Eastern Kisseynew domain (Watts River, Fenton, Harmin, Talbot deposits) are hosted by volcanic and sedimentary rocks formed in a rifted arc and/or back-arc environment and metamorphosed at relatively 'high metamorphic grade'. Reid (2017, 2018) re-examined drillcore and coupled it with aeromagnetic interpretation to characterize the area south of Wekusko Lake, and the Watts, Mitishto and Hargrave rivers areas. Reid (2020) reviewed geochemical and geochronological data from drillcore from these areas with a focus on metasedimentary rocks.

Aeromagnetic data and observation methodology

High-resolution aeromagnetic data used in this interpretation were compiled by Keating et al. (2012) using aeromagnetic surveys from the Geological Survey of Canada and industry that were flown at line spacing ranging from 200 to 400 m and sensor heights ranging from 90 to 150 m. Details regarding microlevelling and upward continuation to merge the datasets is provided in Keating et al. (2012). The total magnetic intensity (TMI) and first vertical derivative (1VD) were gridded using Geosoft plugins in Esri® ArcMap 10.6. Regardless of survey parameters, with the

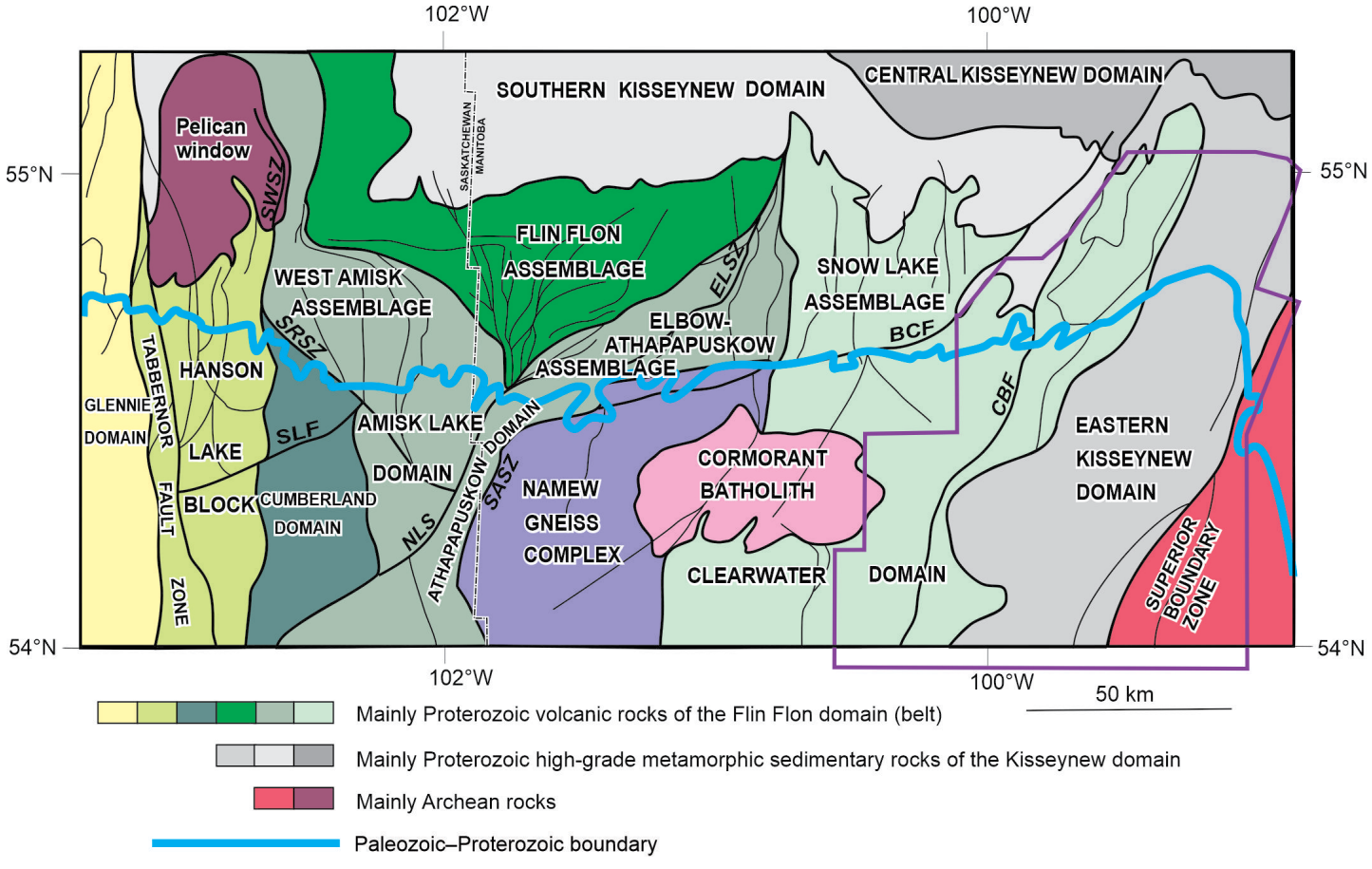

Figure GS2022-8-2: *Interpreted lithotectonic domains of the Flin Flon belt, referred to herein as the Flin Flon domain (after Leclair et al., 1997; NATMAP Shield Margin Project Working Group, 1998). Abbreviations of major faults and shear zones: BCF, Berry Creek fault; CBF, Crowduck Bay fault; ELSZ, Elbow Lake shear zone; NLS, Namew Lake structure; SASZ, South Athapapuskow shear zone; SLF, Suggi Lake fault; SRSZ, Spruce Rapids shear zone; SWSZ, Sturgeon-weir shear zone. The thick blue line is the contact between the exposed Precambrian rocks to the north and Paleozoic-covered Precambrian rocks to the south. The purple line shows the study area.*

increase in depth of the Phanerozoic cover, the distance of the sensor to the target rocks also increases, resulting in lower data resolution. This is observable in Figure GS2022-8-3, moving from where fine detail can be seen in the exposed bedrock area in the north (e.g., East Wekusko, Saw Lake domains) to becoming increasingly blurry with less clarity in more deeply buried areas in the southwest (e.g., Hayward-McClarty, Hargrave high domains). The current interpretation was aided by the availability of electromagnetic (EM) data associated with Spectrem airborne surveys. Though not levelled between surveys, the electromagnetic decay constant (TAU) in the Z-component was gridded to see comparable conductivity between different rocks. Linework and polygons were plotted digitally in ArcMap 10.6.

The reader is referred to Isles and Rankin (2013) for a detailed discussion regarding the interpretation of aeromagnetic data. Based on these authors' guidelines, two distinct classes of

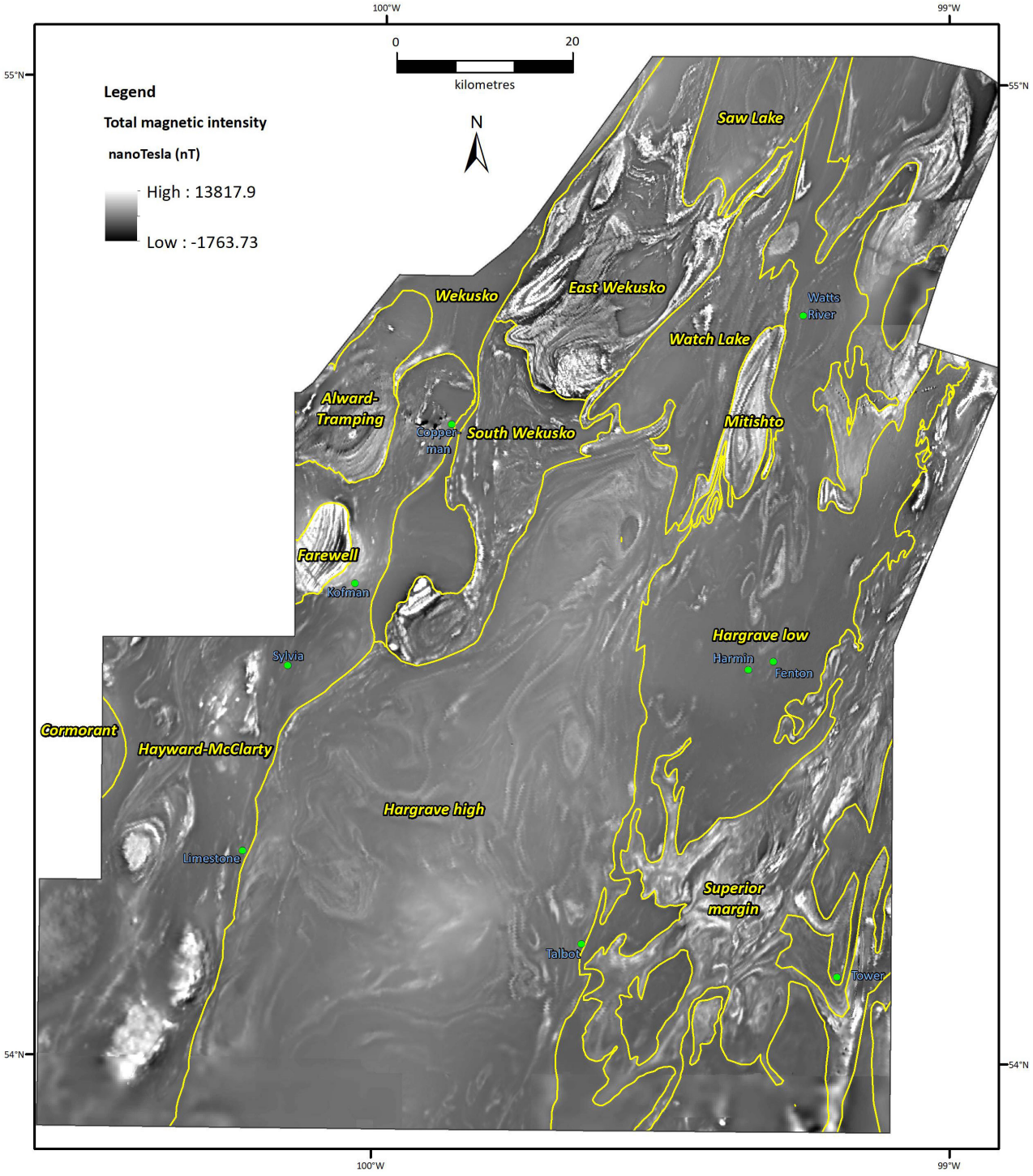

Figure GS2022-8-3: *Greyscale total magnetic intensity overlain by first vertical derivative with 50% transparency, with aeromagnetic domains outlined in yellow. Green dots indicate location of known mineral deposits.*

observations have been made: 1) the magnetic rock units from TMI, and 2) pattern trends and discontinuities (trend breaks) derived from the 1VD. For simplicity in this report, a combination of the TMI overlain by the 1VD with 50% transparency is used here for discussion (Figure GS2022-8-3). Figure GS2022-8-4 shows proposed lithological subdivisions; however, a complete discussion of all lithological subdivisions is beyond the scope of this report. A publication containing all form lines and structural data used to create the aeromagnetic domains and associated lithological subdivisions, is to be released at a later date.

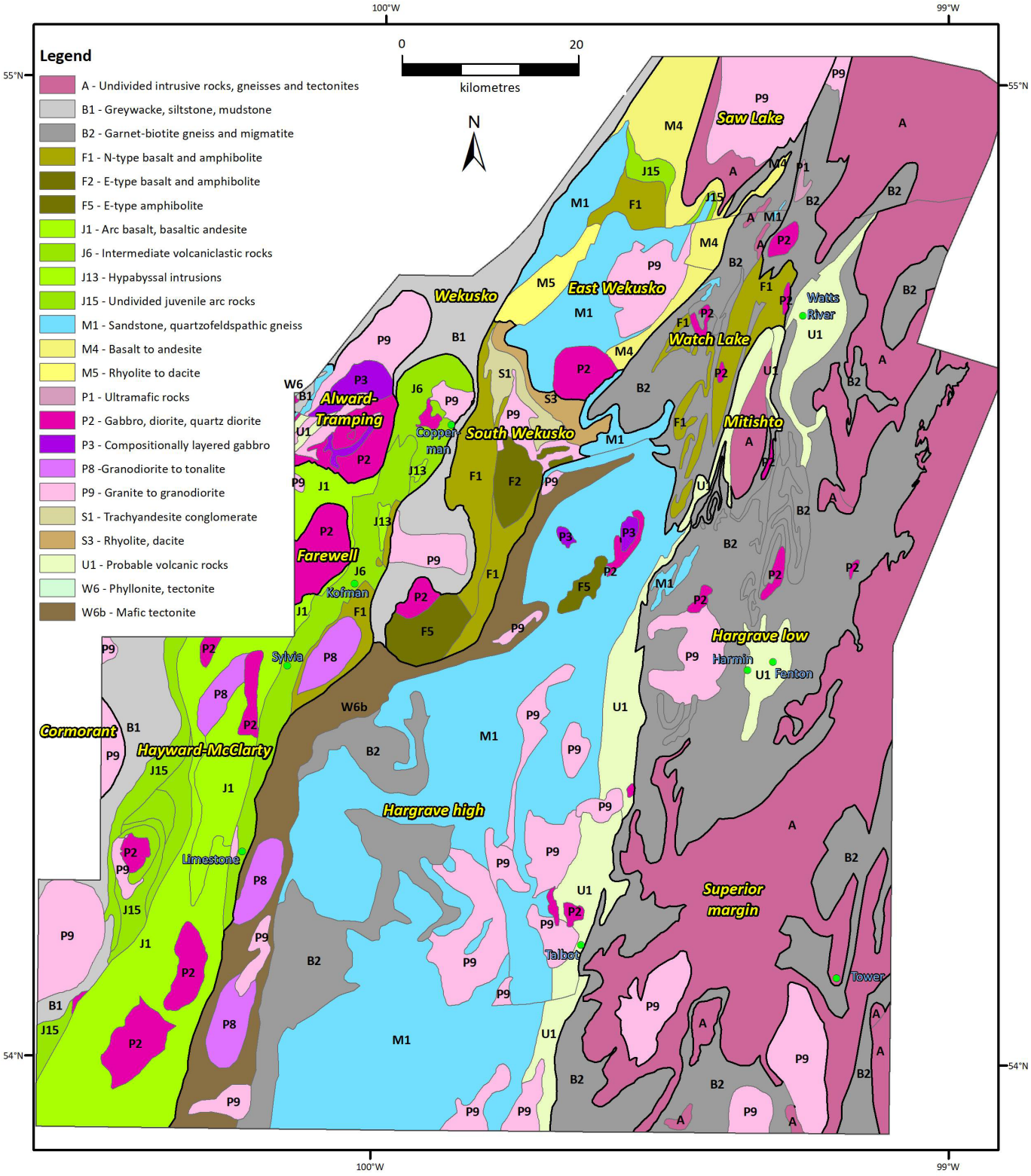

Figure GS2022-8-4: *Lithological subdivision map based on the proposed aeromagnetic domains. The legend is adapted from the NATMAP Shield Margin project (NATMAP Shield Margin Project Working Group, 1998). Green dots show locations of known mineral deposits.*

Aeromagnetic domains

Figure GS2022-8-3 shows the project area divided into 13 aeromagnetic domains that broadly correlate with the Clearwater, Eastern Kisseynew and Southern Kisseynew lithotectonic domains of Leclair et al. (1997). The Hayward-McClarty, Alward-Tramping, Farewell, East Wekusko and South Wekusko aeromagnetic domains are broadly correlative with the Clearwater domain, whereas the Watch Lake, Hargrave high and Hargrave low aeromagnetic domains largely correspond to the Eastern Kisseynew domain (Figures GS2022-8-2 and -3). The Cormorant domain corresponds with the Cormorant batholith as defined by Leclair et al. (1997). The Wekusko domain is associated with the Southern Kisseynew domain. Note, however, that the preliminary interpretation in this report places less emphasis on attempting to identify aeromagnetic domains within the Clearwater or Kisseynew domains, and more emphasis on identifying aeromagnetic domains in the Flin Flon domain. A brief description of the 13 aeromagnetic domains is given below. Figure GS2022-8-4 shows smaller lithological subdivisions; these are based on a number of features, such as TMI, structural pattern, and apparent discontinuities and conductivity (see Table GS2018-4-1 in Reid, 2018 for list of aeromagnetic characteristics of rocks in the eastern Flin Flon domain). Where possible, drillcore data have been incorporated into the interpretation.

Alward-Tramping

This partially exposed aeromagnetic domain is composed of granite and quartz diorite successor-arc plutons and contains subordinate supracrustal rocks (Syme et al., 1995; David et al., 1996). The Wekusko Lake pluton (unit P9; Figure GS2022-8-4) in the northern part of this domain has a very low magnetic signature with almost no internal complexity, and the transition with the Wekusko domain to the northeast is very subtle (Figure GS2022-8-4). The Alward quartz diorite pluton has layered internal complexity and moderate magnetic intensity; its southern extent appears to truncate north-northeast-trending aeromagnetic features in the Hayward-McClarty domain (Figure GS2022-8-3). Although this domain is largely considered to be plutonic, subordinate volcanic and sedimentary rocks are present along its northwest side (units M1, U1; Figure GS2022-8-4).

Wekusko

The Wekusko aeromagnetic domain is a north-south-trending magnetic low; it has varying width and low internal complexity but does contain subtle north-northeast-trending magnetic features and moderate conductivity (EM and TAU; not shown on any figure). The exposed area is mainly composed of mudstone and greywacke that belongs to the Burntwood group at Wekusko Lake (Bailes and Galley, 1992; Gilbert and Bailes, 2005). Moving southward, the Wekusko domain is traced several kilometres under the subsurface via aeromagnetic and drillcore data (Figure GS2022-8-3; Reid, 2017). The Wekusko domain is bounded by the Alward-Tramping domain to the west, the Hayward-McClarty domain to the south and the South Wekusko dome to the east (Figure GS2022-8-3).

Hayward-McClarty

The Hayward-McClarty aeromagnetic domain is broadly analogous to the Clearwater lithotectonic domain identified by Leclair et al. (1997; Figure GS2022-8-2). It is characterized by low to intermediate magnetic intensity and is visible as a series of corrugated north-northeast-trending magnetic fabrics (Figure GS2022-8-3). Irregular to ovoid magnetic lows and highs are interpreted as felsic (unit P9; Figure GS2022-8-4) and mafic (units P2 and P3; Figure GS2022-8-4) intrusive bodies, respectively. In the southwest portion of this domain, macroscopic S-folds flanked by magnetic lows are interpreted as greywacke and mudstone (unit B1; Figure GS2022-8-4), similar to those observed in the Wekusko domain. The eastern portion of the domain hosts the Copper-man, Kofman, Sylvia and Limestone VMS deposits (Figure GS2022-8-3; Simard et al., 2010; Reid, 2017).

Farewell

The Farewell magnetic domain is a prominent north-northeast-trending magnetic high within the Hayward-McClarty domain; it has distinct low and high magnetic corrugations (Figure GS2022-8-3). Two drillholes, WEK-93-13 and WEK-93-14 intersecting massive medium-grained gabbro, test this magnetic high. The corrugated magnetic signature is interpreted to represent a layered mafic intrusion (unit P2; Figure GS2022-8-4) with an approximate 12 km strike length and 9 km width. The 3:2 aspect ratio of this layered intrusion might suggest a much larger intrusion at depth.

Cormorant

A small expression of the Cormorant Lake batholith occurs along the western margin of the project area and has a relatively even, moderately magnetic signature (Figure GS2022-8-3). Work by Leclair et al. (1997) outlined an approximately 60 by 25 km granite intrusion (Figure GS2022-8-2) with an age of 1831 +5/-4 Ma (Stern et al., 1993).

South Wekusko

Rocks of the exposed South Wekusko magnetic domain contain basalt and trachyandesite conglomerate that are structurally juxtaposed against rocks of the Wekusko domain along the Crowduck Bay fault (Gilbert and Bailes, 2005; Reid, 2019). Overall, aeromagnetic response of these rocks is moderate, with minor internal folding and an irregularly folded eastern contact with the East Wekusko and Hargrave high domains. The western half of the South Wekusko domain contains north-south-oriented lows interpreted to represent north-south fault splays running parallel to the Crowduck Bay fault (see Figure GS2022-8-2 for approximate location of the Crowduck Bay fault). An ovoid magnetic

feature, in part interpreted to represent a zoned intrusion with intermediate to mafic composition (unit F5; Figure GS2022-8-4), truncates the southern end of this magnetic domain.

East Wekusko

The East Wekusko magnetic domain covers an area of poorly exposed bedrock east of Wekusko Lake (Figures GS2022-8-1 and -3). Overall TMI signatures that are moderate to high correspond to dominantly Missi group sandstone, conglomerate, felsic–intermediate volcanic, and intermediate intrusive rocks (units M1, M4, M5, P2, P9; Figure GS2022-8-4; NATMAP Shield Margin Project Working Group, 1998; Ansdell et al., 1999; Reid, 2021). Tight to isoclinal folding, recorded by alternating magnetic highs and lows, distinguishes the stratified character of the rocks. The exceptions to the strongly magnetic rocks are ocean-floor basalt and late granite intrusive rocks in the northeast portion of the domain (units F1 and J5; NATMAP Shield Margin Project Working Group, 1998).

Hargrave high

Hargrave high is the largest magnetic domain in the study area; it is a broad magnetic high with variable internal geometry (Figure GS2022-8-3). The contact between the Hayward-McClarty and this domain roughly aligns with the transition to the Eastern Kisseynew domain of Leclair et al. (1997). Similar to Leclair's findings, drillcore from this domain yielded gneissose textures with abundant felsic intrusive sheets. Complexly folded stratigraphy is apparent from magnetic fabrics along the western side of the Hargrave high domain: these resemble interlayered heavy-mineral-rich feldspathic sandstone and conglomerate of the Missi group (unit M1; Figure GS2022-8-4) found in the East Wekusko domain (Figure GS2022-8-3). Drillcore observations support this interpretation; small windows of feldspathic arenite (unit M1; Figure GS2022-8-4) in drillhole HAR077 have a detrital zircon age distribution (Reid, unpublished data) similar to that of Missi group sandstone (e.g., Ansdell et al., 1992, 1999).

Magnetic fabrics along the eastern side of the Hargrave high have been transposed into a north-south orientation; this area hosts the Talbot VMS deposit and may contain intercalated volcanic rocks. Truncation of these north-south magnetic fabrics are considered to be the result of intrusive bodies, possibly granite to granodiorite (unit P9; Figure GS2022-8-4).

Hargrave low

Bordering the Hargrave high domain to the east is a parallel north-northeast-trending magnetic low extending from the very north of the project area to its southern boundary. In contrast to the rocks of the Hargrave high, this domain is characterized by much more subtle magnetic responses (Figure GS2022-8-3). Work by Reid (2020) indicates that a significant amount of rock associated with this broad low aeromagnetic response corresponds with garnet-biotite gneiss that is interpreted to have a sedimentary protolith (unit B2; Figure GS2022-8-4). Similar to rocks in the Hargrave high domain, evidence of in situ melting is often present, with the formation of melanosome and leucosome (Reid, 2018, 2020). Although primary textures are largely absent, Simard et al. (2010) suggested VMS mineralization that occurs in this domain formed in a 'rifted basin' with a mixture of sedimentary and volcanic rocks of younger age (ca. 1865 Ma). Within the broad magnetic lows are areas with subtle increased magnetic response that often coincide with VMS mineralization (e.g., Watts River, Harmin, Fenton deposits; Figure GS2022-8-3); these are considered areas with probable volcanic rocks (Figure GS2022-8-4).

Rocks of the Hargrave low domain have a complexly folded contact with rocks of the Superior margin domain. In the northern part of the domain, a small arrowhead-shaped magnetic high feature (Figure GS2022-8-3) suggests a modified type-2 fold interference. To the south, subtle magnetic features have ovoid patterns, more indicative of type-1 fold interference (Figure GS2022-8-3). Ovoid areas of low aeromagnetic response that are isolated within the Superior margin domain are considered part of the Hargrave low.

Watch Lake

This domain is similar to the Hargrave low in that it has a low magnetic response with subtle magnetic highs; some of these subtle highs appear to be doubly plunging and rootless folds, suggesting these rocks have undergone ductile flow with non-cylindrical folding (Figure GS2022-8-3). The broad magnetic low is assumed to correspond to psammopelite observed in drillcore that is interpreted to be equivalent to Burntwood group (e.g., drillholes KUS343, KUS356 and KUS367; Reid, 2020). However, north-northeast-trending magnetic highs in the very far northern portion of the domain have geochemical characteristics similar to those of Ospwagan group rocks (Reid, 2020), suggesting these rocks may be structurally interleaved.

Mitishto

The Mitishto magnetic domain is a prominent north-northeast-trending ovoid magnetic high with alternating internal complexity that is interpreted to have resulted from type-1 fold interference (Figure GS2022-8-3). Drillholes intersecting this high are limited, but detrital zircons from quartz-rich psammite along its eastern flank (drillhole KUS378) indicate that this unit has Archean provenance, similar to the Saw Lake protoquartzite (Bailes and Böhm, 2008; Reid, 2020). Alternatively, drillholes KUS382 and KUS383 along the western flank intersect calcsilicate-altered intermediate to mafic gneiss interpreted as possible volcanic rocks (Reid, 2020).

Saw Lake

The Saw Lake magnetic domain has low to intermediate magnetic intensity (Figure GS2022-8-3); internal fabrics show

an ovoid centre area, whereas the contact between the East Wekusko and Saw Lake domains is tightly folded. Two main rock types make up the Saw Lake domain (e.g., Bailes, 1985; Bailes and Böhm, 2008); the southern half contains metasedimentary quartzite and subordinate pelite, and the northern half is the multiphase Saw Lake felsic pluton. Detrital zircons from the quartzite yielded only Archean ages, which to some extent overlap with those dominating the Ospwagan group (e.g., Rayner et al., 2006).

Superior margin

Work by Macek et al. (2006) and Zwanzig (1999) demonstrated that the exposed Superior margin stratigraphy extends into the eastern flank of the study area. Strongly magnetic rocks that occur along the eastern flank of the project area and that are in contact and complexly folded with rocks of the Hargrave low are part of the Superior margin domain (Figure GS2022-8-3). These include aspects of Archean orthogneiss and migmatite, and the Paleoproterozoic Ospwagan group passive-margin sedimentary rocks of the northwestern Superior province. The boundary between the Superior margin and the Hargrave low aeromagnetic domains is, in part, adopted from Macek et al. (2006).

Discussion

This report builds on the work of Leclair et al. (1997) by characterizing additional lithological subdivisions of the poorly exposed and sub-Phanerozoic basement rocks along the eastern flank of the Trans-Hudson orogen (Figures GS2022-8-1, -4). As an alternative to the previous subdivision of the studied region into the Clearwater and East Kisseynew lithotectonic domains, the current work divides this area into 13 aeromagnetic domains, each containing probable lithological subdivisions (Figure GS2022-8-4). The current interpretation highlights the following:

- The Hayward-McClarty domain contains arc volcanic and volcaniclastic rocks ranging in composition from basalt to rhyolite. These are, at least in part, an extension of the Hayward Creek juvenile arc volcanic assemblage exposed in the southwest portion of Wekusko Lake (e.g., Gilbert and Bailes, 2005; Reid, 2017).
- The Hargrave high, at least in part, is interpreted to be composed of feldspathic sandstone and conglomerate correlative to the Missi group in the exposed East Wekusko domain.
- The Hargrave low and Watch Lake domains dominantly consist of garnet-biotite gneiss interpreted to be equivalent of Burntwood group, but also contain intercalated intermediate to felsic volcanic rocks (e.g., Simard et al., 2010).
- The Mitishto and Saw Lake domains, although having differing aeromagnetic responses, have quartz-rich sediments with similar Archean provenance (see Bailes and Böhm, 2008; Reid, 2020).

Economic considerations

The poorly exposed and sub-Phanerozoic basement domains of the eastern flank of the Trans-Hudson orogen, particularly the areas east and south of Snow Lake, are well-endowed in a variety of mineral deposit types of economic significance. These include base-metal deposits such as VMS, which contain copper and zinc. Also of economic importance are orogenic structures in the region that are host to gold, and pegmatite dikes containing critical elements such as lithium (Silva et al., 2022). More recently, sulphide-graphite horizons have been recognized to contain elevated vanadium (Huzyk Creek; Couëslan, 2019). Thus, continued baseline documentation and interpretation of poorly exposed and sub-Phanerozoic basement rocks in the Snow Lake region are necessary for finding the critical minerals and elements needed for transitioning to a green electrified economy.

Acknowledgments

The author thanks G. Keller, S. Lee and H. Adediran for their thoughtful guidance and assistance using ArcMap 10.6 and Oasis montaj®.

References

Ansdell, K.M., Connors, K.A., Stern, R.A. and Lucas, S.B. 1999: Coeval sedimentation, magmatism, and fold-thrust domain development in the Trans-Hudson orogen: geochronological evidence from the Wekusko Lake area, Manitoba, Canada; Canadian Journal of Earth Sciences, v. 36, p. 293–312.

Ansdell, K.M., Kyser, T.K., Stauffer, M.R. and Edwards, G. 1992: Age and source of detrital zircon from the Missi Formation: a Proterozoic molasse deposit, Trans-Hudson Orogen, Canada; Canadian Journal of Earth Sciences, v. 29, p. 2583–2594.

Ansdell, K.M., Lucas, S.B., Connors, K.A. and Stern, R.A. 1995: Kisseynew metasedimentary gneiss belt, Trans-Hudson Orogen (Canada): back-arc origin and collisional inversion; Geology, v. 23, no. 11, p. 1039–1043.

Bailes, A.H. 1985: Geology of the Saw Lake area; Manitoba Energy and Mines, Geoscientific Report GR83-2, 47 p. and 1 map at 1:50 000 scale, URL <https://manitoba.ca/iem/info/libmin/GR83-2.zip> [September 2022].

Bailes, A.H. and Böhm, C.O. 2008: Detrital zircon provenance of the Saw Lake protoquartzite, east end of the exposed Flin Flon Domain, Manitoba (NTS 63J13NE); *in* Report of Activities 2008, Manitoba Science, Technology, Energy and Mines, Manitoba Geological Survey, p. 29–37, URL <https://manitoba.ca/iem/geo/field/roa08pdfs/GS-3.pdf> [September 2022].

Bailes, A.H. and Galley, A.G. 1992: Wekusko Lake (north); Manitoba Energy and Mines, Preliminary Map 1992S-2, 1 map, scale 1:20 000. Supersedes 1991S-6, Canada-Manitoba Partnership Agreement on Mineral Development 1990–1995, URL <https://manitoba.ca/iem/info/libmin/PMAP1992_S-2.pdf> [September 2022].

Couëslan, C.G. 2019: Evaluation of graphite- and vanadium-bearing drillcore from the Huzyk Creek property, sub-Phanerozoic Kisseynew domain, central Manitoba (NTS 63J6); *in* Report of Activities 2019, Manitoba Agriculture and Resource Development, Manitoba Geological Survey, p. 60–71, URL <https://manitoba.ca/iem/geo/field/roa19pdfs/GS2019-6.pdf> [September 2022].

David, J., Bailes, A.H. and Machado, N. 1996: Evolution of the Snow Lake portion of the Paleoproterozoic Flin Flon and Kisseynew belts, Trans-Hudson Orogen, Manitoba, Canada; Precambrian Research, v. 80, p. 107–124.

Gilbert, H.P. and Bailes, A.H. 2005: Geology of the southern Wekusko Lake area, Manitoba (NTS 63J12NW); Manitoba Industry, Economic Development and Mines, Manitoba Geological Survey, Geoscientific Map MAP2005-2, scale 1:20 000, URL <https://manitoba.ca/iem/info/libmin/MAP2005-2.pdf> [September 2022].

Gordon, T.M., Hunt, P.A., Bailes, A.H. and Syme, E.C. 1990: U-Pb ages from the Flin Flon and Kisseynew belts, Manitoba: chronology of crust formation at an Early Proterozoic accretionary margin; *in* The Early Proterozoic Trans-Hudson Orogen of North America, J.F. Lewry and M.R. Stauffer (ed.), Geological Association of Canada, Special Paper 37, p. 177–199.

Isles, D.J. and Rankin, L.R. 2013: Geological Interpretation of Aeromagnetic Data; Australian Society of Exploration Geophysicists, Monograph Series, 365 p.

Keating, P., Pilkington, M. and Oneschuk, D. 2012: Geophysical series, high-resolution aeromagnetic data compilation, Flin Flon and Snow Lake regions, Manitoba and Saskatchewan, NTS 63K and parts of NTS 63J, L, M, N and O; Geological Survey of Canada, Open File 7103, scale 1:250 000.

Leclair, A.D., Lucas, S.B., Broome, H.J., Viljoen, D.W. and Weber, W. 1997: Regional mapping of Precambrian basement beneath Phanerozoic cover in southeastern Trans-Hudson Orogen, Manitoba and Saskatchewan; Canadian Journal of Earth Sciences, v. 34, no. 5, p. 618–634.

Lewry, J.F. 1990: Lithoprobe Trans-Hudson Orogen transect: general geology of the transect area and an overview of currently planned and needed research; *in* LITHOPROBE: Trans-Hudson Orogen Transect, LITHOPROBE Secretariat, University of British Columbia, Vancouver, British Columbia, Report 12, p. 5–6.

Lucas, S.B., Stern, R.A., Syme, E.C., Reilly, B.A. and Thomas, D.J. 1996: Intraoceanic tectonics and the development of continental crust: 1.92–1.84 Ga evolution of the Flin Flon Belt, Canada; Geological Society of America Bulletin, v. 108, p. 602–629.

Macek, J.J., Zwanzig, H.V. and Pacey, J.M. 2006: Thompson nickel belt geological compilation map, Manitoba (parts of NTS 63G, J, O, P and 64A and B); Manitoba Science, Technology, Energy and Mines, Manitoba Geological Survey, Open File Report OF2006-33, digital map on CD, URL <https://manitoba.ca/iem/info/libmin/OF2006-33.zip> [October 2022].

Manitoba Geological Survey 2022: New edition of the 1:250 000 scale Precambrian bedrock geology compilation map of Manitoba; Manitoba Natural Resources and Northern Development, Manitoba Geological Survey, GeoFile 3-2022, URL <https://manitoba.ca/iem/info/libmin/geofile3-2022.zip> [October 2022].

NATMAP Shield Margin Project Working Group 1998: Geology, NATMAP Shield Margin Project area, Flin Flon belt, Manitoba/Saskatchewan; Geological Survey of Canada, Map 1968A, scale 1:100 000.

Rayner, N., Zwanzig, H.V. and Percival, J.A. 2006: Detrital zircon provenance of the Pipe Formation, Ospwagan Group, Thompson Nickel Belt, Manitoba, NTS 63O8; *in* Report of Activities 2006, Manitoba Science, Technology, Energy and Mines, Manitoba Geological Survey, p. 116–124, URL <https://manitoba.ca/iem/geo/field/roa06pdfs/GS-11.pdf> [September 2022].

Reid, K.D. 2017: Sub-Phanerozoic basement geology south of Wekusko Lake, eastern Flin Flon belt, north-central Manitoba (parts of NTS63J5, 12, 63K8, 9): insights from drillcore observations and whole-rock geochemistry of mafic rocks; *in* Report of Activities 2017, Manitoba Growth, Enterprise and Trade, Manitoba Geological Survey, p. 65–77, URL <https://manitoba.ca/iem/geo/field/roa17pdfs/GS2017-7.pdf> [September 2022].

Reid, K.D. 2018: Sub-Phanerozoic basement geology from drillcore observations in the Watts, Mitishto and Hargrave rivers area, eastern Flin Flon belt, west-central Manitoba (parts of NTS 63J5, 6, 11, 12, 13, 14); *in* Report of Activities 2018, Manitoba Growth, Enterprise and Trade, Manitoba Geological Survey, p. 37–47, URL <https://manitoba.ca/iem/geo/field/roa18pdfs/GS2018-4.pdf> [September 2022].

Reid, K.D. 2019: Bedrock geological mapping of the Puella Bay area (Weskusko Lake), north-central Manitoba (part of NTS 63J12); *in* Report of Activities 2019, Manitoba Agriculture and Resource Development, Manitoba Geological Survey, p. 42–51, URL <https://manitoba.ca/iem/geo/field/roa19pdfs/GS2019-4.pdf> [September 2022].

Reid, K.D. 2020: Detrital zircon and whole-rock lithogeochemical analyses of poorly exposed and sub-Phanerozoic metasedimentary basement rocks in the Watts, Mitishto and Hargrave rivers area, north-central Manitoba (parts of NTS 63J5, 6, 11–14); *in* Report of Activities 2020, Manitoba Agriculture and Resource Development, Manitoba Geological Survey, p. 21–30, URL <https://manitoba.ca/iem/geo/field/roa20pdfs/GS2020-4.pdf> [September 2022].

Reid, K.D. 2021: Results of bedrock geological mapping in the Stuart Bay–Chickadee Lake area (east of Wekusko Lake), north-central Manitoba (parts of NTS 63J12, 13); *in* Report of Activities 2021, Manitoba Agriculture and Resource Development, Manitoba Geological Survey, p. 29–39, URL <https://manitoba.ca/iem/geo/field/roa21pdfs/GS2021-4.pdf> [September 2022].

Silva, D., Martins, T., Groat, L. and Linnen, R. 2022: Preliminary observations on emplacement controls of pegmatite dikes from the Wekusko Lake pegmatite field, north-central Manitoba (parts of NTS 63J13, 14, 63O4); *in* Report of Activities 2022, Manitoba Natural Resources and Northern Development, Manitoba Geological Survey, p. 49–60, URL <https://manitoba.ca/iem/geo/field/roa22pdfs/GS2022-7.pdf> [November 2022].

Simard, R.-L. and McGregor, C.R. 2009: Toward a new sub-Phanerozoic Precambrian basement map of the Flin Flon Belt, Manitoba (parts of NTS 63J, K, L); *in* Report of Activities 2009, Manitoba Innovation, Energy and Mines, Manitoba Geological Survey, p. 15–21, URL <https://manitoba.ca/iem/geo/field/roa09pdfs/GS-2.pdf> [September 2022].

Simard, R.-L., McGregor, C.R., Rayner, N. and Creaser, R.A. 2010: New geological mapping, geochemical, Sm-Nd isotopic and U-Pb age data for the eastern sub-Phanerozoic Flin Flon Belt, west-central Manitoba (parts of NTS 63J3–6, 11, 12, 14, 63K1–2, 7–10); *in* Report of Activities 2010, Manitoba Innovation, Energy and Mines, Manitoba Geological Survey, p. 69–87, URL <https://manitoba.ca/iem/geo/field/roa10pdfs/GS-6.pdf> [September 2022].

Stauffer, R.A. 1984: Manikewan: an early Proterozoic ocean in central Canada: its igneous history and orogenic closure; Precambrian Research, v. 25, p. 257–281.

Stern, R.A., Lucas, S.B., Syme, E.C., Bailes, A.H., Thomas, D.J., Leclair, A.D. and Hulbert, L. 1993: Geochronological studies in the Flin Flon Domain, Manitoba-Saskatchewan, NATMAP Shield Margin Project area: results for 1992-1993; *in* Radiogenic Age and Isotopic Studies, Report 7, Geological Survey of Canada, Paper 93-2, p. 59–70.

Syme, E.C., Bailes, A.H. and Lucas, S.B. 1995: Geology of the Reed Lake area (parts of 63K/9 and 63K/10); *in* Report of Activities 1995, Manitoba Energy and Mines, Geological Services, p. 42–60, URL <https://manitoba.ca/iem/geo/field/roa95.pdf> [September 2022].

Syme, E.C., Lucas, S.B., Bailes, A.H. and Stern, R.A. 1999: Contrasting arc and MORB-like assemblages in the Paleoproterozoic Flin Flon Belt, Manitoba, and the role of intra-arc extension in localizing volcanic-hosted massive sulphide deposits; Canadian Journal of Earth Sciences, v. 36, p. 1767–1788.

Zwanzig, H.V. 1990: Kisseynew gneiss belt in Manitoba: stratigraphy, structure, and tectonic evolution; *in* The Early Proterozoic Trans-Hudson Orogen of North America, J.F. Lewry and M.R. Stauffer (ed.), Geological Association of Canada, Special Paper 37, p. 95–120.

Zwanzig, H.V. 1999: Mapping in the Setting Lake area (parts of NTS 63J/15 and 63O/1, 63O/2); *in* Report of Activities 1999, Manitoba Industry, Trade and Mines, Manitoba Geological Survey, p. 18–23, URL <https://manitoba.ca/iem/geo/field/roa99pdfs/gs-06-99.pdf> [September 2022].

Zwanzig, H.V. and Bailes, A.H. 2010: Geology and geochemical evolution of the northern Flin Flon and southern Kisseynew domains, Kississing–File lakes area, Manitoba (parts of NTS 63K, N); Manitoba Innovation, Energy and Mines, Manitoba Geological Survey, Geoscientific Report GR2010-1, 135 p., URL <https://manitoba.ca/iem/info/library/downloads/precambrian.html> [September 2022].

GS2022-9

Preliminary results of bedrock geological mapping in the Fox mine–Snake Lake area, Lynn Lake greenstone belt, northwestern Manitoba (part of NTS 64C12)

by X.M. Yang

In Brief:

- Detailed bedrock mapping provides an updated geological framework for various mineralization styles
- Tectonic setting of host rocks to the Fox volcanogenic massive sulphide Cu-Zn deposit is being evaluated
- Quartz diorite intrusions of the post-Sickle intrusive suite may serve as an important guide for potential Au mineralization

Citation:
Yang, X.M. 2022: Preliminary results of bedrock geological mapping in the Fox mine–Snake Lake area, Lynn Lake greenstone belt, northwestern Manitoba (part of NTS 64C12); *in* Report of Activities 2022, Manitoba Natural Resources and Northern Development, Manitoba Geological Survey, p. 71–86.

Summary

In 2022, the Manitoba Geological Survey continued a multiyear bedrock geological mapping project in the Paleoproterozoic Lynn Lake greenstone belt, focusing on the Fox mine–Snake Lake area. The aims were to investigate the geological and structural framework of various rock units, the tectonic setting of the volcanogenic massive sulphide (VMS) Cu-Zn deposit, and the potential relationship between Au and intrusive rocks. Preliminary results of the mapping at 1:10 000 scale indicate that this area contains a variety of volcanic rocks, including basalt, andesite, dacite and rhyolite (BADR), related volcaniclastic rocks, and sedimentary rock units. Reworked volcaniclastic and epiclastic rocks overlie the BADR, suggesting deposition in a setting comparable to modern volcanic arcs to back-arc basins. This supracrustal package is cut by pre-Sickle, post-Sickle and late intrusive suites, and was involved in six regional deformation events (D_1 to D_6). The interpreted tectonic evolution of the greenstone belt includes 1) plate subduction resulting in a magmatic arc to back-arc containing volcanic, volcaniclastic and sedimentary rocks (units 1–3) and associated VMS Cu-Zn mineralization, which are cut by pre-Sickle gabbroic and granitoid rocks (units 4 and 5, respectively); 2) intra-arc extension related to roll-back of a subducting slab, producing synorogenic basins filled by Sickle group sediments (unit 6) and post-Sickle granitoid rocks (unit 7); and 3) juxtaposition and/or terminal collision of the greenstone belt with adjacent domains and relaxation or collapse of the merged orogen, resulting in regional shear-zone formation and associated tectonite (unit 9), and fluid circulation triggered by adakite-like intrusions and Au mineralization in favourable structural-chemical traps, as well as emplacement of a late intrusive suite (unit 8).

Introduction

Detailed bedrock geological mapping at 1:10 000 scale, conducted in the summer of 2022 by the Manitoba Geological Survey (MGS), concentrated on the Fox mine–Snake Lake area in the southwestern part of the Lynn Lake greenstone belt (LLGB; Figure GS2022-9-1). The Fox mine produced about 12 million tons of ore grading 1.82% Cu and 1.78% Zn during the period from 1970 to 1985. It is a volcanogenic massive sulphide (VMS) deposit hosted by the Wasekwan group supracrustal rocks that consist mainly of volcanic, volcaniclastic and sedimentary rocks, informally termed the 'Fox mine succession' (Gilbert et al., 1980; Olson, 1987; Zwanzig et al., 1999). This area provides an excellent opportunity for the MGS to perform detailed bedrock geological mapping to better constrain the field relationships and nature of the supracrustal rocks, the tectonic setting of the VMS deposit, and the various intrusive suites and their associated mineral potential.

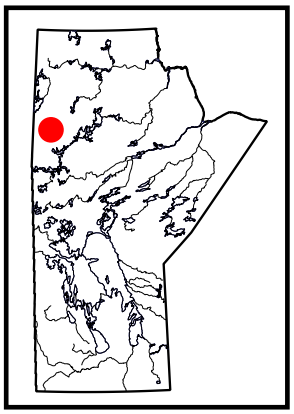

This report presents new field data on the geology, structure and metamorphism of the Fox mine–Snake Lake area, to provide an updated geological map and to discuss tectonic settings of VMS-hosted rocks and implications for Au mineralization by the post-Sickle intrusive suite. The accompanying preliminary map (Yang, 2022) was created from 162 field stations, including 165 new structural measurements, as well as compiled historical data (84 outcrops and 121 structural data points from Gilbert et al. [1980] and a handful of historical drill data), and detailed airborne magnetic data kindly provided by Alamos Gold Inc. During the course of mapping, a Terraplus Inc. KT-10 magnetic susceptibility (MS) meter with a pin was used to measure MS values of outcrops. Each rock type of a visited outcrop was measured at least five times, at different locations if possible, and the average of the measurements was recorded to represent the MS value of the outcrop. The MS data were used, together with the field observations, to constrain lithostratigraphic grouping and unit definition.

Thirty-seven whole-rock samples were collected from the map area for geochemical analysis to study geological processes, including five for Sm-Nd isotopes and one for U-Pb zircon age determina-

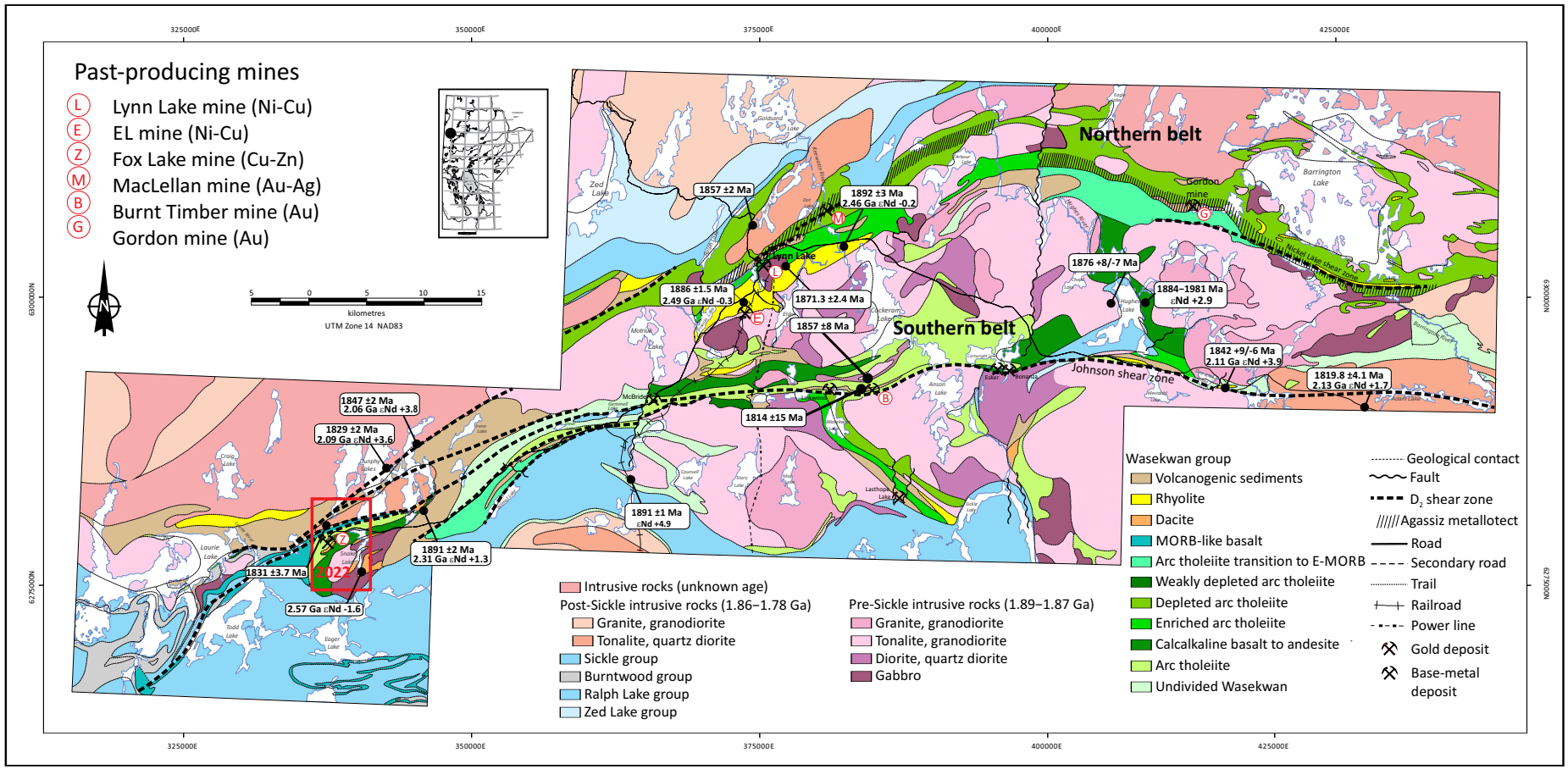

Figure GS2022-9-1: *Regional geology with U-Pb zircon ages and Nd isotopic compositions of the Lynn Lake greenstone belt (modified and compiled from Gilbert et al., 1980; Manitoba Energy and Mines, 1986; Gilbert, 1993; Zwanzig et al., 1999; Turek et al., 2000; Beaumont-Smith and Böhm, 2002, 2003, 2004; Beaumont-Smith et al., 2006; Jones et al., 2006; Beaumont-Smith, 2008; Yang and Beaumont-Smith, 2015b, 2016, 2017; Lawley et al., 2020). The 2022 mapping area is indicated by the red box. Abbreviation: MORB, mid-ocean–ridge basalt.*

tion. The results of these lab analyses are pending and will be reported in subsequent MGS publications.

General geology

The LLGB (Bateman, 1945) is a major tectonic element of the internal Reindeer zone of the Trans-Hudson orogen (Stauffer, 1984; Lewry and Collerson, 1990), which is the largest Paleoproterozoic orogenic belt of Laurentia (Hoffman, 1988; Corrigan et al., 2007, 2009; Corrigan, 2012). It is endowed with several mineral deposit types, such as orogenic Au, magmatic Ni-Cu-Co and volcanogenic massive sulphide Cu-Zn. To the north, the LLGB is bounded by the Southern Indian domain that is composed of variably migmatitic metasedimentary rocks, various granitoids and minor metavolcanic and volcaniclastic rocks (e.g., Kremer et al., 2009; Martins et al., 2019). To the south, the LLGB is flanked by the Kisseynew domain that represents a synorogenic metasedimentary basin (Gilbert et al., 1980; Fedikow and Gale, 1982; Syme, 1985; Zwanzig, 1990, 2000; Zwanzig et al., 1999; White et al., 2000; Zwanzig and Bailes, 2010; Glendenning et al., 2015; Hastie et al., 2018).

The LLGB is composed of two east- to northeast-trending, steeply dipping belts that contain various supracrustal rocks, locally known as the Wasekwan group (Bateman, 1945; Milligan, 1960; Gilbert et al., 1980; Gilbert, 1993), along with the younger Sickle group molasse-type sedimentary rocks (Norman, 1933; Milligan, 1960; Gilbert et al., 1980). The southern and northern belts are separated by granitoid plutons of the 1.89–1.87 Ga Pool Lake intrusive suite (Gilbert et al., 1980; Baldwin et al., 1987; Anderson and Beaumont-Smith, 2001; Beaumont-Smith and Böhm, 2002, 2003, 2004; Beaumont-Smith et al., 2006). In the central and southern parts of the LLGB, the Sickle group overlies the Wasekwan group and felsic–mafic plutonic rocks of the Pool Lake intrusive suite along an angular unconformity (Gilbert et al., 1980). The Sickle group correlates well with the 1850–1840 Ma MacLennan group in the La Ronge greenstone belt of Saskatchewan to the southwest in terms of lithological composition, stratigraphic position and contact relationships (Ansdell et al., 1999; Ansdell, 2005; Corrigan et al., 2009). Volcanic and plutonic rocks in the LLGB underwent peak metamorphism at 1.81–1.80 Ga (Beaumont-Smith and Böhm, 2002, 2003; Lawley et al., 2020).

Significant differences in the geology and geochemistry of the northern and southern belts in the LLGB may reflect regional differences in tectonic settings that were obscured by structural transposition and imbrication during multiple stages of deformation (Gilbert et al., 1980; Syme, 1985; Zwanzig et al., 1999; Beaumont-Smith, 2008). This complexity leads to the suggestion that the term 'Wasekwan group' should be abandoned because it contains disparate volcanic assemblages that were later structurally juxtaposed, and thus may represent a tectonic collage (Zwanzig et al., 1999). The concept was used in a recent geological compilation by Manitoba Agriculture and Resource Development (2021), but this report retains the term 'Wasekwan group' to remain consistent with the literature related to the LLGB.

Geology of the map area

The Fox mine−Snake Lake area is situated in the southwestern part of the LLGB (Figure GS2022-9-1) and is underlain by the Wasekwan group supracrustal rocks intruded by plutons of the Pool Lake intrusive suite (Gilbert et al., 1980). This plutonic suite is unconformably overlain by the Sickle group epiclastic rocks (Figure GS2022-9-2; Yang, 2022). The plutons that only intrude the Wasekwan group are referred to as the 'pre-Sickle suite', and those cutting both the Wasekwan group and the Sickle group are termed the 'post-Sickle suite' (e.g., Milligan, 1960); both are cut by a late intrusive suite (Yang and Beaumont-Smith, 2015a, 2015b, 2017; Yang, 2019, 2021).

Nine map units, including 13 subunits, were defined in the map area and grouped into six affiliations: Wasekwan group, pre-Sickle intrusive suite, Sickle group, post-Sickle intrusive suite, late intrusive suite, and tectonite (Table GS2022-9-1). These map units are shown in Figure GS2022-9-2 and described in the following sections. The supracrustal rocks in the LLGB were mostly deformed and metamorphosed to greenschist and amphibolite facies (Gilbert et al., 1980; Gilbert, 1993; Beaumont-Smith and Böhm, 2004; Yang and Beaumont-Smith, 2015a, 2016, 2017; Yang, 2019, 2021); however, this report omits the prefix 'meta' for brevity.

Wasekwan group (units 1 to 3)

Supracrustal rocks of the Wasekwan group exposed in the map area are divided into the three lithological units and described below.

Volcaniclastic rocks with minor volcanic rocks and sedimentary rocks (unit 1)

Unit 1 is exposed mainly in the northeastern and southwestern (e.g., Snake Lake), west-central (e.g., Mukasew Lake) and southeastern parts of the map area (Figure GS2022-9-2; Yang, 2022). This unit consists of a range of lithologies from mafic to felsic volcanic and volcaniclastic rocks that, in places, appear to have been reworked by sedimentary processes and deposited as volcanic mudstone to sandstone. Locally, some of the unit 1 rocks occur as garnet-biotite schist and amphibolite due to deformation and metamorphism.

Outcrops of foliated dacite and rhyolite (subunit 1a) with minor andesitic rocks and related volcaniclastic rocks occur mainly in the central, west-central and southeastern portions of the map area (Figure GS2022-9-2). These felsic–intermediate rocks are very fine grained, pale grey to white on weathered surfaces and light to medium greyish red or grey on fresh surfaces. Primary features (e.g., flow banding, porphyritic texture) are preserved, despite these rocks being foliated and recrystal-

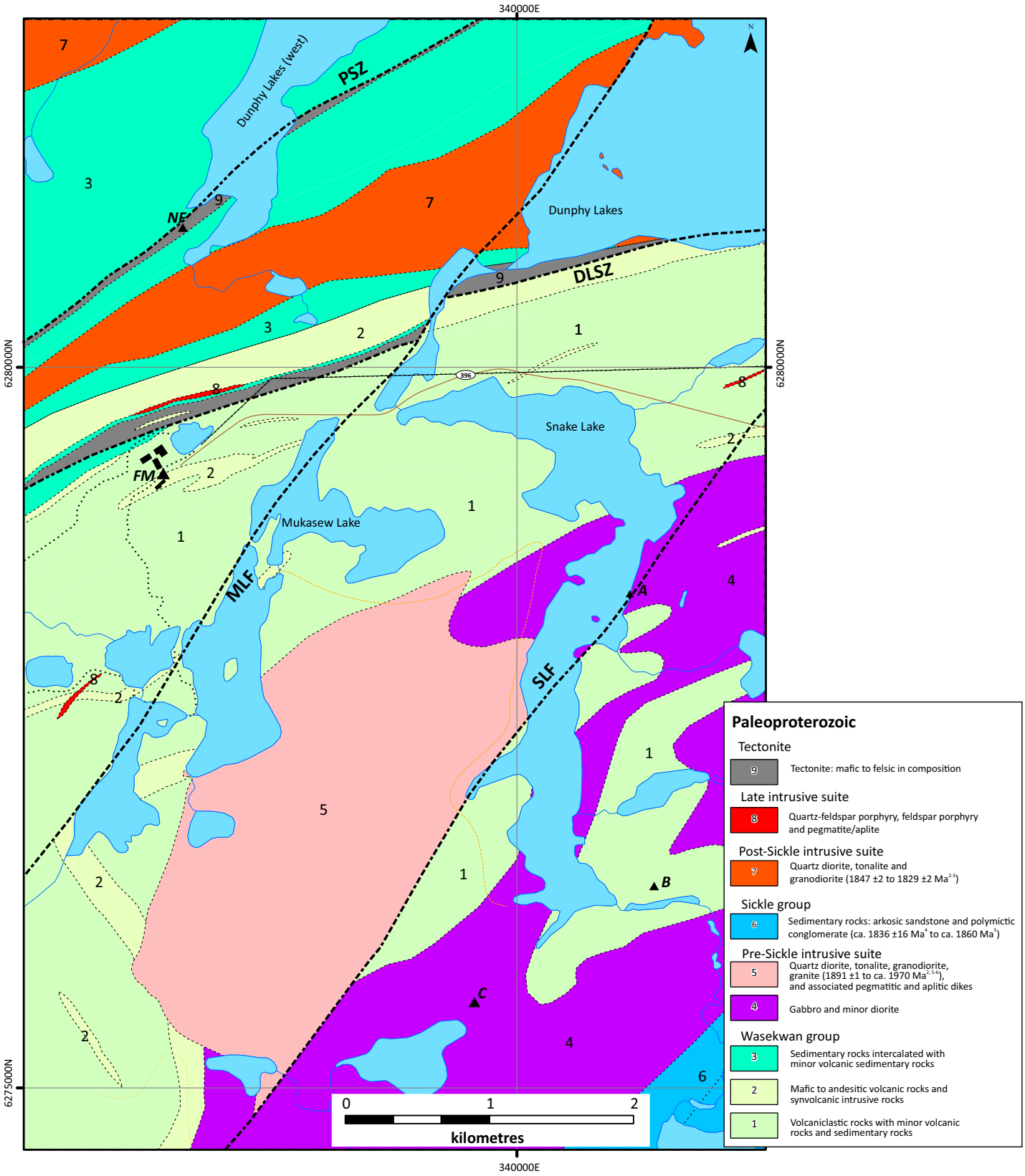

Figure GS2022-9-2: *Simplified geology of the Fox mine–Snake Lake area, Lynn Lake greenstone belt, northwestern Manitoba (simplified from Yang, 2022). Coarse dashed lines indicate a shear zone or fault: DLSZ, Dunphy Lakes shear zone; MLF, Mukasew Lake fault; PSZ, Pumphouse shear zone; SLF, Snake Lake fault. Black triangles indicate a mineral deposit or occurrence: FM, Fox mine (Cu-Zn volcanogenic massive sulphide deposit); NF, North Fox occurrence (Cu-Zn); A, BAG occurrence (Cu); B, GAL occurrence (Cu-Zn-Au-Ag); C, unnamed occurrence (Zn). Superscript numbers following U-Pb zircon ages in legend correspond to references in footnote of Table GS2022-9-1.*

Table GS2022-9-1: Lithostratigraphic units of the Fox mine–Snake lake area, Lynn Lake greenstone belt.

Unit[1]	Rock type	Affiliation
9	Tectonite: mafic to felsic	Tectonite
8	Quartz-feldspar porphyry, feldspar porphyry and pegmatite/aplite	Late intrusive suite
	Intrusive contact	
7	Quartz diorite, tonalite and granodiorite (1847 ±2 to 1829 ±2 Ma[2-3])	Post-Sickle intrusive suite
	Intrusive contact	
6	Sedimentary rocks: arkosic sandstone and polymictic conglomerate (ca. 1836 ±16 Ma[4] to ca. 1860 Ma[5])	Sickle group
6a	Arkosic sandstone, quartz pebbly sandstone	
6b	Polymictic conglomerate with minor pebbly sandstone	
	Structural contact	
5	Quartz diorite, tonalite, granodiorite, granite (1891 ±1 Ma to ~1870 Ma[2, 5-6]) and associated pegmatitic and aplitic dikes	Pre-Sickle intrusive suite
4	Gabbro and minor diorite	
	Intrusive contact	
3	Sedimentary rocks intercalated with minor volcanic sedimentary rocks	Wasekwan group
3a	Argillite, siltstone and greywacke	
3b	Mafic to intermediate tuffaceous sandstone to tuff	
3c	Volcanic mudstone, siltstone, volcanic sandstone and minor volcanic conglomerate	
	Structural contact	
2	Mafic to intermediate volcanic rocks and synvolcanic intrusive rocks	
2a	Diabase and gabbro	
2b	Porphyritic basaltic andesite	
2c	Plagioclase-phyric basalt and aphyric basalt	
2d	Pillow basalt	
	Structural contact	
1	Volcaniclastic rocks with minor volcanic rocks and sedimentary rocks	
1a	Felsic (1891 ±2 Ma[2]) to intermediate volcanic and volcaniclastic rocks	
1b	Intermediate lapillistone, lapilli tuff and tuff	
1c	Mafic lapillistone, lapilli tuff, tuff, amphibolite, minor mafic mudstone and derivative garnet-biotite schist	
1d	Mafic tuff breccia and volcanic breccia	
	?	

[1] Yang (2022)
[2] Beaumont-Smith and Böhm (2003)
[3] Turek et al. (2000)
[4] Lawley et al. (2020)
[5] Beaumont-Smith et al. (2006)
[6] Baldwin et al. (1987)

lized. Amphibole-(plagioclase-)–phyric basaltic andesite (Figure GS2022-9-3a) does not contain any quartz phenocrysts, but porphyritic dacite (Figure GS2022-9-3b) and rhyolite contain equant or subrounded quartz (1–2 mm) and locally subhedral to euhedral feldspar (0.5–1.5 mm) phenocrysts embedded in a very fine grained to aphanitic groundmass.

Intermediate lapillistone, lapilli tuff and tuff (subunit 1b), typically displaying millimetre- to centimetre-scale layers, likely represent beds, although foliated and locally folded. Lapilli tuff contains elongated fragments of various lithologies (e.g., rhyolite, porphyritic andesite, aphanitic basalt) embedded in a fine-grained matrix consisting of amphibole, biotite, chlorite, epidote, plagioclase and aphanitic material (Figure GS2022-9-3c). Alternating dark grey and pale yellow-grey layers, about 0.5–1 cm thick, are common and represent mafic and intermediate–felsic intercalations. Lapilli tuff appears to grade laterally to fine-grained tuff that contains interbedded mafic and felsic laminae (~0.5–2 mm). Some tuff and lapilli tuff contain

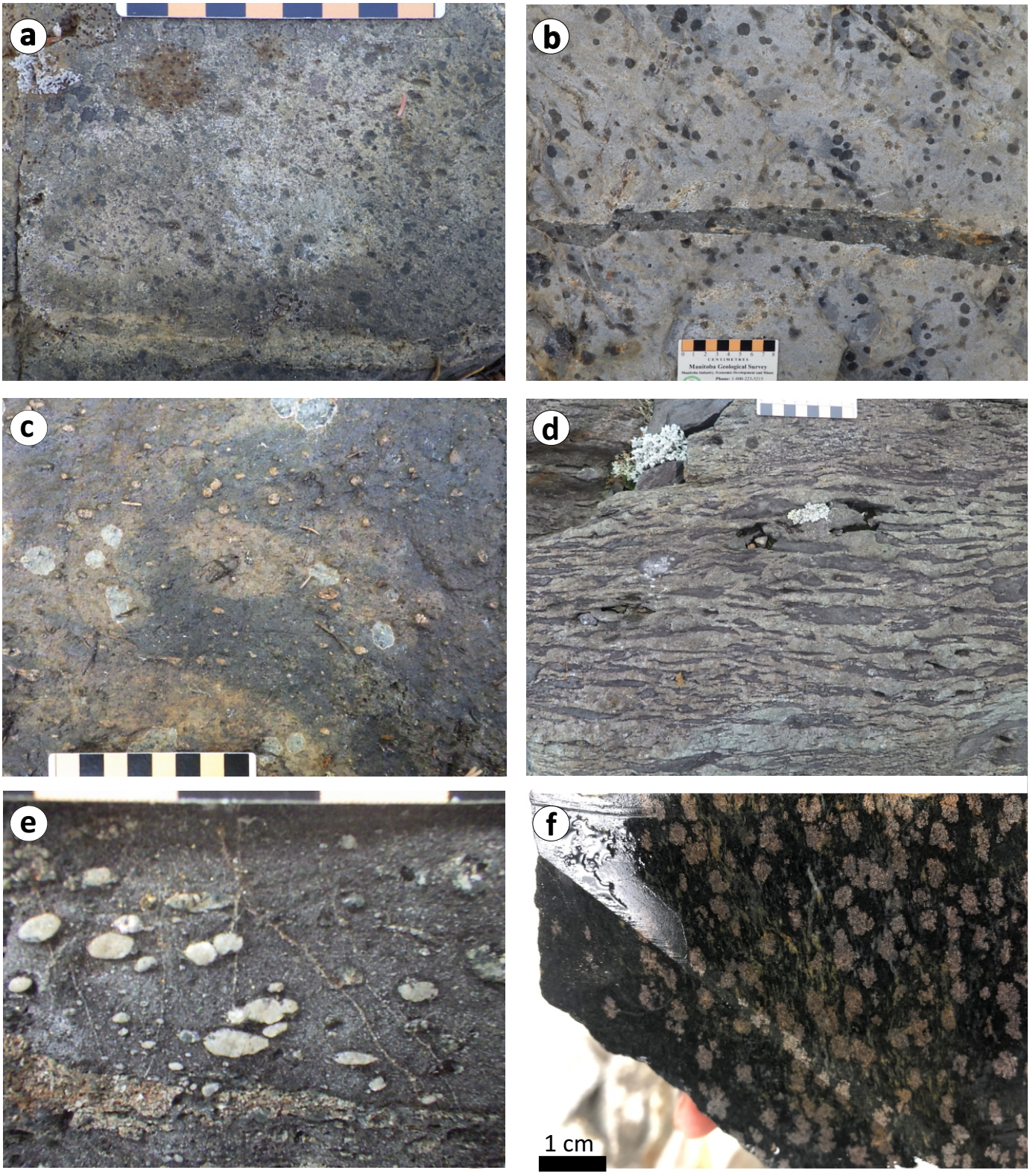

Figure GS2022-9-3: *Field photographs of unit 1 volcaniclastic rocks with minor volcanics and sedimentary rocks of the Wasekwan group in the Fox mine–Snake Lake area:* ***a)*** *amphibole- and plagioclase-phyric basaltic andesite (subunit 1a; UTM Zone 14N, 337470E, 6279101, NAD 83);* ***b)*** *foliated, massive, quartz-phyric dacite cut by a mafic dike up to 4 cm wide (subunit 1a; UTM 337235E, 62777767N);* ***c)*** *foliated andesitic tuff to lapilli tuff containing felsic lithic fragments (subunit 1b; UTM 337147E, 6276091N);* ***d)*** *strongly foliated mafic tuff breccia and breccia with basaltic to andesitic fragments transposed along S_2 foliation (subunit 1d; UTM 341041E, 6279766N);* ***e)*** *some fragments in the mafic volcanic breccia contain stretched oval to subrounded quartz amygdules (same locality as photo d);* ***f)*** *cut slab of sample 111-22-107A01 taken from an outcrop of foliated, medium- to coarse-grained, porphyroblastic garnet amphibolite containing disseminated pyrrhotite (subunit 1c; UTM 336356E, 6278815N) and showing garnet crystals, 5–6 mm in size, that display diffusive grain boundaries and are aligned, together with amphibole and minor plagioclase, in the matrix along S_2 planes. Divisions on scale card are 1 cm.*

reddish garnet porphyroblasts (1–2 mm) that occur preferably in mafic-rich bands or layers and are aligned along S_2 foliation planes.

Mafic volcaniclastic rocks are grouped into two subunits based on size, relative proportion of fragments and composition: subunit 1c includes lapillistone, lapilli tuff, tuff, minor mafic mudstone, and amphibolite and garnet-biotite schist; and subunit 1d includes mafic tuff breccia and breccia (Table GS2022-9-1).

Subunit 1c is characterized by the presence of mafic lithic fragments in an amphibole (and chloritic) matrix. Minor greenish grey, very fine grained, thinly bedded mafic mudstone is included in this subunit. Dark green, acicular actinolite porphyroblasts (up to 5–10 mm), concentrated in foliation or fracture planes in mafic tuff and lapilli tuff, are interpreted to have formed by retrograde greenschist-facies metamorphism. The mafic lapilli tuff and tuff (subunit 1c) are generally moderately to strongly foliated and range from texturally variable to relatively homogeneous. These rocks consist of varied amounts of aphyric lithic fragments and crystal fragments (e.g., plagioclase, chloritic amphibole pseudomorphs after pyroxene) in a fine-grained mafic-tuff matrix. Mafic lapilli-sized fragments make up <25% of subunit 1c but can locally account for up to 80% of the rock, which is then termed mafic lapillistone.

Subunit 1d consists of moderately to strongly foliated mafic tuff breccia and breccia, with various lithic fragments, including plagioclase-phyric basalt, plagioclase-amphibole–phyric basalt, aphyric basalt, lapilli tuff, very fine grained andesite, and minor rhyolite clasts ranging from 8 to 30 cm in length, embedded in a lapilli tuff and tuff matrix. The basaltic fragments are subrounded to subangular, varying in shape from irregular to rarely ellipsoidal, and have been stretched along the generally east-northeast-trending foliation (S_2). In high-strain zones, lithic fragments are sheared and flattened, although the margins of some of the fragments are still discernible (Figure GS2022-9-3d). Some basalt fragments display epidote alteration and others show reaction rims with fine-grained assemblages of chlorite, epidote, sericite and albite. Locally, basalt fragments contain well-preserved quartz amygdules (Figure GS2022-9-3e), and porphyritic fragments display plagioclase and amphibole (after pyroxene) phenocrysts.

Some of the unit 1 volcaniclastic rocks can be classified as garnet-biotite schist because of well-developed schistosity and mineral assemblage (e.g., biotite+plagioclase+garnet+chlorite, quartz and minor magnetite), and others are better termed amphibolite as it is massive rock and contains reddish garnet porphyroblasts in finer amphibole matrix (Figure GS2022-9-3f). The mineral assemblage (i.e., garnet+hornblende±plagioclase) of this garnet amphibolite suggests that its mafic protolith may have experienced middle to upper amphibolite-facies metamorphism at about 5–6 kb and 650–700°C (e.g., Winkler, 1967; Winter, 2014).

Mafic to intermediate volcanic rocks and synvolcanic intrusive rocks (unit 2)

Unit 2 rocks occur mainly south of Dunphy Lakes and in the southwestern part of the map area (Figure GS2022-9-2). This unit consists dominantly of plagioclase-phyric and aphyric basalts and pillow basalt, with subordinate porphyritic basaltic andesite and synvolcanic diabase and gabbro dikes (Table GS2022-9-1).

Synvolcanic diabase and gabbro (subunit 2a) occur mostly as dikes and small plugs in unit 2 volcanic rocks and, in some cases, unit 1 volcaniclastic rocks. The gabbroic rocks are fine to medium grained, porphyritic to equigranular and moderately to strongly foliated. Equant to subhedral plagioclase phenocrysts (up to 10 mm) occur in a fine-grained groundmass of plagioclase, amphibole, chlorite and Fe oxides. Generally, subunit 2a gabbroic rocks consist of 50–60% amphibole and 40–50% plagioclase (Figure GS2022-9-4a). Trace disseminated sulphides (e.g., pyrrhotite; ~0.5–1 mm) are locally evident.

Porphyritic basaltic andesite (subunit 2b) contains amphibole (±biotite) and lesser amounts of plagioclase phenocrysts in a fine-grained groundmass (Figure GS2022-9-4b). Biotite and sericite alteration is common. It is hard to distinguish unit 2b from plagioclase-phyric basalt (subunit 2c), although the latter commonly lacks amphibole (±biotite) phenocrysts (Figure GS2022-9-4c) but commonly exhibits epidote alteration.

Massive aphyric basalt (subunit 2c) is common in the map area. Vesicles and quartz±calcite amygdules are present in some outcrops. Chlorite and epidote alteration is common in the aphyric basalt, as shown by epidote domains as veins and patches ranging from a few centimetres to a metre across.

Pillow basalt (subunit 2d) is exposed and preserved in a relatively low-strain area south and southwest of the Fox mine (Figure GS2022-9-2). Pillow size ranges from 20 to 40 cm and locally reaches up to 100 cm, with well-preserved hyaloclastite selvages up to 3 cm thick. In high-strain areas, pillows are strongly deformed and contain a penetrative foliation. Some pillow selvages are still recognizable and contain stretched vesicles and quartz amygdules transposed along S_2 foliation (Figure GS2022-9-4d). Epidote alteration as veinlets, patches or nodules was commonly observed in basalt with few plagioclase phenocrysts.

Sedimentary rocks intercalated with minor volcanic sedimentary rocks (unit 3)

Unit 3 sedimentary rocks are exposed mainly in the central and northwestern portions of the map area (Figure GS2022-9-2) and can be subdivided into three subunits (Table GS2022-9-1).

Thin- to medium-bedded quartzofeldspathic greywacke, siltstone and argillite (subunit 3a) dominate the sedimentary succession. Primary bedding (S_0) in the sedimentary rocks was transposed by the regional S_2 foliation. The medium- to coarse-grained greywacke is composed mostly of quartz, feldspar, amphibole and lithic clasts (1.5–2 mm) that are well aligned on foliation planes defined by biotite flakes and manifested by felsic-

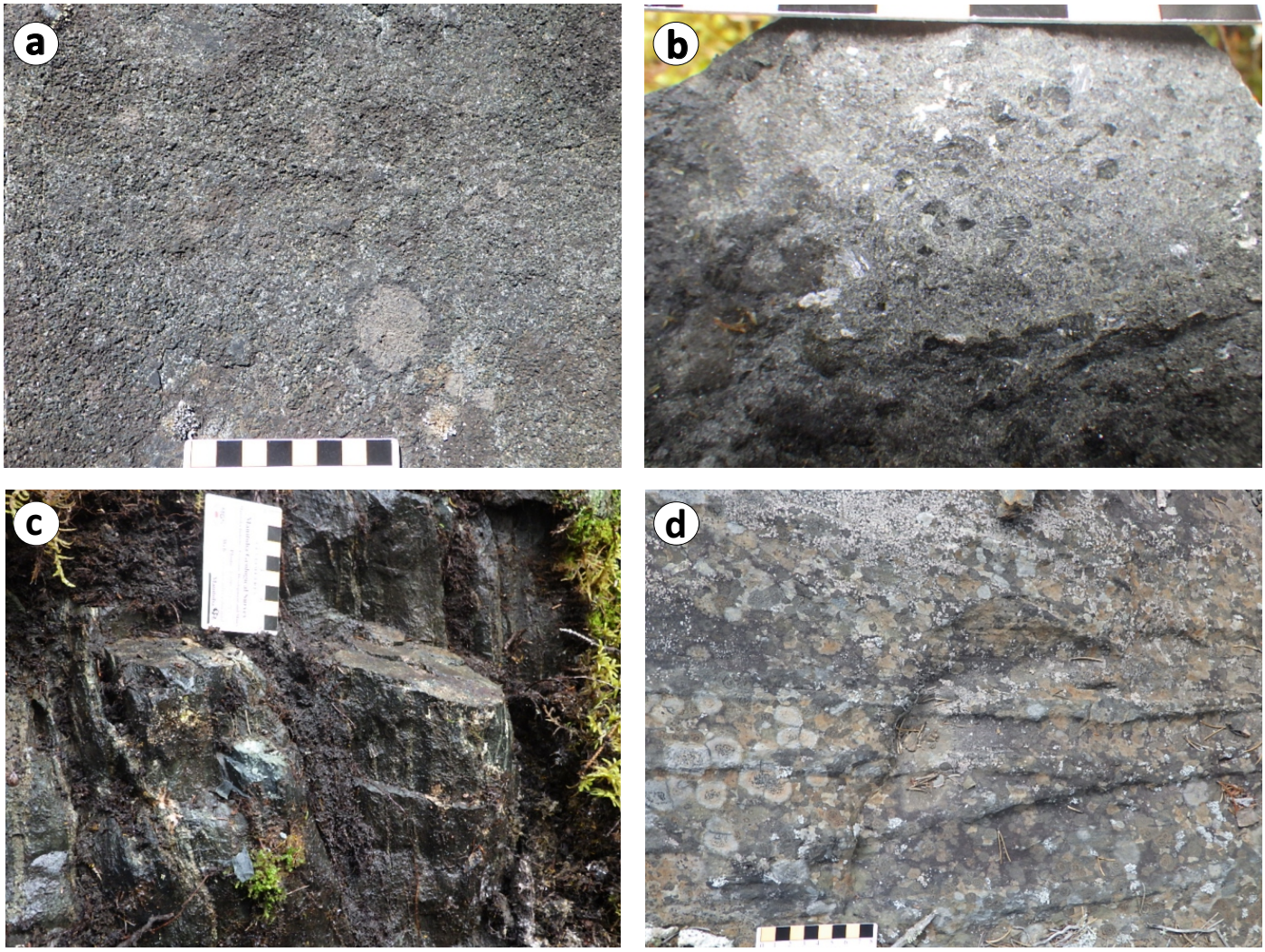

Figure GS2022-9-4: *Field photographs of mafic to intermediate volcanic rocks and synvolcanic intrusive rocks (unit 2) of the Wasekwan group in the Fox mine–Snake Lake area:* ***a)*** *synvolcanic massive gabbro (subunit 2a; UTM Zone 14N, 338119E, 6279300N, NAD 83);* ***b)*** *amphibole-phyric basaltic andesite (subunit 2b; UTM 337803E, 6274906N);* ***c)*** *strongly foliated, aphanitic to plagioclase-phyric basalt (subunit 2c; UTM 338228E, 6280088N);* ***d)*** *strongly foliated pillow basalt with partial hyaloclastite selvage, the stretched pillows aligned along S_2 foliation planes (subunit 2d; UTM 337080E, 6276502N). Divisions on scale card are 1 cm.*

and mafic-rich layering that likely reflects transposed bedding (Figure GS2022-9-5a). Scattered pyrite grains are locally evident in the greywacke and are associated with felsic and/or quartz veins and veinlets. Although strongly foliated and folded (Figure GS2022-9-5b), a unique bed of coarse-grained arkosic greywacke (subunit 3a) with relatively low MS values of 0.179×10^{-3} to 0.215×10^{-3} SI consists dominantly of quartz and feldspar with much less clay material in a matrix containing muscovite and/or biotite, and locally shows graded bedding indicative of younging to the south.

Thin to thick beds of volcanic sedimentary rocks (subunit 3c) consist of volcanic mudstone, siltstone and sandstone, and minor volcanic breccia (Table GS2022-9-1). Tuffaceous sandstone is dominated by laminated, fine- to medium-grained andesitic sandstone consisting mainly of irregular plagioclase, biotite flakes and lithic fragments in a fine sandy matrix; locally, a few large lithic fragments occur along bedding transposed by regional S_2 foliation (Figure GS2022-9-5c). Locally, subunit 3c volcanic sandstone contains fine-grained magnetite grains and displays a relatively high MS value of 1.25×10^{-3} (Figure GS2012-9-5d).

Minor volcanic conglomerate of unit 3c consists dominantly of felsic and intermediate–mafic volcanic clasts in a coarse-grained sandy matrix. These clasts are stretched or flattened and well aligned along S_2 planes that transposed primary bedding. Although not exposed at surface, banded iron formation was intersected by a few historical drillholes in the southeastern part of the map area. It is likely part of the unit 3 sedimentary rocks (e.g., Yang, 2019) and is correlated with highly magnetic, northeast-trending band(s) in the area that are indicated by detailed airborne magnetic data.

Pre-Sickle intrusive suite (units 4 and 5)

Pre-Sickle intrusive suite rocks consist of gabbro and minor diorite of unit 4 and granitoid rocks of unit 5 that occur as plutons

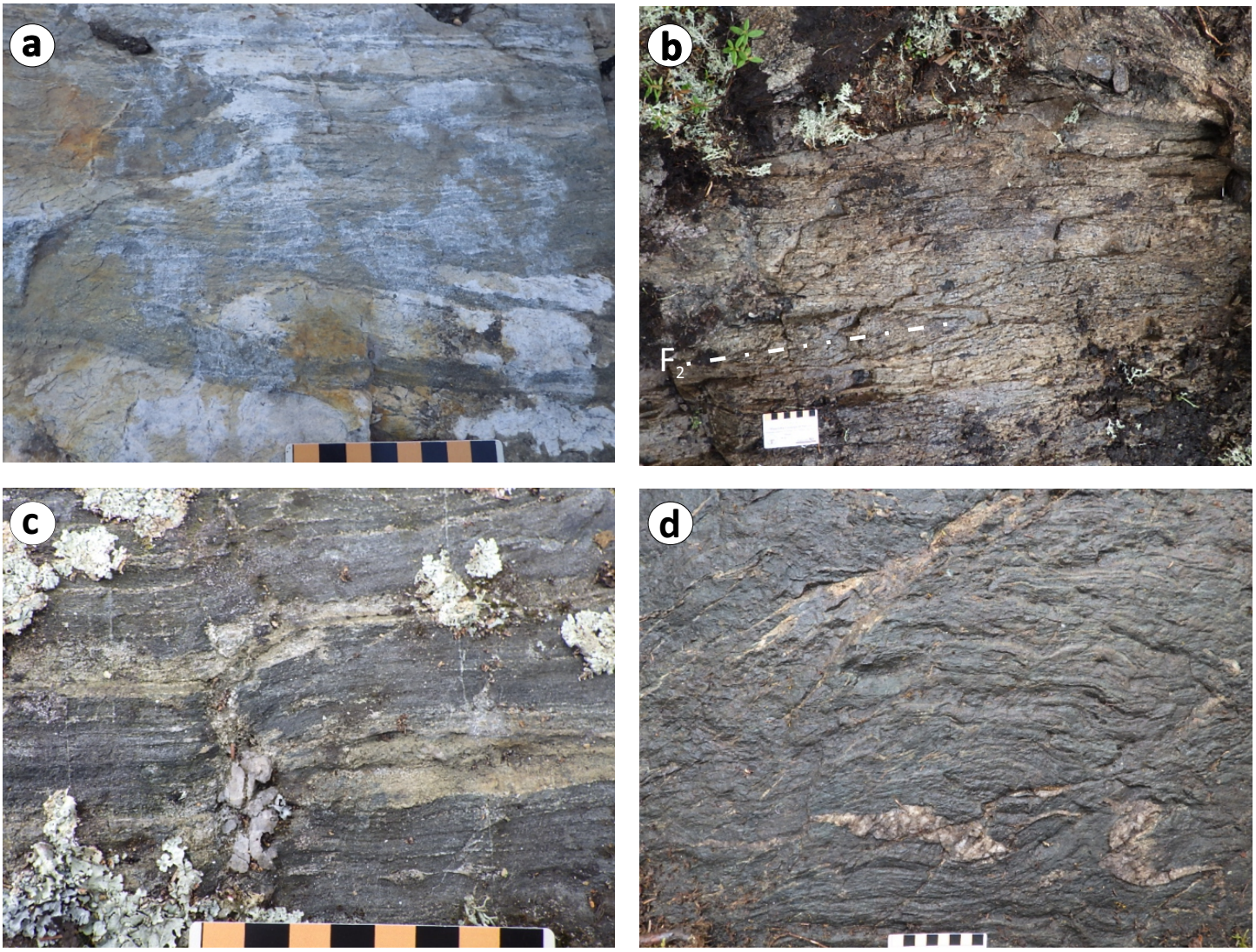

Figure GS2022-9-5: *Field photographs of sedimentary rocks intercalated with minor volcano-sedimentary rocks (unit 3) of the Wasekwan group in the Fox mine–Snake Lake area:* ***a)*** *medium-grained, foliated greywacke with alternating felsic and mafic bands or layering (subunit 3a; UTM Zone 14N, 337634E, 6280046N, NAD 83), which is intruded by fine-grained aplitic dikes (unit 8) up to 10 cm in width;* ***b)*** *strongly foliated arkosic greywacke contains a rootless isoclinal fold (F_2) formed by D_2 formation (unit 3a; UTM 338378E, 6279970N);* ***c)*** *foliated, laminated mafic to intermediate tuffaceous sandstone to tuff (subunit 3b; UTM, 364850E, 6290199N), which is cut and offset by a late quartz vein formed by the D_4 deformation event;* ***d)*** *volcanic sandstone with intermediate to mafic volcanic fragments, its bedding transposed by S_2 foliation that is foliated and folded (subunit 3c; UTM 336954E, 6281033N).*

and/or intrusions in supracrustal rocks of the Wasekwan group, which are overlain unconformably by the Sickle group epiclastic rocks.

Gabbro and minor diorite (unit 4)

Unit 4 occurs mainly in the southern and southeastern parts of the map area (Figure GS2022-9-2). This unit occurs as stock or sill-like intrusions in the Wasekwan group and is cut by unit 5 granitoids. Unit 4 gabbro is foliated, massive, equigranular and medium to coarse grained. It consists of 30–40% plagioclase laths (1–3 mm), 55–60% amphibole (pseudomorphs after pyroxene), minor Fe-oxide minerals and trace pyrrhotite±chalcopyrite (Figure GS202-9-6a). It is locally transitional to medium-grained diorite and texturally grades to very coarse grained gabbro east of Snake Lake. Notably, late quartz (-pyrite) veins cut unit 4 gabbro, resulting in channelized hydrothermal alteration manifested by light red garnets, 3–5 mm across, in the gabbro (Figure GS2022-9-6b).

Granitoid rocks (unit 5)

Unit 5 granitoids occur as a stock (herein termed the 'Snake Lake stock') and are exposed mainly in the southwestern part of the map area (Figure GS2022-9-2). This unit comprises quartz diorite, tonalite, granodiorite and granite, and associated pegmatitic and aplitic dikes.

Unit 5 tonalite is medium to coarse grained, massive, equigranular to locally porphyritic and weakly to moderately foliated. It consists of 20–25% quartz, 40–45% plagioclase, 5–10%

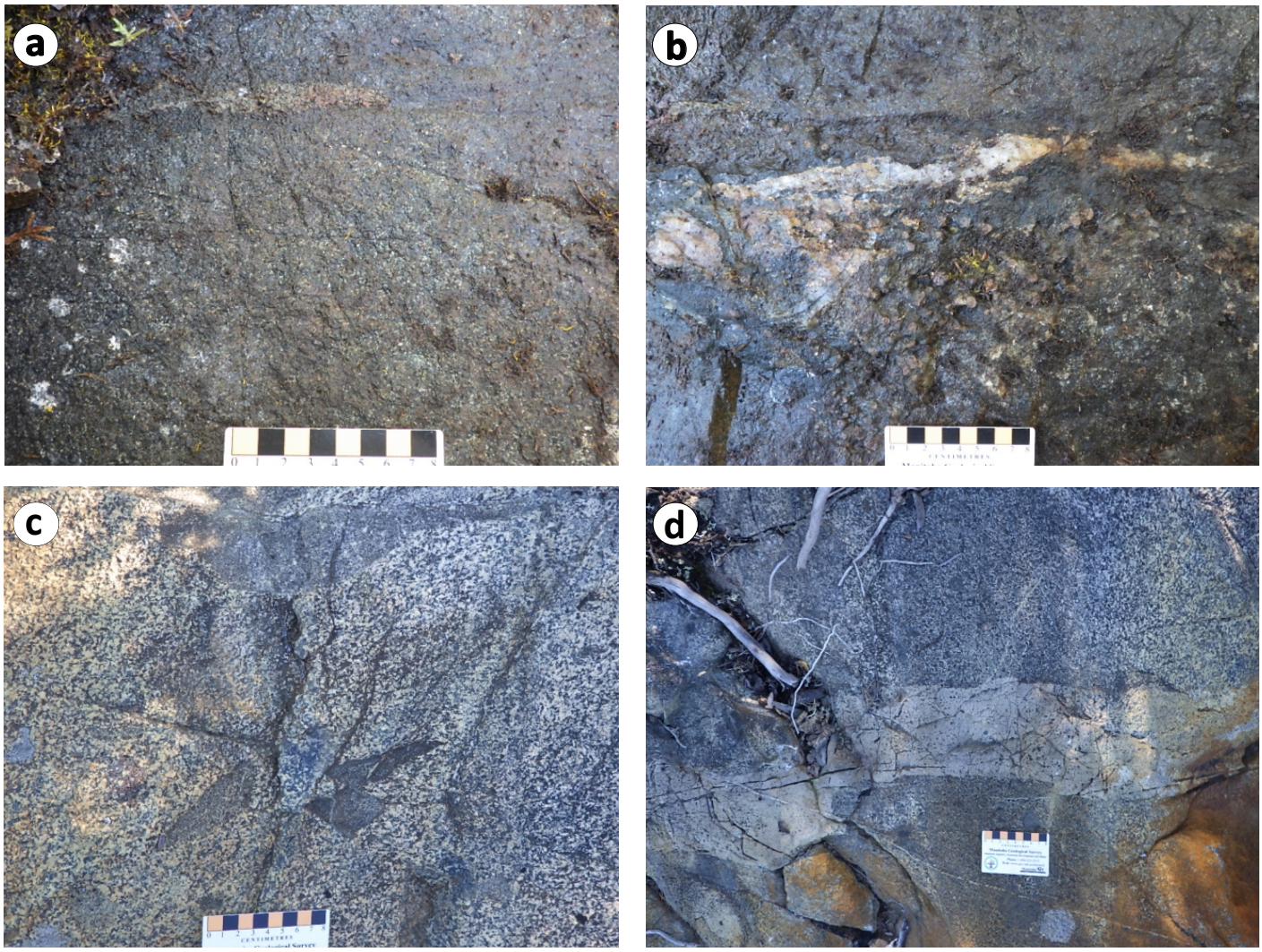

Figure GS2022-9-6: *Outcrop photographs of units 4 and 5 in the Fox mine–Snake Lake area:* ***a)*** *foliated, massive, fine- to medium-grained equigranular gabbro with elongated fragment displaying epidote alteration (unit 4; UTM Zone 14N, 341604E, 6278891N, NAD 83);* ***b)*** *unit 4 gabbro with reddish garnets along north-trending, steeply dipping quartz vein (same location as photo a);* ***c)*** *foliated, massive, medium-grained tonalite (unit 5; UTM 337853E, 6277181N) with angular xenoliths of mafic aphanitic volcanics, plagioclase-phyric basalt and porphyritic diorite;* ***d)*** *foliated, massive, medium-grained quartz diorite cut by an ~20 cm wide aplite dike (unit 5; UTM 337919E, 6277209N).*

K-feldspar, 15–25% hornblende (±biotite) and accessory Fe-oxide minerals. At the contact zone with unit 2 basaltic rocks, tonalite contains variable, angular, mafic volcanic to porphyritic xenoliths (Figure GS2022-9-6c). Some of the porphyritic variety contains ~5% quartz phenocrysts up to 1 cm across, suggesting relatively shallow emplacement into the Wasekwan group supracrustal package.

Quartz diorite occurs mostly as marginal phases of the Snake Lake stock and is fine to medium grained, massive, equigranular and moderately to strongly foliated. It consists of 5–10% anhedral quartz, 50–60% plagioclase, 20–30% hornblende and minor biotite. Granodiorite to granite occur mainly in the southwestern part of the stock, where K-feldspar is more abundant than plagioclase and biotite occurs as the dominant ferromagnesian mineral.

Pegmatite and/or aplite of subunit 5a are not uncommon in association with unit 5 granitoid rocks, which occur as dikes, a few centimetres to a few metres wide, and consist of quartz, feldspar and minor biotite (Figure GS2022-9-6d).

Sickle group (unit 6)

Sickle group sandstone (subunit 6a) and polymictic conglomerate (subunit 6b) outcrop in the southeastern corner of the map area (Figure GS2022-9-2). Subunit 6a sandstone is interpreted as stratigraphically overlying subunit 6b conglomerate (e.g., Gilbert et al., 1980). Medium- to thick-bedded arkosic sandstone and quartz pebbly sandstone of subunit 6a are fine to coarse grained and composed of feldspar, quartz, mica, lithic fragments and finer material. Up to 10% quartz pebbles (3–5 mm) are common in the quartz pebbly sandstone.

Subunit 6b conglomerate is polymictic, poorly sorted, and matrix to clast supported, and contains variably sized (2–30 cm), rounded and subrounded to irregular clasts ranging from pebble

to boulder size. Generally, cobble-size clasts are more common. Clast types include mafic and felsic volcanic rocks, granitoids, vein quartz, epidotized fragments and chert in a sandy to wacke matrix.

Post-Sickle intrusive suite (unit 7)

The post-Sickle intrusive suite (unit 7) is represented by the Fox mine intrusion (1831.0 ±3.7 Ma; Turek et al., 2000) and part of the Dunphy Lakes batholith (1847 ±2 to 1829 ±2 Ma; see Beaumont-Smith and Böhm, 2003; Yang and Beaumont-Smith, 2015b). Unit 7 granitoid rocks occur mainly in the northern part of the map area (Figure GS2022-9-2).

Unit 7 comprises quartz diorite, tonalite and granodiorite. Quartz diorite is fine to medium grained, weakly to moderately deformed and composed of 5–10% quartz, 60–70% plagioclase and 15–20% amphibole (Figure GS2022-9-7a). Tonalite is medium to coarse grained, moderately foliated and contains ~20% quartz and less amphibole (Figure GS2022-9-7b). Quartz diorite and tonalite of the Fox mine intrusion display as magnetic lows on the detailed airborne magnetic imagery. These rocks have high Sr/Y and La/Yb ratios (Yang, in press), resembling post-Sickle quartz diorite at Farley Lake that exhibits geochemical characteristics of adakite-like rocks (Yang and Lawley, 2018). Granodiorite is medium to coarse grained, foliated and equigranular to locally porphyritic.

Late intrusive suite (unit 8)

Unit 8 quartz-feldspar porphyry, feldspar porphyry pegmatite and/or aplite occur mostly as dikes in the central, southwestern and northeastern portions of the map area (Figure GS2022-9-2). Unit 8 rocks do not show any relationship to pre- and post-Sickle

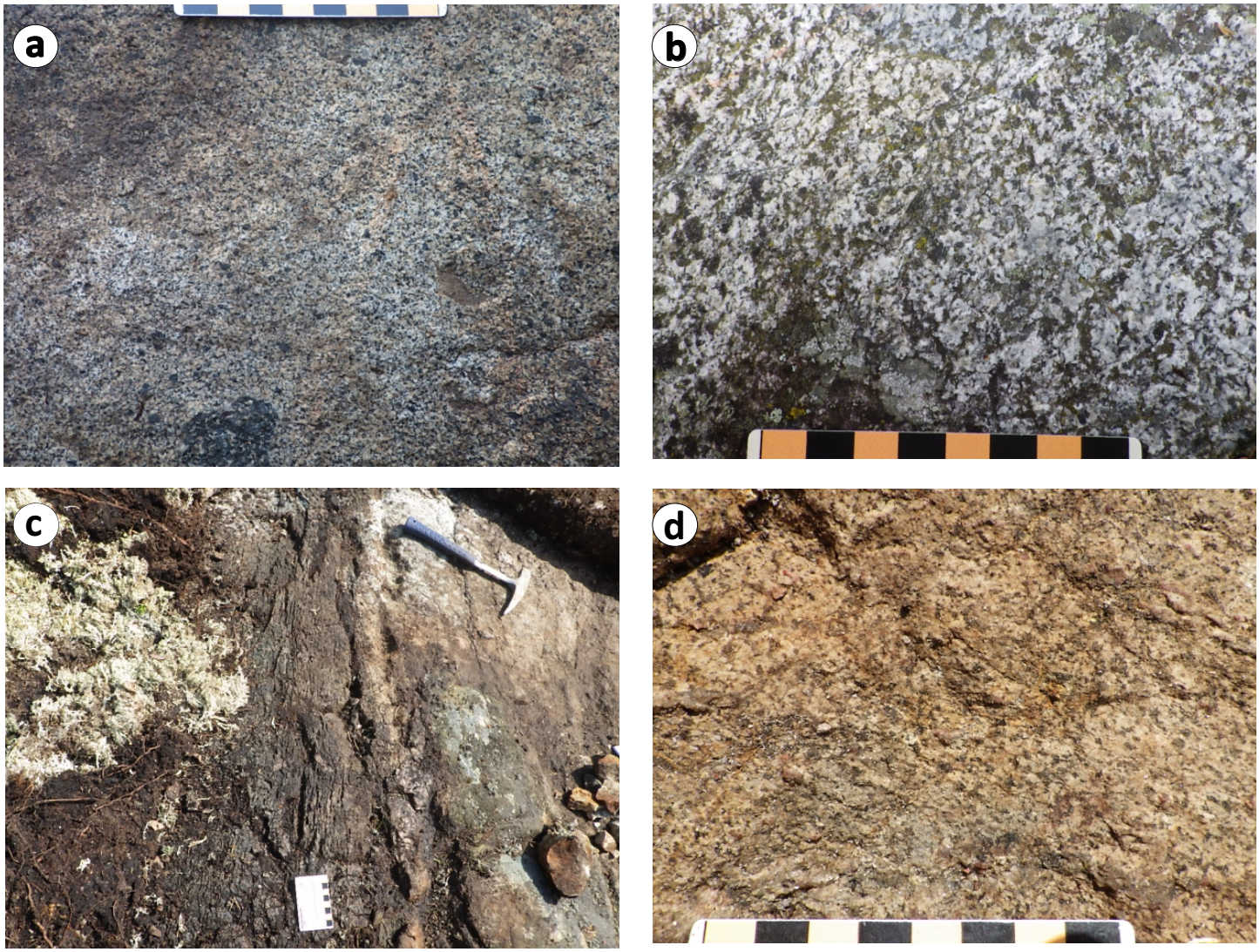

Figure GS2022-9-7: *Outcrop photographs of units 7 and 8 intrusive rocks in the Fox mine–Snake Lake area:* ***a)*** *fine- to medium-grained, massive quartz diorite (unit 7; UTM Zone 14N, 337979E, 6280499N, NAD 83);* ***b)*** *foliated, massive, coarse-grained, equigranular tonalite (unit 7; UTM 338325E; 6282812N);* ***c)*** *quartz-feldspar porphyry (granite) dike (unit 8; UTM 341624E; 6279950N) cuts strongly foliated mafic volcaniclastic rock of subunit 1c (left side; minor malachite is present at the contact; hammer handle points to north);* ***d)*** *massive quartz-feldspar porphyry containing muscovite flakes (~1%) and minor reddish garnet grains, 5 m from the contact with unit 1 amphibolite (unit 8; UTM 341624E; 6279950N).*

intrusive suites (units 5 and 7), and are therefore assigned to the late intrusive suite. Malachite stains were noted along the contact between a quartz-feldspar porphyry dike (up to 15 m wide) and subunit 1c amphibolite, and muscovite flakes (~1%) and minor reddish garnets occur evenly in the porphyritic granite ~5 m away from the contact (Figure GS2022-9-7a, b). The presence of muscovite and garnet indicates that this quartz-feldspar porphyry is likely an S-type granite, although it has relatively high MS values of 0.404 × 10^{-3} SI due to disseminated primary pyrrhotite (e.g., Yang et al., 2019). Pegmatite and aplite of unit 8 commonly contain muscovite (±tourmaline) in addition to biotite.

Tectonite (unit 9)

Tectonite of unit 9 comprises mafic to felsic protomylonite to mylonite within the Dunphy Lakes shear zone (DLSZ) and Pumphouse shear zone (Figure GS2022-9-2), characterized by the development of intense S_2 tectonic fabrics (Beaumont-Smith and Böhm, 2002; this study). Although the protoliths of such high-strain rocks are difficult to determine in the field, some of the feldspar, quartz and lithic relicts may be partly preserved in tectonite that shows ductile deformation (Figure GS2022-9-8a, b). Mafic tectonites derived from mafic volcanic flows and/or volcaniclastic rocks are indistinguishable, particularly those that were altered to very fine grained chlorite and sericite materials. Some S-C fabrics are well

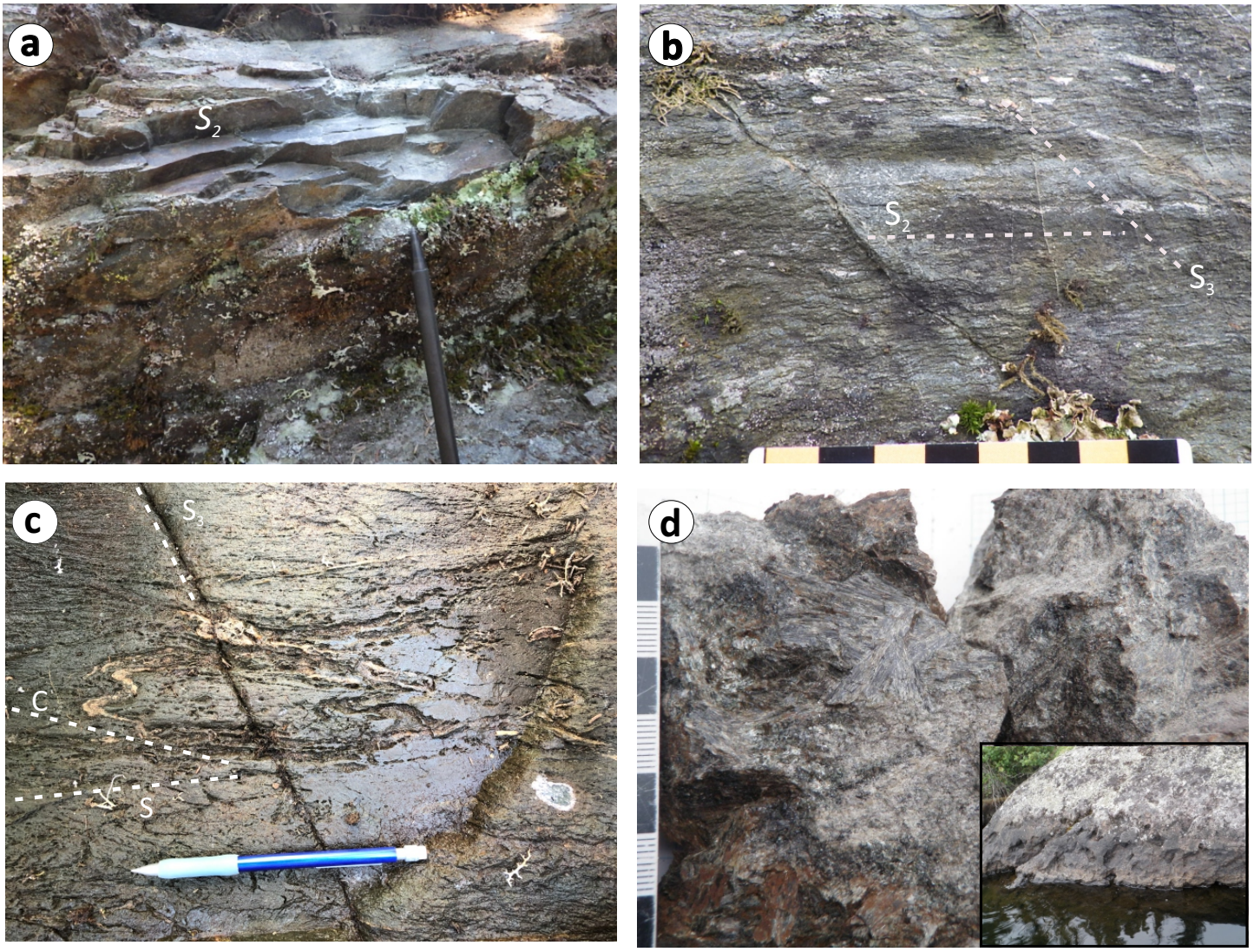

Figure GS2022-9-8: *Outcrop photographs of unit 9 tectonite in the Fox mine–Snake Lake area:* ***a)*** *shallowly dipping S_1 fabrics cut by subvertical S_2 foliation plane (indicated by the pencil) developed in mafic mylonite (unit 9; UTM Zone 14N, UTM 339887E; 6280527N, NAD83);* ***b)*** *protomylonite derived from unit 3 volcanic sandstone and conglomerate, in which relicts of quartz, feldspar and mafic to felsic volcanic fragments are preserved and aligned along S_2 foliation planes and cut by S_3 cleavages (UTM 338012E, 6281178N);* ***c)*** *S-C fabrics indicative of dextral shear in mafic mylonite, with folded quartz veins cut by S_3 fabrics (UTM 340579E, 6280688; pencil points to the east);* ***d)*** *radial aggregates of megacrystic actinolite (UTM 340421E, 6277000N) formed by retrograde greenschist-facies metamorphism, evident in a structural-breccia zone in unit 4 gabbro that is about 10–15 m wide, trends 350° and dips at about 80° to east; inset in lower right shows the gabbroic breccia at the shoreline of Snake Lake.*

developed within the DLSZ, providing a reliable shear-sense indicator (e.g., dextral shear; Figure GS202022-9-8c).

Structural geology

The LLGB was involved in six generations of regional deformation (D_1 to D_6; Beaumont-Smith and Böhm, 2002, 2004), although these structures are not necessarily encountered in one area. In the map area, D_1 fabrics are locally evident as penetrative, shallow-dipping S_1 foliation (Figure GS2022-9-8a) overprinted by vertical S_2 fabrics associated with D_2 deformation. D_1 fabrics, which are not found in the Sickle group, Pool Lake suite (Gilbert et al., 1980) or pre-Sickle intrusive suite rocks, likely formed due to the assembly of volcanic terranes (Beaumont-Smith and Böhm, 2002, 2003, 2004).

The D_2 structures are dominant and penetrative, and manifest as a steeply north-dipping S_2 foliation and tight to isoclinal folds (F_2) that have shallowly plunging hinges and associated minor chevron folds. The S_2 fabrics were observed in all map units except the late intrusive suite (unit 8). Typically, S_2 foliations dip steeply north and contain a down-dip to steeply plunging mineral and stretching lineation. Ductile shear zones that generally define map-unit contacts are commonly related to D_2 deformation, as the intensity of S_2 fabrics and tightness of F_2 folds increase toward the contacts. The D_2 shear zones are characterized by a steep south to north strain gradient culminating in a 30–50 m wide mylonitic core, dextral shear-sense indicators (e.g., Figure GS2022-9-8c) on horizontal surfaces, and steeply plunging, generally down-dip to slightly oblique (easterly pitch) stretching lineations. The northeast-trending DLSZ and PSZ are dextral transpressional shear zones formed during D_2 deformation (Beaumont-Smith and Böhm, 2002; Figure GS2022-9-2). The DLSZ appears to be the western extension of the regional JSZ, whereas the PSZ is likely the continuation of the North Star Lake shear zone (Yang, 2019; Beaumont-Smith, 2000), which could be part of a southern splay of the JSZ (Beaumont-Smith and Böhm, 2002).

The D_3 deformation is represented by close to tight, S-asymmetric F_3 folds and northwest-trending, axial-planar S_3 crenulation cleavage. F_4 folds produced by the D_4 deformation event are also pervasive throughout the map area. These folds plunge steeply to the northeast and are associated with steeply dipping, northeast-striking, axial-planar S_4 crenulation cleavage. The Mukasew Lake and Snake Lake faults (Figure GS2022-9-2) strike north-northeast and display sinistral movement, and are associated with D_4 deformation. Some fault breccia contains megacrystic, radial actinolite aggregates (Figure GS2022-9-8d) in the Snake Lake fault, which was likely formed during greenschist-facies metamorphism.

Economic considerations

Mafic to felsic volcaniclastic rocks, volcanic rocks characterized by coexistence of plagioclase- and amphibole-phyric varieties, and derivative volcanic sedimentary rocks in the map area suggest that the Wasekwan group (units 1–3) may have been derived from hydrous calcalkaline to tholeiitic magmas in a volcanic-arc to back-arc setting. Plotting of published geochemical data (Zwanzig et al., 1999; Beaumont-Smith, 2008) from mafic to felsic volcanic rock samples (n = 26) from the map and adjacent areas on a diagram (not shown) of Nb/Y versus σ values, based on the parameters defined respectively by Pearce (1996) and Yang (2007), indicate that volcanic rocks of units 1 and 2 are exclusively calcalkaline, consistent with their emplacement into a magmatic arc to back-arc setting. Unit 1 calcalkaline dacitic to rhyolitic rocks are geochemically similar to FII felsic rocks identified by Lesher et al. (1986) and Hart et al. (2004), suggesting the felsic rocks of unit 1 are a good but rare example of a Paleoproterozoic felsic volcanic package that could host VMS Cu-Zn deposits.

The Wasekwan group supracrustal rocks (units 1–3) were intruded by the pre-Sickle intrusive suite (units 4 and 5), post-Sickle granitoid (unit 7) and, subsequently, late intrusive suite (unit 8). Unit 4 gabbroic intrusions contain disseminated pyrrhotite and, locally, chalcopyrite, and thus need to be further evaluated for magmatic Ni-Cu-PGE minerals. Unit 7 granitoid rocks display adakite-like signatures and may have played a role in Au mineralization (Thorne et al., 2002; Yang and Lawley, 2018; Yang, 2019, 2021). The occurrences of I-type adakite-like granitoids in the map area suggests that tectonic settings may have evolved from intra-arc extension induced by slab roll-back to terrane terminal collision (Yang and Lawley, 2018).

Based on the Manitoba Mineral Inventory Cards (https://mrsearch.gov.mb.ca/Itm-cat/web/minsearch.html), the Fox VMS deposit and four mineral occurrences (Figure GS2022-9-2) suggest the presence of diverse styles of mineralization within the map area (Ferreira, 1993). Appreciable amounts of residual mineral resources are evidently present below the mined-out orebodies of the Fox mine, suggestive of high exploration potential. The North Fox occurrence on the southwestern shore of Dunphy Lakes, located about 1.76 km north of the Fox mine, contains a sulphide zone up to 18.8 m in width (pyrrhotite+arsenopyrite+chalcopyrite+pyrite; Ferreira, 1993) hosted in sedimentary rocks and minor volcanic sedimentary rocks that were strongly deformed and mylonitized to be termed tectonite (unit 9). The BAG occurrence (labelled A on Figure GS2022-9-2) shows disseminated pyrite and chalcopyrite in siliceous anthophyllite-corderite-biotite±garnet porphyroblastic schist (Stewart and Brewer, 1984), similar to the alteration zone of the Fox VMS deposit (Obinna, 1974; Lustig, 1979). This metamorphic mineral assemblage may have been derived from a primary chlorite±sericite hydrothermal alteration associated with VMS mineralization overprinted by middle- to upper-amphibolite–facies metamorphism. Felsic rocks similar to those of the Fox deposit occur southeast of Snake Lake, where chip samples collected from exploration trenches south of the pond on the GAL occurrence (labelled B) contain mineralization with up to 61.7 g/t Au, 2011 g/t Ag, 22% Cu and 7.7%

Pb (https://manitoba.ca/iem/geo/gis/mds/m64c_12_009.pdf). At an unnamed occurrence (labelled C), historical drilling intercepted mineralization, including a 1.6 m pyrrhotite zone containing trace Zn and Ni (Assessment File 91016, Manitoba Natural Resources and Northern Development, Winnipeg), hosted in unit 1 felsic volcanic rocks cut by intrusions of units 4 and 5.

Acknowledgments

The author thanks M. Fahim for providing enthusiastic field assistance, and C. Epp and P. Belanger for thorough logistical support, cataloguing and processing of the samples. Thanks go to L. Chackowsky and H.O. Adediran for assistance with GIS and drafting of the preliminary map and Figure GS2022-9-2, respectively. Alamos Gold Inc. is thanked for generously providing detailed geophysical data. B.R. King at Oakridge Environmental Ltd. kindly provided underground drilling data from the Fox mine. Willeson Metals Corp. is acknowledged for allowing field crew to enter their property. Nutrien and its contractors (Strilkiwski and Arcadis) are thanked for permitting use of the access road passing through their property. Constructive reviews by K.D. Reid and C.O. Böhm, technical editing by R.F. Davie and report layout by C. Steffano are gratefully acknowledged.

References

Anderson, S.D. and Beaumont-Smith, C.J. 2001: Structural analysis of the Pool Lake–Boiley Lake area, Lynn Lake greenstone belt (NTS 64C/11); *in* Report of Activities 2001, Manitoba Industry, Trade and Mines, Manitoba Geological Survey, p. 76–85, URL <https://manitoba.ca/iem/geo/field/roa01pdfs/01gs-12.pdf> [October 2021].

Ansdell, K.M. 2005: Tectonic evolution of the Manitoba-Saskatchewan segment of the Paleoproterozoic Trans-Hudson Orogen, Canada; Canadian Journal of Earth Sciences, v. 42, p. 741–759.

Ansdell, K.M., Corrigan, D., Stern, R. and Maxeiner, R. 1999: SHRIMP U-Pb geochronology of complex zircons from Reindeer Lake, Saskatchewan: implications for timing of sedimentation and metamorphism in the northwestern Trans-Hudson Orogen; Geological Association of Canada–Mineralogical Association of Canada, Joint Annual Meeting, May 26–29, 1999, Sudbury, Ontario, Program with Abstracts, v. 24, p. 3.

Baldwin, D.A., Syme, E.C., Zwanzig, H.V., Gordon, T.M., Hunt, P.A. and Stevens, R.P. 1987: U-Pb zircon ages from the Lynn Lake and Rusty Lake metavolcanic belts, Manitoba: two ages of Proterozoic magmatism; Canadian Journal of Earth Sciences, v. 24, p. 1053–1063.

Bateman, J.D. 1945: McVeigh Lake area, Manitoba; Geological Survey of Canada, Paper 45-14, 34 p.

Beaumont-Smith, C.J. 2000: Structural analysis of the Johnson Shear Zone in the Gemmell Lake–Dunphy Lakes area, Lynn Lake greenstone belt (parts of NTS 64C/11, /12); *in* Report of Activities 2000, Manitoba Industry, Trade and Mines, Manitoba Geological Survey, p. 57–63, URL <https://manitoba.ca/iem/geo/field/roa00pdfs/00gs-12.pdf> [September 2022].

Beaumont-Smith, C.J. 2008: Geochemistry data for the Lynn Lake greenstone belt, Manitoba (NTS 64C11-16); Manitoba Science, Technology, Energy and Mines, Manitoba Geological Survey, Open File OF2007-1, 5 p., URL <https://manitoba.ca/iem/info/libmin/OF2007-1.zip> [October 2021].

Beaumont-Smith, C.J. and Böhm, C.O. 2002: Structural analysis and geochronological studies in the Lynn Lake greenstone belt and its gold-bearing shear zones (NTS 64C10, 11, 12, 14, 15 and 16), Manitoba; *in* Report of Activities 2002, Manitoba Industry, Trade and Mines, Manitoba Geological Survey, p. 159–170, URL <https://manitoba.ca/iem/geo/field/roa02pdfs/GS-19.pdf> [October 2021].

Beaumont-Smith, C.J. and Böhm, C.O. 2003: Tectonic evolution and gold metallogeny of the Lynn Lake greenstone belt, Manitoba (NTS 64C10, 11, 12, 14, 15 and 16), Manitoba; *in* Report of Activities 2003, Manitoba Industry, Economic Development and Mines, Manitoba Geological Survey, p. 39–49, URL <https://manitoba.ca/iem/geo/field/roa03pdfs/GS-06.pdf> [October 2021].

Beaumont-Smith, C.J. and Böhm, C.O. 2004: Structural analysis of the Lynn Lake greenstone belt, Manitoba (NTS 64C10, 11, 12, 14, 15 and 16); *in* Report of Activities 2004, Manitoba Industry, Economic Development and Mines, Manitoba Geological Survey, p. 55–68, URL <https://manitoba.ca/iem/geo/field/roa04pdfs/GS-06.pdf> [October 2021].

Beaumont-Smith, C.J., Machado, N. and Peck, D.C. 2006: New uranium-lead geochronology results from the Lynn Lake greenstone belt, Manitoba (NTS 64C11–16); Manitoba Science, Technology, Energy and Mines, Manitoba Geological Survey, Geoscientific Paper GP2006-1, 11 p., URL <https://manitoba.ca/iem/info/libmin/GP2006-1.pdf> [October 2021].

Corrigan, D. 2012: Paleoproterozoic crustal evolution and tectonic processes: insights from the LITHOPROBE program in the Trans-Hudson orogen, Canada; Chapter 4 *in* Tectonic Styles in Canada: The LITHOPROBE Perspective, J.A. Percival, F.A. Cook and R.M. Clowes (ed.), Geological Association of Canada, Special Paper 49, p. 237–284.

Corrigan, D., Galley, A.G. and Pehrsson, S. 2007: Tectonic evolution and metallogeny of the southwestern Trans-Hudson Orogen; *in* Mineral Deposits of Canada: A Synthesis of Major Deposit-Types, District Metallogeny, the Evolution of Geological Provinces, and Exploration Methods, W.D. Goodfellow (ed.), Geological Association of Canada, Mineral Deposits Division, Special Publication 5, p. 881–902.

Corrigan, D., Pehrsson, S., Wodicka, N. and de Kemp, E. 2009: The Palaeoproterozoic Trans-Hudson Orogen: a prototype of modern accretionary processes; *in* Ancient Orogens and Modern Analogues, J.B. Murphy, J.D. Keppie, and A.J. Hynes (ed.), Geological Society of London, Special Publications, v. 327, p. 457–479.

Fedikow, M.A.F. and Gale, G.H. 1982: Mineral deposit studies in the Lynn Lake area; *in* Report of Field Activities 1982, Manitoba Department of Energy and Mines, Mineral Resources Division, p. 44–54, URL <https://manitoba.ca/iem/geo/field/rfa1982.pdf> [October 2022].

Ferreira, K.J. 1993: Mineral deposits and occurrences in the Laurie Lake area, NTS 64C/12; Manitoba Energy and Mines, Geological Services, Mineral Deposit Series, Report No. 9, 101 p., URL <https://manitoba.ca/iem/info/libmin/MDS9.zip> [September 2022].

Gilbert, H.P. 1993: Geology of the Barrington Lake–Melvin Lake–Fraser Lake area; Manitoba Energy and Mines, Geological Services, Geological Report GR87-3, 97 p., URL <https://manitoba.ca/iem/info/libmin/GR87-3.zip> [October 2021].

Gilbert, H.P., Syme, E.C. and Zwanzig, H.V. 1980: Geology of the metavolcanic and volcaniclastic metasedimentary rocks in the Lynn Lake area; Manitoba Energy and Mines, Mineral Resources Division, Geological Paper GP80-1, 118 p., URL <https://manitoba.ca/iem/info/libmin/GP80-1.zip> [October 2021].

Glendenning, M.W.P., Gagnon, J.E. and Polat, A. 2015: Geochemistry of the metavolcanic rocks in the vicinity of the MacLellan Au-Ag deposit and an evaluation of the tectonic setting of the Lynn Lake greenstone belt, Canada: evidence for a Paleoproterozoic-aged rifted continental margin; Lithos, v. 233, p. 46–68.

Hart, T.R., Gibson, H.L. and Lesher, C.M. 2004: Trace element geochemistry and petrogenesis of felsic volcanic rocks associated with volcanogenic massive Cu-Zn-Pb sulfide deposits; Economic Geology, v. 99, p. 1003–1013.

Hastie, E.C.G., Gagnon, J.E. and Samson, I.M. 2018: The Paleoproterozoic MacLellan deposit and related Au-Ag occurrences, Lynn Lake greenstone belt, Manitoba: an emerging, structurally controlled gold camp; Ore Geology Reviews, v. 94, p. 24–45.

Hoffman, P.H. 1988: United plates of America, the birth of a craton: Early Proterozoic assembly and growth of Laurentia; Annual Reviews of Earth and Planetary Sciences, v. 16, p. 543–603.

Jones, L.R., Lafrance, B. and Beaumont-Smith, C.J. 2006: Structural controls on gold mineralization at the Burnt Timber Mine, Lynn Lake Greenstone Belt, Trans-Hudson Orogen, Manitoba; Exploration and Mining Geology, v. 15, p. 89–100.

Kremer, P.D., Rayner, N. and Corkery, M.T. 2009: New results from geological mapping in the west-central and northeastern portions of Southern Indian Lake, Manitoba (parts of NTS 64G1, 2, 8, 64H4, 5); *in* Report of Activities 2009, Manitoba Science, Innovation, Energy and Mines, Manitoba Geological Survey, p. 94–107, URL <https://manitoba.ca/iem/geo/field/roa09pdfs/GS-9.pdf> [October 2021].

Lawley, C.J.M., Yang, X.M., Selby, D., Davis, W., Zhang, S., Petts, D.C. and Jackson, S.E. 2020: Sedimentary basin controls on orogenic gold deposits: new constraints from U-Pb detrital zircon and Re-Os sulphide geochronology, Lynn Lake greenstone belt, Canada; Ore Geology Reviews, v. 126, art. 103790.

Lesher, C.M., Goodwin, A.M., Campbell, I.H. and Gorton, M.P. 1986: Trace-element geochemistry of ore-associated and barren, felsic metavolcanic rocks in the Superior province, Canada; Canadian Journal of Earth Sciences, v. 23, p. 222–237.

Lewry, J.F. and Collerson, K.D. 1990: The Trans-Hudson Orogen: extent, subdivisions and problems; *in* The Early Proterozoic Trans-Hudson Orogen of North America, J.F. Lewry and M.R. Stauffer (ed.), Geological Association of Canada, Special Paper 37, p. 1–14.

Lustig, G.N. 1979: Geology of the Fox orebody, northern Manitoba; M.Sc. thesis, University of Manitoba, Winnipeg, Manitoba, 87 p.

Manitoba Agriculture and Resource Development 2021: Lynn Lake, Manitoba (NTS 64C14); Manitoba Agriculture and Resource Development, Manitoba Geological Survey, Lynn Lake Bedrock Compilation Map 64C14, scale 1:50 000, URL <https://manitoba.ca/iem/info/libmin/lynn_lake_compilation_2021.zip> [October 2021].

Manitoba Energy and Mines 1986: Granville Lake, NTS 64C; Manitoba Energy and Mines, Minerals Division, Bedrock Geology Compilation Map 64C, scale 1:250 000, URL <https://manitoba.ca/iem/info/libmin/bgcms/bgcms_granville_lake.pdf> [October 2022].

Martins, T., Kremer, P.D., Corrigan, D. and Rayner, N. 2019: Geology of the Southern Indian Lake area, north-central Manitoba (parts of NTS 64G1, 2, 7–10, 64H3–6); Manitoba Growth, Enterprise and Trade, Manitoba Geological Survey, Geoscientific Report GR2019-1, 51 p. and 4 colour maps at 1:50 000 scale, URL <https://manitoba.ca/iem/info/libmin/GR2019-1.zip> [October 2021].

Milligan, G.C. 1960: Geology of the Lynn Lake district; Manitoba Department of Mines and Natural Resources, Mines Branch, Publication 57-1, 317 p., URL <https://manitoba.ca/iem/info/libmin/PUB57-1.zip> [October 2022]

Norman, G.W.H. 1933: Granville Lake district, northern Manitoba; Geological Survey of Canada, Summary Report, Part C, p. 23–41.

Obinna, F.C. 1974: The geology and some genetic aspects of Fox mine mineralization, northern Manitoba; M.Sc. thesis, University of Manitoba, Winnipeg, Manitoba, 96 p.

Olson, P.E. 1987: The stratigraphy, structural geology and geochemistry of the Fox Lake massive sulfide deposit; M.Sc. thesis, University of Manitoba, Winnipeg, Manitoba, 220 p.

Pearce, J.A. 1996: A user's guide to basalt discrimination diagrams; *in* Trace Element Geochemistry of Volcanic Rocks: Applications for Massive Sulphide Exploration, D.A. Wyman (ed.), Geological Association of Canada, Short Course Notes 12, p. 79–113.

Stauffer, M.R. 1984: Manikewan: an Early Proterozoic ocean in central Canada, its igneous history and orogenic closure; Precambrian Research, v. 25, p. 257–281.

Stewart, P.W. and Brewer, K. 1984: Mineral deposit studies in the western Lynn Lake greenstone belt; *in* Report of Field Activities 1984; Manitoba Energy and Mines; Mineral Resources Division, p. 17–19, URL <https://manitoba.ca/iem/geo/field/roa84pdfs/rofa1984.pdf> [October 2022].

Syme, E.C. 1985: Geochemistry of metavolcanic rocks in the Lynn Lake Belt; Manitoba Energy and Mines, Geological Services/Mines Branch, Geological Report GR84-1, 84 p.

Turek, A., Woodhead, J. and Zwanzig H.V. 2000: U-Pb age of the gabbro and other plutons at Lynn Lake (part of NTS 64C); *in* Report of Activities 2000, Manitoba Industry, Trade and Mines, Manitoba Geological Survey, p. 97–104, URL <https://manitoba.ca/iem/geo/field/roa00pdfs/00gs-18.pdf> [October 2021].

Thorne, K.G., Lentz, D.R., Hall, D.C. and Yang, X.M. 2002: Petrology, geochemistry, and geochronology of the granitic pegmatite and aplite dikes associated with the Clarence Stream gold deposit, southwestern New Brunswick; Geological Survey of Canada, Current Research 2002-E12, 13 p.

White, D.J., Zwanzig, H.V. and Hajnal, Z. 2000: Crustal suture preserved in the Paleoproterozoic Trans-Hudson orogeny, Canada; Geology, v. 28, p. 527–530.

Winkler, H.G.F. 1967: Petrogenesis of metamorphic rocks; Springer-Verlag, New York, New York, 237 p.

Winter, J.D. 2014: Principles of Igneous and Metamorphic Petrology, second edition; Pearson Education Limited, Essex, United Kingdom, 738 p.

Yang, X.M. 2007: Using the Rittmann Serial Index to define the alkalinity of igneous rocks; Neues Jahrbuch für Mineralogie, v. 184, p. 95–103.

Yang, X.M. 2019: Preliminary results of bedrock mapping in the Gemmell Lake area, Lynn Lake greenstone belt, northwestern Manitoba (parts of NTS 64C11, 14); *in* Report of Activities 2019, Manitoba Agriculture and Resource Development, Manitoba Geological Survey, p. 10–29, URL <https://manitoba.ca/iem/geo/field/roa19pdfs/GS2019-2.pdf> [October 2021].

Yang, X.M. 2021: Bedrock mapping at Ralph Lake, Lynn Lake greenstone belt, northwestern Manitoba (part of NTS 64C14): preliminary results and geological implications; *in* Report of Activities 2021, Manitoba Agriculture and Resource Development, Manitoba Geological Survey, p. 40–58, URL <https://manitoba.ca/iem/geo/field/roa21pdfs/GS2021-5.pdf> [November 2021].

Yang, X.M. in press: Progress report on the study of granitoids in Manitoba: petrogenesis and metallogeny; Manitoba Natural Resources and Northern Development, Manitoba Geological Survey, Open File OF2022-3.

Yang, X.M. 2022: Bedrock geology of the Fox mine–Snake Lake area, Lynn Lake greenstone belt, northwestern Manitoba (part of NTS 64C12); Manitoba Natural Resources and Northern Development, Manitoba Geological Survey, Preliminary Map PMAP2022-2, scale 1:10 000, URL <https://manitoba.ca/iem/info/libmin/PMAP2022-2.pdf> [October 2021].

Yang, X.M. and Beaumont-Smith, C.J. 2015a: Geological investigations of the Keewatin River area, Lynn Lake greenstone belt, northwestern Manitoba (parts of NTS 64C14, 15); *in* Report of Activities 2015, Manitoba Mineral Resources, Manitoba Geological Survey, p. 52–67, URL <https://manitoba.ca/iem/geo/field/roa15pdfs/GS-4.pdf> [October 2021].

Yang, X.M. and Beaumont-Smith, C.J. 2015b: Granitoid rocks in the Lynn Lake region, northwestern Manitoba: preliminary results of reconnaissance mapping and sampling; *in* Report of Activities 2015, Manitoba Mineral Resources, Manitoba Geological Survey, p. 68–78, URL <https://manitoba.ca/iem/geo/field/roa15pdfs/GS-5.pdf> [October 2021].

Yang, X.M. and Beaumont-Smith, C.J. 2016: Geological investigations in the Farley Lake area, Lynn Lake greenstone belt, northwestern Manitoba (part of NTS 64C16); *in* Report of Activities 2016, Manitoba Growth, Enterprise and Trade, Manitoba Geological Survey, p. 99–114, URL <https://manitoba.ca/iem/geo/field/roa16pdfs/GS-9.pdf> [October 2021].

Yang, X.M. and Beaumont-Smith, C.J. 2017: Geological investigations of the Wasekwan Lake area, Lynn Lake greenstone belt, northwestern Manitoba (parts of NTS 64C10, 15); *in* Report of Activities 2017, Manitoba Growth, Enterprise and Trade, Manitoba Geological Survey, p. 117–132, URL <https://manitoba.ca/iem/geo/field/roa17pdfs/GS2017-11.pdf> [October 2021].

Yang, X.M. and Lawley, C.J.M. 2018: Tectonic setting of the Gordon gold deposit, Lynn Lake greenstone belt, northwestern Manitoba (parts of NTS 64C16): evidence from lithogeochemistry, Nd isotopes and U-Pb geochronology; *in* Report of Activities 2018, Manitoba Growth, Enterprise and Trade, Manitoba Geological Survey, p. 89–109, URL <https://manitoba.ca/iem/geo/field/roa18pdfs/GS2018-8.pdf> [October 2021].

Yang, X.M., Drayson, D. and Polat, A. 2019: S-type granites in the western Superior Province: a marker of Archean collision zones; Canadian Journal of Earth Sciences, v. 56, p. 1409–1436.

Zwanzig, H.V. 1990: Kisseynew gneiss belt in Manitoba: stratigraphy, structure, and tectonic evolution; *in* The Early Proterozoic Trans-Hudson Orogen of North America, (ed.) J.F. Lewry and M.R. Stauffer; Geological Association of Canada, Special Paper 37, p. 95–120.

Zwanzig, H.V. 2000: Geochemistry and tectonic framework of the Kisseynew Domain–Lynn Lake belt boundary (part of NTS 63P/13); *in* Report of Activities 2000, Manitoba Industry, Trade and Mines, Manitoba Geological Survey, p. 91–96, URL <https://manitoba.ca/iem/geo/field/roa00pdfs/00gs-17.pdf> [October 2021].

Zwanzig, H.V. and Bailes, A.H. 2010: Geology and geochemical evolution of the northern Flin Flon and southern Kisseynew domains, Kississing–File lakes area, Manitoba (parts of NTS 63K, N); Manitoba Innovation, Energy and Mines, Manitoba Geological Survey, Geoscientific Report GR2010-1, 135 p., URL <https://manitoba.ca/iem/info/libmin/GR2010-1.zip> [October 2021].

Zwanzig, H.V., Syme, E.C. and Gilbert, H.P. 1999: Updated trace element geochemistry of ca. Ga metavolcanic rocks in the Paleoproterozoic Lynn Lake belt; Manitoba Industry, Trade and Mines, Geological Services, Open File Report OF99-13, 46 p., URL <https://manitoba.ca/iem/info/libmin/OF99-13.zip> [October 2021].

GS2022-10

Stratigraphy and distribution of the potash-bearing members of the Devonian Prairie Evaporite, southwestern Manitoba (parts of NTS 62F, K)

by M.P.B. Nicolas and C. Yang[1]

In Brief:

- New mapping of potash has increased exploration space
- Prairie Evaporite has three separate potash beds extending into Manitoba from the west

Citation:
Nicolas, M.P.B. and Yang, C. 2022: Stratigraphy and distribution of the potash-bearing members of the Devonian Prairie Evaporite, southwestern Manitoba (parts of NTS 62F, K); *in* Report of Activities 2022, Manitoba Natural Resources and Northern Development, Manitoba Geological Survey, p. 87–95.

Summary

In Manitoba, the Devonian Prairie Evaporite is a thick sequence of evaporitic beds with three potash members—Esterhazy, White Bear and Belle Plaine—near the top of the formation. Of these three, the White Bear Member is the most extensive, followed by the Esterhazy Member, then the Belle Plaine Member. The Esterhazy Member hosts Manitoba's first proposed potash mine, located near the town of Russell.

New mapping of the potash distribution has increased the potash exploration area from previous potash distribution maps, with extensions north up to Twp. 25 and farther east to Rge. 27, W 1st Mer. In addition, new mapping of the zero edge of total salt distribution in the Manson and Virden oil fields supports the hypothesis that salt dissolution and collapse strongly effected oil pool formation and development in those areas.

Introduction

The Devonian Prairie Evaporite is a thick sequence of evaporitic beds, dominantly halite beds with sylvite- and carnallite-rich beds, with anhydrite and minor clay and dolostone interbeds. The formation overlies the reefal and platform carbonates of the Winnipegosis Formation and underlies the platform carbonates of the Dawson Bay Formation. In Manitoba, the Prairie Evaporite stratigraphy, from the bottom up, includes the anhydritic basal Winnipegosis transitional beds, the Shell Lake anhydrite and the three potash members—Esterhazy, White Bear and Belle Plaine (Figure GS2022-10-1). Each of these members is separated by thick, unnamed halite beds. Through recent cross-border collaborations between the geological surveys of Manitoba and Saskatchewan, the extension of the Belle Plaine Member into Manitoba was confirmed. Bannatyne (1983), with a follow-up by Nicolas (2015), provides a detailed description of the geology of the potash beds in Manitoba and their economic prospectivity.

This report outlines the distribution of the three individual potash members, and includes revised mapping of potash distribution and the zero edge of salt distribution in Manitoba.

Potash exploration and development

Bannatyne (1960) completed the earliest study on the halite and potash deposits in the Prairie Evaporite, just as economic potash deposits in Saskatchewan were discovered and exploration efforts began in Manitoba. Bannatyne (1983) provided the first look at the economics and potash grades of the St. Lazare deposit. Nicolas (2015, 2019) provided an update on potash distribution and the first look at the grade distribution of the Russell deposit (Figure GS2022-10-2). There are three known areas of potash occurrences in Manitoba: 1) Russell-McAuley, 2) Daly-Sinclair and 3) Pierson (Figure GS2022-10-2).

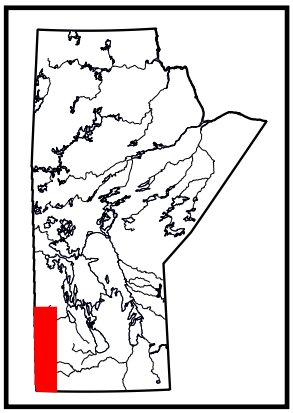

Recently, there has been renewed interest in the Russell deposit, with the drilling of the first pair of horizontal potash production wells by Potash and Agri Development Corporation of Manitoba Ltd. (PADCOM) in L.S. 12, Sec. 21, Twp. 20, Rge. 29 W 1st Mer. (abbreviated 12-21-20-29W1; Figure GS2022-10-3), oil and gas well licences 11642 and 11643 (Manitoba Natural Resources and Resource Development, Winnipeg). PADCOM's Environmental Act licence no. 3375 (Manitoba Environment, Climate and Parks, Winnipeg) for this development indicates a selective dissolution process will be used to extract the potash, leaving halite in the ground. At the time of writing, production had not yet started.

[1] Saskatchewan Geological Survey, Saskatchewan Ministry of Energy and Resources, Regina, Saskatchewan, chao.yang@gov.sk.ca

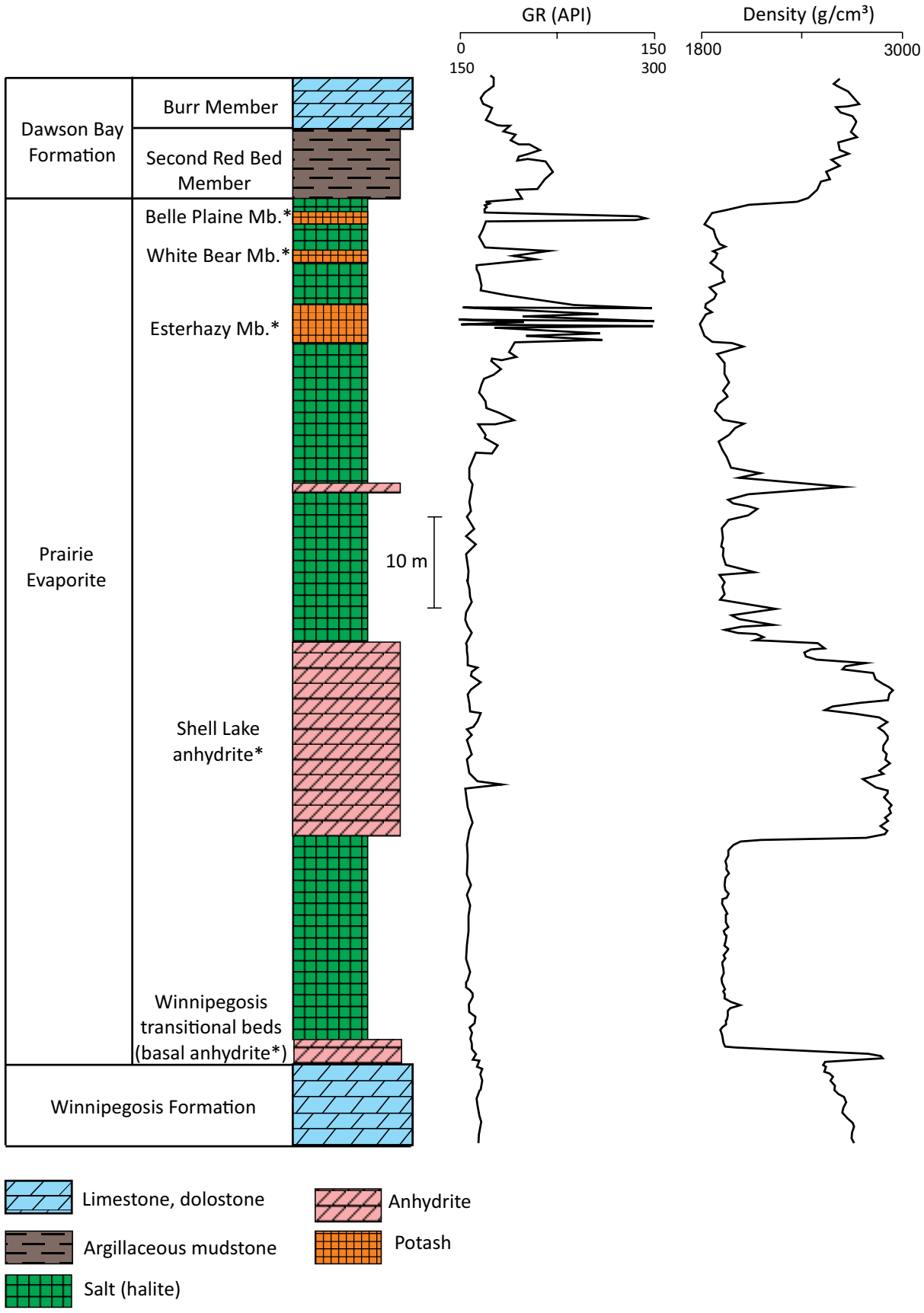

Figure GS2022-10-1: *Schematic stratigraphic column of the Devonian Prairie Evaporite in Manitoba, with a representative composite gamma-ray and bulk density downhole geophysical log. The vertical scale is approximate. The asterisk (*) indicates beds that are not always present. Abbreviations: GR, gamma ray; Mb., Member.*

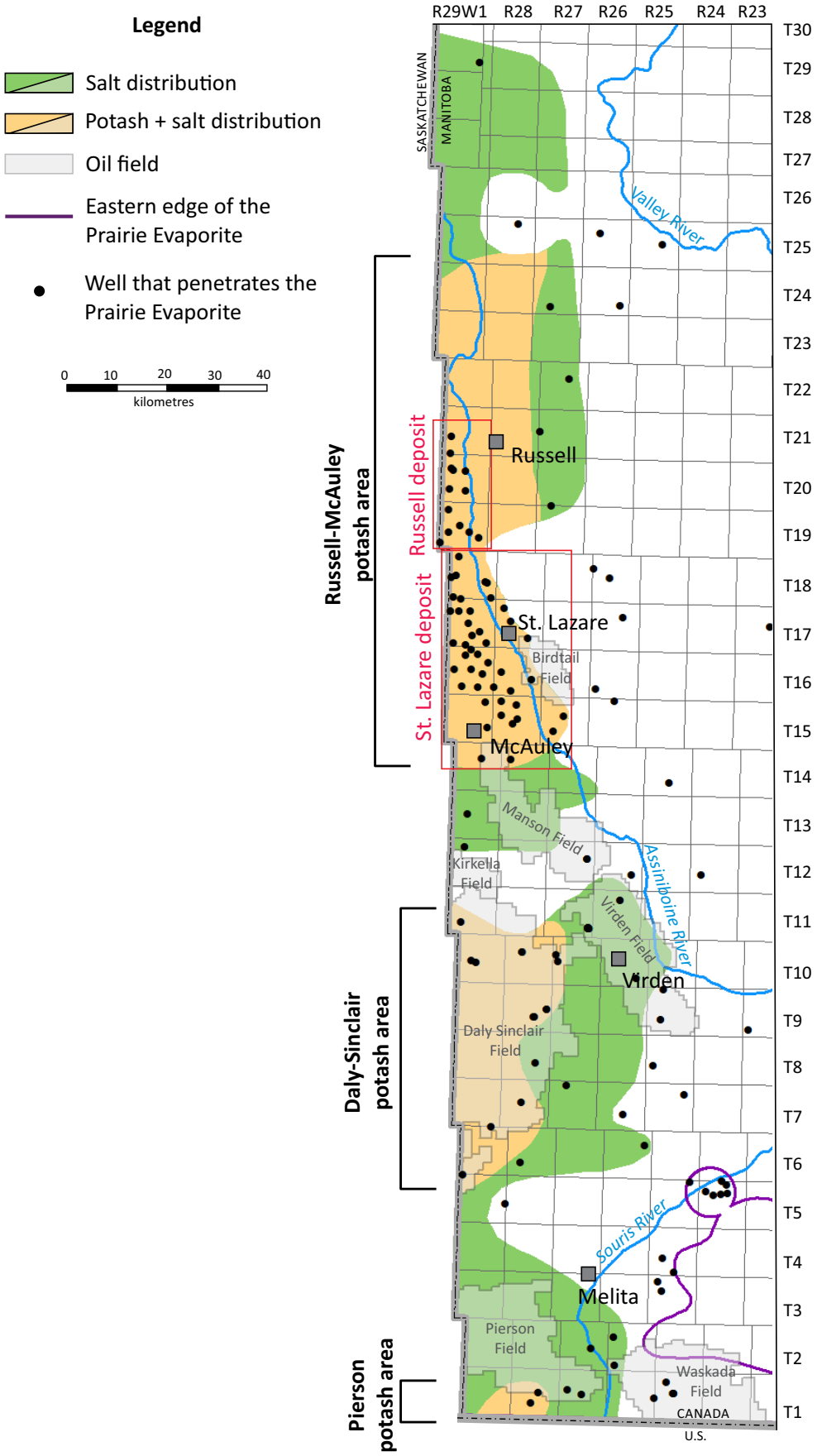

Figure GS2022-10-2: *Distribution of salt, potash + salt, oil fields, and wells that penetrate the Prairie Evaporite in southwestern Manitoba.*

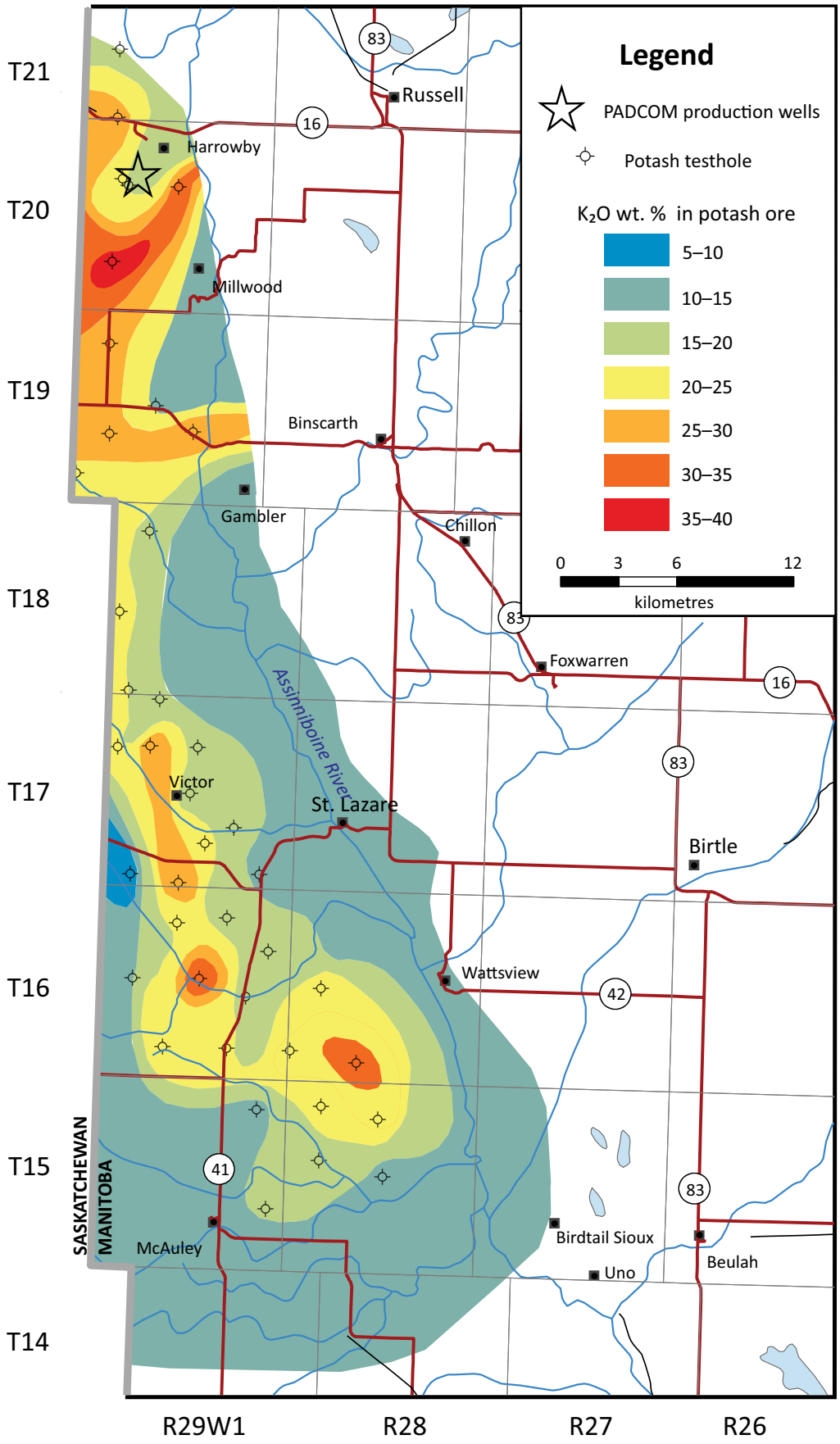

Figure GS2022-10-3: *Potash distribution and K_2O wt. % in potash ore (sylvinite) calculated as a weighted average over the best 2.44 m of ore of the Russell and St. Lazare deposits in the Russell-McAuley potash area, southwestern Manitoba (modified from Nicolas, 2019).*

Stratigraphy and potash distribution

Detailed mapping of potash in Manitoba by the Manitoba Geological Survey and industry was generally focused on the northern deposits of the Russell-McAuley potash area, due to historical exploration being confined to those areas. Previous potash distribution mapping was restricted to areas of potash confirmed from testholes, which in turn, restricted the exploration area evaluated by companies. Bannatyne (1983) formally identified and confirmed the White Bear and Esterhazy members in southwestern Manitoba. Bannatyne (1983) suspected the presence of the Belle Plaine Member in two wells in the Daly-Sinclair potash area (Figure GS2022-10-2). Through new correlations and interpretive mapping, the White Bear Member now has the most expansive distribution in Manitoba, followed by the Esterhazy Member. The Belle Plaine Member is confirmed to extend into Manitoba more than originally speculated.

Belle Plaine Member

The stratigraphy of the Prairie Evaporite in Manitoba is now revised to include the Belle Plaine Member. Yang et al. (2018) mapped the distribution of the potash members in Saskatchewan, providing updated zero-edge mapping of the Patience Lake, Belle Plaine and Esterhazy members up to the Manitoba border; these maps incorporated new off-confidential data points from potash test wells. Using these maps and interprovincial cross-sections, the continuity of the Belle Plaine Member into Manitoba was confirmed (Figure GS2022-10-4). In the Daly-Sinclair potash area, the Belle Plaine Member is the dominant potash bed, whereas in the Russell-McAuley potash area, it is restricted to a small area in Twp. 20 and 21, Rge. 29W1, near the Saskatchewan border. The distribution of the Belle Plaine Member is shown in Figure GS2022-10-5a.

The southwest to northeast cross-section A–A' in Figure GS2022-10-4 shows the distribution and preservation of three distinct potash members into Manitoba. The well at 6-16-10-29W1 shows the potash beds are locally thinner, with weak gamma-ray signatures in comparison to the other wells. This may be the result of localized complete salt dissolution, evident in a nearby well at 9-17-10-29W1; the resulting collapse and dissolution affects are slightly overprinted in the 6-16-10-29W1 well. In

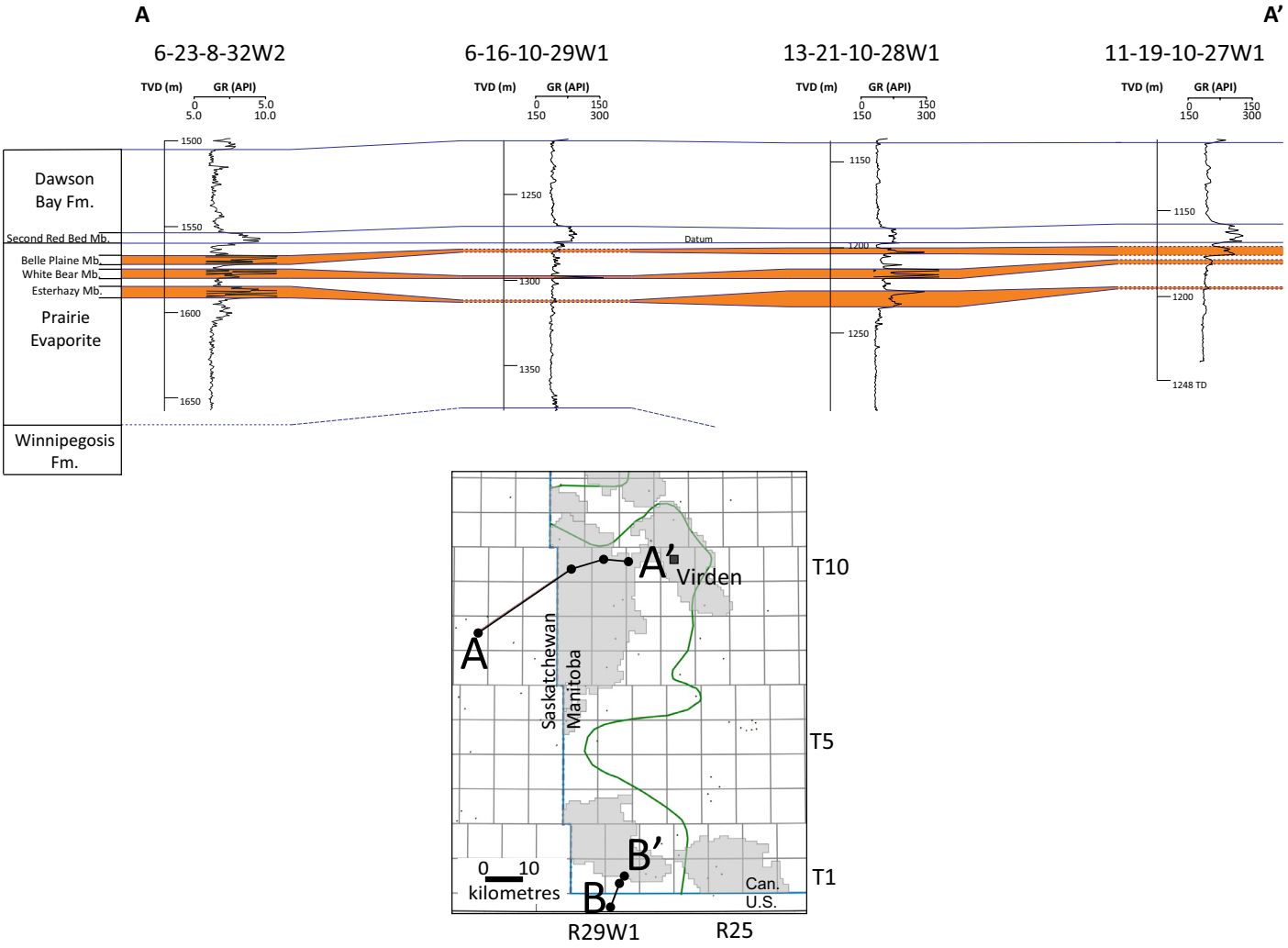

Figure GS2022-10-4: *Southwest to northeast cross-section A–A' from Saskatchewan to Daly-Sinclair potash area, southwestern Manitoba. Datum is top of Prairie Evaporite. Inset map shows the location of the cross-section and the eastern edge of salt distribution (green line). Abbreviations: 6-23-8-32W2, well at L.S. 6, Sec. 23, Twp. 8, Rge. 32, W 2nd Mer.; Fm., Formation; GR, gamma ray; Mb., Member; TD, total depth; TVD, true vertical depth.*

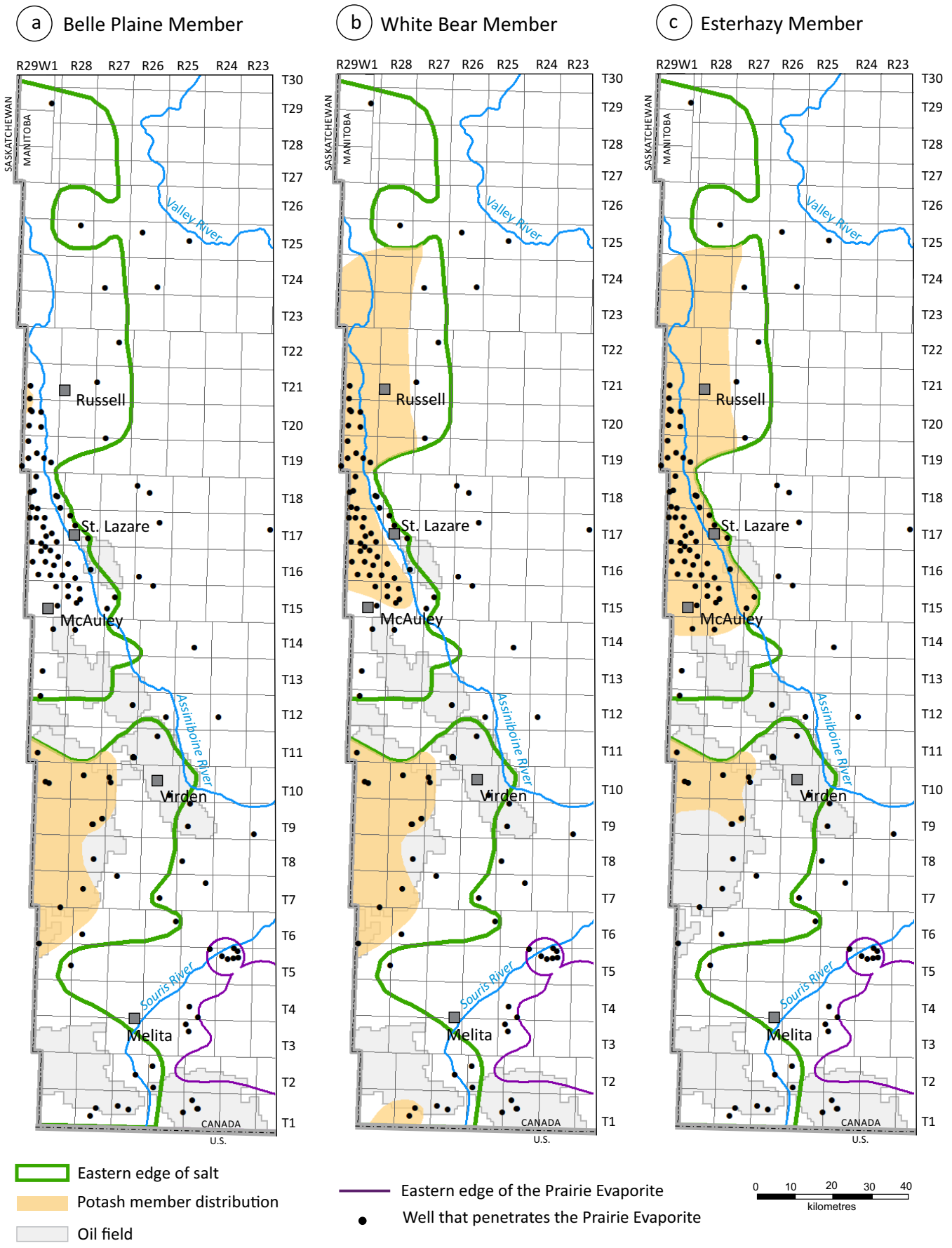

Figure GS2022-10-5: *Distribution of the individual potash members in southwestern Manitoba:* ***a)*** *Belle Plaine Member,* ***b)*** *White Bear Member,* ***c)*** *Esterhazy Member.*

the well at 11-19-10-27W1, the gamma-ray signature only suggests a very thin Esterhazy Member, alternatively, this signature may represent a remnant or clay seam extension of the member as it approaches the zero edge of the member.

White Bear Member

In wells where all three potash members are not present, it can be difficult to identify which potash member is present. This is exemplified in the south to north cross-section B–B', extending from North Dakota into the Pierson potash area of Manitoba (Figure GS2022-10-6), which uses the northeasternmost well from Kruger (2014) as the southernmost well in the cross-section. Mapping by Kruger (2014) suggests the potash member that extends into Manitoba's Pierson potash area is the White Bear Member, which is further supported by Bannatyne's (1983) mapping. Mapping and cross-border correlations from Saskatchewan are nonconclusive on the stratigraphic assignment of this potash member. The White Bear Member has a wider distribution on the United States side of the basin. In North Dakota, it is the most expansive of the potash-bearing members (Kruger, 2014). The same can be said for Manitoba, since most of the potash-bearing wells in Manitoba include the White Bear Member (Figure GS2022-10-5b), with the exception of a few wells nearing the zero edge of the potash distribution in the northern area. The White Bear Member in Saskatchewan has attracted less attention because of its lower ore grade, thinner thickness and poorer continuity compared to the other three economic potash members. The White Bear Member was mapped in Saskatchewan by Yang et al. (2009), but not updated in the later maps of Yang and Love (2015) and Yang et al. (2018). Figure GS2022-10-5b, cross-sections in Figure GS2022-10-6 and Figure GS2022-10-7 show the best estimation of the extent of the White Bear Member in Manitoba, based on current information.

Esterhazy Member

The Esterhazy Member occurs in both the northern extent of the Daly-Sinclair and the entire Russell-McAuley potash areas (Figure GS2022-10-5c). This member is the most cored and explored potash member in Manitoba, representing the eastward extension of Nutrien Ltd.'s Rocanville mine and The Mosaic Company's K1 and K2 mines near Esterhazy, Saskatchewan. This extension into Manitoba has known economic grades (Bannatyne, 1983; Nicolas, 2015) and is the location of PADCOM's proposed selective-solution mine (Figure GS2022-10-3).

The Esterhazy Member has a well-defined log signature in the northern deposits, due to its high gamma-ray signature (e.g., 4-36-15-29W1 in Figure GS2022-10-7) and K_2O grades (Figure GS2022-10-3). Correlation of this member in the northern deposits is straightforward and commonly occurs with the White Bear Member above, except when approaching the zero edge of the salt distribution. In the St. Lazare deposit, there is a thickening of the Prairie Evaporite section above the Esterhazy Member, where there may be a thin localized remnant of Belle Plaine Member preserved in wells at 8-6-17-29W1 and 5-10-17-29W1. Localized preservation of the Belle Plaine Member is not unexpected in this area, as similar localized occurrences were mapped by Yang et al. (2018) in Twp. 17, Rge. 30W1 in Saskatchewan.

Northern extension of potash area

The potash distribution north of Twp. 19 and east of Rge. 29W1 represents a new interpretation of the potash extent in Manitoba (Figure GS2022-10-2). Well control is scarce in this area, however, three components suggested that the potash extended farther north and east. These components are 1) the isopach contours of the Prairie Evaporite salt (Bezys and Conley, 1998), 2) the log signatures and presence of clay beds in the control wells in Rge. 27W1, and 3) the zero edge of the Esterhazy Member from Yang et al. (2018). This revised potash zero edge in the area between Twp. 19 and 25 follows approximately the 90 m Prairie Evaporite salt isopach contour of Bezys and Conley (1998). In other areas, 90 m is the approximate salt thickness needed for any potash beds to be deposited and/or preserved in Manitoba. It is possible the potash extends farther north into Twp. 25–28, but the zero edge in Saskatchewan, as it is drawn at the time of writing (Yang et al., 2018), is the determining factor to stop the northern extension at Twp. 25. The revision of the potash edge in this area resulted in approximately 840 km^2 (approximately nine townships in area) of new potash exploration area in Manitoba, although only new exploration test wells can verify the actual presence of potash in these areas.

Total salt zero edge

The zero edge of total salt distribution outlines the eastern extent of the thick package of evaporitic minerals consisting of halite, sylvite and carnallite within the Prairie Evaporite. This edge was also updated in this report (Figure GS2022-10-2), specifically in the area in the southeastern end of the Manson Field in Twp. 12–13, Rge. 27W1 and along the eastern edge of the Virden Field in Twp. 10–11, Rge. 25–26W1.

In the Manson Field, stratigraphic information gathered through recent oil pool development uncovered a complex series of multistage structural disturbances related to salt dissolution and collapse. The oil pool development method (vertical and direction wells dominating), oil pool distribution (small isolated pools) and producing intervals that span multiple horizons in the southeastern end of this oil field are strikingly different from those in the northwestern part of the Manson Field and even to the south in the Virden Field. The latter are dominated by horizontal well developments in large expansive oil pools with production from a focused stratigraphic interval. These factors together inform the more precise location of the salt edge in this area. Additionally, core from the southeastern area shows large open fractures, slickensides indicative of faulting and brecciation in the overlying interval from the Mississippian Lodgepole For-

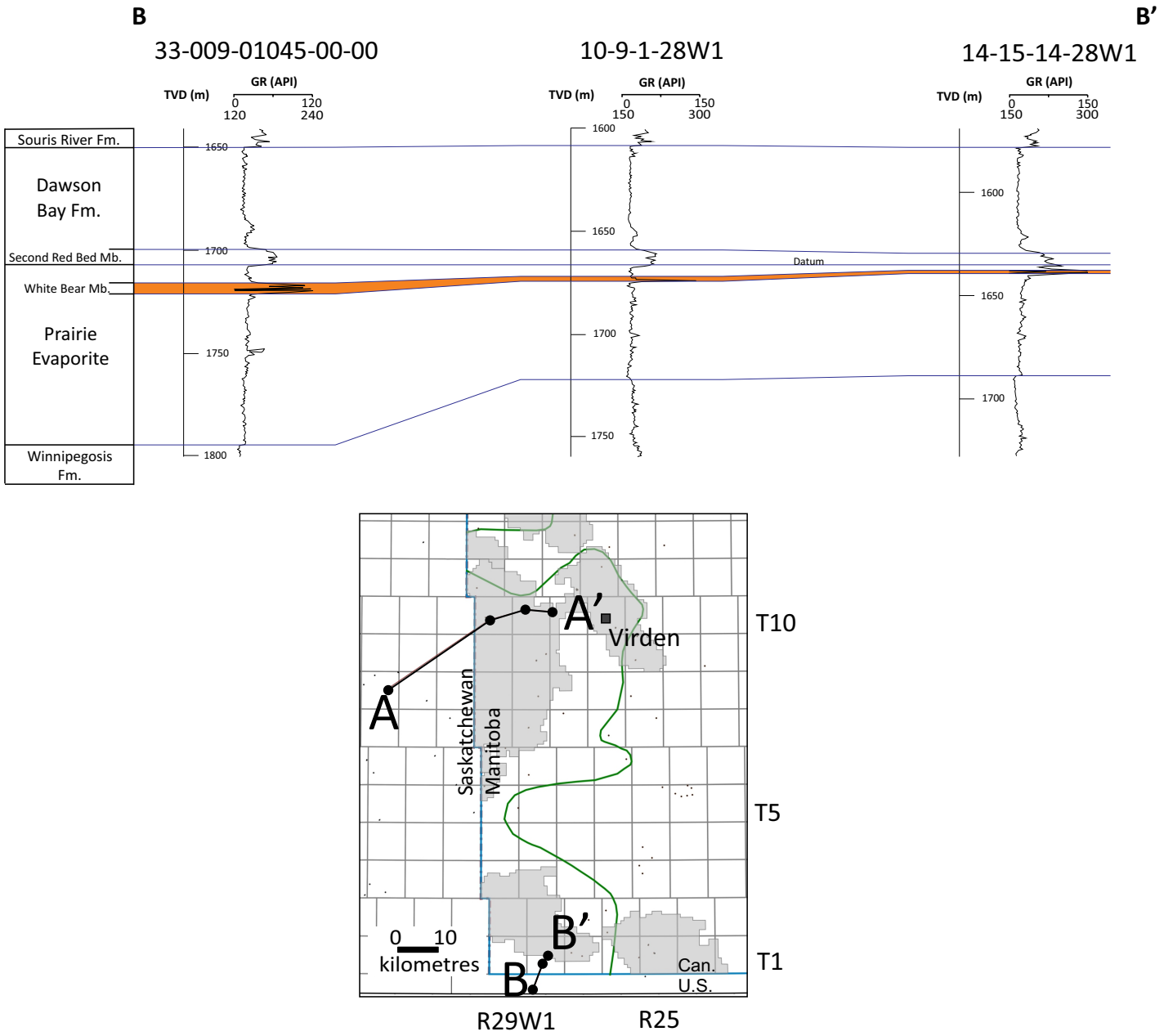

Figure GS2022-10-6: *South to north cross-section B–B' from North Dakota (well 33-009-01045-00-00) to Pierson potash area, southwestern Manitoba. Datum is top of Prairie Evaporite. Inset map shows the location of the cross-section and the eastern edge of salt distribution (green line). Abbreviations: 10-9-1-28W1, well at L.S. 10, Sec. 9, Twp. 1, Rge. 28, W 1st Mer.; Fm., Formation; GR, gamma ray; Mb., Member; TVD, true vertical depth.*

mation to the Jurassic Melita Formation resulting from the complete dissolution of the salt below.

In the Virden Field, the salt zero edge was moved to match more closely the edge of the oil pools; this was done based on the location of dry wells, oil pool boundaries and the structural mapping of the Lodgepole Formation (Klassen, 1996; Nicolas, 1999). The deposition of the Lodgepole Formation and development of this oil field is known to have been strongly controlled by structural disturbances in the Birdtail-Waskada Zone—a known structural feature, which postdated Prairie Evaporite deposition (Klassen, 1996), directly affected by the partial to complete dissolution of the salt beds.

Economic considerations

Potash deposits are mined for use dominantly by the fertilizer industry to increase crop yields. With growing global demand for potash, identifying new deposits helps to add reserves, which will ensure security of product for generations to come. The development of the first potash mine in Manitoba is attracting global interest to the province. Through renewed research and mapping of the potash layers across the basin, and better geoscientific understanding of the distribution of the potash members in Manitoba, the area of potential potash occurrences has been expanded and fine-tuned, resulting in approximately 840 km^2 of new potash exploration area.

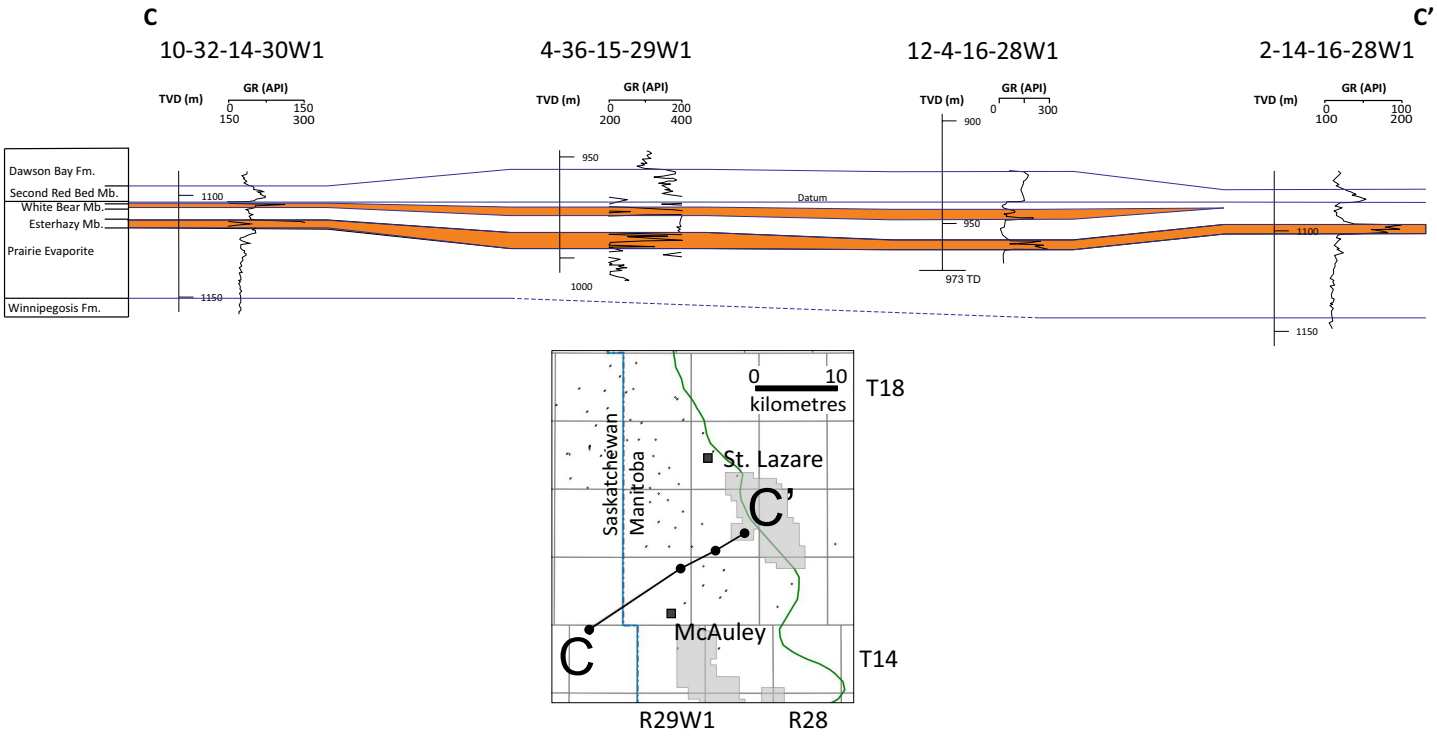

Figure GS2022-10-7: *Southwest to northeast cross-section C–C' from Saskatchewan to the southern extent of the McAuley-Russell potash area in southwestern Manitoba. Datum is top of Prairie Evaporite. Inset map shows the location of the cross-section and the eastern edge of salt distribution (green line). Abbreviations: 10-32-14-30W1, well at L.S. 10, Sec. 32, Twp. 14, Rge. 30, W 1st Mer.; Fm., Formation; GR, gamma ray; Mb., Member; TD, total depth; TVD, true vertical depth.*

Acknowledgments

The authors would like to thank T. Hodder and T. Kennedy for their technical and critical review of this report.

References

Bannatyne, B.B. 1960: Potash deposits, rock salt, and brines in Manitoba; Manitoba Department of Mines and Natural Resources, Mines Branch, Publication 59-1, 30 p., URL <https://manitoba.ca/iem/info/libmin/PUB59-1.pdf> [October 2022].

Bannatyne, B.B. 1983: Devonian potash deposits of Manitoba (parts of 62F/3, 6, 11 and 14); Manitoba Department of Energy and Mines, Mineral Resources Division, Open File Report OF83-3, 27 p., URL <https://manitoba.ca/iem/info/libmin/OF83-3.pdf> [October 2022].

Bezys, R.K. and Conley, G.G. 1998: Manitoba stratigraphic database and the Manitoba stratigraphic map series; Manitoba Energy and Mines, Geological Services, Open File Report OF98-7, CD-ROM.

Klassen, H.J. 1996: An overview of the regional geology and petroleum potential, Lodgepole Formation, southwestern Manitoba; Manitoba Energy and Mines, Petroleum and Energy Branch, Petroleum Open File Report POF 15-96, 42 p., URL <https://manitoba.ca/iem/petroleum/pubcat/pof_15-96.zip> [October 2022].

Kruger, N. 2014: The potash members of the Prairie Formation in North Dakota; North Dakota Geological Survey, Report of Investigations No. 113, 43 p.

Nicolas, M.P.B. 1999: Structure contour map of the Mississippian Upper Virden Member, Lodgepole Formation, Virden Field area; Manitoba Conservation, Petroleum and Energy, Stratigraphic Map Series M-4, scale 1:250 000, URL <https://manitoba.ca/iem/petroleum/pubcat/new/m_4.tif> [October 2022].

Nicolas, M.P.B. 2015: Potash deposits in the Devonian Prairie Evaporite, southwestern Manitoba; *in* Report of Activities 2015, Manitoba Mineral Resources, Manitoba Geological Survey, p. 97–105, URL <https://manitoba.ca/iem/geo/field/roa15pdfs/GS-8.pdf> [October 2022].

Nicolas, M.P.B. 2019: Beyond oil: mineral potential within and below Manitoba's oil fields; Central Canada Mineral Exploration Convention, November 18–19, 2019, Winnipeg, Manitoba, Geoscientific Presentation PRES2019-6, poster, URL <https://manitoba.ca/iem/geo/techposters/2019/PRES2019-6.pdf> [October 2022].

Yang, C. and Love, M. 2015: Potash-rich members of the Devonian Prairie Evaporite in Saskatchewan: isopachs, carnallite contours and K_2O grade; Saskatchewan Ministry of Economy, Saskatchewan Geological Survey, Open File 2015-2, 3 maps.

Yang, C., Jensen, G. and Berenyi, J. 2009: The stratigraphic framework of the potash-rich members of the Middle Devonian Upper Prairie Evaporite Formation, Saskatchewan; *in* Summary of Investigations 2009, Volume 1, Saskatchewan Geological Survey, Saskatchewan Energy and Resources, Miscellaneous Report 2009-4.1, Paper A-4, p. 1–28.

Yang, C., Schuurmans, E. and Love, M. 2018: Updated isopach maps of the potash-rich members of the Devonian Prairie Evaporite in Saskatchewan; Saskatchewan Ministry of Energy and Resources, Saskatchewan Geological Survey, Open File 2018-1, 6 maps.

GS2022-11

Surficial geology mapping and till composition of the western Fox River greenstone belt area, northeastern Manitoba (NTS 53M15, 16, parts of 53N13, 54C4, 54D1): year two

by M.S. Gauthier and T.J. Hodder

In Brief:

- Surficial mapping in NTS 53M15 and 53M16, year 2
- Collection of till samples to determine provenance and drift-exploration potential, including for diamonds—includes release of year 1 KIM analyses
- Collection of ice-flow data to reconstruct the glacial history and aid drift exploration

Citation:
Gauthier, M.S. and Hodder, T.J. 2022: Surficial geology mapping and till composition of the western Fox River greenstone belt area, northeastern Manitoba (NTS 53M15, 16, parts of 53N13, 54C4, 54D1): year two; *in* Report of Activities 2022, Manitoba Natural Resources and Northern Development, Manitoba Geological Survey, p. 96–109.

Summary

Quaternary geology fieldwork, including till sampling and ice-flow–indicator mapping, was conducted over a portion of the buried Fox River greenstone belt in northeastern Manitoba (NTS 53M15, 16; parts of 53N13, 54C4, 54D1). This follow-up to 2020 fieldwork included visits to 143 field sites to ground-truth the surficial geology mapping, collect till samples and identify ice-flow indicators. Sixty-five 2 kg till samples were collected for geochemical (<63 µm size fraction) and clast-lithology (2–8 mm size fraction) analyses in 2022. At 40 of these sample sites, an additional 11.4 L was collected for heavy mineral analysis (magmatic or metamorphosed massive-sulphide–indicator minerals, kimberlite-indicator minerals and visible gold).

Sediment cover in the area varies from 0 m, along some river beds, to at least 60 m, as indicated by drillholes in the study area. The study area is draped by a light-coloured diamict with a sandy-silt or silty-sand matrix. A darker-coloured and finer-textured diamict, with a crumbly or blocky texture, can also be found at surface. At six mapping sites, older buried tills, which are denser than the overlying diamicts, blocky with oxidation rinds on joints, darker-coloured and usually finer-grained, were also identified.

Most parts of the study area are covered by a veneer of glaciolacustrine clay or silt (0.1 to ~1.0 m thick), though thicker glaciolacustrine deposits were observed (up to 1.5 m). A proglacial lake washed the existing substrate, commonly to depths of 0.6 m. Consequently, till samples collected for drift exploration purposes must be taken at depth to avoid sampling till that has been washed of fines and/or leached of water-soluble elements and/or sampling displaced material.

Paleo-ice flow was interpreted from both erosional field-based ice-flow indicators (total of seven sites) and till fabrics (total of 13 sites). The till-fabric interpretations suggest young south- to south-southwest-trending ice flow (170–215°), west-trending ice flow (283°) and either a northwest- or southeast-trending ice flow (300–334° or 120–154°). Older ice-flow phases were oriented to the northwest-southeast (bimodal, twice), west (twice), southwest, south-southwest and south. The study area is covered by erosional streamlined landforms, which trend toward the southwest (215–245°) and were formed by the deglacial Hayes Lobe of the Laurentide Ice Sheet.

Introduction

Quaternary geology fieldwork, including till sampling and ice-flow–indicator mapping, was conducted for 21 days in August 2022, over a portion of the buried Fox River greenstone belt in northeastern Manitoba (NTS 53M15, 16; parts of 53N13, 54C4, 54D1). This complements work done in 2020 (Gauthier and Hodder, 2020, 2021). The goals of this project are to

- conduct 1:50 000 scale mapping;
- sample till to assess the till composition of the area;
- sample till to analyze for heavy minerals (magmatic or metamorphosed massive-sulphide–indicator minerals [MMSIMs®], kimberlite-indicator minerals [KIMs], visible gold); and
- conduct paleo–ice-flow mapping to assist reconstructions of the glacial dynamics of the area, which in turn guide drift exploration studies in northeastern Manitoba.

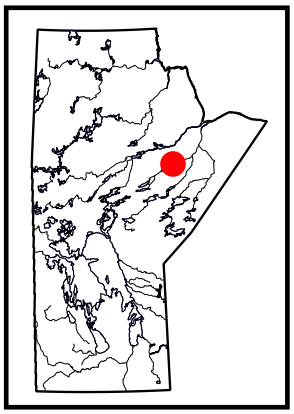

Bedrock geology

The study area is underlain by rocks of the Fox River greenstone belt, which is part of the circum-Superior belt in northeastern Manitoba (Figure GS2022-11-1). The Fox River belt demonstrates potential to host nickel±copper and platinum-group-element (PGE) mineralization (Rinne, 2018, 2020). The belt consists of Paleoproterozoic metamorphosed sedimentary rocks (mudstone, sandstone, minor

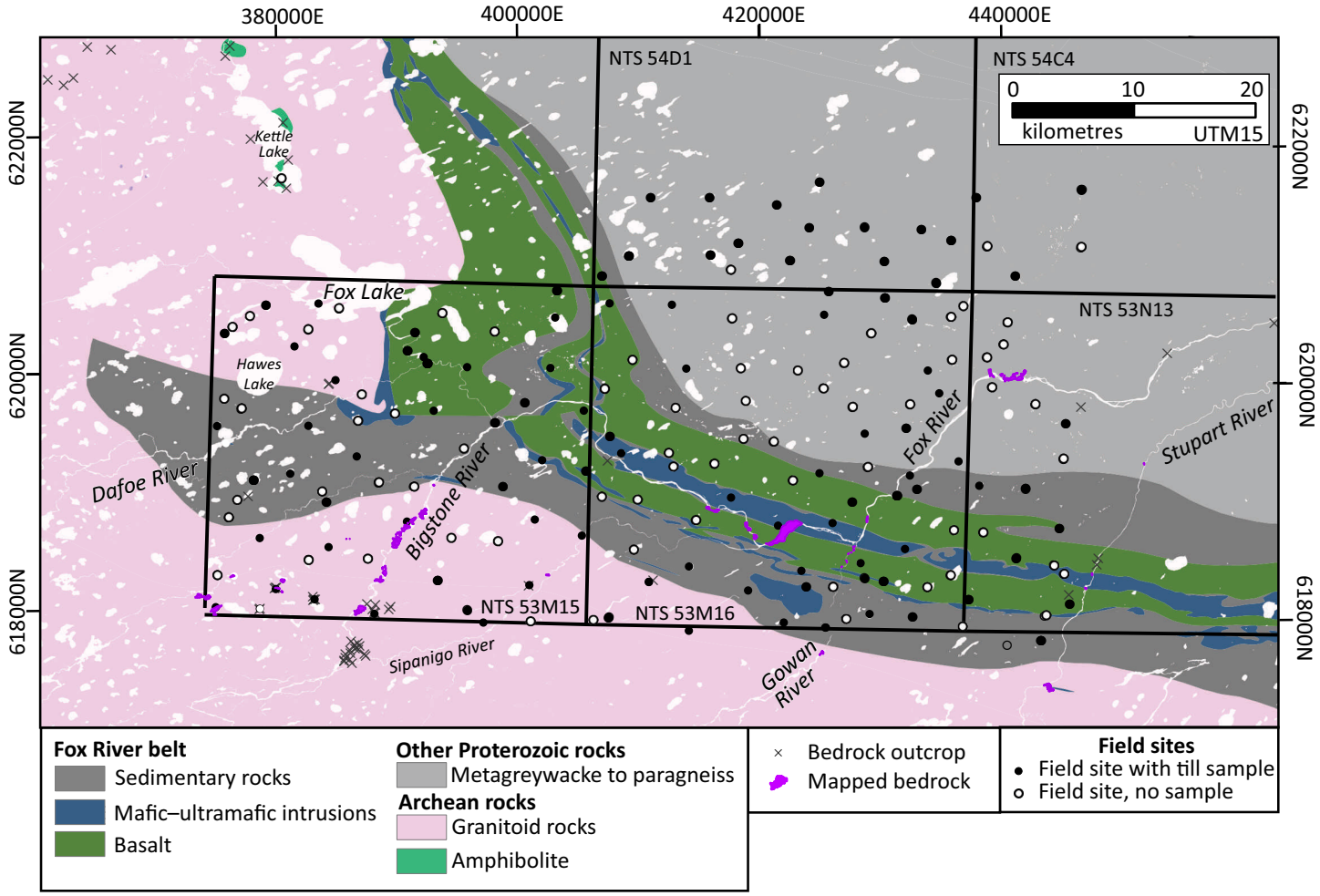

Figure GS2022-11-1: *Field sites and till sample sites overlying a portion of the Fox River greenstone belt, northeastern Manitoba. Bedrock geology is from Rinne (2018, 2020). All co-ordinates are in UTM Zone 15, NAD83.*

iron formation and calcareous beds), mafic to ultramafic rocks (basalt to komatiitic basalt with minor interflow mudstones) and mafic to ultramafic intrusions (serpentinized peridotite, pyroxenite, gabbro and minor leucogabbro). Archean granitoid rocks of the Superior province border the western and southern parts of the Fox River belt, whereas the area north of the belt is dominated by Paleoproterozoic metagreywacke and derived gneiss of the Trans-Hudson orogen (eastern Kisseynew belt).

Quaternary history

The study area was previously mapped in the late 1970s, using aerial photographs at 1:250 000 scale with limited to no ground-truthing (Klassen and Netterville, 1979). More recent work has been conducted to the north and south of the study area (Trommelen, 2015; Gauthier et al., 2019). These areas are dominated by gently sloping, moderately to very poorly drained topography. Stunted spruce bogs and forests drape most areas and surface permafrost is common beneath blankets of organic deposits. Elevation varies between 68 and 198 metres above sea level (m asl). Local relief is typically 1 to 30 m, generated by smooth, bare to thinly drift-covered outcrops separated by low ground.

The study area was glaciated by ice flowing from multiple migratory domes of the Laurentide Ice Sheet during the last glacial cycle, comprising marine isotope stages (MISs) 2–5 (Klassen, 1986; Gauthier et al., 2019). At some point during MIS 2 a thick ice ridge, the Hudson Bay Ice Saddle, formed between two main domes (Dyke and Prest, 1987; Thorleifson et al., 1993). During deglaciation, the lobate Hayes Lobe ice stream flowed southwest from this saddle, and across the study area (Dredge and Cowan, 1989; Gauthier et al., 2021). In an area 55 km to the south, the Hayes Lobe is interpreted as a late-stage erosional event (Trommelen and Ross, 2014), which did not affect the composition of the underlying till(s). The results from this study will determine whether that interpretation holds true for this area as well.

Methods

Helicopter-supported fieldwork was undertaken over 21 days in August 2022, based out of the town of Gillam, which is located 40 km north of the study area. The Bell Jet Ranger heli-

copter was equipped with floats, as the area is forested and landing is limited to fens. A total of 143 field sites were visited to ground-truth the surficial geology mapping, collect till samples and identify ice-flow indicators (Figure GS2022-11-1). The surficial material at each field station was investigated by means of a hand-dug shovel hole, a Dutch auger (1.2 m long) hole and/or a natural sediment exposure.

In 2022, sixty-five 2 kg till samples were collected for geochemical analysis by partial and total digestion of the silt and clay size fraction (<63 µm) and clast-lithology (2–8 mm size fraction) analysis. Till samples were collected from the C-horizon soil, both at surface and at depths of up to 14 m. At 40 of these sample sites, an additional 11.4 L was collected for heavy mineral analysis (MMSIMs, KIMs, visible gold).

For the 80 till samples collected in 2020, results from till geochemistry and heavy mineral analyses were released in Gauthier and Hodder (2021). Kimberlite-indicator-mineral counts with microprobe results from 2020 were released in Hodder and Gauthier (2022)[1].

2020 indicator mineral processing

During the 2020 field program, 59 till samples were collected for heavy mineral analysis. These till samples were initially processed by the De Beers Group of Companies (De Beers; Sudbury, Ontario). The KIM sample locations were withheld from De Beers to allow equal opportunity for follow-up by all interested parties. Heavy mineral concentrate from the <0.5 mm size fraction of the till sample was passed over a 0.3 mm aperture sieve and the <0.3 mm size fraction was discarded, leaving the 0.3–0.5 mm size fraction. The remaining heavy mineral concentrate was shipped to Overburden Drilling Management (ODM; Ottawa, Ontario) where it was recombined and reprocessed. Suspected KIM grains from both labs were visually selected, and then analyzed by electron microprobe. The resultant KIM grains were initially classified using electron microprobe results, following the methodology outlined in the Manitoba KIM database (Keller, 2019). The chemistry of certain KIM grain types was then further investigated with bivariate plots.

Results

Surficial geology

Organics

Organic, treed bog deposits are common on very poorly drained surfaces in the study area, and are usually underlain by permafrost (Figure GS2022-11-2a). Other flat-lying areas are draped by thick fen deposits (Figure GS2022-11-2b). Organic cover is commonly thin (5–30 cm) where it overlies drumlinoid ridges, and thicker in low-lying areas between drumlins or where the underlying surficial material is finer textured (Figure GS2022-11-2c). In some areas, permafrost mudboils (frost boils) are visible from the air and indicative of thin organic cover (Figure GS2022-11-2d).

Glaciomarine and glaciolacustrine sediments

Glaciolacustrine sediments

Massive glaciolacustrine clay and/or silt drapes most of the study area (Figure GS2022-11-3a, b). These sediments are thickest (>1.2 m depth) near the esker-meltwater corridor system (Figure GS2022-11-4), and thin to absent overlying drumlinoid ridges. Wave-washed till was observed at elevations between 120 and 175 m asl. Wave-washing was particularly strong in the southwestern portion of the study area, where low-lying bedrock is exposed between 170 and 185 m asl (Figure GS2022-11-3c).

Beaches and trimlines

Southwest-trending beaches formed around a small esker (northeasternmost study area) and along a topographic high (southeastern study area) at ~131 m asl (Figure GS2022-11-4). In the southeast, several trimlines (wave-washed scarps) were mapped at 136 m asl (Figure GS2022-11-3d). Above the scarps are unwashed tills, whereas below the scarps are massive brown clay or washed tills. Nonetheless, given that the marine limit was mapped at 135 m asl in the Gillam area, 35 km to the north (Gauthier et al., 2020), these are tentative marine features.

Glaciomarine sediments

Significant beach development, subparallel to the modern ocean shoreline, occurred at 120 m asl, just east and northeast of the study area. Possible glaciomarine sediments include 1.5 m of interbedded brown clay, light brown fine to medium sand and brown diamict at 121 m asl, in the eastern half of the study area along the Fox River (Figure GS2022-11-5). Silt (0.4 m) over clay (0.2 m) over moderately to poorly sorted, medium to coarse sand (0.5 m) was encountered at 122 m asl near the southeasternmost part of the study area. On the other hand, thick (>1.2 m) massive brown clay was encountered at two separate locations around 122 m asl. This clay is identical to glaciolacustrine clay mapped throughout the study area. As such, it was noted that the marine limit is at least 120 m asl, and also that glaciolacustrine sediments may have been deposited below marine limit. In areas to the north and northeast, glaciolacustrine sediments were mapped as low as 100 m asl (Gauthier et al., 2020).

[1] MGS Data Repository Item DRI2022010, containing the data or other information sources used to compile this report, is available online to download free of charge at https://manitoba.ca/iem/info/library/downloads/index.html, or on request from minesinfo@gov.mb.ca, or by contacting the Resource Centre, Manitoba Natural Resources and Northern Development, 360-1395 Ellice Avenue, Winnipeg, Manitoba R3G 3P2, Canada

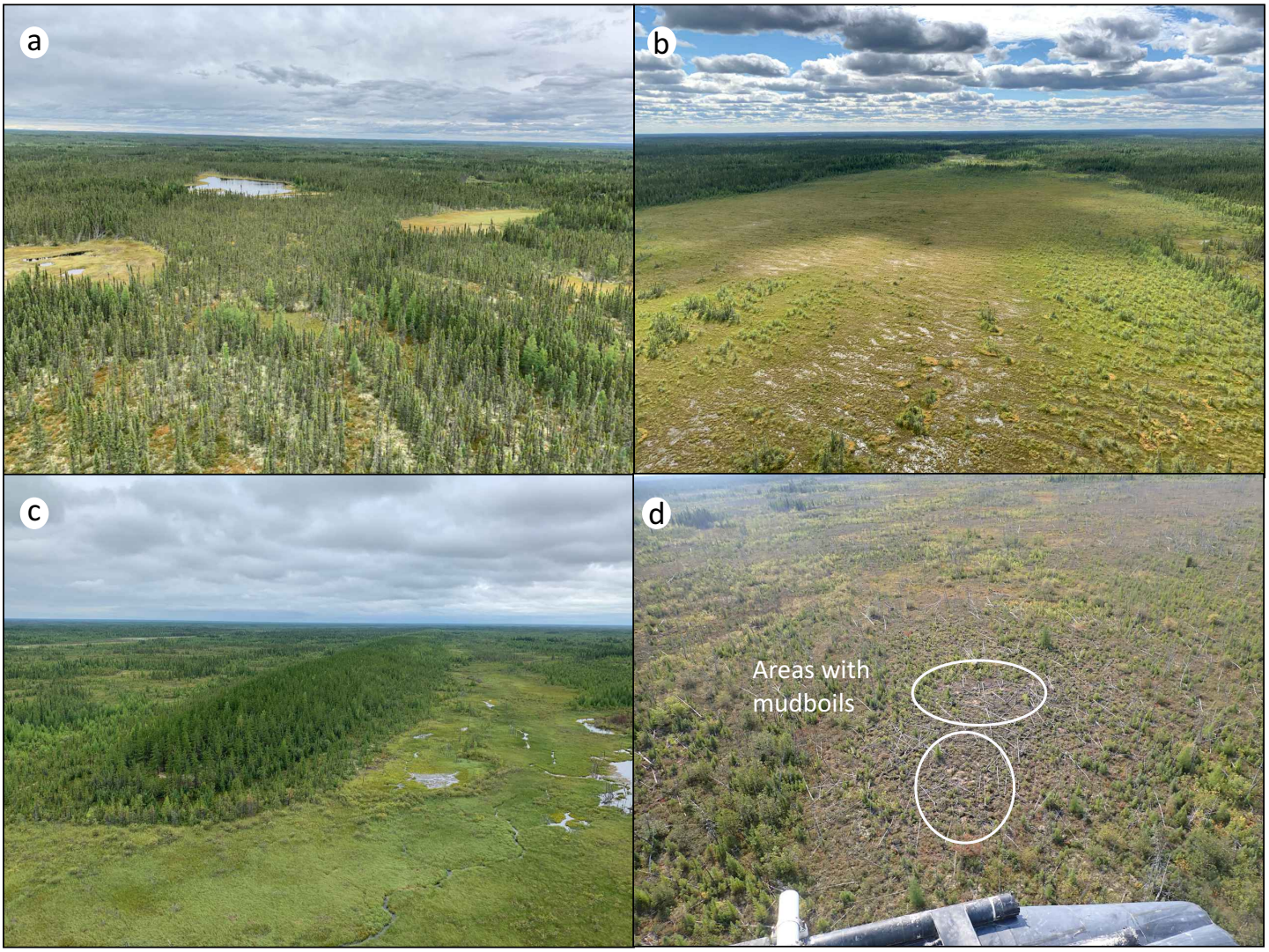

Figure GS2022-11-2: *The majority of the study area is draped by* ***a)*** *organic bogs and* ***b)*** *fens. Organic cover is thin* ***c)*** *where it overlies long linear drumlinoid ridges or* ***d)*** *in better-drained elevated areas, the site of permafrost mudboils.*

Glaciofluvial sediments

The study area is crossed by a large esker-meltwater corridor system, up to 2.5 km wide, that initiates near the confluence of the Stupart and Fox rivers (Figure GS2022-11-4), and extends at least 190 km towards the west-southwest. The corridor has been infilled by at least 11 m of silt and sand, which may relate to the esker, or to later infill by glaciolacustrine and/or glaciomarine sediment. Near the east end of Fox Lake, the surface of the esker is cut by iceberg scours between 170 and 185 m asl. This is the height of land in the study area, and the only place with mapped iceberg scours.

Numerous meltwater channels crosscut the area, including the channels now occupied by the northeast-flowing Bigstone, Fox, Sipanigo and Gowan rivers. These meltwater channels cut down into bedrock (Figures GS2022-11-1, -6a, b), and flowed to the southwest beneath the Hayes Lobe.

Tills

The study area is draped by a light-coloured diamict with a sandy-silt or silty-sand matrix (Figure GS2022-11-7a, b). A rarer darker-coloured and/or finer-textured diamict, with a crumbly or blocky texture, was found below that till at three sections (Figure GS2022-11-7a, c). Both diamicts are loose to crumbly, and interpreted to have been deposited during the last glaciation.

Six sections also exposed underlying older tills that are denser than the upper diamicts, blocky with oxidation staining on joints, darker coloured and usually finer grained (Figure GS2022-11-7d, e). The blocky and relatively dense nature suggests that these tills are significantly older, and that any potential overlying sorted sediments, deposited during an ice-free period, are missing from the area (eroded or not deposited).

Data from the 2020 till samples show that both younger and older tills contain ~65% carbonate clasts (2–8 mm size fraction) and 45% total carbonate in the till matrix (<63 um size fraction), with variable concentrations of greenstone, greywacke and granitoid clasts. A full examination of till composition will occur once the 2022 till sample results are obtained.

Figure GS2022-11-3: *Glaciolacustrine sediments deposited within glacial Lake Agassiz include* ***a)*** *massive brown clay and* ***b)*** *light brown silt. Lowering of lake levels resulted in* ***c)*** *rare removal of Quaternary sediment overlying bedrock and* ***d)*** *the formation of wave-washed scarps (trimline denoted by arrows).*

Washed tills

Drift exploration programs using till samples must be wary of what material to sample. Till in the study area was commonly washed by glacial Lake Agassiz waves, which may have caused removal of the fine-textured size fraction at depths up to 0.6 m, or remobilization and partial sorting of the surface sediments. Wave-washing can leach the water-soluble elements from the sediments and hence lead to a decreased elemental concentration compared to what might have been there originally. Alternatively, if sampling the sand size fraction for heavy mineral analysis, the concentration of indicator minerals within a sample volume may be increased.

In areas of washed till, sediment sampled at depth is usually finer textured, less sorted and denser than the upper washed sediments (Figure GS2022-11-8a–d). Clasts that are clean on one side and have a 'clay skin' adhering to the other side are also indicative of washing and fines removal (Figure GS2022-11-8e, f). In other areas, perhaps due to permafrost mixing, brown clay can be mixed in with beige diamict at depths up to 0.8 m (Figure GS2022-11-8g, h).

Ice-flow history

Erosional field-based ice-flow indicators

Bedrock outcrops are rare in the study area, and new erosional ice-flow measurements were obtained from striations, grooves, chattermarks, crescentic gouges and fractures at just two field sites in 2022 and five field sites in 2020 (Figure GS2022-11-9c; Gauthier and Hodder, 2022)[2]. Based on

[2] MGS Data Repository Item DRI2022009, containing the data or other information sources used to compile this report, is available online to download free of charge at https://manitoba.ca/iem/info/library/downloads/index.html, or on request from minesinfo@gov.mb.ca, or by contacting the Resource Centre, Manitoba Natural Resources and Northern Development, 360-1395 Ellice Avenue, Winnipeg, Manitoba R3G 3P2, Canada

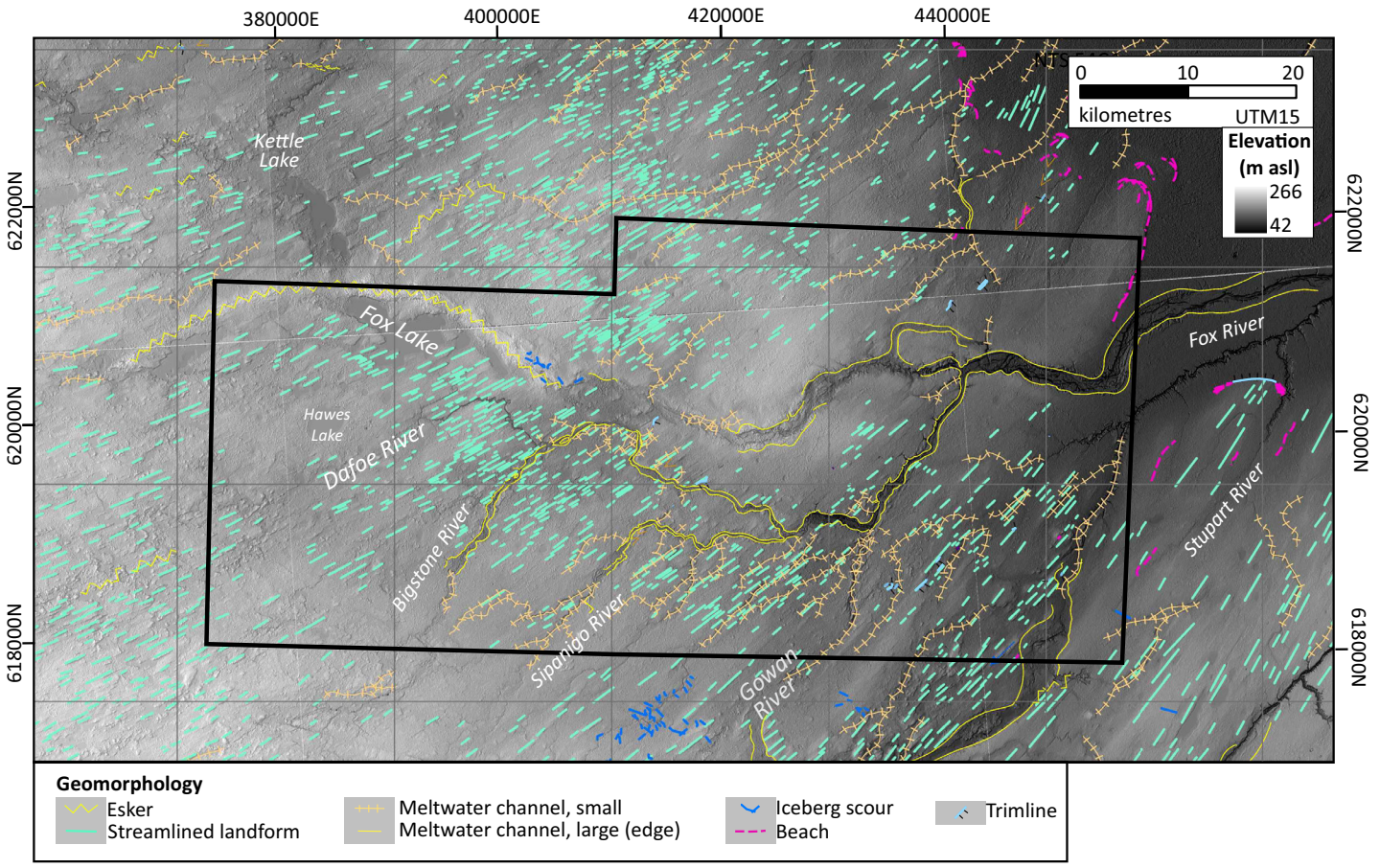

Figure GS2022-11-4: *Surface geomorphology in the study area is dominated by southwest-trending streamlined landforms, which are accompanied by subparallel meltwater channels. A larger esker-meltwater corridor system crosses the area, and was likely active during formation of the Hayes Lobe. During deglaciation, iceberg scours formed on the bed of glacial Lake Agassiz. Final deglaciation resulted in incursion of the Tyrrell Sea, which formed beaches and trimlines between 131 and 136 m asl. Background imagery is a hillshade created from data provided by Earth Observation Research Center and Japanese Aerospace Exploration Agency (2022). All co-ordinates are in UTM Zone 15, NAD83.*

these erosional field-based ice-flow indicators, paleo-ice flow was to the northwest (308–310°), then west (270°, 286°) and then southwest (235–258°). Ice flowed to the south before the southwest, as demarcated by a protected crescentic fracture to 176° at one site.

Streamlined landforms

Streamlined landforms were mapped across the study area, at a variety of resolutions from remotely sensed imagery (Figure GS2022-11-4). All streamlined landforms trend toward the southwest in the study area, in a fan shape spread toward ~215° in the east and 245° in the northwest, and were formed by the Hayes Lobe ice stream (Dredge and Cowan, 1989; Gauthier et al., 2021).

Till-fabric analyses

Till-fabric analyses were conducted on the surface till at seven sample sites, and on the subsurface till at an additional 13 sample sites. Separating the tills based on presumed relative age (see also Gauthier et al., 2022), the till fabrics suggest that ice during previous glacial cycle(s) flowed to the northwest-southeast twice (direction undetermined), west twice, southwest, south-southwest and south (Figure GS2022-11-9b). The relatively less dense surface till was deposited and/or deformed by south- to south-southwest-trending ice flow, west-trending ice flow and either a northwest- or southeast-trending ice-flow (Figure GS2022-11-9a). The order of these ice-flow phases is unknown, though it is noted that most areas of till were later eroded into southwest-trending streamlined landforms.

Till-fabric analyses are particularly useful in areas where bedrock outcrops are scarce. However, given that the orientations of the surface till fabrics contradict the orientation of streamlined landforms, this study highlights the importance of conducting till-fabric analyses in all areas. The mismatch of orientations between different types of ice-flow indicators likely means that the streamlined landforms are erosional, and have exposed till(s) unrelated to the young southwest-trending ice-flow direction. Although forthcoming till-composition studies will assess this hypothesis, it should be noted that erosional streamlined-landform genesis is confirmed in the Knee Lake area, 55 km to the south (Trommelen and Ross, 2014).

Figure GS2022-11-5: *Interbedded brown clay, light brown fine to medium sand and brown diamict, interpreted as glaciomarine deposits at the top of a section along the Fox River, northeastern Manitoba.*

2020 kimberlite indicator mineral results

A total of 193 KIM grains were recovered from the 59 samples collected in 2020, averaging 1.7 KIM recovered per 10 kg of till processed. The KIM chemistry and sample abundances are provided in Hodder and Gauthier (2022). The KIM grains include 26 kimberlitic garnets, which are further classified as two G1 garnets, two G11 garnets, two G3 garnets and 20 G9 garnets based on the criteria set out in Grütter et al. (2004; Figure GS2022-11-10a). A single Cr-diopside grain was recovered and plots within the diamond inclusion and intergrowth field defined by Nimis (2002; Figure GS2022-11-10b). A total of 14 kimberlitic Mg-ilmenite grains were recovered (Figure GS2022-11-10c, d). The 19 forsterite grains that were recovered have Mg numbers that range from 0.88 to 0.96 and some grains have detectable concentrations of chromium. Three of the grains fall within and two lie on the border of the diamond inclusion and intergrowth field defined by Fipke et al. (1995; Figure GS2022-11-10e).

The majority of the KIMs recovered are chromite and Cr-spinel grains (69%; n = 133). Of these grains, 54.9% are Mg-chromite (n = 73 of 133), 39.8% are chromite (n = 53 of 133), 3.8% are Ti-chromite (n = 5 of 133) and 1.5% are spinel (n = 2 of 133) based on the criteria used in Smith et al. (2021). Chromite grains are grouped with Cr-spinel herein and in Hodder and Gauthier (2022), in accordance with the terminology established in the Manitoba KIM database (Keller, 2019). One Cr-spinel grain plots within the diamond inclusion and intergrowth field based on two indices (Figure GS2022-11-11a, c), and is interpreted to be a Di-Cr-spinel. Two other grains plot within the diamond inclusion and intergrowth field of one index and are interpreted as possible Di-Cr-spinel grains (Figure GS2022-11-11a).

Importantly, chromite grains are not exclusive to kimberlites and their interpretation as a KIM needs to be approached cautiously. Locally, the Fox River sill contains chromite in concentrations of more than 4% (Scoates, 1990). Even grains that plot within the diamond inclusion and intergrowth fields are also not restricted to kimberlites (Figure GS2022-11-11), as chromite with this composition has been documented from chromite deposits

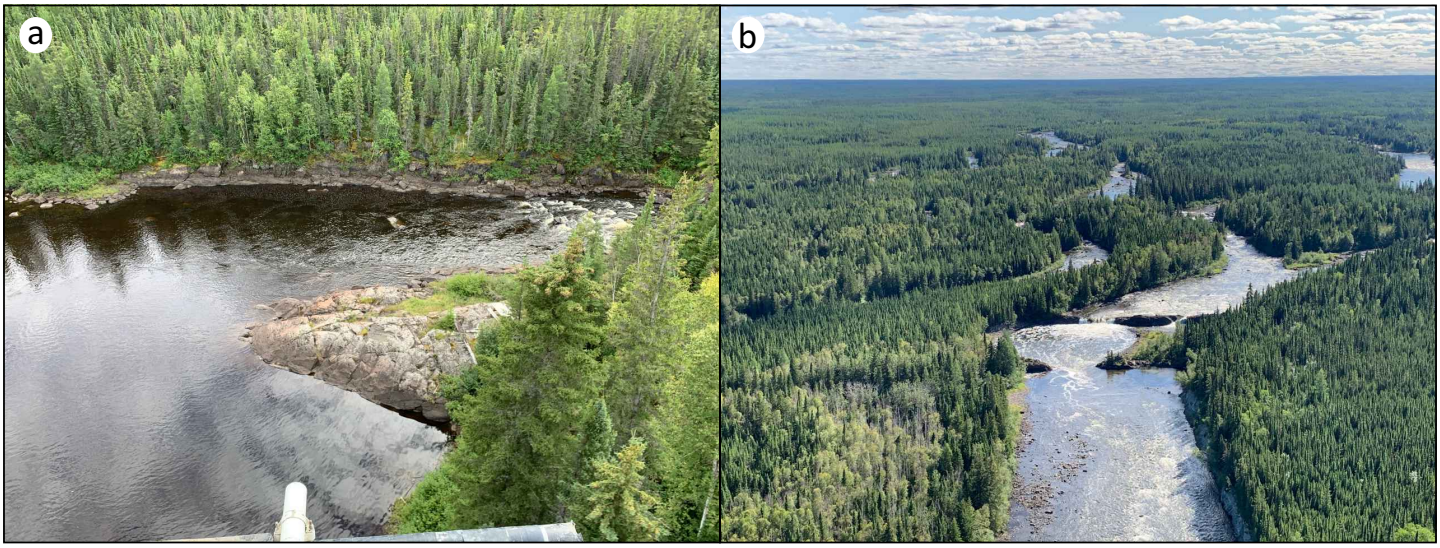

Figure GS2022-11-6: *Glacial waters flowing beneath the Hayes Lobe cut down through Quaternary sediments into bedrock along multiple rivers in the study area, including at the confluence of the Gowan River with the Fox River* ***(a)*** *and just downstream of the confluence of the Sipanigo and Fox rivers* ***(b)****.*

Figure GS2022-11-7: *The surface till in the study area is light coloured and coarse textured* ***(a, b)****, and overlies either bedrock or older darker-coloured and finer-textured* ***(a, c)*** *tills. Some river sections expose even older dense, blocky diamicts with oxidation rind on joint surfaces* ***(d, e)****.*

in the McFaulds Lake ('Ring of Fire') area of northern Ontario (Gao and Crabtree, 2016). Chromite grains from the Fox River sill have Cr_2O_3 concentrations that range from 25.3 to 46.5 wt. % (n = 73; Turnock et al., 2005). Relationships between grains recovered from till samples and those from in situ bedrock will be more thoroughly analyzed following receipt of the 2022 sampling results.

Spatial trends

On Figure GS2022-11-12a, the spatial distribution of KIM grains is plotted as towers that are proportional in height to the total number of KIMs recovered, normalized to 10 kg of till processed. These towers are then broken down according to the type of KIMs recovered. Since chromite grains can be locally sourced from mafic to ultramafic rocks, the spatial distribution of KIMs without Cr-spinel is plotted separately (Figure GS2022-11-12b).

The distribution of kimberlitic garnet grains is not even across the survey area (Figure GS2022-11-12b). There are two spatial patches with relatively elevated concentrations of garnet. The first patch ('patch 1') is situated in the southeastern corner of the NTS 53M16 map area and the second patch ('patch 2') is

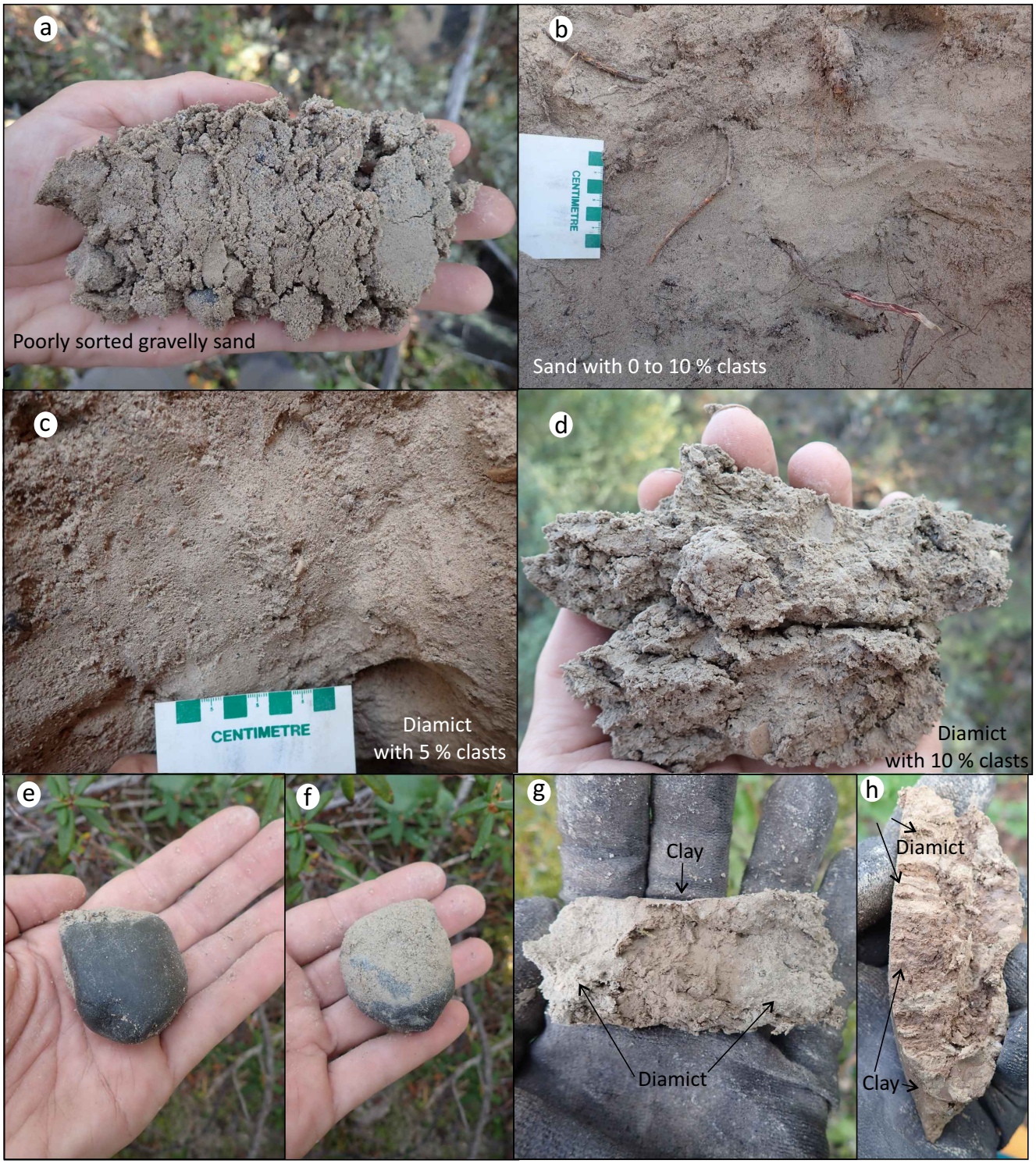

Figure GS2022-11-8: *Wave-washing at a site can lead to the removal of fines* ***(a)*** *or sorting of sediment* ***(b)*** *from the diamict parent material* ***(c, d)****. Clasts that are clean on one side* ***(e)*** *and have a 'clay skin' adhering to the other side* ***(f)*** *are also indicative of washing and fines removal. In other cases, remobilized till becomes interbedded with clay* ***(g, h)****.*

situated in the central region of the NTS 53M15 map area (Figure GS2022-11-12b). The spatial distribution of Mg-ilmenite and forsterite is largely restricted to these two patches as well.

Dispersal patterns will be further analyzed following receipt of the 2022 indicator-mineral sample results and in consultation with till clast-lithology and matrix geochemistry provenance analysis. The 2022 sampling occurred within and amongst the samples shown in Figure GS2022-11-12, as well as to the east and northeast (Figure GS2022-11-1). The western boundary of patch 1 is oriented to the southwest, which aligns with the streamlined landform orientation in that area (Figure GS2022-11-9a). Only one site in patch 1 has measured till-fabric orien-

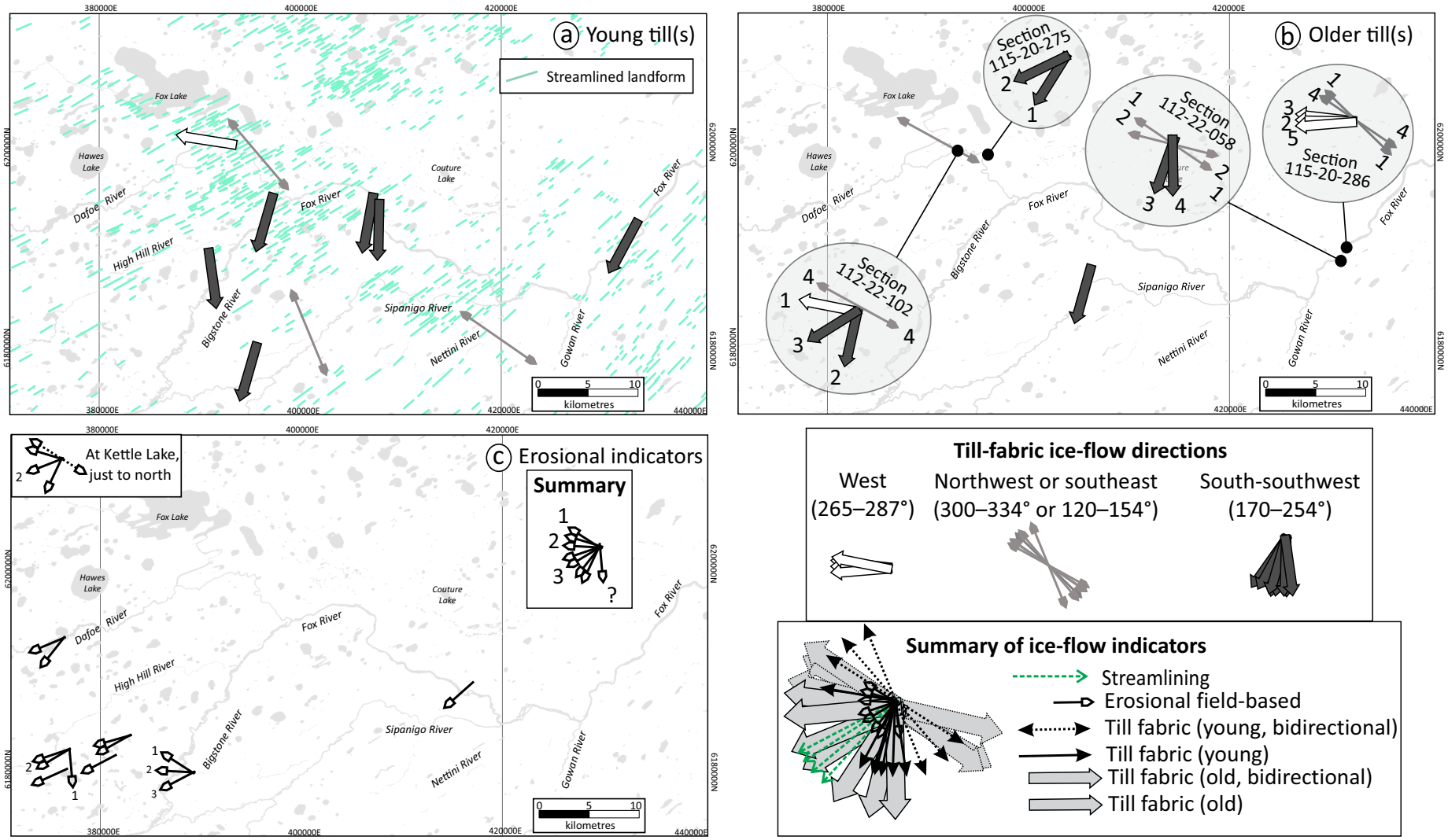

Figure GS2022-11-9: *Ice-flow indicators for the Fox River belt study area, separated into **a)** a young phase (from till-fabric and landform analyses), **b)** a presumed old phase (from till-fabric analysis) and **c)** erosional field-based. Indicators are denoted by relative age when observed either up-section (till fabrics) or by cross-cutting relationships (erosional field-based ice-flow indicators). All co-ordinates are in UTM Zone 15, NAD83.*

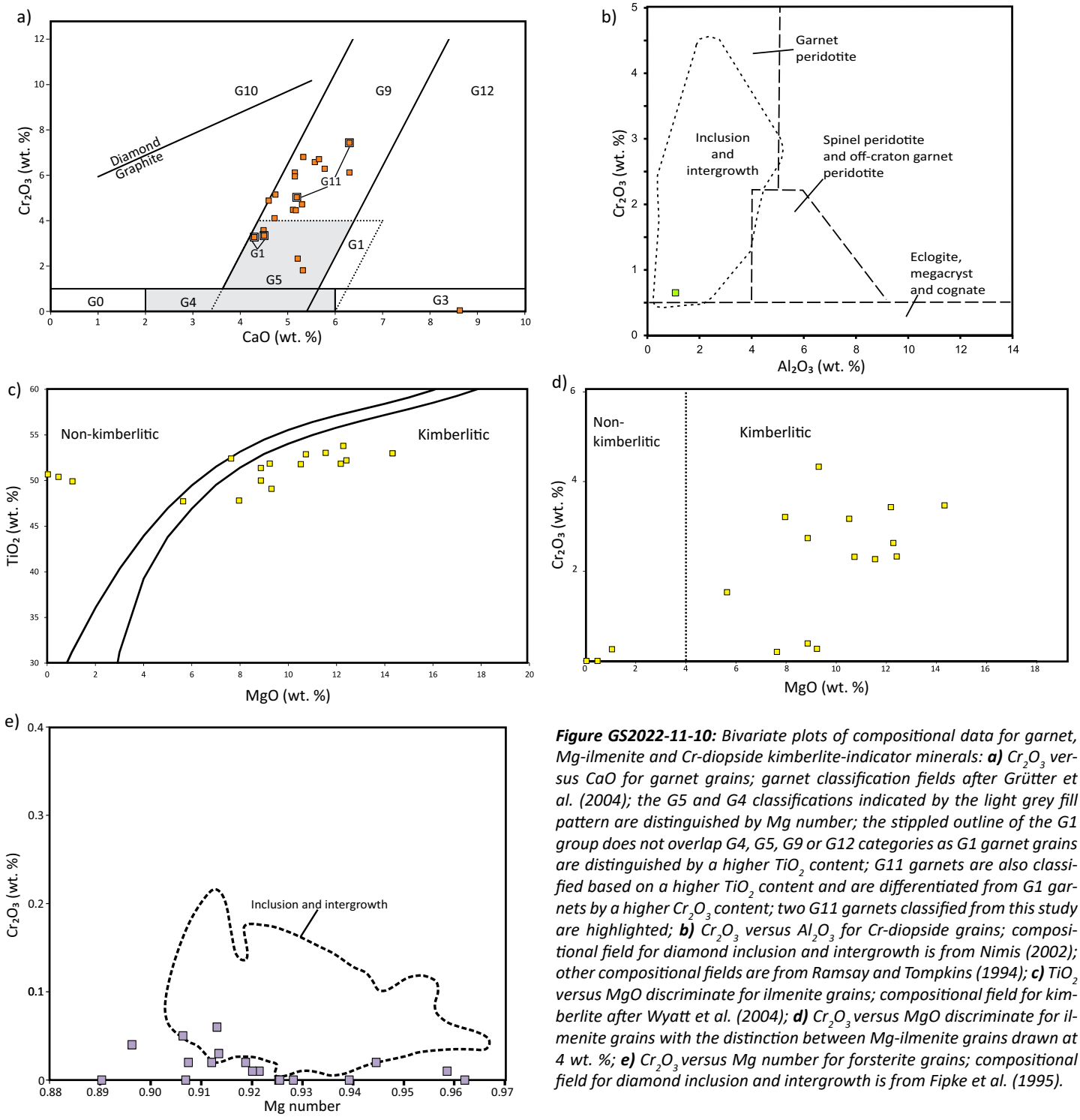

Figure GS2022-11-10: *Bivariate plots of compositional data for garnet, Mg-ilmenite and Cr-diopside kimberlite-indicator minerals:* ***a)*** *Cr_2O_3 versus CaO for garnet grains; garnet classification fields after Grütter et al. (2004); the G5 and G4 classifications indicated by the light grey fill pattern are distinguished by Mg number; the stippled outline of the G1 group does not overlap G4, G5, G9 or G12 categories as G1 garnet grains are distinguished by a higher TiO_2 content; G11 garnets are also classified based on a higher TiO_2 content and are differentiated from G1 garnets by a higher Cr_2O_3 content; two G11 garnets classified from this study are highlighted;* ***b)*** *Cr_2O_3 versus Al_2O_3 for Cr-diopside grains; compositional field for diamond inclusion and intergrowth is from Nimis (2002); other compositional fields are from Ramsay and Tompkins (1994);* ***c)*** *TiO_2 versus MgO discriminate for ilmenite grains; compositional field for kimberlite after Wyatt et al. (2004);* ***d)*** *Cr_2O_3 versus MgO discriminate for ilmenite grains with the distinction between Mg-ilmenite grains drawn at 4 wt. %;* ***e)*** *Cr_2O_3 versus Mg number for forsterite grains; compositional field for diamond inclusion and intergrowth is from Fipke et al. (1995).*

tations; at site 115-20-286, sample B01 has a strong till fabric toward 215°, sample F02 has a moderate till fabric oriented to 308° or 128°, sample H01 has a strong till fabric oriented to 270°, and sample I02 has a very strong till fabric oriented to 315° or 135° (Gauthier and Hodder, 2022). In patch 2, eight of the KIM till samples have associated till-fabric measurements (Gauthier and Hodder, 2022). Those with nonchromite KIMs include young tills with interpreted ice flow to the south-southwest (201°) and northwest or southeast (334 or 154°), as well as a possibly older till with interpreted ice flow to the southwest (254°).

Future work

Ongoing surficial geology analyses will focus on 1:50 000 scale surficial mapping, as well as tracing lithological indicators from known bedrock source areas. The latter will be conducted by clast-lithology counts, indicator-mineral counts and analyzing the geochemical composition of the collected till samples.

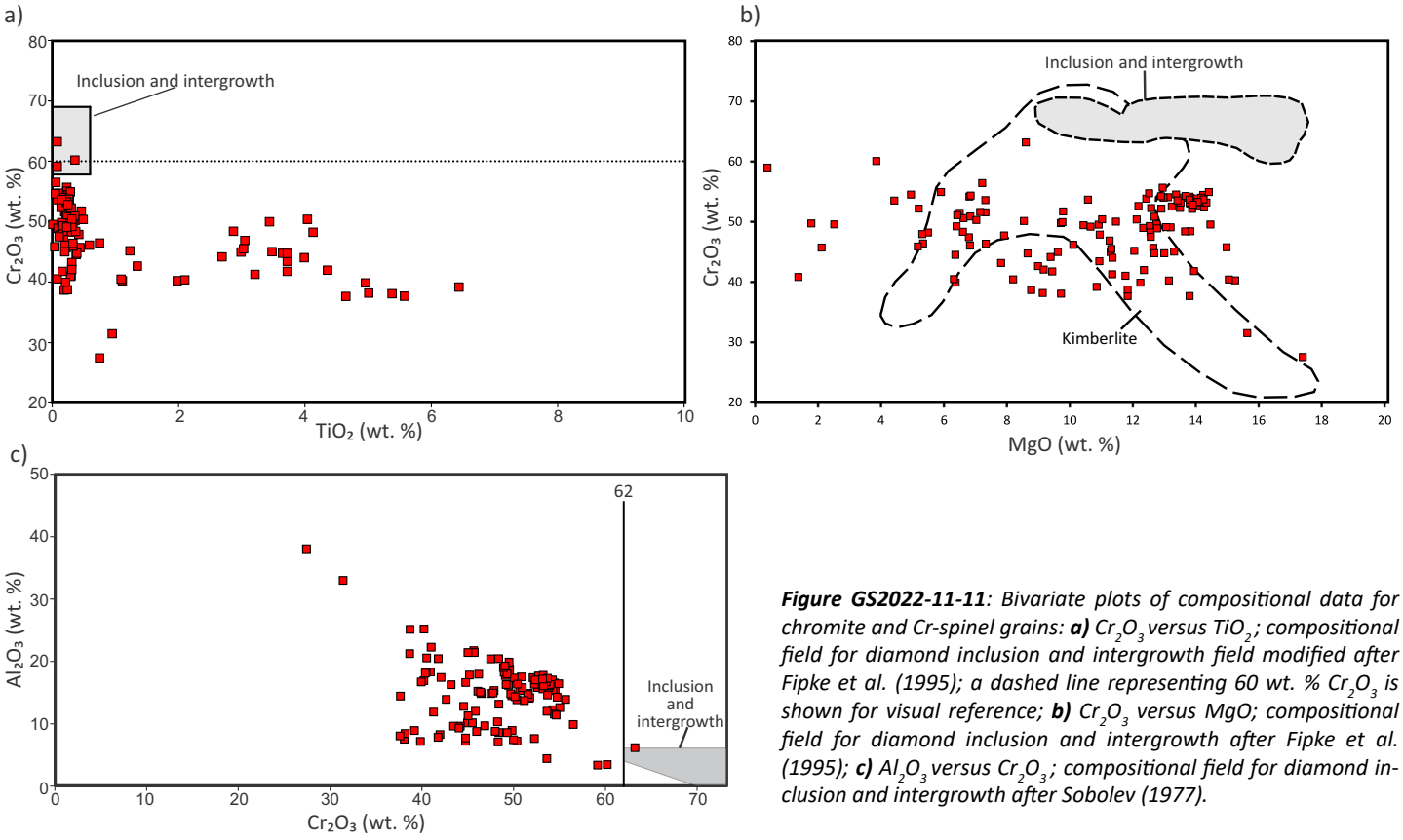

***Figure GS2022-11-11**: Bivariate plots of compositional data for chromite and Cr-spinel grains: **a)** Cr_2O_3 versus TiO_2; compositional field for diamond inclusion and intergrowth field modified after Fipke et al. (1995); a dashed line representing 60 wt. % Cr_2O_3 is shown for visual reference; **b)** Cr_2O_3 versus MgO; compositional field for diamond inclusion and intergrowth after Fipke et al. (1995); **c)** Al_2O_3 versus Cr_2O_3; compositional field for diamond inclusion and intergrowth after Sobolev (1977).*

Economic considerations

As bedrock outcrops are rare in much of Manitoba's northern region, a thorough understanding of surficial geology is essential for drift prospecting. Till-sample analysis is commonly used in drift-covered regions to help determine the source area for mineralized erratics and boulder trains, but is more difficult to interpret in palimpsest terrains such as in this study area. Ongoing surficial geology studies aim to provide a detailed framework for the directions, timing and nature (e.g., erosive or depositional) of major and minor ice-flow events in the region. The outcomes of these studies are geared toward providing mineral exploration geologists with an up-to-date surficial geology knowledge base and the adequate tools to more accurately locate exploration targets in Manitoba's drift-covered areas. More specifically, the results of this study may inform drift exploration for nickel, copper and platinum-group-element mineralization in the Fox River belt, and new KIM results will help assess the regional-scale diamond potential of the study area.

Acknowledgments

The authors thank K. Dunthorne of Prairie Helicopters Ltd. for his good nature and calm flying. The 2022 till samples for heavy mineral analyses are funded by Geological Survey of Canada's Geo-mapping for Energy and Minerals, GeoNorth program (GEM-GeoNorth). Logistical support was provided by C. Epp throughout the project.

References

Dredge, L.A. and Cowan, W.R. 1989: Quaternary geology of the southwestern Canadian Shield; *in* Quaternary Geology of Canada and Greenland, R.J. Fulton (ed.), Geological Survey of Canada, Geology of Canada, no. 1, p. 214–248.

Dyke, A.S. and Prest, V.K. 1987: Late Wisconsinan and Holocene history of the Laurentide Ice Sheet; Geographie physique et Quaternaire, v. 41, no. 2, p. 237–263.

Earth Observation Research Center and Japanese Aerospace Exploration Agency 2022: ALOS Global Digital Surface Model; Earth Observation Research Center and Japanese Aerospace Exploration Agency, ALOS World 3D - 30m, URL <https://www.eorc.jaxa.jp/ALOS/en/dataset/aw3d30/aw3d30_e.htm> [March 2022].

Fipke, C.E., Gurney, J.J. and Moore, R.O. 1995: Diamond exploration techniques emphasising indicator mineral geochemistry and Canadian examples; Geological Survey of Canada, Bulletin 423, 96 p.

Gao, C. and Crabtree, D.C. 2016: Results of regional till and modern alluvium sampling in the McFaulds Lake ("Ring of Fire") area, northern Ontario; Ontario Geological Survey, Open File Report 6309, 164 p.

Gauthier, M.S. and Hodder, T.J. 2020: Surficial geology mapping and till composition of the western Fox River greenstone belt area, northeastern Manitoba (NTS 53M15, 16); *in* Report of Activities 2020, Manitoba Agriculture and Resource Development, Manitoba Geological Survey, p. 47–54, URL <https://manitoba.ca/iem/geo/field/roa20pdfs/GS2020-7.pdf> [October 2022].

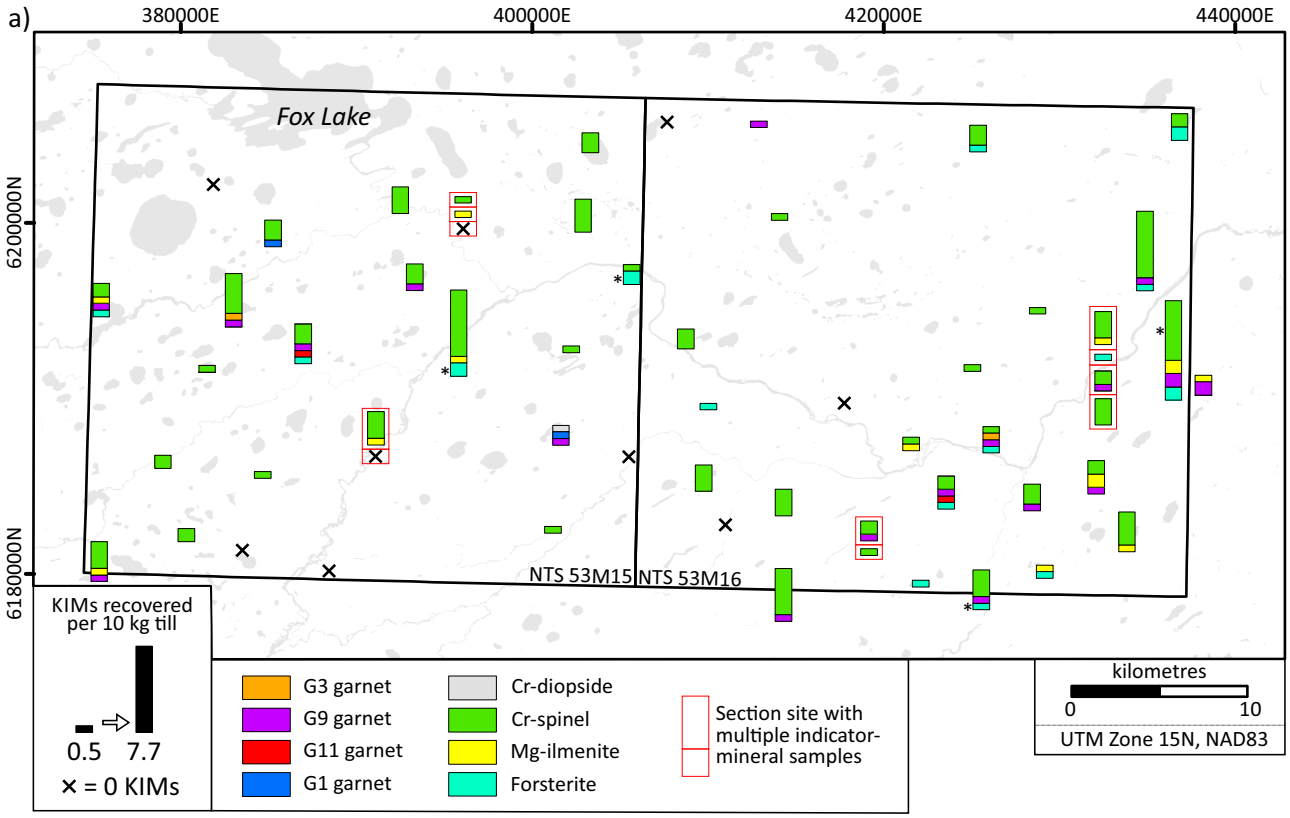

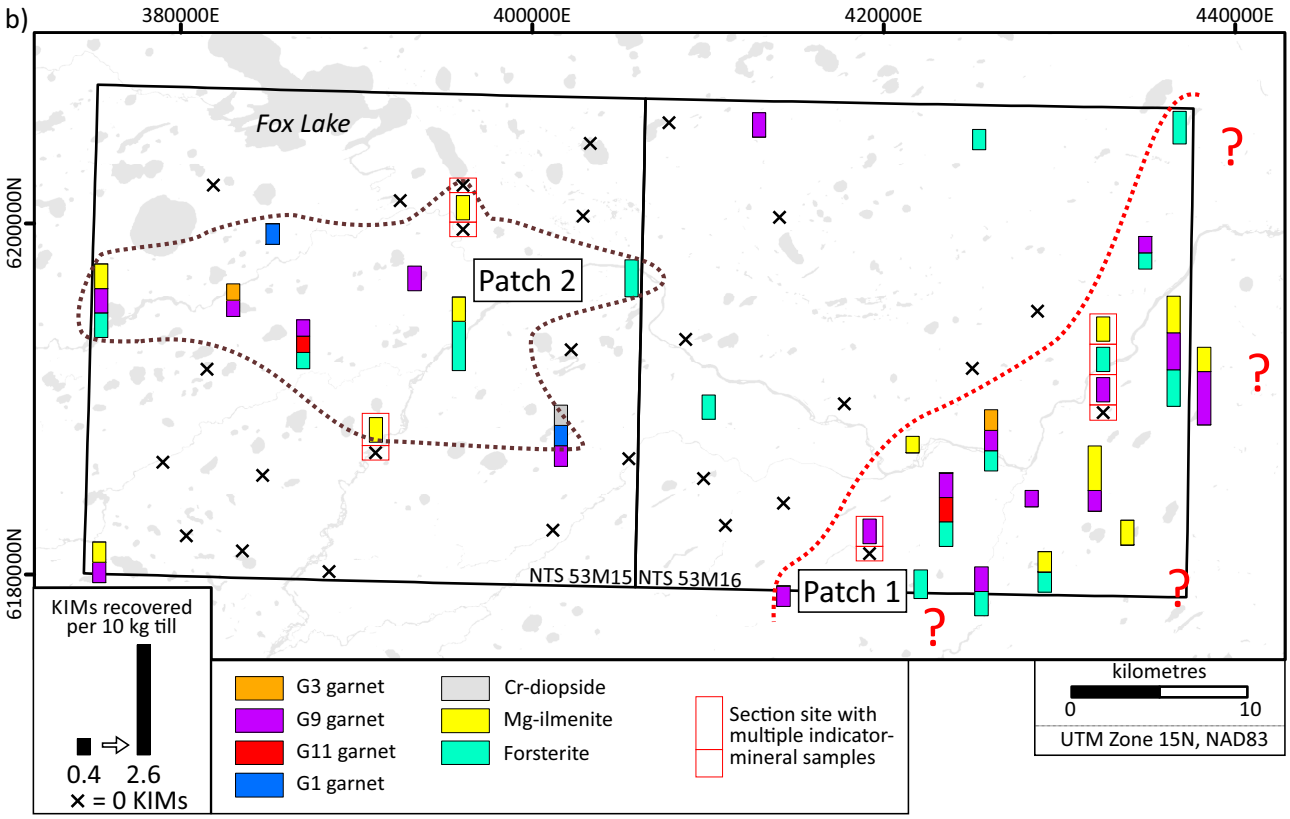

Figure GS2022-11-12: *Spatial distribution of kimberlite-indicator-mineral (KIM) grains recovered from till presented as towers that are proportional in height to the number of KIMs recovered, normalized to 10 kg of till processed:* ***a)*** *all KIMs as defined by the Manitoba KIM database (Keller, 2019); the asterisk denotes samples with either a Di-forsterite (n = 3) or a Di-Cr-spinel (n = 1) recovered, see text for details;* ***b)*** *KIM grains recovered with Cr-spinel removed, since these grains can be locally sourced from mafic to ultramafic rocks in the Fox River sill.*

Gauthier, M.S. and Hodder, T.J. 2021: Till geochemistry and heavy mineral analyses of the western Fox River greenstone belt area, northeastern Manitoba (NTS 53M15, 16), plus 4 samples from the Gillam area (parts of 54D7, 11); Manitoba Agriculture and Resource Development, Manitoba Geological Survey, Data Repository Item DRI2021010, Microsoft® Excel® file, URL <https://manitoba.ca/iem/info/libmin/DRI2021010.xlsx> [October 2022].

Gauthier, M.S. and Hodder, T.J. 2022: Field-based ice-flow indicator data from the Split Lake and Fox River belt areas, northeastern Manitoba (parts of NTS 53M15, 16, 54D2, 4, 64A2); Manitoba Natural Resources and Northern Development, Manitoba Geological Survey, Data Repository Item DRI2022009, Microsoft® Excel® file, URL <https://manitoba.ca/iem/info/libmin/DRI2022009.xlsx> [November 2022].

Gauthier, M.S., Breckenridge, A. and Hodder, T.J. 2021: Patterns of ice recession and ice stream activity for the MIS 2 Laurentide Ice Sheet in Manitoba, Canada; Boreas, v. 51, no. 2, p. 274–298, URL <https://doi.org/10.1111/bor.12571>.

Gauthier, M.S., Hodder, T.J. and Ross, M. 2022: Quaternary stratigraphy and ice-flow indicator data for the Gillam region, Manitoba (parts of NTS 54C, D, 64A); Manitoba Natural Resources and Northern Development, Manitoba Geological Survey, Geoscientific Paper GP2022-2, 37 p. plus 7 appendices, URL <https://manitoba.ca/iem/info/libmin/GP2022-2.zip> [November 2022].

Gauthier, M.S., Hodder, T.J., Ross, M., Kelley, S.E., Rochester, A. and McCausland, P. 2019: The subglacial mosaic of the Laurentide Ice Sheet; a study of the interior region of southwestern Hudson Bay; Quaternary Science Reviews, v. 214, p. 1–27, URL <https://doi.org/10.1016/j.quascirev.2019.04.015>.

Gauthier, M.S., Kelley, S.E. and Hodder, T.J. 2020: Lake Agassiz drainage bracketed Holocene Hudson Bay Ice Saddle collapse; Earth and Planetary Science Letters, v. 554, no. 15, p. 116372, URL <https://doi.org/10.1016/j.epsl.2020.116372>.

Grütter, H.S., Gurney, J.J., Menzies, A.H. and Winter, F. 2004: An updated classification scheme for mantle-derived garnet, for use by diamond explorers; Lithos, v. 77, p. 841–857.

Hodder, T.J. and Gauthier, M.S. 2022: Kimberlite-indicator-mineral data derived from glacial sediments (till) in the western Fox River greenstone belt area, northeastern Manitoba (NTS 53M15, 16); Manitoba Natural Resources and Northern Development, Manitoba Geological Survey, Data Repository Item DRI2022010, Microsoft® Excel® file, URL <https://manitoba.ca/iem/info/libmin/DRI2022010.xlsx> [November 2022].

Keller, G.R. 2019: Manitoba Kimberlite Indicator Mineral Database (version 3.2); Manitoba Growth, Enterprise and Trade, Manitoba Geological Survey, zipped Microsoft® Access® 2016 database, URL <https://manitoba.ca/iem/geo/diamonds/MBKIMDB_32.zip> [October 2021].

Klassen, R.W. 1986: Surficial geology of north-central Manitoba; Geological Survey of Canada, Memoir 419, 57 p.

Klassen, R.W. and Netterville, J.A. 1979: Surficial geology, Knee Lake, Manitoba; Geological Survey of Canada, Preliminary Map 11-1978, scale 1:250 000.

Nimis, P. 2002: The pressures and temperatures of formation of diamond based on thermobarometry of chromian diopside inclusions; The Canadian Mineralogist, v. 40, p. 871–884.

Ramsay, R.R. and Tompkins, L.A. 1994: The geology, heavy mineral concentrate mineralogy, and diamond prospectivity of the Boa Esperança and Cana Verde pipes, Corrego D'anta, Minas Gerais, Brazil; *in* Kimberlites, Related Rocks and Mantle Xenoliths, H.O.A. Meyer and O.H. Leonardos (ed.), Proceedings of the 5th International Kimberlite Conference, Araxá, Brazil, Companhia de Pesquisa de Recursos Minerais (CRPM), Special Publication, v. 2, p. 329–345.

Rinne, M.L. 2018: Summary of key results and interpretations for the Fox River belt compilation project, northeastern Manitoba (parts of NTS 53M, N, O, 54B, C, D); *in* Report of Activities 2018, Manitoba Growth, Enterprise and Trade, Manitoba Geological Survey, p. 25–26, URL <https://manitoba.ca/iem/geo/field/roa18pdfs/GS2018-3.pdf> [September 2020].

Rinne, M.L. 2020: Bedrock geology of the Fox River belt, Manitoba (parts of NTS 53M–O, 54B, D); Manitoba Agriculture and Resource Development, Manitoba Geological Survey, Open File OF2020-4, 2 maps at 1:525 000 scale, 1 map at 1:250 000 scale and 1 map at 1:50 000 scale, URL <https://manitoba.ca/iem/info/libmin/OF2020-4.zip> [October 2022].

Scoates, R.J. 1990: The Fox River sill, northeastern Manitoba – a major stratiform intrusion; Manitoba Energy and Mines, Geological Services, Geological Report GR82-3, 192 p., 1 map, scale 1:50 000, URL <https://manitoba.ca/iem/info/libmin/GR82-3.zip> [October 2022].

Smith, I.R., Day, S.J.A., Paulen, R.C. and Pearson, D.G. 2021: Chemical studies of kimberlite indicator minerals from stream sediment and till samples in the southern Mackenzie region (NTS 85B, C, F, G), Northwest Territories, Canada; Geological Survey of Canada, Open File 8799, 29 p., URL <https://doi.org/10.4095/329080>.

Sobolev, N.V. 1977: Deep-seated inclusions in kimberlites and the problem of the Upper Mantle composition; translated from Russian by D.A. Brown, F.R. Boyd (ed.), American Geophysical Union, Washington, D.C., 259 p.

Thorleifson, L.H., Wyatt, P.H. and Warman, T.A. 1993: Quaternary stratigraphy of the Severn and Winisk drainage basins, northern Ontario; Geological Survey of Canada, Bulletin 442, 65 p.

Trommelen, M.S. 2015: Glacial history and till composition, Knee Lake area, northeastern Manitoba (NTS 53L14, 15, 53M1, 2); Manitoba Mineral Resources, Manitoba Geological Survey, Geoscientific Paper GP2013-3, 30 p. plus 13 appendices, URL <https://manitoba.ca/iem/info/libmin/GP2013-3.zip> [September 2020].

Trommelen, M.S. and Ross, M. 2014: Distribution and type of sticky spots at the centre of a deglacial streamlined lobe in northeastern Manitoba, Canada; Boreas, v. 43, p. 557–576, URL <https://doi.org/10.1111/bor.12064>.

Turnock, A.C., Raudsepp, M. and Scoates, R.F.J. 2005: Electron-microprobe analyses of minerals from the Fox River sill, northeastern Manitoba; Manitoba Industry, Economic Development and Mines, Manitoba Geological Survey, Data Repository Item DRI2005001, Microsoft® Excel® file, URL <https://manitoba.ca/iem/info/libmin/2005001.xlsx> [October 2022].

Wyatt, B.A., Baumgartner, M., Anckar, E. and Grütter, H.S. 2004: Compositional classification of 'kimberlitic' and 'non-kimberlitic' ilmenite; Lithos, v. 77, p. 841–857.

GS2022-12

Quaternary stratigraphic investigations near the confluence of the Hayes and Gods rivers, northeastern Manitoba (part of NTS 54C7)

by T.J. Hodder and M.S. Gauthier

Summary

The occurrence of a relatively elevated concentration of kimberlite-indicator-mineral (KIM) grains, identified during a previous survey, at a site near the confluence of the Hayes and Gods rivers has led to a further investigation of the kimberlite potential in the region. Previous work interpreted the Quaternary stratigraphy at this site as a single till that was deposited by south- to southeast-trending ice flow. This site was revisited and a reinterpretation identified two tills that were deposited by separate ice-flow events; both were likely deposited by northwest-trending ice flow. Two additional nearby sites were described and sampled to 1) further assess the KIM potential in the region and 2) help establish the Quaternary stratigraphy and till provenance.

In Brief:

- Investigation of the Quaternary stratigraphy and till provenance near previous KIM high

Citation:
Hodder, T.J. and Gauthier, M.S. 2022: Quaternary stratigraphic investigations near the confluence of the Hayes and Gods rivers, northeastern Manitoba (part of NTS 54C7); *in* Report of Activities 2022, Manitoba Natural Resources and Northern Development, Manitoba Geological Survey, p. 110–120.

Introduction

The Manitoba Geological Survey (MGS) conducted an investigation of the Quaternary stratigraphy exposed along three river sections near the confluence of the Hayes and Gods rivers in northeastern Manitoba (Figure GS2022-12-1). This helicopter-supported work was completed over a half day in 2019 and two days in 2022. The purpose of this study is to gather additional observations of the Quaternary stratigraphy in the area, and collect indicator mineral samples to assess the kimberlite potential in the region.

Previous work

The MGS conducted a reconnaissance-scale glacial sediments (till) KIM survey in the Hudson Bay Lowland (HBL) in 2001 and 2002 (Nielsen, 2001, 2002). Results from this survey indicated that the KIM distribution across the region was not uniform; there was a relatively elevated concentration of KIMs at a site on the north shore of the Hayes River near the confluence with the Gods River (Syme et al., 2004; Hodder et al., 2017).

Sediments exposed at this site were previously described in three separate studies (Figure GS2022-12-1; Operation Winisk [B.G. Craig, H. Gwyn and B.C. McDonald, unpublished notes, 1967; McDonald, 1969]; Klassen, 1986; Nielsen, 2002). The Quaternary stratigraphy comprises postglacial sorted sediments overlying two till beds, which are separated by 1.5–2.4 m of sorted intertill sediments (Figure GS2022-12-1). Two of the studies reported that the river bank exposed between 17.9 and 21.3 m of sediments (Operation Winisk [B.G. Craig, H. Gwyn and B.C. McDonald, unpublished notes, 1967; McDonald, 1969]; Klassen, 1986; Figure GS2022-12-1), whereas Nielsen (2002) indicated that 38 m of sediments were exposed; nearly twice as thick as previous studies.

Nielsen (2002) interpreted both diamicton beds as till, and correlated them to the Long Spruce till (Nielsen et al., 1986). The Long Spruce till was originally defined in the Gillam area as light olive grey with a blocky appearance and light oxidation rind on joint surfaces. Initial studies indicated large variations in the concentration of undifferentiated greenstone and greywacke within this 'one' named till (Nielsen et al., 1986). Till-fabric measurements from the Long Spruce till were interpreted to indicate deposition by west- and west-southwest-trending ice flow (Nielsen et al., 1986). Additional work in the lower Hayes River area expanded the mapped extent of the Long Spruce till (Nielsen, 2001; Nielsen and Fedikow, 2002). Till-fabric measurements from the Long Spruce till were now interpreted to indicate deposition by southwest-trending ice flow (~195–215°; Nielsen and Fedikow, 2002). Additional work in 2002 led to mapping of the Long Spruce Till at every section investigated, primarily based on stratigraphic position relative to nonglacial sediments (Nielsen, 2002). On the basis of 30 till fabrics, it was then interpreted that the lower part of the Long Spruce till was deposited by southwest-trending ice flow and the upper part was deposited by south- to southeast-trending ice flow (Nielsen, 2002). These studies have shown that there is significant variability in the characteristics of the named Long Spruce till, including the direction of ice flow that deposited the sediment.

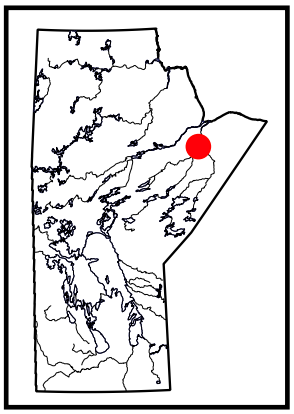

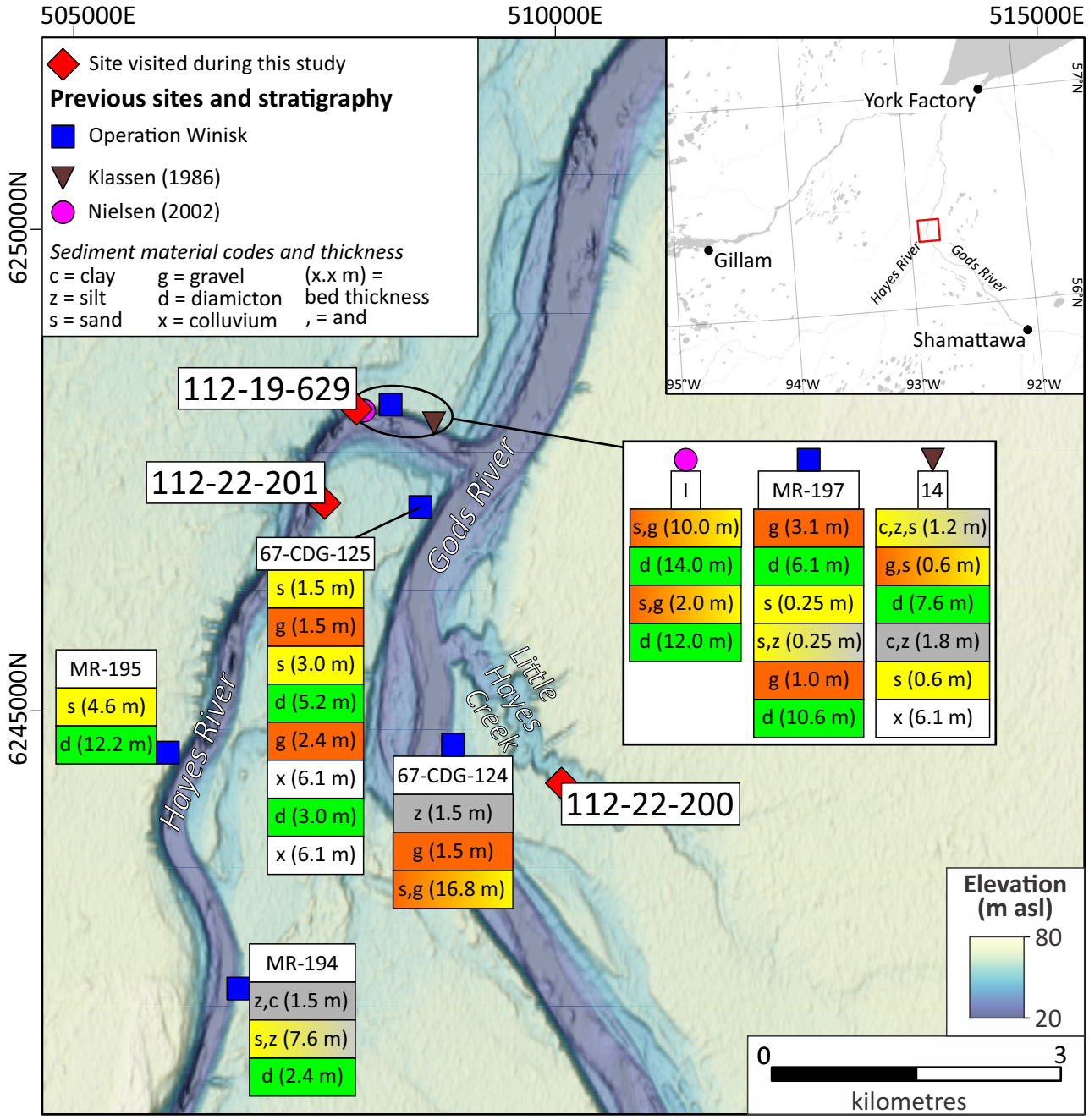

Figure GS2022-12-1: *Location of the study area (red square on inset) near the confluence of the Hayes and Gods rivers, northeastern Manitoba. Previous sites investigated, and the stratigraphy at each site, are shown alongside the three sites investigated as part of this study. Operation Winisk data from B.G. Craig, H. Gwyn and B.C. McDonald (unpublished notes, 1967) and McDonald (1969). Background digital surface model is provided by Earth Observation Research Center and Japanese Aerospace Exploration Agency (2022).*

The understanding of Quaternary stratigraphy records has continued to evolve since these initial investigations. Whereas geologists once strived to correlate these stratigraphic records over great distances, assuming rather continuous deposition during ice-flow events (e.g., Thorleifson et al., 1993), there is now a better appreciation for the fragmented nature of continental glacial records (e.g., Trommelen et al., 2013; Lee, 2018; Gauthier et al., 2019, 2022). Fragmentation needs to be considered when conducting Quaternary stratigraphic investigations in complex glacial terrains, such as northeastern Manitoba, where stratigraphic ice-flow indicators range from northwest-trending (310°) to east-southeast-trending (105°) over at least three glacial cycles (Gauthier et al., 2019). A recent stratigraphic study of 83 sections in the Gillam area suggests that the terms Long Spruce till and Sky Pilot till (overlying unit; Nielsen et al., 1986; Dredge and McMartin, 2011) be retired, and instead be recognized as one 'upper' till unit that overlies nonglacial sediments (Gauthier et al., 2022). This new upper till is interpreted as a cumulative record of erosion, deposition and deformation over at least one glacial cycle. Importantly, careful interpretations of

till texture, density and fabrics suggest that the upper till consists of fragmented patches of sediment belonging to two separate glaciations (occurring where nonglacial sediments are missing between the two chronologically different tills [Gauthier et al., 2022]). Current MGS work in the HBL attempts to better understand the patchy stratigraphic record (Gauthier et al., 2021) and decipher these shifts in ice-flow directions through multiple glaciations.

Current work

River and creek sections in the study area expose 10–24 m of Quaternary sediments. The Quaternary stratigraphy was documented at two new locations and one previously investigated section (Figure GS2022-12-1). Sediment exposures were first cleared of slumped detritus, exposing a continuous section with no gap, and then described in detail. A total of 10 till samples (two in 2019 and eight in 2022) were collected, each weighing 2–3 kg. The till samples were split for archival purposes at the MGS Midland Sample and Core Library (Winnipeg, Manitoba) and then analyzed for grain size, matrix geochemistry (<63 µm size fraction) and clast lithology. An additional 11.4 L till sample was collected at seven till sample sites for indicator mineral analysis. Indicator mineral samples were submitted for analyses to Overburden Drilling Management Limited (Ottawa, Ontario) in collaboration with the Geological Survey of Canada.

Ice-flow data was obtained from studied sections by measuring the long-axes orientation, or fabric, of clasts within till. Elongate clasts, defined by a minimum 1.5:1.0 ratio of the a-axis (longest) to the b-axis (middle), will rotate within the till matrix and orient parallel to the direction of stress that the overriding glacier exerts on the till (Holmes, 1941). A minimum of 30 elongated clasts were measured at each of the nine clast-fabric sites to ensure a statistically valid result.

Section 112-19-629

The north shore of the Hayes River near the confluence with the Gods River was revisited to verify the stratigraphy and thickness of the Quaternary sediments exposed here. Five different stratigraphic beds (SB; SB A–E) were denoted within the upper 24 m of the investigated section. These beds were underlain by ~12 m of colluvium to the river level in 2022. The thicknesses of the two till beds reported here are proportional to the thicknesses reported in Nielsen (2002), but at a ratio of ~0.5:1. For example, Nielsen (2002) reported that the upper SB B till is 14.0 m thick, whereas it has been reported to be 6.1–7.8 m thick across three other studies (including this one). This needs to be considered when revisiting sections reported in Nielsen (2002), since this pattern of overestimating sediment bed thicknesses is not limited to this site.

The uppermost SB A consists of bedded sand and gravel with minor clay (Figure GS2022-12-2). Shell fragments were observed throughout the upper sediments and some beds contain paired whole valves of *Hiatella arctica*, which are indicative of deposition within a marine environment. The bedded sequence and grain-size variations of SB A are interpreted to represent postglacial marine transgression at this site.

A 7.8 m thick layer of brown (Munsell colour 10YR 4/3; Munsell Color–X-Rite, Incorporated, 2015), massive, matrix-supported diamicton (SB B; Figure GS2022-12-3a) sharply underlies SB A. The diamicton contains 10–15% clasts and has a sandy-silt matrix. The diamicton has a crumbly appearance with minor oxidation rind developed on joint surfaces.

A 0.6 m thick layer of matrix-supported, massive, sandy gravel (SB C) underlies SB B. The gravel is poorly sorted and contains 40% clasts that are granule- to large pebble-sized. The lower 0.2 m of this gravel contains rip-up clasts of diamicton. This gravel is interpreted as a glaciofluvial or fluvial deposit based on the poorly sorted nature of the sediments.

A 1.6 m thick layer of well sorted, bedded, very fine sand and medium- to coarse-grained sand (SB D) underlies SB C gravel. Shell fragments were observed in the upper 0.1 m of the bedded sands. The sands are interpreted to have been deposited in a marine environment, based on the rhythmic bedding, the elevation (41 m asl), the position beneath postglacial Tyrrell Sea sediments and the proximity to the modern shoreline (~90 km).

More than 6.0 m of dark greyish-brown (Munsell colour 2.5Y 4/2), massive, matrix-supported diamicton (SB E; Figure GS2022-12-3a) sharply underlies SB D sand. The diamicton contains 15% clasts and has a clayey sandy-silt matrix. The diamicton has a blocky structure with oxidation rind on the joint surfaces, and is relatively denser compared to the upper diamicton (Figure GS2022-12-3a). Both SB B and E diamicton are interpreted as till based on their massive structure, their texture, the glaciogenic shape of the clasts (bullet shaped, faceted and striated), the modality and strength of the clast fabrics, and the lateral continuity.

Ice-flow data, till composition and sediment provenance interpretation

Ice-flow data for both tills (SB B, E) were measured during this study and by Nielsen (2002). The complete dataset is published in Hodder and Gauthier (2022)[1]. To allow a comparison of data from the two studies, the depth of Nielsen (2002) till-fabric measurements were scaled to fit the stratigraphic observations obtained in this study. Two till-fabric analyses were completed in SB B at a similar depth. For this study, the till-fabric measurements were conducted 0.5 m above the lower contact of the till, and were interpreted to indicate deposition by northwest- or southeast-

[1] MGS Data Repository Item DRI2022011, containing the data or other information sources used to compile this report, is available online to download free of charge at https://manitoba.ca/iem/info/library/downloads/index.html, or on request from minesinfo@gov.mb.ca, or by contacting the Resource Centre, Manitoba Natural Resources and Northern Development, 360-1395 Ellice Avenue, Winnipeg, Manitoba R3G 3P2, Canada.

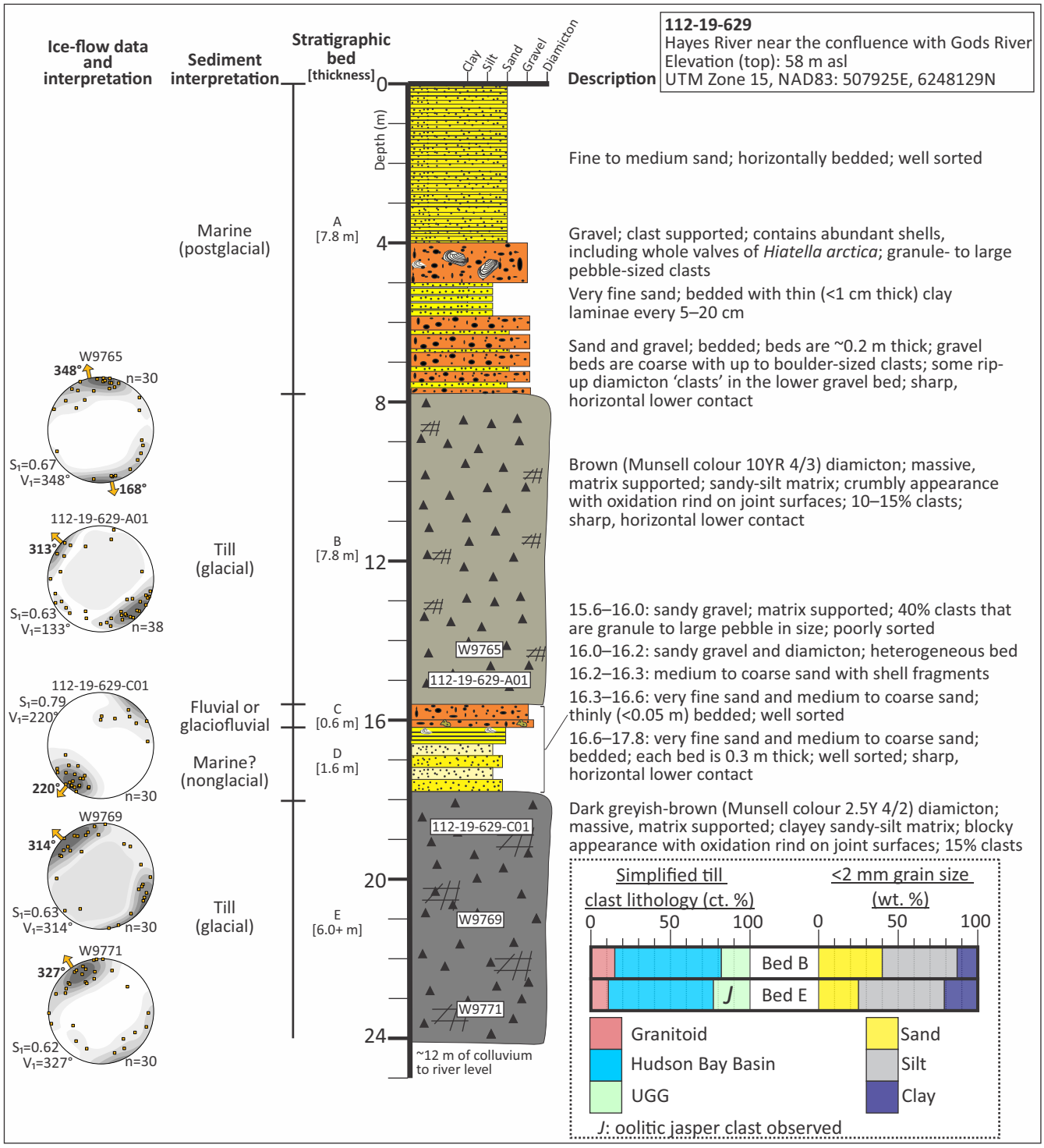

Figure GS2022-12-2: *Quaternary stratigraphy on the north shore of the Hayes River near the confluence with the Gods River (section 112-19-629). Till sample numbers and till-fabric sites are labelled within the white boxes. Till-fabric data is plotted on equal area, lower hemisphere projection stereonets. The value of the principal eigenvalue (S_1) and direction of the principal eigenvector (V_1) are provided and an interpretation of the ice-flow direction is indicated (orange arrow). Diamicton colour from Munsell Color–X-Rite, Incorporated (2015).*

oriented ice flow (site 112-19-629-A01; Figure GS2022-12-2). The second till fabric indicates deposition by north-northwest- or south-southeast-oriented ice flow (site W9765; Figure GS2022-12-2). The SB B till contains 18 ct. % undifferentiated greenstone and greywacke (UGG) clasts in the 2–8 mm size fraction (see Figure GS2022-12-3b for 2–4 mm size fraction). This is in agreement with counts on the 4–8 mm fraction from three other samples from this till bed, which ranged from 12.8 to 19.0 wt. % and increased in concentration with depth (Hodder et al., 2017). Three till-fabric analyses were completed in SB E. The two lower fabrics indicate deposition by northwest- or southeast-oriented ice flow and the uppermost fabric indicates deposition by south-

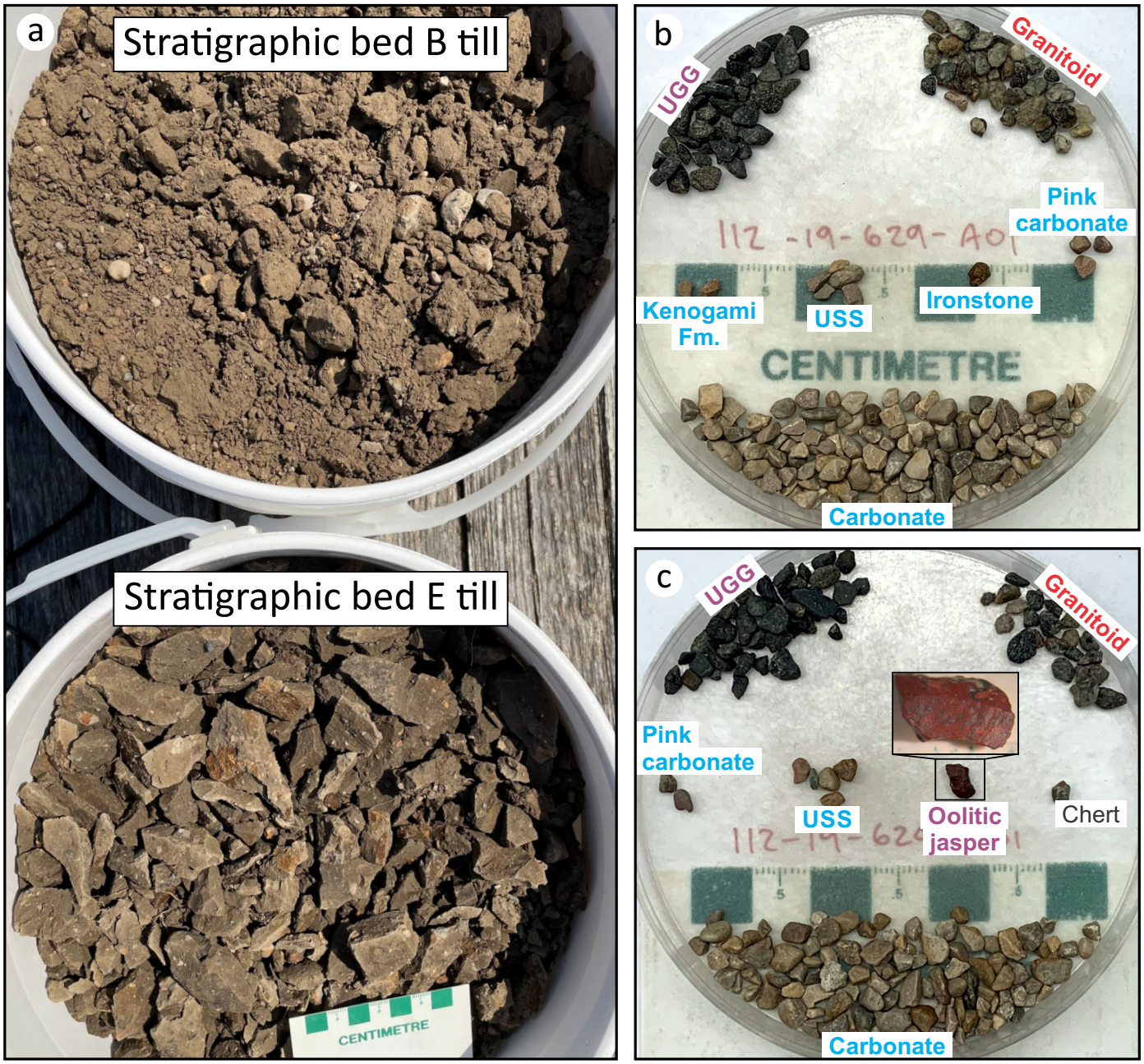

Figure GS2022-12-3: *Glacial sediment and clast count examples for section 112-19-629 on the Hayes River near the confluence with the Gods River:* ***a)*** *comparison of the upper crumbly till (stratigraphic bed [SB] B) and lower blocky till (SB E);* ***b)*** *sorted 2–4 mm granules from SB B till;* ***c)*** *sorted 2–4 mm granules from SB E till. Abbreviations: Fm., Formation; UGG, undifferentiated greenstone and greywacke; USS, undifferentiated sandstone and siltstone.*

west- or northeast-oriented ice flow (sites W9769, W9771, 112-19-629-C01; Figure GS2022-12-2). The lower till contains 23 ct. % UGG clasts at 18.7 m depth (Figure GS2022-12-3c). This is in agreement with counts on the 4–8 mm fraction from seven other samples from this till bed, which ranged from 17–25 wt. % (Hodder et al., 2017). An oolitic jasper clast from the Proterozoic Kipalu Formation, which has an eastern provenance (Hodder and Kelly, 2018), was observed in the 2–4 mm size fraction of the till sample counted during this study (Figure GS2022-12-3c).

The largest bedrock source by aerial extent for UGG clasts recovered in the Hudson Bay Basin is interpreted to be the Belcher Group and Sutton Inlier to the east and southeast (Shilts, 1980; Hodder and Kelley, 2018). Scattered greenstone belts throughout the Canadian Shield are also potential source rocks for these indiscriminate dark grey erratics. The UGG concentrations of SB B and E tills are consistent with till interpreted to have an eastern provenance based on a regional-scale study over the Kaskattama highland area (~80 km to the east; Hodder and Kelley, 2018) and ongoing provenance work in this area. This is further supported by the recovery of an oolitic jasper from SB E till. Thus, it is interpreted that both tills at section 112-19-629 have an east to southeast provenance. The lower (SB E) till was depos-

ited by northwest-trending ice flow and was overprinted by a later southwest-trending ice flow, but this did not change the till composition. The upper (SB B) till was deposited by northwest- to north-northwest-trending ice flow.

Qualitatively, the lower till is significantly denser than the upper till and there is a difference in the ice-flow direction indicated above and below the intertill sorted sediments. These changes suggest that the tills were deposited during separate ice-flow events and the intertill sediments were deposited during an ice-free period following retreat of the ice that deposited the lower till. A sample of the sand (SB D) was collected for optically stimulated luminescence dating, which should help to confirm the chronology at this site.

Section 112-22-200

Section 112-22-200 on the Little Hayes Creek exposes 10.4 m of Quaternary sediments (Figure GS2022-12-4). The uppermost sediments consist of texturally bedded silt and fine sand (SB A; Figure GS2022-12-5a). These postglacial sediments are in sharp horizontal contact with an underlying 15 cm thick diamicton (SB B). The SB B diamicton is massive, matrix supported, contains 5% clasts and is sharply separated from the underlying 0.4 m thick

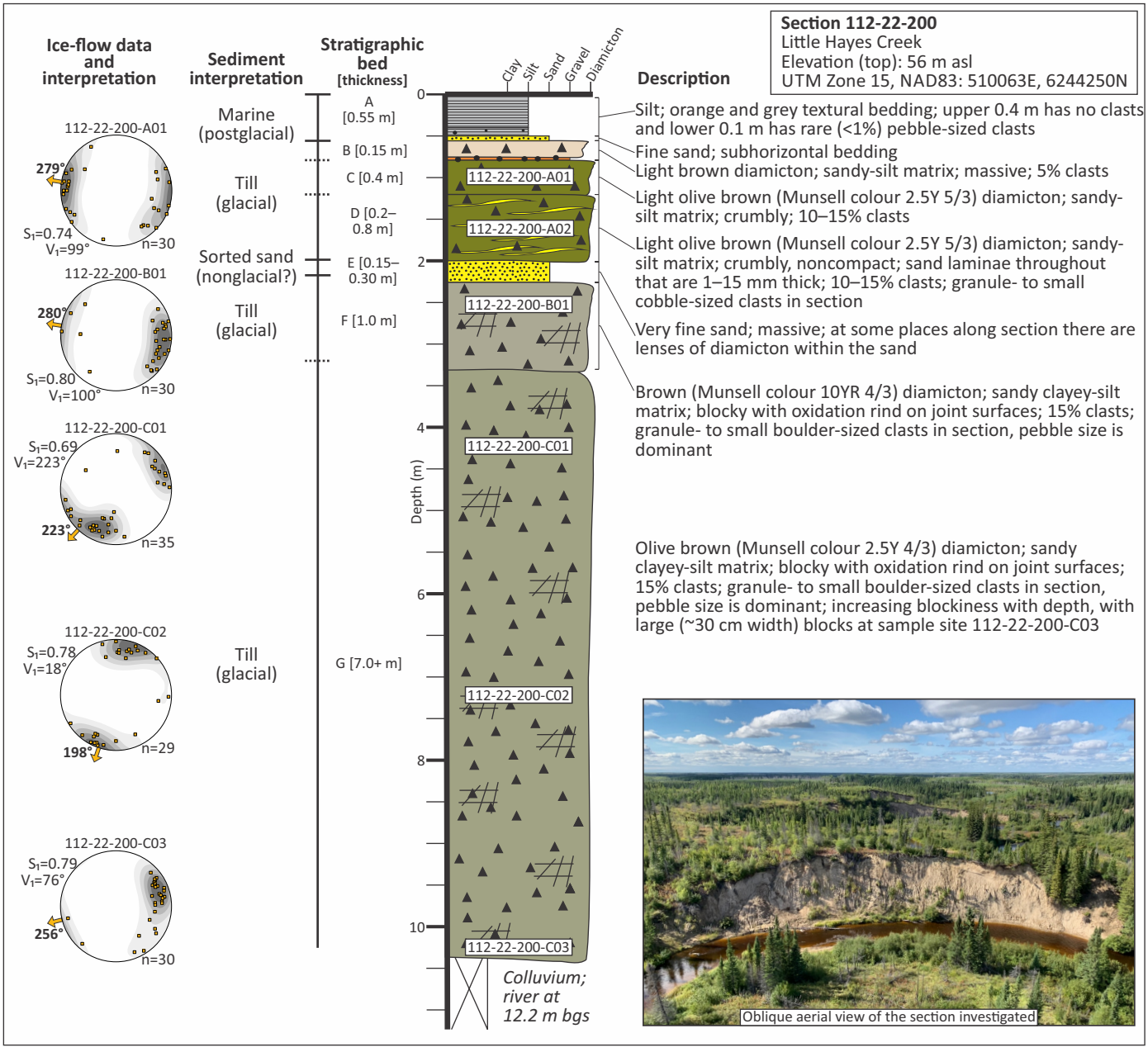

Figure GS2022-12-4: *Quaternary stratigraphy exposed at section 112-22-200 on the Little Hayes Creek. Till sample numbers and till-fabric sites are labelled within the white boxes. Till-fabric data is plotted on equal area, lower hemisphere projection stereonets. The value of the principal eigenvalue (S_1) and direction of the principal eigenvector (V_1) are provided and an interpretation of the ice-flow direction is indicated (orange arrow). Diamicton colour from Munsell Color–X-Rite, Incorporated (2015). Abbreviation: bgs, below ground surface.*

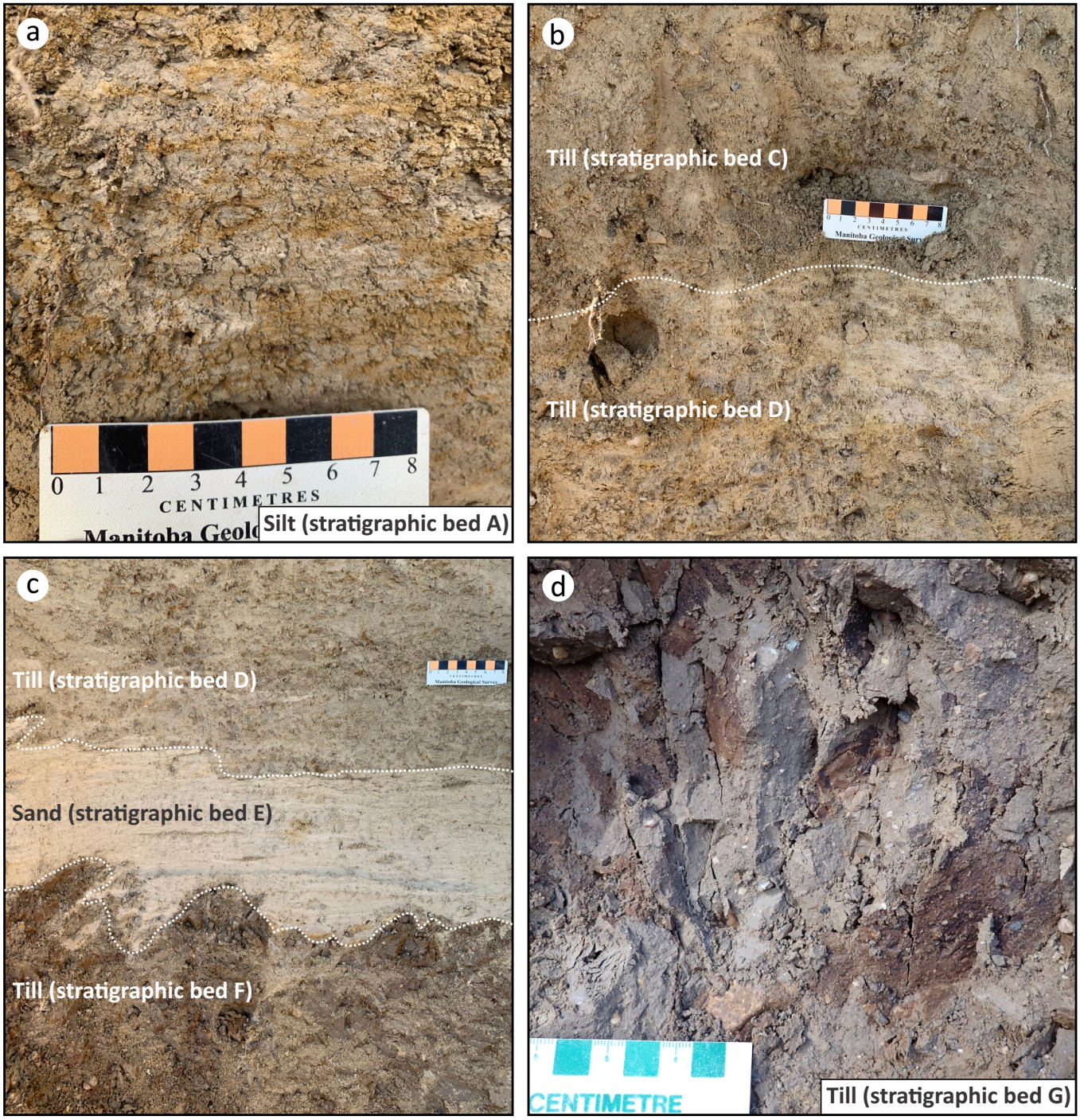

Figure GS2022-12-5: *Sediments exposed at section 112-22-200 on the Little Hayes Creek:* ***a)*** *stratigraphic bed (SB) A texturally bedded silt;* ***b)*** *SB C and D tills highlighting the sharp subhorizontal contact separating the two tills;* ***c)*** *SB D and F tills separated by very fine sand (intertill);* ***d)*** *dense blocky till of SB G.*

diamicton (SB C). Stratigraphic bed C is a light olive brown (Munsell colour 2.5Y 5/3) diamicton that is massive, matrix supported and contains 10–15% clasts (Figure GS2022-12-5b). The SB C diamicton has a sharp subhorizontal contact with an underlying 0.2–0.8 m thick diamicton (SB D; Figure GS2022-12-5b). Stratigraphic bed D is a light olive brown (Munsell colour 2.5Y 5/3) diamicton that contains sand laminae that are 1–15 mm thick throughout the sediment (Figure GS2022-12-5b). The diamicton is matrix supported and contains 10–15% clasts. The SB D diamicton has a sharp undulatory lower contact with a 15–30 cm thick sand (SB E; Figure GS2022-12-5c). Stratigraphic bed E consists of well sorted, very fine sand, though laterally this unit becomes heterogeneous and contains lenses of diamicton. The lower contact of SB E is sharp and undulatory with the underlying 1 m thick diamicton (SB F; Figure GS2022-12-5c). Stratigraphic bed F is a brown (Munsell colour 10YR 4/3) diamicton that is massive, matrix supported and contains 15% clasts. The diamicton has a blocky appearance with oxidation rind on joint surfaces. There is

a gradational contact between SB F and the underlying diamicton (SB G); the diamicton beds are qualitatively very similar except for their colour. The SB G diamicton is olive brown (Munsell colour 2.5Y 4/5), massive, matrix supported and contains 15% clasts (Figure GS2022-12-5d). The diamicton has a blocky appearance with oxidation rind on joint surfaces. Density increases with depth in SB G, and large (~20 by 30 cm) blocks are broken off at sample site 112-22-200-C03. The SB B, C, D, F and G diamictons are interpreted as tills, based on their massive structure, their texture, the glaciogenic shape of the clasts (bullet shaped, faceted and striated), the modality and strength of the clast fabrics, and the lateral continuity of beds.

Till fabrics were measured for five sample sites at section 112-22-200. A till fabric measured in SB C is interpreted to show deposition by west-trending (279°) ice flow, as is a till fabric conducted in SB F (280°; Figure GS2022-12-4). Though the ice-flow direction indicated for these two beds is identical, they are interpreted to have been deposited during separate ice-flow events based on qualitative differences, including density of the tills and presence of sorted sediments separating the beds. Next, three till fabrics were measured in SB G. The upper and middle fabrics indicate deposition by southwest-trending (198°, 223°) ice flow. The lower fabric is interpreted to show deposition by west-southwest-trending (256°) ice flow, indicating a transition in ice flow up unit from west-southwest- to southwest-trending. Future work on the composition of the till will aid in understanding this transition as it relates to this change in ice-flow orientation.

Section 112-22-201

Section 112-22-201 on the Hayes River exposes 21.1 m of Quaternary sediments (Figure GS2022-12-6). The uppermost sediments are 10 m of bedded sand and gravel with minor silt (SB A). The uppermost gravel bed contains whole valves of *Hiatella arctica,* indicating deposition within a marine environment. The bedded sand and gravel underlying this gravel contains shell fragments that are presumably of marine origin. Stratigraphic bed A is interpreted to represent a cycle of postglacial marine transgression and regression.

Postglacial sediments of SB A are in sharp horizontal contact with 2.2 m of diamicton (SB B; Figure GS2022-12-7a). The SB B diamicton is very dark greyish-brown (Munsell colour 2.5Y 3/2), massive, matrix supported and contains 15% clasts. The diamicton has a blocky appearance with oxidation rind on joint surfaces and sharply overlies a 1.2 m thick diamicton (SB C; Figure GS2022-12-7b). Stratigraphic bed C is olive brown (Munsell colour 2.5Y 4/3) diamicton that is massive, matrix supported and contains 15% clasts. Within this diamicton there is a laterally discontinuous pod of gravel that is ~1.1 m wide by 0.2 m high (Figure GS2022-12-7c). Both the SB C and D diamictons are interpreted as tills based on their massive structure, their texture, the glaciogenic shape of the clasts (bullet shaped, faceted and striated), the modality and strength of the clast fabrics, and the lateral continuity of the beds.

Stratigraphic bed C is in sharp contact with more than 7.7 m of the underlying bedded sand and diamicton (SB D). Individual beds range from 0.1 to 0.8 m in thickness and there are two distinctly different diamicton beds within SB D. The diamicton beds are either silty dark greyish-brown or sandy light brown (Figure GS2022-12-7d). The sand and diamicton beds are horizontal from 13.4 to 18.4 m below ground surface (bgs) and disturbed beyond 18.4 m bgs, with vertical contacts and convoluted bedding. Stratigraphic bed D is interpreted to have been deposited in a proglacial subaqueous setting with significant glacial input.

Till fabrics were measured in SB B and C, and both indicate deposition by northwest- or southeast-trending ice flow (Figure GS2022-12-6). Till composition data will be assessed to determine which of the ice-flow orientations deposited these beds, and if there is any variation in composition between the two beds.

Implications for diamond exploration

The two till beds at section 112-19-629 have previously been interpreted to be deposited by the same ice-flow event (Long Spruce till) and by south- to southeast-trending ice flow (Syme et al., 2004). This study, however, has determined that both tills likely have an east to southeast provenance, based on their clast-lithology composition and ice-flow data, indicating that both tills were deposited by northwest-trending ice flow. The lowermost till was later modified by southwest-trending ice flow, but this ice-flow direction change did not change the clast-lithology composition (Hodder et al., 2017). This ice-flow directional change does add an additional parameter to consider for drift prospecting since this could create complex palimpsest dispersal patterns (McClenaghan et al., 2020). Furthermore, it is suggested that the two tills were deposited by separate ice-flow events, and that there was an ice-free period between these two glacial events that deposited nonglacial sorted sediments. This new interpretation recognizes that the upper and lower tills are different in colour, texture, density and till fabrics, in addition to their separation by 2.2 m of sorted sediments.

The eastern to southeastern till provenance interpreted here implies a similar provenance for the KIM grains recovered from these tills. The recovery of relatively elevated KIM counts from samples deposited by west- to northwest-trending ice flow has emerged as a trend across two additional surveys that are situated to the east and northeast of this study area in the HBL (Hodder and Kelley, 2018; Hodder and Gauthier, 2021).

Economic considerations

Manitoba's far northeast is a remote and largely unexplored frontier area with thick drift covering much of the bedrock in the region. Results from this study continue to document the Quaternary stratigraphy, glacial history and indicator-mineral patterns

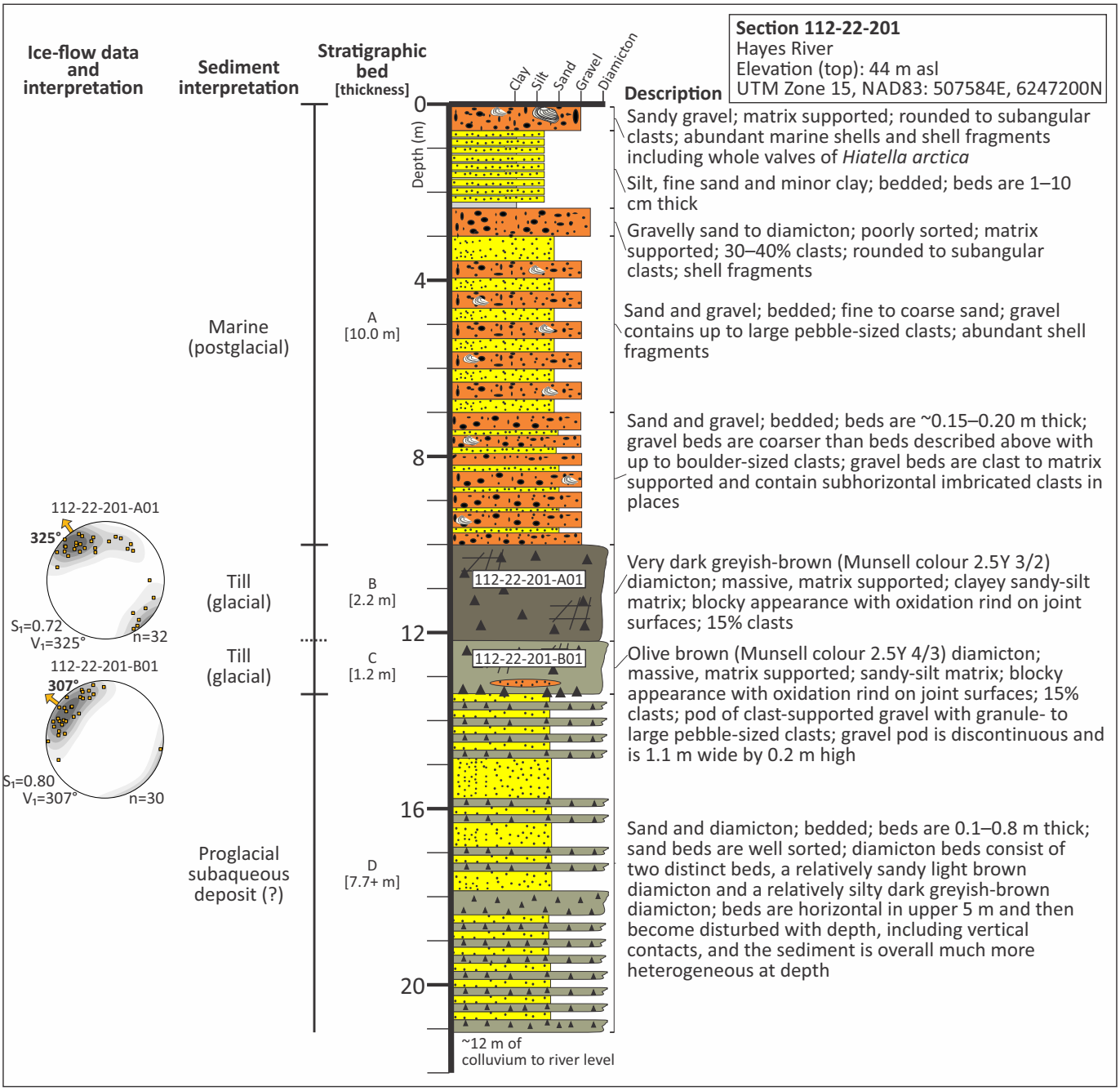

Figure GS2022-12-6: *Quaternary stratigraphy exposed at section 112-22-201 on the Hayes River. Till sample numbers and till-fabric sites are labelled within the white boxes. Till-fabric data is plotted on equal area, lower hemisphere projection stereonets. The value of the principal eigenvalue (S_1) and direction of the principal eigenvector (V_1) are provided and an interpretation of the ice-flow direction is indicated (orange arrow). Diamicton colour from Munsell Color–X-Rite, Incorporated (2015).*

in the study area. This is necessary to support drift prospecting efforts in this region of thick drift, which contains a depositional record spanning multiple glaciations.

Acknowledgments

Pilot K. Dunthorne and Prairie Helicopters Inc. are thanked for providing excellent air-support during this project. This research is funded by the Manitoba Geological Survey and the Geological Survey of Canada's Geo-mapping for Energy and Minerals GeoNorth program (GEM-GeoNorth).

References

Dredge, L.A. and McMartin, I. 2011: Glacial stratigraphy of northern and central Manitoba; Geological Survey of Canada, Bulletin 600, 27 p.

Earth Observation Research Center and Japanese Aerospace Exploration Agency 2022: ALOS Global Digital Surface Model; Earth Observation Research Center and Japanese Aerospace Exploration Agency, ALOS World 3D - 30m, URL <https://www.eorc.jaxa.jp/ALOS/en/dataset/aw3d30/aw3d30_e.htm> [August 2022].

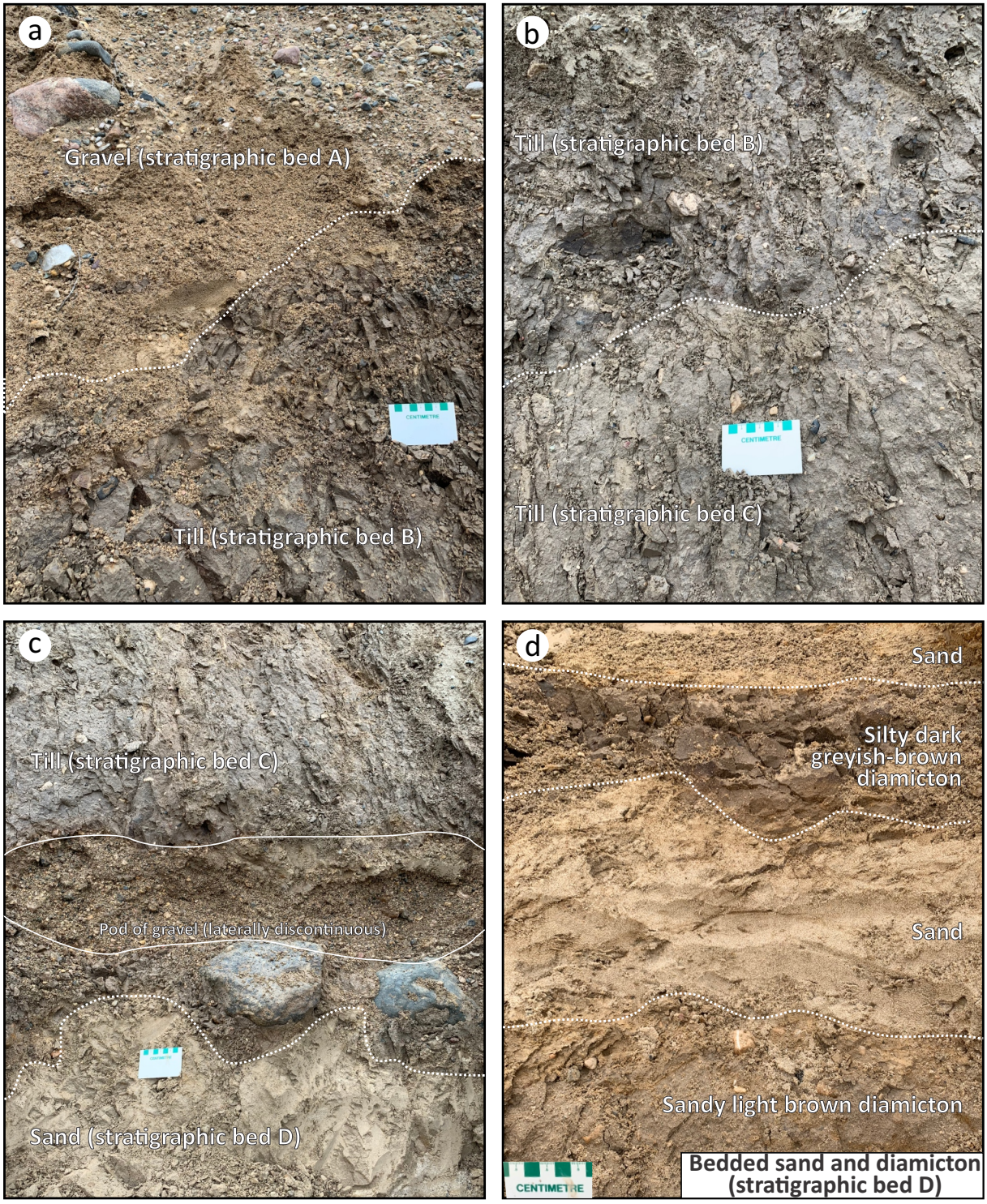

Figure GS2022-12-7: *Sediments exposed at section 112-22-201 on the Hayes River:* ***a)*** *stratigraphic bed (SB) A gravel in sharp contact with SB till;* ***b)*** *sharp contact between SB B and C tills;* ***c)*** *pod of gravel within SB C till and view of the sharp undulatory contact between SB C and D;* ***d)*** *horizontally bedded sand and diamicton of SB D.*

Gauthier, M.S., Hodder, T.J., Lian, O.B., Finkelstein, S.A., Dalton, A.S. and Paulen, R.C. 2021: Stratigraphic, paleoenvironmental and geochronological investigations of intertill nonglacial deposits in northeastern Manitoba (parts of NTS 54BF, K, L, 64A, H, I); *in* Report of Activities 2021, Manitoba Agriculture and Resource Development, Manitoba Geological Survey, p. 71–76, URL <https://manitoba.ca/iem/geo/field/roa21pdfs/GS2021-8.pdf> [October 2022].

Gauthier, M.S., Hodder, T.J. and Ross, M. 2022: Quaternary stratigraphy and ice-flow indicator data for the Gillam region, Manitoba (parts of NTS 54C, D, 64A); Manitoba Natural Resources and Northern Development, Manitoba Geological Survey, Geoscientific Paper GP2022-2, 37 p. plus 7 appendices, URL <https://manitoba.ca/iem/info/libmin/GP2022-2.zip> [November 2022].

Gauthier, M.S., Hodder, T.J., Ross, M., Kelley, S.E., Rochester, A. and McCausland, P. 2019: The subglacial mosaic of the Laurentide Ice Sheet; a study of the interior region of southwestern Hudson Bay; Quaternary Science Reviews, v. 214, p. 1–27.

Hodder, T.J. and Gauthier, M.S. 2021: Kimberlite-indicator-mineral results from till sampled in the Machichi–Kettle rivers area, far northeastern Manitoba (parts of NTS 54A–C); *in* Report of Activities 2021, Manitoba Agriculture and Resource Development, Manitoba Geological Survey, p. 77–83, URL <https://manitoba.ca/iem/geo/field/roa21pdfs/GS2021-9.pdf> [October 2022].

Hodder, T.J. and Gauthier, M.S. 2022: Till-fabric measurements and statistics from sections near the confluence of the Hayes and Gods rivers, northeastern Manitoba (part of NTS 54C7); Manitoba Natural Resources and Northern Development, Manitoba Geological Survey, Data Repository Item DRI2022011, Microsoft® Excel® file, URL <https://manitoba.ca/iem/info/libmin/DRI2022011.xlsx> [November 2022].

Hodder, T.J. and Kelley, S.E. 2018: Kimberlite-indicator minerals and clast-lithology composition of till, Kaskattama highland region, northeastern Manitoba (parts of NTS 53N, O, 54B, C); *in* Report of Activities 2018, Manitoba Growth, Enterprise and Trade, Manitoba Geological Survey, p. 150–165, URL <https://manitoba.ca/iem/geo/field/roa18pdfs/GS2018-13.pdf> [October 2022].

Hodder, T.J., Gauthier, M.S. and Nielsen, E. 2017: Quaternary stratigraphy and till composition along the Hayes, Gods, Nelson, Fox, Stupart, Yakaw, Angling and Pennycutaway rivers, northeast Manitoba (parts of NTS 53N, 54C, 54D, 54F); Manitoba Growth, Enterprise and Trade, Manitoba Geological Survey, Open File OF2017-4, 20 p., URL <https://manitoba.ca/iem/geo/field/roa17pdfs/GS2017-18.pdf> [October 2022].

Holmes, C.D. 1941: Till fabric; Bulletin of the Geological Society of America, v. 52, p. 1299–1354.

Klassen, R.W. 1986: Surficial geology of north-central Manitoba; Geological Survey of Canada, Memoir 419, 57 p.

Lee, J. 2018: Glacial lithofacies and stratigraphy; Chapter 11 *in* Past Glacial Environments, J. Menzies and J.J.M. van der Meer (ed.), Elsevier Science, Amsterdam, The Netherlands, p. 377–429.

McClenaghan, M.B., Spirito, W.A., Plouffe, A., McMartin, I., Campbell, J.E., Paulen, R.C., Garrett, R.G., Hall, G.E.M., Pelchat, P. and Gauthier, M.S. 2020: Till-sampling and analytical protocols: from field to archive, 2020 update; Geological Survey of Canada, OF8591, 73 p.

McDonald, B.C. 1969: Glacial and interglacial stratigraphy, Hudson Bay Lowland; *in* Earth Science Symposium on Hudson Bay, P.J. Hood (ed.), Geological Survey of Canada, Paper 68-83, p. 78–99.

Munsell Color–X-Rite, Incorporated 2015: Munsell Soil Color Book; Pantone LLC, Carlstadt, New Jersey, 42 p.

Nielsen, E. 2001: Quaternary stratigraphy, till provenance and kimberlite indicator mineral surveys along the lower Hayes River; *in* Report of Activities 2001, Manitoba Industry, Trade and Mines, Manitoba Geological Survey, p. 121–125, URL <https://manitoba.ca/iem/geo/field/roa01pdfs/01gs-18.pdf> [October 2022].

Nielsen, E. 2002: Quaternary stratigraphy and ice-flow history along the lower Nelson, Hayes, Gods and Pennycutaway rivers and implications for diamond exploration in northeastern Manitoba; *in* Report of Activities 2002, Manitoba Industry, Trade and Mines, Manitoba Geological Survey, p. 209–215, URL <https://manitoba.ca/iem/geo/field/roa02pdfs/GS-24.pdf> [October 2022].

Nielsen, E. and Fedikow, M.A.F. 2002: Kimberlite indicator mineral surveys, lower Hayes River; Manitoba Industry, Trade and Mines, Manitoba Geological Survey, Geological Paper GP2002-1, 39 p., URL <https://manitoba.ca/iem/info/libmin/GP2002-1.zip> [October 2021].

Nielsen, E., Morgan, A.V., Morgan, A., Mott, R.J., Rutter, N.W. and Causse, C. 1986: Stratigraphy, paleoecology and glacial history of the Gillam area, Manitoba; Canadian Journal of Earth Sciences, v. 23, p. 1641–1661.

Shilts, W.W. 1980: Flow patterns in the central North American ice sheet; Nature, v. 286, p. 213–218.

Syme, E.C., Bezys, R.K., Bogdan, D.J., Böhm, C.O., Kaszycki, C.A., Keller, G.R., Lenton, P.G. and Matile, G.L.D. 2004: Kimberlite potential in Manitoba: an update; *in* Report of Activities 2004, Manitoba Industry, Economic Development and Mines, Manitoba Geological Survey, p. 309–319, URL <https://manitoba.ca/iem/geo/field/roa04pdfs/GS-30.pdf> [October 2022].

Thorleifson, L.H., Wyatt, P.H. and Warman, T.A. 1993: Quaternary stratigraphy of the Severn and Winisk drainage basins, northern Ontario; Geological Survey of Canada, Bulletin 442, 65 p.

Trommelen, M.S., Ross, M. and Campbell, J.E. 2013: Inherited clast dispersal patterns: implications for paleoglaciology of the southeast Keewatin Sector of the Laurentide Ice Sheet; Boreas, v. 42, no. 3, p. 693–713.

PUBLICATIONS

Data Repository Items

DRI2021014

Lithogeochemical database, Sm-Nd isotopic data and U-Pb geochronological data for the Wuskwatim–Granville–Laurie lakes corridor, Manitoba (parts of NTS 63O, P, 64A–C)

by L.A. Murphy, H.V. Zwanzig and C.O. Böhm

Microsoft® Excel® file accompanies:

Murphy, L.A. and Zwanzig, H.V. 2021: Geology of the Wuskwatim–Granville lakes corridor, Kisseynew domain, Manitoba (parts of NTS 63O, P, 64A–C); Manitoba Agriculture and Resource Development, Manitoba Geological Survey, Geoscientific Report GR2021-2, 94 p.

DRI2021021

Bedrock geochemical data of the Ralph Lake area, Lynn Lake greenstone belt, northwestern Manitoba (parts of NTS 64C14)

by X.M. Yang

Microsoft® Excel® file supplements:

Yang, X.M. 2021: Bedrock mapping at Ralph Lake, Lynn Lake greenstone belt, northwestern Manitoba (part of NTS 64C14): preliminary results and geological implications; *in* Report of Activities 2021, Manitoba Natural Resources and Northern Development, Manitoba Geological Survey, p. 40–58.

DRI2022001

Whole-rock geochemistry results of Cretaceous shale outcrop samples from the Pembina Hills area, southwestern Manitoba (NTS 62G1, 2, 8, 10)

by M.P.B. Nicolas

DRI2022002

Bedrock geochemistry from the Stuart Bay–Chickadee Lake area (east of Wekusko Lake), north-central Manitoba (parts of NTS 63J12, 13)

by K.D. Reid

Microsoft® Excel® file supplements:

Reid, K.D. 2019: Bedrock geological mapping of the Puella Bay area (Wekusko Lake), north-central Manitoba (part of NTS 63J12); *in* Report of Activities 2019, Manitoba Natural Resources and Northern Development, Manitoba Geological Survey, p. 42–51.

Reid, K.D. 2021: Results of bedrock geological mapping in the Stuart Bay–Chickadee Lake area (east of Wekusko Lake), north-central Manitoba (parts of NTS 63J12, 13); *in* Report of Activities 2021, Manitoba Natural Resources and Northern Development, Manitoba Geological Survey, p. 29–39.

DRI2022003

Compilation of Sm-Nd isotope results from the Manitoba Geological Survey 2021/2022 field season

by Manitoba Geological Survey

DRI2022004

Till-matrix geochemistry data from the Gillam area, northeastern Manitoba: additional 2021 data (NTS 54D7, 9, 11)

By M.S. Gauthier and T.J. Hodder

DRI2022005

Till-matrix geochemistry data from the Churchill–Little Churchill rivers area, northeastern Manitoba (part of NTS 54E)

By T.J. Hodder and M.S. Gauthier

DRI2022006

Till-matrix geochemistry data from the Machichi–Kettle rivers area, far northeastern Manitoba (parts of NTS 54A–C)

By T.J. Hodder and M.S. Gauthier

DRI2022007

Whole-rock geochemistry results of pegmatites from the Superior province (parts of NTS 53L10, 11, 14, 15)

By T. Martins

DRI2022008

Laser-ablation inductively coupled plasma–mass spectrometry analyses of detrital zircon grains from metasedimentary rocks of the Ospwagan group, Thompson nickel belt, Manitoba (parts of NTS 63O8, 9; 63P12)

By C.G. Couëslan

DRI2022009

Field-based ice-flow indicator data from the Split Lake and Fox River belt areas, northeastern Manitoba (parts of NTS 53M15, 16, 54D2, 4, 64A2)

by M.S. Gauthier and T.J. Hodder

Microsoft® Excel® file supplements:

Gauthier, M.S. and Hodder, T.J. 2022: Surficial geology mapping and till composition of the western Fox River greenstone belt area, northeastern Manitoba (NTS 53M15, 16, parts of 53N13, 54C4, 54D1): year two; *in* Report of Activities 2022, Manitoba Natural Resources and Northern Development, Manitoba Geological Survey, p. 96–109.

DRI2022010

Kimberlite-indicator-mineral data derived from glacial sediments (till) in the western Fox River greenstone belt area, northeastern Manitoba (NTS 53M15, 16)

by T.J. Hodder and M.S. Gauthier

Microsoft® Excel® file supplements:

Gauthier, M.S. and Hodder, T.J. 2022: Surficial geology mapping and till composition of the western Fox River greenstone belt area, northeastern Manitoba (NTS 53M15, 16, parts of 53N13, 54C4, 54D1): year two; *in* Report of Activities 2022, Manitoba Natural Resources and Northern Development, Manitoba Geological Survey, p. 96–109.

DRI2020011

Till-fabric measurements and statistics from sections near the confluence of the Hayes and Gods rivers, northeastern Manitoba (part of NTS 54C7)

by T.J. Hodder and M.S. Gauthier

Microsoft® Excel® file supplements:

Hodder, T.J. and Gauthier, M.S. 2022: Quaternary stratigraphic investigations near the confluence of the Hayes and Gods rivers, northeastern Manitoba (part of NTS 54C7); *in* Report of Activities 2022, Manitoba Natural Resources and Northern Development, Manitoba Geological Survey, p. 110–120.

GeoFiles

GeoFile 1

Digital compilation of surficial point and line features for Manitoba, including ice-flow data

by M.S. Gauthier, A. Santucci and G.R. Keller

GeoFile 2

Manitoba till-matrix geochemistry compilation: silt plus clay (<63 µm) size-fraction by inductively coupled plasma–mass spectrometry after an aqua-regia or modified aqua-regia digestion

by M.S. Gauthier

GeoFile 3

New edition of the 1:250 000 scale Precambrian bedrock geology compilation map of Manitoba

by Manitoba Geological Survey

GeoFile 4

Compilation of lithogeochemistry from Precambrian rocks in Manitoba

by Manitoba Geological Survey

GeoFile 5

Updates to the Manitoba Mineral Deposits Database, east-central and northern Manitoba (parts of NTS 53; 54; 64)

by M.L. Rinne

Geoscientific Papers

GP2022-1

Characterization of ultramafic-hosting metasedimentary rocks and implications for nickel exploration at Phillips Lake, Thompson nickel belt, central Manitoba (part of NTS 63O1)

by C.G. Couëslan

GP2022-2

Quaternary stratigraphy and ice-flow indicator data for the Gillam region, Manitoba (parts of NTS 54C, D, 64A)

by M.S. Gauthier, T.J. Hodder and M. Ross

Geoscientific Report

GR2021-2

Geology of the Wuskwatim–Granville lakes corridor, Kisseynew domain, Manitoba (parts of NTS 63O, P, 64A–C)

by L.A. Murphy and H.V. Zwanzig

Open Files

OF2022-1

Palynological analyses of subtill sediments from four sites in the western Hudson Bay Lowland region (parts of NTS 53O; 54A, C, D)

by A.S. Dalton, S.A. Finkelstein, T.J. Hodder and M.S. Gauthier

OF2022-2

Bedrock geology of Manitoba

by Manitoba Geological Survey (scale 1:1 000 000)

Preliminary Maps

PMAP2022-1
Bedrock geology of the Halfway Lake area, central Manitoba (parts of NTS63O1, 2)
by C.G. Couëslan (scale 1:25 000)

PMAP2022-2
Bedrock geology of the Fox mine–Snake Lake area, Lynn Lake greenstone belt, northwestern Manitoba (part of NTS 64C12)
by X.M. Yang (scale 1:10 000)

Surficial Geology Compilation Maps

Updated maps can be downloaded at https://manitoba.ca/iem/geo/surficial/digitalcompilation.html

Benn, D., Linnen, R., and Martins, T. 2021: Evaluating white mica as an indicator mineral for lithium bearing pegmatites, Wekusko Lake pegmatite field, Manitoba, Canada; *in* Targeted Geoscience Initiative 5: grant program final reports (2018-2020), Geological Survey of Canada, Open File 8755, p. 45–58, URL <https://doi.org/10.4095/328982>.

Benn, D., Martins, T. and Linnen, R. in press: Fractionation and enrichment patterns in white mica from Li pegmatites of the Wekusko Lake pegmatite field, Manitoba, Canada; The Canadian Mineralogist.

Breasley, C.M., Linnen, R.L., Barker, I.R., Groat, L.A. and Martins, T. 2022: Utilizing X-ray computed tomography to visualise lithium silicate minerals: insights into mineralization at the Tanco pegmatite, Manitoba; AME Roundup 2022, January 31–February 3, 2022, Vancouver, BC, poster presentation.

Breasley, C.M., Martins, T., Linnen, R.L. and Groat, L.A. 2022: Textures and trace element geochemistry of spodumene at the Tanco Pegmatite, Manitoba, Canada; 2022 Goldschmidt Conference, July 10–15, 2022, Honolulu, Hawaii, poster presentation.

Couëslan, C.G. 2022: Affinity and petrogenesis of the Huzyk Creek metal-enriched graphite deposit: a metamorphosed metalliferous black shale in the Trans-Hudson Orogen of Manitoba, Canada; The Canadian Mineralogist, v. 60, no. 6, p. 1–28.

Couëslan, C.G. 2022: Genesis of the Paleoproterozoic Huzyk Creek polymetallic graphite deposit, and the potential benefits of high-grade metamorphism of metalliferous black shales; Geological Association of Canada–Mineralogical Association of Canada, Joint Annual Meeting, May 15–18, 2022, Halifax, Nova Scotia, Volume of Abstracts, v. 45, p. 75.

Gauthier, M.S. 2022: Using radiocarbon ages on organics affected by freshwater–a geologic and archaeologic update on the freshwater reservoir ages and freshwater diet effect in Manitoba, Canada; Radiocarbon, v. 64, no. 2, p. 253–264, URL <https://doi.org/10.1017/RDC.2022.30>.

Gauthier, M.S. and Hodder, T.J. 2022: Glacial terrain zones reveal patchy erosion and deposition; Quaternary Research Association Annual Meeting 2022, January 5–7, 2022, Sheffield, U.K., oral presentation.

Gauthier, M.S., Breckenridge, A. and Hodder, T.J. 2022: Patterns of ice recession and ice stream activity for the MIS 2 Laurentide Ice Sheet in Manitoba, Canada; Boreas, v. 51, no. 2, p. 274–298, URL <https://doi.org/10.1111/bor.12571>.

Gauthier, M.S., Brewer, V., Hodder, T.J., Lian, O.B. and Schaarschmidt, M. 2022: Laurentide Ice Sheet withdraw and advance in the Roseau River area of southern Manitoba, Canada; American Quaternary Association Biennial Meeting (AMQUA 2022), June 7–11, 2022, Madison, Wisconsin, poster presentation.

Haynes, S., Nicolas, M.P.B., MacCormack, K., McKenzie, B., Lynch, G., Hills, D., Coutts, K. and Watson, N. 2022: Building a strong foundation: progress on the 2027 Geological Atlas of the Western Canada Sedimentary Basin; Geoconvention 2022, June 20–22, 2022, Calgary, Alberta, Program with Abstracts and poster presentation, URL <https://geoconvention.com/wp-content/uploads/abstracts/2022/73339-building-on-a-strong-foundation_-progress-on-the-2.pdf> [October 2022].

Martins, T. and Nicolas, M.P.B. 2022: Lithium – Manitoba leading the way; Northern Prospector 2022-2023, p. 14–15.

Martins, T., Benn, D. and Linnen, R. 2022: Cs enrichment in white mica from Manitoba Li-bearing pegmatites. Is it always a product of fractional crystallization?; GAC-MAC-IAH-CNC-CSPG Joint Meeting, May 15–18, 2022, Halifax, Nova Scotia, Program with Abstracts and oral presentation, URL <https://halifax2022.atlanticgeosciencesociety.ca/technical-program/> [September 2022].

McMartin, I., Gauthier, M.S. and Page, A.V. 2022: Updated post-glacial marine limits along western Hudson Bay, central mainland Nunavut and northern Manitoba; Geological Survey of Canada, Open File 8921, 19 p., URL <https://doi.org/10.4095/330940>.

Nicolas, M.P.B. 2022: Helium potential of southwestern Manitoba; Williston Basin Petroleum Conference 2022, May 17–18, 2022, Regina, Saskatchewan, Program with Abstracts and oral presentation.

Nicolas, M.P.B., Hills, D., Watson, N., Lynch, G. and McKenzie, B. 2022: Geological Atlas of the Western Canada Sedimentary Basin 2027: compiling the world's most comprehensive geological atlas; Williston Basin Petroleum Conference 2022, May 17–18, 2022, Regina, Saskatchewan, Program with Abstracts and poster presentation.

Polat, A., Frei, R., Deng, H., Yang, X.M. and Sotiriou, P. 2022: Anatomy of a Neoarchean continental arc-backarc system in the Cross Lake-Pipestone Lake region, northwestern Superior Province, Canada; Precambrian Research, v. 370, art. 106556, URL <https://doi.org/10.1016/j.precamres.2021.106556>.